RESEARCH REPORT

HEALTH EFFECTS INSTITUTE

Number 133
March 2006

Characterization of Metals Emitted from Motor Vehicles

James J Schauer, Glynis C Lough, Martin M Shafer, William F Christensen, Michael F Arndt, Jeffrey T DeMinter, and June-Soo Park

Includes a Commentary by the Institute's Health Review Committee

HEALTH
EFFECTS
INSTITUTE

The Health Effects Institute was chartered in 1980 as an independent and unbiased research organization to provide high quality, impartial, and relevant science on the health effects of air pollution. All results are provided to industry and government sponsors, other key decisionmakers, the scientific community, and the public. HEI funds research on all major pollutants, including air toxics, diesel exhaust, nitrogen oxides, ozone, and particulate matter. The Institute periodically engages in special reviews and evaluations of key questions in science that are highly relevant to the regulatory process. To date, HEI has supported more than 220 projects at institutions in North America, Europe, and Asia and has published over 160 Research Reports and Special Reports.

Typically, HEI receives half of its core funds from the US Environmental Protection Agency and half from 28 worldwide manufacturers and marketers of motor vehicles and engines who do business in the United States. Other public and private organizations periodically support special projects or certain research programs. Regardless of funding sources, HEI exercises complete autonomy in setting its research priorities and in reaching its conclusions.

An independent Board of Directors governs HEI. The Institute's Health Research Committee develops HEI's five-year Strategic Plan and initiates and oversees HEI-funded research. The Health Review Committee independently reviews all HEI research and provides a Commentary on the work's scientific quality and regulatory relevance. Both Committees draw distinguished scientists who are independent of sponsors and bring wide-ranging multidisciplinary expertise.

The results of each project and its Commentary are communicated widely through HEI's home page, Annual Conference, publications, and presentations to professional societies, legislative bodies, and public agencies.

HEI STATEMENT
Synopsis of Research Report 133

Characterization of Metals Emitted from Motor Vehicles

BACKGROUND

Metals comprise a complex group of elements with a broad range of toxicity, including effects on genes, nervous and immune systems, and the induction of cancer. Some metals are toxic at very low levels; others are essential to living systems at low concentrations, but may be toxic at higher concentrations. Metals may exist in several valence states that differ in toxicity and may be associated with organic matter and inorganic materials that can affect their toxicity. The presence of metals in the environment has received a great deal of attention in recent years. Their accumulation in the environment is of concern because of their persistence. Some scientists believe that transition metals are particularly toxic components of particulate matter (PM).

In 1998, HEI issued Request for Preliminary Applications 98-4, *Research on Metals Emitted by Motor Vehicles.* The goal of the RFA was a broad investigation of metals that may be found in automobile emissions, in particular those found in tailpipe exhaust. Metallic components of fuel additives were a high priority, but metals found in other emissions (such as those derived from fuel lubricant, engine wear, catalytic converter, or brake pads) were also of interest.

APPROACH

Dr Schauer collected and characterized metals in fine and coarse particles from a variety of sources associated with on-road motor vehicles in summer and winter, including tailpipe emissions (from both gasoline and diesel vehicles), dust from brake wear and tire wear, roadway dust, and roadway dust containing salt applied to roadways in winter. In addition, total roadway emissions were measured in two roadway tunnels. Metals were also characterized in ambient air from three urban sites. Use of sensitive analytic techniques such as inductively coupled plasma mass spectrometry (ICP-MS) allowed measurement of a variety of elements in these emissions and subsequent development of profiles for each source. These profiles were compared to the profiles developed for the roadway tunnels by using a chemical mass balance (CMB) model, in order to determine the relative contribution of various sources to total roadway emissions. Iterated confirmatory factor analysis (ICFA) was used to determine the relative contribution of various sources to ambient particulate matter collected at the three ambient locations. To preliminarily address bioavailability of metals, ambient and tunnel samples were examined in a study that determined solubility in a synthetic fluid that was designed to mimic human epithelial lung lining fluid to better estimate the biologically available pool of metals in particulate matter.

Dr Schauer's study evaluated the use of tunnels for identifying the source contributions of metals from a variety of different types of automobile emissions. The study objectives address the use of improved methods for measuring many metals that occur at low levels and application of these methods to tunnels, automobile-associated emissions, and ambient air. Measurements from tunnels were thought to be useful for evaluating exposures to emissions from in-use vehicles. He used the two newer methods, ICP-MS and ICFA, along with more conventional analytic techniques such as x-ray fluorescence spectrometry (XRF) and CMB models, to identify source profiles for various components of mobile source emissions.

RESULTS

The combined use of ICP-MS and XRF allowed detection of 43 elements. The concentrations of 12 elements (aluminum, silicon, phosphorus, sulfur, potassium, calcium, scandium, germanium, selenium, bromine, iodine, and cerium) were determined by XRF elemental analysis. The application of ICP-MS allowed measurement of concentrations of 31 additional elements. Use of ICP-MS, with its greater sensitivity for metals, allowed the detailed profiling of elements that was necessary

Continued

This Statement, prepared by the Health Effects Institute, summarizes a research project funded by HEI and conducted by Dr James J Schauer, Environmental Chemistry and Technology Program and Wisconsin State Laboratory of Hygiene, University of Wisconsin, Madison WI. The following Research Report contains both the detailed Investigators' Report and a Commentary on the study prepared by the Institute's Health Review Committee.

for the subsequent identification of profiles that can be used for assessing the contribution of different sources to metal levels in the tunnel.

Using a CMB model, the investigators compared source profiles for total roadway emissions, as measured in tunnels, to profiles for the individual emissions sources (resuspended road dust, brake dust, tire dust, and tailpipe emissions from gasoline- and diesel-powered vehicles). Using these source profiles, and excluding results from light weekend traffic in summer in one tunnel, CMB modeling predicted 63% to 160% of the total PM mass in the tunnels. Measured emission rates and values calculated using CMB modeling added further support for the modeling results.

ICFA combines elements of confirmatory and exploratory factor analysis in a way that makes use of knowledge of some source profiles while generating updated profiles for sources that are less well defined. Results of this analysis indicated that the two organic source profiles were dominant contributors of ambient PM_{10} and that the road salt profile was a dominant contributor to ambient chloride. Not surprisingly, organic and elemental carbon dominated the results of the analysis; however, by removing these values from the model, the investigators were able to perform a source attribution for metals. They concluded that organic sources were major contributors for 14 species in ambient PM_{10}: organic carbon, elemental carbon, magnesium, aluminum, potassium, calcium, iron, vanadium, manganese, arsenic, strontium, cadmium, barium, and cerium. Road salt was found to be a major contributor of chloride and sodium.

The solubility tests used samples from ambient air and from tunnels in a synthetic lung fluid. The results indicated that many elements could be leached into the fluid. The investigators found eight transition metals (silver, titanium, iron, tungsten, copper, zinc, manganese, and cadmium) from tunnel samples, and eight (titanium, tungsten, copper, zinc, manganese, chromium, vanadium, and molybdenum) from ambient samples, in the leachate, with a high solubility observed for several elements.

SUMMARY AND CONCLUSIONS

This was a valuable study, performed by an investigator team with expertise in measuring trace levels of metals in environmental samples. The methods they used to approach the study problem were excellent, and the study generated solid information that could be important for a range of activities, including emissions inventories. The team took a multidisciplinary approach to the examination of metals from mobile sources (including vehicle sources besides the tailpipe), weaving together biology, chemistry, and source apportionment techniques. An important aim of this study, to measure exposure in people conducting activities near traffic, was not addressed, however, the results from the other aims are valuable individually, and even more valuable when examined together.

Although this study provides a large amount of useful information, several limitations should be noted before more general conclusions are drawn: (1) Care should be taken if extending the roadway emissions results from this study in these specific locations more broadly. (2) Similar care should be taken in extending the ambient air sampling and subsequent source apportionment results. (3) ICFA needs to be validated through replication in other studies, including studies in different environments and with different compositions of vehicles, and evaluated against other methods. (4) The data generated from this study should be considered exploratory in nature, providing new information for and insight into the application of techniques to studies of air pollution related to mobile sources.

The study provides useful data, especially with respect to exposure from all types of mobile sources (not just tailpipes). The study by Schauer and colleagues brings a novel approach, ICP-MS, to the characterization of metals in PM, which has been a problem because measurement of trace elements has heretofore been hindered by limits of detection. This technique lowers the detection limits significantly, making measurement of trace metals possible. The application of another new technique, ICFA, allows these measurements to be used in subsequent source apportionment. This research also involved using synthetic fluid to determine the fraction of metals that is soluble in a biological environment and thus may interact with cellular components. This study, with its multidisciplinary approach, provides important tools and presents a useful approach for gathering information about which metals (and sources of these metals) are linked with pathology of the respiratory systems in asthma and other diseases.

Library of Congress Catalog Number for the HEI Report Series: WA 754 R432.
The paper in this publication meets the minimum standard requirements of the ANSI Standard Z39.48-1984 (Permanence of Paper) effective with Report 21 in December 1988; and effective with Report 92 in 1999 the paper is recycled from at least 30% postconsumer waste with Reports 25, 26, 32, 51, 65 Parts IV, VIII, and IX, 91, 105, 117, and 128 excepted. These excepted Reports are printed on acid-free coated paper.

HEALTH EFFECTS INSTITUTE

CONTENTS

Research Report 133

Characterization of Metals Emitted from Motor Vehicles

James J Schauer, Glynis C Lough, Martin M Shafer, William F Christensen, Michael F Arndt, Jeffrey T DeMinter, and June-Soo Park

Environmental Chemistry and Technology Program and Wisconsin State Laboratory of Hygiene, University of Wisconsin, Madison, Wisconsin; and Department of Statistics, Brigham Young University, Provo, Utah

HEI STATEMENT

This Statement is a nontechnical summary of the Investigators' Report and the Health Review Committee's Commentary.

INVESTIGATORS' REPORT

When an HEI-funded study is completed, the investigators submit a final report. The Investigators' Report is first examined by three ouside technical reviewers and a biostatistician. The report and the reviewers' comments are then evaluated by members of the HEI Health Review Committee, who had no role in selecting or managing the project. During the review process, the investigators have an opportunity to exchange comments with the Review Committee and, if necessary, revise the report.

Continued

COMMENTARY HEALTH REVIEW COMMITTEE

The Commentary about the Investigators' Report is prepared by the HEI Health Review Committee and staff. Its purpose is to place the study into a broader scientific context, to point out its strengths and limitations, and to discuss remaining uncertainties and implications of the findings for public health.

RELATED HEI PUBLICATIONS

Publishing history: This document was posted as a preprint on *www.healtheffects.org* and then finalized for print.

Citation for whole document:

Schauer JJ, Lough GC, Shafer MM, Christensen WF, Arndt MF, DeMinter JT, Park J-S. March 2006. Characterization of Metals Emitted from Motor Vehicles. Research Report 133. Health Effects Institute, Boston MA

When specifying a section of this report, cite it as a chapter of the whole document.

INVESTIGATORS' REPORT

Characterization of Metals Emitted from Motor Vehicles

James J Schauer, Glynis C Lough, Martin M Shafer, William F Christensen, Michael F Arndt, Jeffrey T DeMinter, and June-Soo Park

ABSTRACT

A systematic approach was used to quantify the metals present in particulate matter emissions associated with on-road motor vehicles. Consistent sampling and chemical analysis techniques were used to determine the chemical composition of particulate matter less than 10 µm in aerodynamic diameter (PM_{10}*) and particulate matter less than 2.5 µm in aerodynamic diameter ($PM_{2.5}$), including analysis of trace metals by inductively coupled plasma mass spectrometry (ICP-MS). Four sources of metals were analyzed in emissions associated with motor vehicles: tailpipe emissions from gasoline- and diesel-powered vehicles, brake wear, tire wear, and resuspended road dust. Profiles for these sources were used in a chemical mass balance (CMB) model to quantify their relative contributions to the metal emissions measured in roadway tunnel tests in Milwaukee, Wisconsin.

Roadway tunnel measurements were supplemented by parallel measurements of atmospheric particulate matter and associated metals at three urban locations: Milwaukee and Waukesha, Wisconsin, and Denver, Colorado. Ambient aerosol samples were collected every sixth day for one year and analyzed by the same chemical analysis techniques used for the source samples. The two Wisconsin sites were studied to assess the spatial differences, within one urban airshed, of trace metals present in atmospheric particulate matter. The measurements were evaluated to help understand source and seasonal trends in atmospheric concentrations of trace metals.

ICP-MS methods have not been widely used in analyses of ambient aerosols for metals despite demonstrated advantages over traditional techniques. In a preliminary study, ICP-MS techniques were used to assess the leachability of trace metals present in atmospheric particulate matter samples and motor vehicle source samples in a synthetic lung fluid.

INTRODUCTION

Motor vehicles are known to be a major source of particulate matter and are thought to contribute to the presence of some metals in urban air. Exposure to inhalable $PM_{2.5}$ and PM_{10} emissions from roadways has been implicated in adverse human health effects and linked to increased risk of respiratory illnesses (Tsai et al 2000; Lin et al 2002). Because health effects have also been associated with metals (Gavotte and Koren 2001; Aust et al 2002; Claiborn et al 2002), better characterization of the metal emissions from motor vehicles is needed. Exposure to particulate matter from roadways implies simultaneous exposure to PM_{10} and $PM_{2.5}$ emissions from tailpipes, brake wear, tire wear, and road dust. The relative contributions of these sources to total concentrations of metals in roadway emissions are not well understood. Correspondingly, patterns of human exposure to metals from these sources and the related possibility of public health effects are not known.

Improved information about the elemental composition of emissions from on-road motor vehicles will be important to health effects studies and efforts to model source contributions. Although many elements are present at only trace levels in roadway emissions from motor vehicles, these contributions may constitute a large fraction of the elements' total atmospheric concentrations. Therefore, roadway emissions may dominate human exposures to many elements, particularly in some urban environments. To understand these relations, in this study we used a systematic approach to integrate measurements of roadway

* A list of abbreviations and other terms appears at the end of the Investigators' Report.

This Investigators' Report is one part of Health Effects Institute Research Report 133, which also includes a Commentary by the Health Review Committee and an HEI Statement about the research project. Correspondence concerning the Investigators' Report may be addressed to Dr James J Schauer, Environmental Chemistry and Technology Program, University of Wisconsin, 660 N Park St, Madison WI 53706, *jjschauer@wisc.edu*.

Although this document was produced with partial funding by the United States Environmental Protection Agency under Assistance Award R82811201 to the Health Effects Institute, it has not been subjected to the Agency's peer and administrative review and therefore may not necessarily reflect the views of the Agency, and no official endorsement by it should be inferred. The contents of this document also have not been reviewed by private party institutions, including those that support the Health Effects Institute; therefore, it may not reflect the views or policies of these parties, and no endorsement by them should be inferred.

emissions of particulate matter, emissions from specific roadway sources, and ambient concentrations of metals. Additionally, this study explored the leachability, in a synthetic lung fluid, of metals in particulate matter, a measure that is indicative of biological availability and possible health effects of particles deposited in human lungs.

Many metals emitted from motor vehicles and present in atmospheric particulate matter have not been sufficiently studied to assess their possible effects on human health, largely because the low levels of trace elements in most ambient particulate matter samples have not been routinely quantified. Methods for analyzing particulate matter that utilize ICP-MS enable reliable measurement of trace amounts of a wide range of elements. With ICP-MS techniques, more than 30 elements present at levels less than 1 ng/m^3 are routinely detected in typical low-volume (6–10 L/min), 24-hour, ambient particulate matter samples. In this study, particulate matter samplers and sample handling techniques were designed to minimize metal contamination and enable quantification of ultratrace metal levels.

A variety of previous studies have investigated motor vehicle emissions and ambient particulate matter; however, analysis of the results is complicated by the range of methods applied within the studies. Therefore, an important factor in the design of the present study was the application of parallel methods for collection and analysis of samples in every facet of the study, allowing direct comparison of all results.

EMISSIONS MEASUREMENTS

Vehicle tunnels can be used to measure total roadway emissions of particulate matter from in-use fleets (El-Fadel and Hashisho 2001), which are generally much higher than expected on the basis of dynamometer tests of tailpipe emissions. Given this disparity, tunnel emission results should not be directly compared with dynamometer results. Tunnel emission measurements are higher because they include a mixture of emissions from tailpipes (Sagebiel et al 1997; Cadle et al 1999), brake and tire debris (Hildemann et al 1991; Garg et al 2000), and road dust resuspended by passing vehicles (Nicholson et al 1989; Rogge et al 1993; Jaecker-Voirol and Pelt 2000; Sternbeck et al 2002). The overall composition and metal content of particulate matter emitted by motor vehicle traffic depends on inputs from these specific sources, each of which has a distinct elemental composition and a signature profile of trace metals. Therefore, efforts to assess the effects of roadway emissions on metal levels in the atmosphere and their possible health effects must consider the relative contributions of these sources.

Tunnel tests were conducted to characterize roadway particulate matter and metal emissions from a mixed, on-road fleet and to investigate contributions of specific roadway sources to metal emissions. Previous studies of in-use vehicle emissions have primarily focused on gaseous, semivolatile, and particulate organic compounds (Hildemann et al 1991; Zielinska et al 1996; Fraser et al 1999; Schauer et al 1999), with minimal emphasis on characterization of trace metals. Several studies have reported elemental emission rates for tailpipe exhaust of vehicles on dynamometers (Watson et al 1994; Cadle et al 1997, 1999; Schauer et al 1999; Kleeman et al 2000); others have reported concentrations near roadways (Wrobel et al 2000).

Gillies and colleagues (2001) reported PM_{10} and $PM_{2.5}$ emission rates for 40 elements, measured by x-ray fluorescence spectrometry (XRF), in the Sepulveda Tunnel; however, the analytic techniques employed yielded significant emission rates for only five elements in each size fraction. Gertler and coworkers (2002) reported roadway tunnel emission rates for light-duty and heavy-duty vehicles. That study used particle-induced x-ray emission (PIXE) and XRF to quantify emission rates of 20 elements in $PM_{2.5}$ but measured significant emission rates for only 6. Allen and associates (2001) used instrumental neutron activation analysis to quantify fine and coarse emissions of 36 elements from light-duty and heavy-duty fleets in the Caldecott Tunnel, but only 13 elements were found in significant amounts in any sample. Pierson and Brachaczek (1983) reported the most comprehensive analysis of metals emitted from motor vehicle roadways, but they presented results for total suspended particles only, and the study was conducted more than 20 years ago.

In the present study, both ICP-MS and XRF were used for metal analysis to ensure low detection limits for a wide range of elements. Combination of the two techniques allowed quantification of a total of 42 elements, 32 of which were emitted in significant amounts in individual tests. XRF, widely used in the past for analysis of metals in atmospheric particulate matter samples, is well suited to analysis of light elements. New methods involving ICP-MS have strengths in quantification of ultralow levels of heavier trace elements. These two methods are not equivalent and are used to achieve different objectives.

The aim of ICP-MS use in the present study was the detection of low levels of trace elements in order to determine the contributions of different roadway sources to emissions of metals from motor vehicle traffic. To that end, tests were planned for two tunnels in Milwaukee under a variety of conditions, including winter and summer weather, weekend and weekday traffic, and the presence of fleets with higher and lower proportions of trucks. These

conditions were chosen not to represent the average fleet in the urban area but to use the differences between seasonal conditions and fleet conditions to investigate the specific sources of metals emitted from motor vehicles. Multiple tests were conducted in the two tunnels with different fleet characteristics to elucidate the effects of traffic volume and heavy-duty vehicle fraction. Variation between emissions from a weekday rush-hour fleet and a weekend fleet was explored in one tunnel. Emissions in this tunnel were also measured in both summer (nominally 25°C) and winter (nominally 0°C) to examine seasonal differences in emissions.

These tunnel tests were conducted to allow investigation of the relative effects of specific roadway sources of metals, including tailpipe emissions, brake wear, tire wear, and resuspended road dust. Contributions of these sources under typical roadway conditions are not well understood. Therefore, in the present study methods were designed to help provide a basis for understanding the effects of these sources and the potential for control strategies to reduce motor vehicle emissions of trace metals. These methods included obtaining samples of each specific roadway source of metals that were directly comparable to the total roadway emissions in the tunnels. They also included developing compositional profiles to allow source apportionment of total roadway emissions.

SOURCE CHARACTERIZATION

Composition of brake wear dust and resuspended road dust differs from region to region with differences in vehicles and equipment, driving patterns, climate, geology, and other factors. Source samples were collected and analyzed by methods parallel to those for measurement of total roadway emissions to ensure the relevancy of the source profiles to the tunnel emissions. To apportion the total emissions of trace metals from an on-road fleet of vehicles sampled in the tunnel tests in Milwaukee, road dust from the tunnels and brake wear and tire wear dust from Wisconsin vehicles were used to construct source profiles.

Although brake and tire wear contribute only one fraction of total roadway particulate matter emissions, brake wear has been suggested as a major contributor to levels of some trace metals detected in motor vehicle emissions and in the urban atmosphere (Davis et al 2001; Sternbeck et al 2002; Pakkanen et al 2003). However, measurement of brake and tire wear emissions is complicated by the proximity of many other motor vehicle emission sources, including tailpipe exhaust and resuspended road dust. Tunnel tests measure emissions of a large fleet under real-world driving conditions, but the measurements include the entire roadway mixture of sources. Although brake dynamometers have been used to measure emissions from brake pads, they require specialized equipment that is not widely accessible. Additionally, any set of dynamometer test conditions can only approximate the variable conditions of on-road driving. Because of the difficulties of obtaining a reasonable number of representative brake and tire wear emission samples, a method for estimating emissions composition was developed from a survey of commercial and proprietary brake pads and tires in a geographic area.

Average compositional profiles for brake and tire wear emissions were combined with profiles for tailpipe emissions and resuspended road dust to apportion particulate matter from measured total roadway motor vehicle emissions and ambient aerosol samples. Relative compositions of sources are used in CMB models to apportion source contributions to total particulate matter levels (Watson et al 1994; Schauer et al 1996). Therefore, only representative chemical compositions for brake and tire wear emissions are required, not actual on-road emission rates. Because the bulk material compositions of brake pads and tires are easy to measure, determining the relation between the bulk composition and the chemical composition of emissions is a simple way to attain representative profiles.

To identify the relation between bulk compositions of and emissions from brakes and tires, chassis dynamometer tests were completed in a specialized chamber for a small number of vehicles. Separately, samples of brake dust and tire dust from those vehicles were resuspended for size-resolved particulate matter sampling and chemical characterization. Synthesis of the dynamometer data and resuspension test data provided insight into the relation between the chemical composition of brakes and tires and the composition of particulate matter emissions from wearing of brakes and tires. Using this information, samples of brake pads and tires were collected from a larger, random fleet of vehicles and assessed the composition of actual brake and tire wear emissions.

Although measurements of wear emissions from vehicles run on the chassis dynamometer are reasonable estimates of emission compositions in actual driving conditions, several factors confound extrapolation to roadway emissions. First, only one axle—the two driving wheels of the vehicle—does the work, and only one set of brakes is used. During actual driving, therefore, emissions could be greater (from four rather than two wheels) or wear could be diminished when friction from starting and stopping the vehicle is distributed among all four tires and brake pads. Second, the tires roll on a stainless-steel cylinder, which is smoother than most road surfaces. The roller may also be

subject to more rapid temperature fluctuations than road surfaces are. However, considering the variety of surfaces that an average urban vehicle crosses (such as gravel, concrete, fresh pavement, and ice and snow), conditions on the smooth roller can be considered a well-defined, but not necessarily typical, driving surface. Third, the effects of airflow past the test vehicle and past a moving vehicle are not the same. Fans are directed at the stationary vehicle as it is run on the dynamometer, but differences in airflow could alter surface temperatures and liberation of wear products (Sanders et al 2002). For these reasons, emission rates are not necessarily applicable to actual conditions, but relative chemical composition of the emissions is of interest for source apportionment of total roadway emissions. In these tests, we compared the relative composition of measured emissions and the actual bulk composition of the brake pads and tires used. The results were used to develop compositional profiles for brake and tire wear.

Road dust, enriched by deposition of roadway and urban pollutants, becomes a source of metals in atmospheric particulate matter when it is resuspended by vehicle traffic (Sternbeck et al 2002; Pakkanen et al 2003). The content of trace metals (such as Pt, Cu, and Ba) in road dust has been studied as an indicator of the effect of motor vehicles in some locations (Petrucci et al 2000; Rauch et al 2000; Davis et al 2001). Brake wear is considered an important source of the trace metals in road dust, and it also emits particulate matter directly into the atmosphere (Garg et al 2000; Sanders et al 2002). Tire wear has also been investigated for its contribution to road dust and to urban atmospheric particulate matter, but it has been considered primarily a source of organic compounds (Hildemann et al 1991; Reddy and Quinn 1997; Kumata et al 2002).

In addition to brake wear, tire wear, and resuspension of road dust, motor vehicle tailpipe emissions are widely recognized as an important source of particulate matter in the urban atmosphere. Emission tests of vehicles driven on dynamometers have been widely conducted to characterize tailpipe emissions under specific, defined operational conditions. A dilution chamber is used to cool the exhaust before sampling so that emissions condense into the particle phase as they do in the atmosphere.

Alternatively, numerous studies have measured emissions from motor vehicles in roadway tunnels, which allows study of the mixture of specific roadway source contributions that comprise motor vehicle emissions. Tunnel tests are used to determine the total roadway emissions from real-world motor vehicles, whereas dynamometer tests are used to characterize tailpipe exhaust under controlled conditions. Most studies that have measured particulate matter emissions from gasoline and diesel vehicles have focused on organic compounds. Although a number of studies have investigated emissions of metals, traditional analytic techniques have allowed few metals to be accurately quantified.

Specific sources of particulate matter from motor vehicle tailpipe emissions in tunnels include combusted fuel and lubricating oil. Apportioning the tunnel roadway emissions that are due to tailpipe emissions requires applying equivalent sample collection methods and identical analytic methods. To that end, tailpipe emissions of gasoline and diesel vehicles were characterized through dynamometer tests. Samples were collected and analyzed parallel to total roadway emissions measured in tunnels with a focus on fully describing the sources of trace metals in total roadway emissions.

APPLICATION OF CMB MODEL

The contributions of brake wear, tire wear, resuspended road dust, and tailpipe emissions to total roadway emissions of metals were determined using a CMB model, which requires only well-defined, representative chemical compositions of each source, rather than actual on-road emission rates. The use of parallel sample collection and analysis methods in all sections of this study allowed application of a CMB model. This use of analogous data for determining compositions of sources and total roadway emissions is important to avoid bias in the mass balance calculations. Metal composition profiles for brake wear, tire wear, resuspended road dust, gasoline tailpipe, and diesel tailpipe emissions developed in this study were used for source apportionment of metal emissions in different types of roadway tunnel tests.

The model used in the present study was designed and configured to best apportion emissions of metals from motor vehicles, not to optimize the apportionment of particle mass. Although, from a statistical perspective, a CMB model optimized to apportion mass emissions would be the same as one optimized for metal emissions, several subtle factors associated with the construction of source profiles greatly affects CMB model operation.

First, the methods used to construct average source profiles affect the relative variability of the profile elements. For example, emissions of particle-phase organic tracers (molecular markers) that have been used in CMB models are significantly less variable when normalized to organic carbon (OC) emissions than when normalized to particle mass emissions. Therefore, CMB models that seek to optimize the apportionment of carbonaceous particulate emissions should be constructed to apportion organic aerosol emissions, which can then be converted to particle mass source contributions.

Second, the effective variance solution used in most CMB models assumes that members of the source profile are independent, which is not rigorously true. For example, CMB models that include many tracers for crustal materials tend to overestimate the apportionment of crustal-dominated sources, which tends to improve the fit for crustal elements at the expense of noncrustal species and sources. Although this bias is common to many CMB calculations, the modeling focus in this study avoided it by using similar numbers of species for all sources in the mass balance.

The ultimate goal of the tunnel CMB calculations was to determine the sources of metal emissions associated with motor vehicle traffic. Thus, organic tracers were not used in the model in order to avoid apportionment of the organic fraction of the particulate matter at the expense of metal emissions.

AMBIENT METAL CONCENTRATIONS

Another major focus of the present study was investigation of the spatial distributions of metals in the urban atmosphere and their relations to motor vehicle roadway emissions. The effects of motor vehicles on ambient concentrations of metals are of interest because epidemiologic studies reported in the past decade have demonstrated that human mortality and morbidity are associated with increased levels of atmospheric particulate matter concentrations (US Environmental Protection Agency [EPA] 2002).

Most epidemiologic studies of particulate matter exposure have used data from a centralized air quality monitoring site to represent the exposure of the study cohort. However, the health effects and exposure assessment communities have recognized that these data do not represent the actual exposure of the cohort (US National Research Council 1998). To better characterize actual exposure, a number of studies have quantified the relations between ambient concentrations of particulate matter at centralized monitoring sites, indoor particle concentrations, and personal exposures to particulate matter (Evans et al 2000; Williams et al 2000; Gauvin et al 2002; Adgate et al 2003; Liu et al 2003). Studies such as that of Goswami and colleagues (2002) have demonstrated that the spatial distribution of airborne particle mass is moderately uniform across an urban area. This finding provides a basis for developing exposure models that reference centralized urban monitoring sites.

Most of these epidemiologic and exposure studies have, however, focused on exposure to atmospheric particulate mass and a few constituent species such as SO_4^{2-}, OC, and elemental carbon (EC). In the absence of information about spatial variation for trace metals and other toxic components of particulate matter, many in the health effects community have assumed that all airborne pollutants are equally homogenous across an urban airshed. As efforts proceed to elucidate and mitigate the effects of exposure to atmospheric particulate matter, health researchers and regulators need accurate information about how exposure patterns differ among groups of pollutants.

Metals in atmospheric particulate matter have been linked to the observed associations between increased levels of fine particulate matter and health effects (Laden et al 2000; Aust et al 2002). However, the low levels of trace elements in most ambient particulate matter samples have not in the past been routinely quantifiable. Current methods employing ICP-MS to analyze atmospheric particulate matter samples enable reliable measurement of trace amounts over a wide range of elements.

In this study, sample collection and handling were specifically designed to minimize metals contamination and enable quantification of ultratrace levels of metals, and detailed metals data were combined with bulk chemical data. To obtain a large set of samples in which to quantify metal concentrations, particulate matter was collected every sixth day for a full year. Simultaneous collection in three US locations allowed comparison of the metal content of aerosols in different areas and seasons. The Milwaukee and Waukesha sampling sites in Wisconsin are 20 km (about 12 miles) apart. These sites were chosen to investigate trends in metals concentrations in ambient particulate matter across an urban airshed. The third site, in Denver, Colorado, was selected because of the trends observed in data from the Northern Front Range Air Quality Study (NFRAQS; Watson et al 1998). These data have indicated that particle emissions from gasoline engines are a major contributor to atmospheric fine particulate matter in the area.

ITERATED CONFIRMATORY FACTOR ANALYSIS

Goals of the ambient monitoring included quantification of ambient metal concentrations and determination of the effects of measured motor vehicle emissions on the urban atmosphere. To observe ambient concentrations only in areas heavily affected by motor vehicles would overestimate traffic contributions. Therefore, the three ambient sampling sites chosen differed in traffic volume and roadway proximity. To further investigate the contributions of motor vehicle roadway emissions to ambient concentrations of metals, statistical analysis was undertaken for source apportionment. Several approaches to pollution source apportionment have been reported, each of which requires a different degree of knowledge about potential sources. When little or nothing is known about the nature of the pollution sources, exploratory factor analysis models have been used (Thurston and Spengler 1985; Koutrakis

and Spengler 1987; Henry et al 1994). Other techniques include confirmatory factor analysis models (Yang 1994; Gleser 1997; Christensen and Sain 2002), Bayesian analysis (Park et al 2001, 2002), and measurement-error modeling (Watson et al 1984; Christensen and Gunst 2004). In recent years, interest has increased in more flexible approaches that assume some knowledge of pollution source profiles, such as UNMIX (outlined in Henry 1997) and positive matrix factorization (PMF; Paatero and Tapper 1994). Neither these nor any other purely exploratory approach can guarantee a uniquely identified solution, however, without additional constraints on the source profiles.

The current study aimed to determine the contributions of roadway emissions to ambient metal concentrations, without parallel measurements of other major sources in the Milwaukee area. The approach applied, iterated confirmatory factor analysis (ICFA), utilizes both the factor analysis structure and a priori information when estimating source profiles. ICFA can take on aspects of both exploratory factor analysis and confirmatory factor analysis, by assigning varying degrees of constraint to each element of the source profiles during the estimation process. Therefore, the source profiles for emissions of metals from roadways can be constrained to be similar to the actual, measured roadway emissions. Profiles that are not as well defined are less constrained and are updated by the model. This approach attempts to maximally utilize source profile information to reduce indeterminacy and enhance interpretability in a multivariate receptor model. Like other factor analysis methods, ICFA is not flawless, but it provides unique insights into source apportionment and promises value as it is developed as a new approach.

SYNTHETIC LUNG FLUID EXTRACTIONS

The final focus of this study was furthering the understanding of the potential health effects of metals in particulate matter deposited in the lungs. The processes and mechanisms through which pollutant compounds exert toxicity vary considerably as a function of endpoint, but a soluble, uncomplexed species is generally accepted as the toxicologically relevant component within a biological system (Prieditis and Adamson 2002; Zelikoff et al 2002). Mineralogic characteristics, particle size, oxidation state, organic complexation, and specific chemical associations all influence the lability and biological availability of an aerosol's elemental components. Therefore, the bulk total elemental analysis of an aerosol sample provides only an crude estimate of potential biological effects. To better characterize the chemical and biological behavior of aerosols within human systems, the mechanisms through which specific aerosol components interact with relevant biological tissues and fluids must be assessed. A mounting set of direct and indirect evidence implicates many trace elements (eg, Ag, As, Cd, Cr, Fe, and Ni) in observable health effects (Sun et al 2001; Aust et al 2002; Molinelli et al 2002; Oller 2002; Wise et al 2002).

One critical toxicologic pathway is the dissolution of aerosol particulate matter in fluids associated with the human respiratory system (Knaapen et al 2002; Kodavanti et al 2002). Although published studies have addressed the dissolution of fibers and other well-defined laboratory aerosols, information about the solubility of actual environmental aerosols, and in particular their trace element components, is limited. A major roadblock to acquiring this type of information has been the lack of instrumentation and methods with sensitivity and accuracy sufficient to measure trace components in samples of atmospheric aerosols and complex biological fluids. Recent advances in ICP-MS techniques and associated clean chemistry now enable researchers to acquire this critical information. For example, a large suite of elements are now quantifiable at levels in the range of a few picograms per milliliter of fluid. The fluid sample matrix of ICP-MS makes it ideal for such leaching studies.

The alveoli and surfaces of the lung are bathed in a pH-buffered fluid containing inorganic salts, proteins, and organic surfactants. Dissolution of particulate matter in this fluid is a marker of potential bioavailability and cell damage from particles deposited in the lungs. Species that are solubilized quickly are expected to have greater potential for acute effects through several pathways, including changing the composition and function of the lung surfactant system.

In this study, a synthetic lung fluid that incorporates physiologically relevant inorganic salts was used. It was modeled after the Gamble solution, a physiologic saline widely used as such a surrogate. Of the major factors influencing dissolution and solubility of trace elements in human lung fluid, this synthetic solution should closely mimic actual fluid in terms of pH, ionic strength, and major interactions of specific ions. Although this leaching method is similar to other chemical analysis methods, the sole focus was to compare metals leached by a biologically relevant fluid with total metals in the sample. Leaching experiments were not used to investigate sources or behavior of metals from different sources in ambient particulate matter.

The current work with synthetic lung fluid was exploratory in the sense that it sought only to develop an understanding of the solubility of metals in ambient particulate matter, an indicator of their potential biological activity.

This somewhat preliminary work was not able to address every part of the puzzle posed by the relations of human health effects and ambient metal concentrations. For example, dissolution of particles in lung fluid is not the only mechanism through which particulate matter can become more biologically available or cause cell damage; it may not even be the dominant mechanism. Interactions of other species present in particulate matter may attenuate or exacerbate the effects of metals, as may those organic components of lung fluid that were excluded from the synthetic fluid. Dissolution of particulate matter collected on filters may differ considerably from that of individual inhaled particles.

PM_{10} was used in the leaching experiments to ensure adequate mass loadings, but smaller particles penetrate more deeply into the lungs. Like particle size, physiologic factors may dominate the dose and response of metals deposited in the human lung. Nonetheless, this present work allowed investigation of the variation in solubility of individual metals in particulate matter samples. Such variation indicates differences in chemical and physical properties and is therefore clearly related to the fate of particulate matter in the lungs.

SUMMARY

This report presents results of a systematic study that investigated the sources of metals that contribute to total emissions of metals from motor vehicles, as well as the effect of these emissions on atmospheric particulate matter. The methods used were source sampling, source apportionment modeling of motor vehicle roadway emissions, ambient sampling, analysis of atmospheric samples, and an exploratory study of the leachability, in a synthetic lung fluid, of trace metals in particulate matter samples. The results of this study are intended to help regulators, health effects scientists, and vehicle manufacturers understand the effects of emissions of trace metals from motor vehicles.

METHODS

SOURCE SAMPLING

Tunnel Tests

Particulate matter emission rates were measured in two tunnels in Milwaukee. One, referred to as the *Kilborn Tunnel*, is an entrance ramp for Interstate 43, a major highway downtown. In this tunnel, traffic merges from two lanes to one lane and then accelerates through an approximately 45° curve and up a 1% upgrade onto the interstate. Vehicles brake in the tunnel while merging and are forced to turn slightly while accelerating. Vehicle speeds recorded at the tunnel entrance and exit averaged 51 and 62 kph (32 and 39 mph), respectively, during the tests. The tunnel was periodically swept, so dirt on the roadway was minimal. The tunnel also has a forced exhaust outlet in the middle for ventilation.

Sampled were collected only from the first half of the tunnel, between the vehicle entrance and the forced exhaust outlet. Samplers were located several feet from the wall, on the sidewalk next to the tunnel roadway. Figure 1 diagrams the experimental layouts in both test tunnels. Upwind samplers were placed 5 m (about 16 ft) inside the Kilborn Tunnel entrance; exit samplers were placed 15 m (about 49 ft) upwind of the forced exhaust outlet. The samplers were 200 m (about 656 ft) apart. Five 4-hour tests were conducted during summer weekday rush hours in the Kilborn Tunnel (tests A–E, Table 1). Each test involved 700 vehicles per hour on average, approximately 2.2% of which were heavy-duty trucks.

The other tunnel, referred to as the *Howell Tunnel*, is on Howell Avenue and is very similar to the Van Nuys Tunnel in California, where several previous tunnel tests have been conducted (Fraser et al 1998; El-Fadel and Hashisho 2001). This tunnel has two completely separate three-lane bores, for northbound and southbound traffic. We sampled from the southbound bore (Figure 1). The tunnel has no grade, no curve, and no mechanical ventilation. Traffic cruises in the tunnel with little braking; average vehicle speeds at the entrance and exit during the tests were around 50 kph (31 mph). The Howell Tunnel was not swept, and dirt was noticeable on the roadway and roadside.

As in the Kilborn Tunnel, samplers were located on the sidewalk inside the Howell Tunnel, 5 m (about 16 ft)

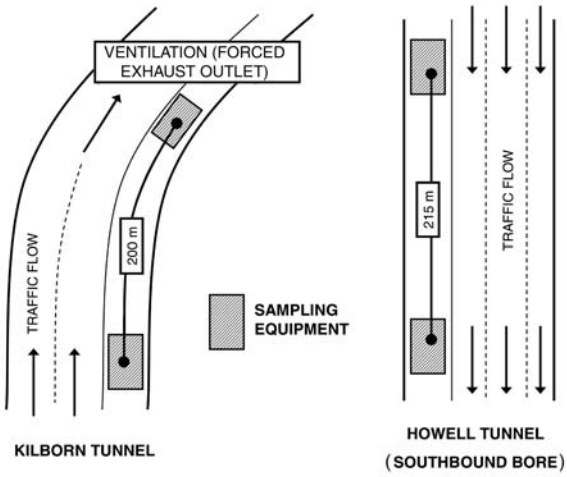

Figure 1. Experimental layout in Kilborn and Howell Tunnels.

Table 1. Tunnel Studies Conducted in Milwaukee, Wisconsin[a]

Test	Tunnel	Date	Day	Hours of Sampling	Total Number of Vehicles	Number (%) of Trucks	SF_6 Release
Summer							
A	Kilborn	07/31/2000	Mon	4	2310	37 (1.6)	No
B	Kilborn	08/03/2000	Thurs	4	2792	70 (2.5)	No
C	Kilborn	08/08/2000	Tues	4	3665	62 (1.7)	Yes
D	Kilborn	08/09/2000	Wed	4	2403	55 (2.3)	Yes
E	Kilborn	08/10/2000	Thurs	4	2364	71 (3.0)	No
F	Howell	08/23/2000	Wed	4	4486	274 (6.1)	Yes
G	Howell	08/27/2000	Sun	4	2336	35 (1.5)	Yes
H	Howell	08/27/2000	Sun	4	2621	63 (2.4)	No
I	Howell	08/28/2000	Mon	4	3112	293 (9.4)	No
J	Howell	08/28/2000	Mon	4	4822	313 (6.5)	No
Winter							
K	Howell	12/13/2000	Wed	7[b]	6720	470 (7.0)	Yes
L	Howell	12/14/2000	Thurs	8	7579	546 (7.2)	No
M	Howell	01/10/2001	Wed	8	7062	544 (7.7)	No
N	Howell	01/11/2001	Thurs	8	7860	605 (7.7)	Yes
O	Howell	01/16/2001	Tues	8	7964	573 (7.2)	Yes
P	Howell	01/17/2001	Wed	8	7977	526 (6.6)	No

[a] One of six summer tests in each tunnel was determined to be invalid. Those results are not included here.

[b] Test K sampling was cut short.

inside the tunnel entrance and 15 m (about 49 ft) upwind of the tunnel exit, 215 m (about 705 ft) apart. We conducted three 4-hour tests during summer weekday rush hours (tests F, I, and J), two 4-hour summer weekend tests (tests G and H), and six or 8-hour winter weekday tests (tests K–P; Table 1). Weekday tests in the Howell Tunnel (summer and winter) involved approximately 1000 vehicles per hour, 7.2% of which were heavy-duty trucks; summer weekend tests involved approximately 600 vehicles per hour, 2.0% of which were heavy-duty trucks. (One summer test in each tunnel was determined to be invalid because of equipment problems; those results are not included in Table 1 or elsewhere in this report.)

Vehicles were counted and classified using two sets of video recordings of passing vehicles. One set showed vehicle license plates, which provided vehicle registration data used to determine vehicle ages. The other set allowed classification of vehicle types and actual heavy-duty and light-duty vehicle counts. In addition, the Wisconsin Department of Transportation provided loop counts (rubber strips laid across the roadway to count vehicles), which were used to corroborate basic vehicle counts and were available only in the summer.

Particulate matter was collected with samplers built at the University of Wisconsin–Madison. As shown in Figure 2, the sampler separates particle sizes with a PM_{10} inlet (URG Corp, Chapel Hill NC) and Air and Industrial Hygiene Laboratory (AIHL) $PM_{2.5}$ cyclone separators (Thermo-Andersen Instruments). Particles of both size fractions were collected on multiple collocated filters for mass and chemical analyses. Each sampler had five PM_{10} filters and six $PM_{2.5}$ filters. Flow rates through PM_{10} filters were 6.4 L/min; through $PM_{2.5}$ filters, 8.0 L/min. Flow rates were calibrated in the laboratory and rechecked in the field before and after each test.

During winter tests O and P, 11-stage micro-orifice uniform deposit impactors (MOUDIs, MSP Corp, Shoreview MN) were operated alongside the Howell Tunnel entrance and exit samplers to investigate the size distribution of emissions in the tunnel. One set of MOUDI substrates was used over two consecutive tests to obtain sufficient mass for analysis on each stage.

Volumetric flow rates of air through the tunnels were calculated using inert sulfur hexafluoride (SF_6) gas as a tracer, together with measurements of wind speed at the entrances and exits of the tunnels (Pierson et al 1996; Rogak et al 1998). In some tests (Table 1), small known amounts of inert SF_6 (1.5 to 3.0 g/min) were released downwind of the tunnel entrance samplers at a constant flow rate over the entire test period. Stainless-steel canisters with passivated

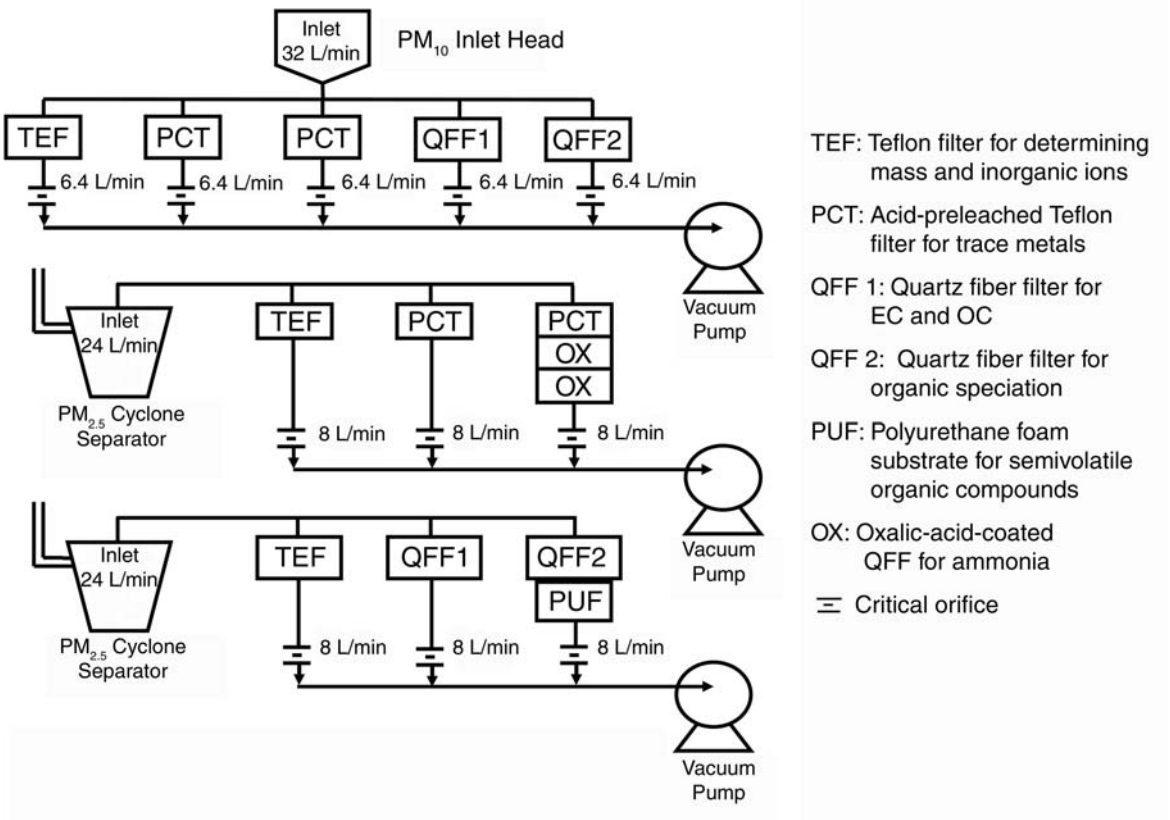

Figure 2. Particulate matter sampler.

internal surfaces (SUMMA cans), positioned near the aerosol samplers at the tunnel entrance and exit, were filled slowly at a constant flow rate over the course of the tests. Concentrations of SF_6 in the SUMMA cans were measured by using gas chromatography–electron capture detection.

From the increase in SF_6 concentration at the tunnel exit and air velocity measurements, an empirical relation was determined between volumetric flow rate through the tunnel and air velocity. This factor was then applied to air velocities measured in all tests to determine specific volumetric dilution rates. Uncertainties associated with these measurements were dominated by the ability to accurately measure air velocities and SF_6 release rates, as SF_6 can be accurately measured by using gas chromatography–electron capture detection.

Through comparison of SF_6 results and airflow measurements, the total effect of these uncertainties on tunnel air dilution rate measurements was estimated to be 5% in tests with SF_6 release. On the basis of variation in the measured factors for airflow, uncertainty of airflow measurements in tests with no SF_6 release was determined to be approximately 15%. Dilution rates were combined with vehicle counts and carbon monoxide and carbon dioxide measurements, also made with the SUMMA cans, to calculate average vehicle-miles traveled per gallon of fuel consumed in the tunnels. Average fleet fuel mileage was determined to be in the range of 20 to 30 mi/gal (8.5 to 13 km/L).

In addition to SF_6 release to determine tunnel ventilation rates, one test in the Kilborn Tunnel was performed to check for back-mixing across the central forced exhaust outlet. SUMMA cans were placed with the aerosol samplers as usual, but SF_6 was released 50 feet (15.2 m) beyond the exhaust outlet, in the second half of the tunnel. No SF_6 was detected in these test canisters; thus back-mixing of air and emissions from the second half of the tunnel to the tested tunnel section was found to be negligible.

Increases in concentrations ($\mu g/m^3$) of particulate matter and chemical species between the tunnel entrance and exit samplers were converted to emission rates. Total increase in concentration was multiplied by the calculated tunnel dilution rate (m^3/hr) and divided by the number of vehicles that passed through the tunnel during the sampling period and the distance between samplers to obtain an emission rate on a per-kilometer basis (mg/km per vehicle). These calculations are parallel to those performed in other tunnel studies (Pierson et al 1996). Analytic and measurement uncertainties, which incorporate the uncertainty of repeated field

blank measurements, were propagated through the calculation of emission rates for individual species as the square root of the sum of the squared uncertainties. Emission rates for individual species in tests of the same type (summer weekday Kilborn, summer weekday Howell, summer weekend Howell, and winter weekday Howell) were averaged. The uncertainty associated with each average is presented as the standard error of the averaged measurements, which is equal to the standard deviation of the n individual measurements, divided by the square root of n.

Brake and Tire Wear Tests

To sample actual emissions from brake and tire wear, a specialized dynamometer was used at the California Air Resources Board Haagen-Smit Laboratory (El Monte CA). This facility has a chassis dynamometer in running-loss sealed housing for evaporative determinations (RL-SHED, model 60000-DRL1, 1995, Webber Engineering and Manufacturing, Ontario CA), illustrated in Figure 3. A 48-inch-diameter, single-roll cylindrical electric dynamometer (model DCE48MDV, 1995, Clayton Industries, El Monte CA) is installed in the floor of a stainless-steel chamber. The chamber is the size of a single-car garage, approximately $3 \times 4 \times 10$ m (about $10 \times 13 \times 33$ ft). It has a door for vehicle entry and a door for people entry. The chamber can be completely sealed by inflating small bladders on the perimeters of both doors. Two large fans in the wall circulate air away from and back into the chamber, while keeping it separate from external air. A third fan blows directly on the engine to cool it, as the car is stationary. Temperature in the sealed chamber can be controlled: the roof can be raised and lowered to allow expansion and contraction with temperature changes. In the tests for this study, temperature was held constant at 75°F (23.9°C), maintaining a total chamber volume of 130 m^3 (about 4591 ft^3) including the fan system.

Inside the sealed chamber, the front, driving wheels of the vehicle were centered on the dynamometer, and the rear wheels were clamped to the floor with bolted-down blocks and straps. The air inlet of the vehicle was disconnected upstream of the air filter so that ambient air from outside the chamber could be piped to the engine inlet with a long flexible hose, 6 inches in diameter. A second tube was clamped to the tailpipe to remove all exhaust from the chamber. Levels of carbon dioxide in the chamber were monitored to ensure that exhaust did not leak into the chamber. From the start of each test until the end of the driving cycle, carbon dioxide increased 200 to 400 ppm, consistent with the effect of the human vehicle operator breathing in the chamber. With these measures for isolating inlet and exhaust air, the chamber contained no tailpipe emissions; the only emissions in the chamber were those from tire wear, brake wear, resuspended dust, and fugitive evaporative emissions.

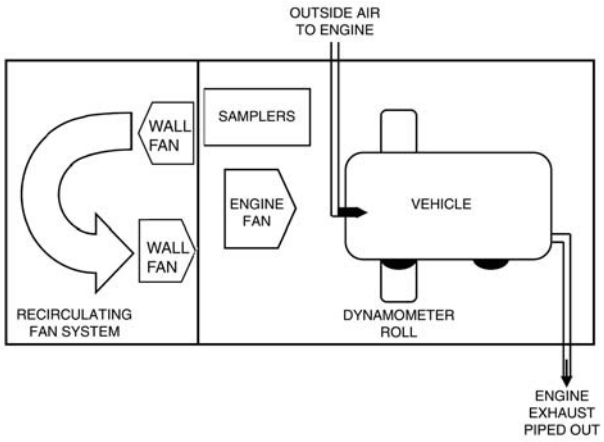

Figure 3. Experimental setup for vehicle dynamometer tests in RL-SHED.

Two vehicles were tested on the dynamometer under three different types of driving cycle and three different types of blank test (Table 2). Late-model vehicles with original brakes were tested to avoid complication from residues of previous brake pads. In accordance with standard procedures for testing tailpipe emissions, the dynamometer was programmed with the specific inertial weight and actual horsepower for each vehicle. Such programming allows the dynamometer to simulate actual driving conditions by exerting forces equivalent to the inertial and aerodynamic resistances that would be experienced on the road.

For each test, sampling continued for a total of 2 hours: 1 hour of the driving cycle and 1 hour with the vehicle turned off while particulate matter returned to background levels. For each of the three different driving cycles, a professional driver followed a speed trace on a monitor next to the vehicle.

The federal test protocol (FTP) driving cycle approximated city driving, with medium speeds and moderate rates of braking and acceleration (Table 2; Figure 4). The unified cycle (UC) was more similar to highway driving; it required higher speeds and included some hard accelerations and decelerations. For each of these two test types, the standard protocol included a hot-soak period, 10 minutes between cycles during which the vehicle was turned off. For a standard FTP test, the hot soak is usually followed by a repeated part of the first segment of the test, but in these tests, the first driving segment (1372 seconds) was repeated in its entirety after the hot soak.

The third driving cycle was a steady-state (SS) cycle with no braking, meant to reproduce driving conditions in

Table 2. Summary of RL-SHED Dynamometer Tests

Test	Vehicle Engine Running	External Engine Fan On	Dynamometer Running	DustTrak Inlet Cutpoint (μm)	Distance Driven (km)	Driving Cycle[a]
Vehicle A[b]						
FTP 1A	Yes	Yes	Yes	10	24	FTP test, 10-min hot soak, FTP test
UC A	Yes	Yes	Yes	10	32	UC test, 10-min hot soak, UC test
Blank 1	No	No	Yes	2.5	0	Dynamometer run 60 min at 48 kph
SS A	Yes	Yes	Yes	2.5	48	Dynamometer run 60 min at 48 kph, no braking
FTP 2A	Yes	Yes	Yes	2.5	24	FTP test, 10-min hot soak, FTP test
Vehicle B[c]						
Blank 2	No	Yes	No	2.5	0	Only chamber fans on
FTP 1B	Yes	Yes	Yes	2.5	24	FTP test, 10-min hot soak, FTP test
UC B	Yes	Yes	Yes	2.5	32	UC test, 10-min hot soak, UC test
Blank 3	No	No	Yes	10	0	Dynamometer run 60 min, with repeated cycles of acceleration to 48 kph and deceleration to 8 kph
SS B	Yes	Yes	Yes	10	48	Dynamometer run 60 min at 48 kph, no braking
FTP 2B	Yes	Yes	Yes	10	24	FTP test, 10-min hot soak, FTP test

[a] For the first hour of sampling. In the second hour, the vehicle and dynamometer were turned off; the chamber fans were left on for the remaining hour. See text for full descriptions of test types.

[b] Vehicle A is a Dodge Caravan minivan, 1998 model year; inertial weight, 4250 lb; actual horsepower, 10.4.

[c] Vehicle B is a Ford Escort, 3-door, 1995 model year; inertial weight, 2750 lb; actual horsepower, 6.1.

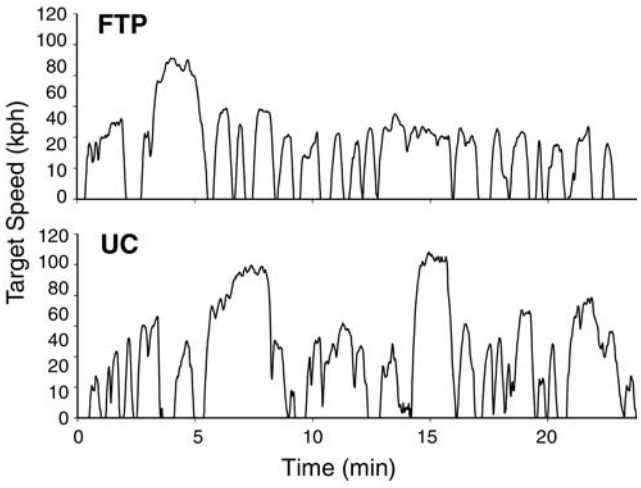

Figure 4. FTP and UC driving cycle traces of target speeds followed by drivers during dynamometer tests.

the sampled vehicle tunnels. No hot soak segment was included. The vehicle was driven at 48 kph (30 mph) for 60 minutes and then allowed to coast to a stop over approximately 3 minutes without braking.

Blank tests (Table 2) were performed to determine the background levels of particulate matter resulting from basic operation of the dynamometer and chamber fans. During the blank tests, the vehicle was not running and the wheels were not on the dynamometer. The chamber was sealed, and sampling was conducted for 2 hours, as in the driving cycle tests. Chamber fans were operated during all blank tests. In one blank test, the dynamometer was run at 48 kph to sample the background dust resuspended by its operation. In the second blank test, only the chamber fans were operating. In the third blank test, the dynamometer accelerated to 48 kph and decelerated to 8 kph (5 mph) repeatedly, to investigate the possibility that dynamometer deceleration and acceleration increased particle emissions.

Particulate matter samplers were placed in the chamber with the vehicle and dynamometer (Figure 3). Several types of samplers were used; all were placed within 2 m (about 6.6 ft) of the operating wheels. The sampler for PM_{10} and $PM_{2.5}$ used in the chamber was identical to those used in the tunnel tests (described earlier; Figure 2). Multiple filters were collected simultaneously for both size cuts, enabling full chemical characterization. MOUDIs were used for single tests or for pairs of tests of the same vehicle, to obtain higher sample masses. For two pairs of tests, two MOUDIs were collocated with aluminum and Teflon substrates to allow analysis of organic and inorganic fractions.

An optical instrument (DUSTTRAK aerosol monitor model 8520, TSI, Shoreview MN) was used for semiquantitative real-time measurements of particulate matter mass in the chamber. Mass was not quantified with the DustTrak, but the data were used to observe trends in mass concentration in the chamber. To observe these trends in both fine and coarse size fractions, the instrument was fitted with PM_{10} and $PM_{2.5}$ inlets in the different tests (Table 2).

Figure 5 shows example DustTrak PM_{10} data for each of the three driving cycle tests (FTP, UC, and SS). Peak concentrations occurred at the end of each driving cycle. Also shown are DustTrak data from the blank 3 test, in which the dynamometer accelerated and decelerated continuously. In this and every blank test, DustTrak measurements were at a maximum at the start of sampling and declined steadily to below ambient concentrations, indicating that the chamber had no leaks or major sources of particulate matter during blank tests.

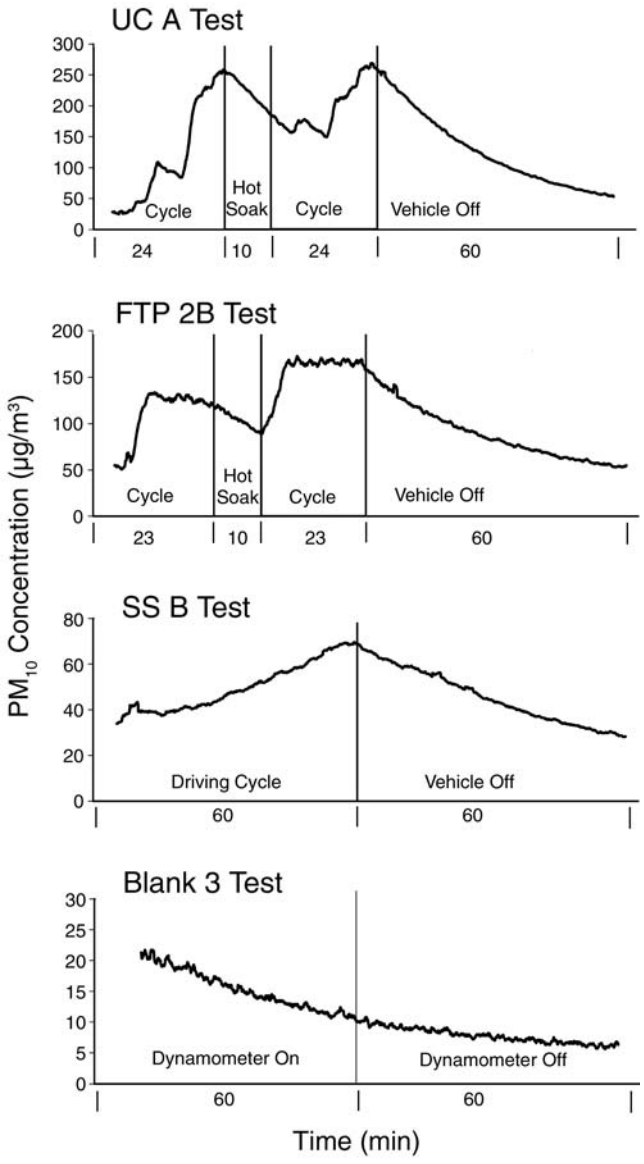

Figure 5. DustTrak data for PM_{10} mass in RL-SHED. For test specifications, see Table 2.

The two blank tests in which the dynamometer was running (blank 1 and blank 3) had low levels for all species measured, similar to those of the blank 2 test, in which the dynamometer was turned off. Therefore, operation of the dynamometer itself was not a notable source of particulate matter in the chamber. Analytic results of the three blank tests were averaged for each species and size fraction. The average blank value was 10% of the average vehicle test mass, for both PM_{10} and $PM_{2.5}$. Average blank values for each species, by size fraction, were subtracted from all vehicle test data. The standard deviation of the blank test measurements for each species was combined with the analytic uncertainty of each vehicle test measurement to more accurately reflect measurement uncertainty.

Concentrations of species in the RL-SHED, quantified from filter samples ($\mu g/m^3$), were averages for the 2-hour sampling period. DustTrak data showed levels of particulate matter mass increasing during driving cycles and decreasing when the vehicle was stopped. This decrease was due to removal by samplers and deposition onto surfaces in the RL-SHED and in the recirculating fan system. Therefore, to convert filter measurements to emission rates in mass per kilometer driven, a decay rate for particulate matter concentrations was needed.

The decline of particulate matter mass concentrations in the DustTrak data when the vehicles were turned off followed first-order decay. Mathematically, concentration C at time t is equivalent to the initial concentration multiplied by e^{-kt}, where k is the decay constant. Under such conditions, the decay rate r is proportional to concentration: $r = k \times C$. Therefore, the fractional loss is independent of concentration. Concentrations measured with the DustTrak in the last half-hour of each of the driving cycle tests and blank tests were used to calculate the decay constant for that period in each test. Values of k in blank tests were 0.52/sec to 0.74/sec; in vehicle tests, 0.83/sec to 1.68/sec, with a vehicle-test average of 0.93/sec and an SD of 0.32/sec. This average decay constant was applied to all tests as part of the mass balance equation to calculate emission rates of measured species.

Although the emissions conditions in each test were different, the chamber and sampling configurations that affect decay of particle concentrations were the same. The only emission-related factor that could affect the decay rate would be a change in the size distribution of particles resulting from differences in test conditions. However,

because some uncertainty is necessarily associated with the DustTrak measurements and the determination of decay rates, an average decay constant was determined to be the most robust application of the DustTrak data.

Because the RL-SHED is a closed system, a mass balance for generation, accumulation, and consumption of particulate matter is easily constructed. A mass balance derived by Wooley and coworkers (1990) for emissions and sampling in a similar closed system is relevant here. Incremental generation in the system is equal to accumulation plus consumption:

$$s = V\frac{dC}{dt} + \mathrm{k}CV,$$

where s is the emissions in the system, V is volume of the closed system, C is concentration of particulate matter, and t is time. Integrating over time gives the emission rate:

$$S = \int_{\text{initial}}^{\text{final}} s\,dt = V\left[\left(C_{\text{final}} - C_{\text{initial}}\right) + \mathrm{k}C_{\text{average}}t\right].$$

Because concentrations peaked in the middle of the tests, the difference between final and initial concentrations measured with the DustTrak was small, and the ($C_{\text{final}} - C_{\text{initial}}$) term in the equation could be ignored. Therefore, the emission rate S is equivalent to $V\mathrm{k}C_{\text{average}}t$. With known distances driven in each test, emission rates could be expressed as mass emitted per kilometer (µg/km).

To compare the composition of measured brake and tire wear emissions with the composition of bulk material, brake pads, brake housing dust, and tires were removed from the dynamometer test vehicles for use in resuspension tests and size-resolved sampling. Pulverized brake pads, sieved brake-housing dust, and ground tires were introduced to a dilution chamber, from which PM_{10} and $PM_{2.5}$ samples were collected on filters. The size separation and sampling procedures were parallel to those used in the dynamometer tests, to allow direct comparison of the data.

Resuspension Tests

Resuspension of bulk samples in air in a laboratory environment is an established method for achieving size resolution of dust particles. Samples were resuspended and collected by using a dilution chamber similar to that described and illustrated by Hildemann and associates (1989, 1991). The sample dust was placed in a flask, and pressurized, clean, particle-free air was flowed into the flask to suspend the dust. The air carried the suspended sample through stainless-steel tubing into a clean stainless-steel dilution chamber, a cylinder approximately 0.3 m in diameter and 1.5 m high. $PM_{2.5}$ and PM_{10} samples were collected by drawing air from the dilution chamber through cyclone separators and filters. The size separation and filter collection methods were parallel to collection methods for ambient aerosols in the field, ensuring that the data could be directly compared. Duplicate filters were collected simultaneously for each size cut. As part of quality control for the resuspension process, mass loadings of duplicate filters were compared.

Between resuspension tests of sample dusts, blank tests were performed in which no sample dust was placed in the flask, but air was flowed through the flask and dilution chamber, and filter samples were collected from the chamber. This procedure results in higher blank values than when blanks are collected without drawing air through the flask and chamber. This bias is typical of such samples and needs to be properly addressed as part of sample blank correction. Average blank test measurements from each series of resuspension tests were subtracted from each measurement, for each species, by size cut. The standard deviation of blank test measurements in a series was added to the analytic uncertainty associated with each measurement and was propagated through all calculations.

For both PM_{10} and $PM_{2.5}$, average blank test values represented 0.3% to 11% of the mass in sample resuspension tests. For Fe, the most abundant element in resuspended brake dust, the average PM_{10} and $PM_{2.5}$ dynamic blank values were 7.2% ± 1.6% and 3.4% ± 0.6% of the resuspended samples, respectively. Average OC values in blank tests conducted between tire dust resuspension tests represented less than 0.5% of any sample. Dynamic blank values for less abundant species in all tests represented larger fractions of the species measurements, with correspondingly larger uncertainties. For example, blank values for As in the brake-dust series represented 20% to 300% of sample As, and the large standard deviation—150% of the blank value—was propagated with the measurement uncertainty.

Road Dust Collection During each series of roadway tunnel tests, summer tests at the Kilborn Tunnel and summer and winter tests at the Howell Tunnel, composite samples of the dust and dirt from the surface of the road were collected. Although no winter tests were conducted at the Kilborn Tunnel, a winter road-dust sample was collected for comparison. Collecting dust from each tunnel in each season tested ensured that the dust would be equivalent to that resuspended by vehicles and measured as part of the total roadway emissions profile. Samples were collected, by using a small vacuum cleaner (Porta-Mite vacuum with paper filter bags), from several points along the lengths of

the tunnels. Each paper vacuum bag was sealed in two layers of plastic bags and frozen with the tunnel emissions samples until resuspension. Before the dust was resuspended to collect size-resolved filter samples for analysis, it was passed through a 63-μm sieve to remove gravel and large pieces of dirt.

Brake and Tire Dust Collection We collected a total of 10 sets of brake pads and corresponding brake housing dust (dust found in the vehicle brake housing when the pads were removed) from on-road vehicles. All vehicles were from the Midwest, the region of the tunnel tests, to ensure the relevancy of the brake dust data to apportioning specific sources of metal emissions in the tunnels. We obtained 2 of the 10 sample sets from the vehicles used in the dynamometer tests for brake and tire emissions and 8 from vehicles serviced at garages in Wisconsin.

When brake pads were removed from the vehicles, plastic bags were held beneath the wheel to collect brake housing dust. Dust and pads were sealed separately in plastic bags. The brake pads were pulverized. The brake housing dust, though it contained fine material and larger pieces of material, was not pulverized. The crushed brake pads and the brake housing dust samples were passed through a 63-μm sieve, and the fine material was used in resuspension tests.

Tires were taken from the two vehicles used in the dynamometer tests for sampling. To avoid embedded dirt, a thin layer of the tread was removed from the section to be sampled. Several methods were attempted to obtain tire dust, but it was not possible to collect a dry sample that was resuspendable and not electrostatically charged (a problem previously noted by Hildemann and colleagues [1991]). Therefore, to introduce tire samples to the dilution sampler, a small, fine sanding drill bit was used to abrade the tire surface near the inlet of the sampler, so that the smoke from the sanding was sucked directly into the dilution chamber. Samples were size separated and collected on filters in the same way as the resuspended dusts were.

Tailpipe Emissions Measurement

Tailpipe emissions from gasoline- and diesel-powered motor vehicles were measured as part of a study funded by the US Department of Energy (DOE), the Gasoline/Diesel Split Study. The goal of the project was to compare source apportionment methods that were simultaneously used to assess the relative effects of motor vehicles on atmospheric particulate matter samples in the Los Angeles basin. Several research centers (including the University of West Virginia, the EPA, the Desert Research Institute, and the University of Wisconsin–Madison) collaborated with DOE to test a range of vehicles on chassis dynamometers and collect and analyze particulate matter samples. Complete details of the tests and analytic results are given in the project report (Gabele 2003). The measurements reported here are limited to the average bulk chemical profiles and the trace metal analyses of the particulate matter samples.

Gasoline-powered automobiles were driven twice through the same driving cycle to sample emissions from cold engine and warm engine operation. The cold phase included a cold engine start, a driving cycle of 1436 seconds, and an average speed of 40.2 kph (25 mph). The cold phase was followed by a 10-minute soak with the engine turned off, and then the warm phase was begun. The warm phase was identical to the cold phase in driving cycle, speed trace, and time, but the engine was warm at the start.

Heavy-duty diesel-powered trucks were driven through three driving cycles. Two were city–suburban heavy vehicle route cycles, 10.8 km (6.68 mi) over 27.5 minutes; one of these was a cold start and the other a warm start. The third was a highway cycle, equivalent to 25.0 km (15.54 mi) in 27.5 minutes.

Tailpipe exhaust was piped into a dilution chamber, an 8-inch-diameter stainless-steel tube, where it was mixed with air that had been pretreated by flowing it through a charcoal bed to remove hydrocarbons and then through a high-efficiency particulate air (HEPA) filter to remove particulate matter. Sample air was drawn from the dilution chamber isokinetically, through a cyclone to separate particulate matter sizes, and $PM_{2.5}$ samples were collected on filters. Flows were controlled downstream of the filter holders using critical orifices. Methods for collection, handling, and analysis of filter samples were identical to the methods used in the tunnel tests, to ensure that the data were directly comparable.

Dynamic blank tests, in which the dilution sampler was operated with no vehicle attached, were performed at intervals throughout the vehicle tests. The average concentration of each species in the sampler during the blank tests was subtracted from the test measurements. The standard deviation of the blank test measurements during a series of vehicle tests was added to the measurement uncertainties of those tests and propagated through all calculations.

To reduce the number of samples submitted for ICP-MS, some samples for metals analysis were composited in pairs. Compositing was consistent with other chemical measurements being conducted by University of Wisconsin–Madison and the Desert Research Institute as part of the larger DOE-funded study.

COLLECTION OF ATMOSPHERIC PARTICULATE MATTER SAMPLES

All three sites where ambient particulate matter samples were collected—in Milwaukee, Waukesha, and Denver—are established EPA sampling sites. The Milwaukee and Waukesha sites are in the Greater Milwaukee area, selected to discern trends in ambient trace metal concentrations in two residential areas in the same urban airshed. The Milwaukee site is near downtown, on the roof of the 16th Street Community Health Center, a three-story building at the intersection of Greenfield and 16th Streets. The area is urban, with constant traffic and many small businesses and restaurants in between urban residential blocks. Approximately 20 km west is the Waukesha site, on Cleveland Street not far from Highway 18/JJ, a four-lane suburban road. The site is fenced in, and samplers sit on platforms 1 m (3.3 ft) above the ground. The area is a mix of residences and heavy industry, and the site itself is adjacent to an automobile body shop. In Denver, samples were collected at the central Adams County site, on the roof of a two-story building in an area that is both residential and industrial. This third site is near an industrial incinerator and a quarry.

PM_{10} and $PM_{2.5}$ were collected at each site with samplers constructed at the University of Wisconsin–Madison. The samplers and analytic methods used for ambient measurements were identical to samplers and methods used for Milwaukee tunnel tests of motor vehicle roadway emissions, to permit direct comparison of the data. Samplers and filter substrates were prepared and handled specifically for each targeted chemical measurement.

Ambient samples were collected from midnight to midnight on the EPA sixth-day schedule from February 2001 to January 2002. The sixth-day schedule rotates sampling days through days of the week; it is used for ambient sampling to avoid bias from trends that follow weekly patterns. Filters were loaded in the samplers the day before sampling, picked up the day after, and frozen until analysis. PM_{10} and $PM_{2.5}$ were collected on multiple filters simultaneously. Both size fractions were analyzed for gravimetric mass, EC and OC, and SO_4^{2-}, NO_3^-, Cl^-, and NH_4^+ ions. In PM_{10}, metals were also analyzed. Analytic methods are described in the next section (and in Appendix A, available on request from HEI).

To correct for contamination from handling, field blank samples were taken at regular intervals at each site throughout the year. Field blank filters were handled in the same manner as sample filters. They were prepared, taken to the field, loaded into the samplers, and stored and analyzed with the samples. The same person operated the two Wisconsin samplers, the field blanks at the two sites were handled similarly, and their data were averaged. The sampler in Denver was treated separately because it was operated separately and because the filters and samples were shipped between Wisconsin and Denver.

Blanks from the field were generally very low in value. Average (± SD) field blank values for the year represented 2.6% ± 3.1% of the average PM_{10} mass at the Denver site and 0.0% ± 6.7% of that at the Wisconsin sites. For $PM_{2.5}$ mass, average field blank values for the year were 5.2% ± 6.6% of the average mass in Denver and 0.0% ± 9.2% of that in Wisconsin. For each species, individual ambient measurements were corrected by subtracting the appropriate average PM_{10} or $PM_{2.5}$ field blank value. The standard deviation of the blank measurements was combined with analytic uncertainty and propagated through all calculations. Additional error of ± 5% was included to account for uncertainty in flow rate measurements.

CHEMICAL ANALYSIS

Bulk Chemical Measurements

All substrates were prepared in the laboratory before sampling. For mass measurements, Teflon filters were equilibrated in a temperature- and humidity-controlled room for 24 hours. Acid-precleaned Teflon filters for MOUDI sampling were preweighed to allow quantification of mass and trace metals with the same substrate. Quartz fiber filters (47 mm in diameter; Pall Life Sciences, Ann Arbor MI), used for measurement of EC and OC, were prepared by heating to 550°C for 12 hours and were stored in Petri dishes lined with aluminum foil baked at 550°C for 12 hours.

Samples on tared filters were equilibrated for 24 hours in a temperature- and humidity-controlled room before being weighed on a microbalance (Metler MX-5). EC and OC were quantified with a thermal–optical analyzer (Sunset Laboratory, Forest Grove OR) by using the US National Institute for Occupational Safety and Health 5040 method (Schauer et al 2003). Inorganic SO_4^{2-}, NO_3^-, Cl^-, and NH_4^+ ions were analyzed by using water extraction and ion chromatography. All of these measurements were conducted at the Wisconsin State Laboratory of Hygiene in Madison.

Metal Measurements

Teflon substrates (Teflo, 2 µm thick, 47 mm in diameter; Pall Life Sciences) used to collect trace metal samples were preleached with high-purity acids in a room clean of trace metals. Details of substrate and material cleaning are given in Appendix A. When preleached filters were not available (for one test and for some samples for XRF analysis), the greater variability of field blank results for unleached filters was used to determine the uncertainty of the measurements of samples on unleached filters.

Elemental composition of the particulate matter samples was measured using ICP-MS techniques (PQ Excell; Thermo Elemental, Franklin MA), which allowed quantification of 35 elements. Digestion and analysis methods are

described in detail in Appendix A. Sample dissolution was achieved by using microwave-assisted digestion with hydrochloric acid, nitric acid, and hydrofluoric acid, according to techniques specifically developed for analyzing low levels of metals in airborne particulate matter samples. These techniques effectively solubilize samples with minimal contamination.

When coupled with microwave-assisted acid digestion, ICP-MS techniques provide the accuracy and sensitivity to analyze atmospheric particulate matter samples for a wide range of elements. Propagated uncertainties were calculated from the standard deviation of field blank measurements and the standard deviation of replicate analyses of standard reference materials (SRMs; US National Institute of Standards and Technology [NIST], Gaithersburg MD). A minimum of six solid samples of three SRMs were digested and analyzed with every batch of 25 samples. The average recoveries of SRMs, compared with their reported values, are shown in Appendix A (figure). The relative uncertainties in each measurement were represented by the uncertainties in the extraction and analysis of replicate SRM samples plus the absolute uncertainty of the field blanks, with the assumption that these errors were normally distributed and independent.

The concentrations of 13 reported elements (Al, Si, P, S, Cl, K, Ca, Sc, Ge, Se, Br, I, and Ce) were determined by using XRF elemental analysis conducted by the EPA (Research Triangle Park NC) with an energy-dispersive XRF instrument (Kevex EDX-771). Calibration checks were performed by using an SRM (Thin Glass Film on Polycarbonate, NIST 1833). Details of XRF analysis are described elsewhere (Kellog and Winberry 1999).

Synthetic Lung Fluid Leaching

Our exploratory research examined the short-term solubility of a large set of elements from actual sampled emissions of motor vehicles in roadway tunnels and from sampled urban ambient particulate matter. Leaching with a synthetic lung fluid was used to investigate the fraction of total elements in the lung that is likely to be mobilized through dissolution in lung fluid. Acid digestion and analysis of duplicate particulate matter samples provided measurements of total metals in each sample.

Table 3 presents the chemical composition of the synthetic lung fluid. Although the fluid was prepared with the highest-purity salts available, blank samples indicated that trace quantities of contaminants present in the salts could be problematic when leaching submilligram masses of aerosols. Therefore, the synthetic lung fluid was processed through a Chelex resin column to remove these trace contaminants from the concentrated salt solution. The functional groups on Chelex resin (iminodiacetate) have a high affinity for transition metals, even in the presence of high concentrations of major cations, and Chelex resin has been shown to be highly effective in cleaning-up seawater-type matrices (Shafer et al 2004).

Trace elements in synthetic lung fluid before and after chelation are shown in Figure 6 by element concentration and in Figure 7 by removal efficiency of the chelation step. Major reductions in background levels of Al, Mn, Zn, Ag, Cd, Ba, Ce, and Pb were observed. Reductions in background levels of Cu and Sb were less notable. Little or no change was apparent for Ti, Rb, or Cs, or for Ru and Rh (not shown). The results for Ti, Rb, Cs, Ru, and Rh were expected given their solution chemistry; however, their background levels were in most cases near the limit of detection, so the ineffectiveness of the Chelex cleanup was not problematic.

When the synthetic lung solution was passed through the Chelex resin twice, background levels of trace metals were very low, and approximately 100% ± 10% of 1 µg/L spikes of all elements was recovered, except Ag, Cd, and Zn, of which approximately 100% ± 20% was recovered (Figure 8).

PM_{10} was used in this preliminary research to ensure adequate mass loadings. Particulate matter samples were collected on Teflon membrane filters (47 mm in diameter) preleached with hydrochloric and nitric acids and rinsed with 18 MΩ water. All supplies used in sample collection and analysis were leached with high-purity acids, and all preparation and analysis was performed in dedicated laboratories clean of trace metals.

Table 3. Composition of Synthetic Lung Fluid

	Synthetic Lung Fluid			Human Serum
Species	mM	mg/L	mEq	mEq
Cations				
Na^+	142	3265	142	142
K^+	5.0	195.5	5.0	4
Mg^{2+}	0.5	12.16	1.0	2
Ca^{2+}	0.5	20.04	1.0	5
Sum of cations	148	3493	149	153
Anions				
CL^-	115.5	4095	115.5	101
HCO_3^-	31.0	1891	31.0	27
HPO_4^{2-}	0.5	48.49	0.5	2
SO_4^{2-}	1.0	96.06	2.0	1
Sum of anions	148	6131	149	131

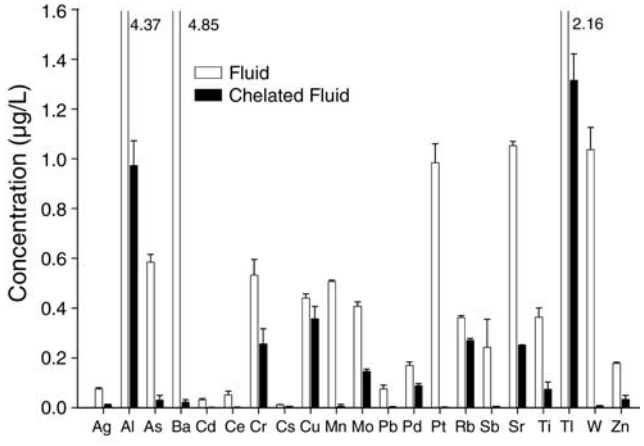

Figure 6. Trace element levels in synthetic lung fluid, with and without Chelex resin cleanup. Error bars indicate the standard error of the average.

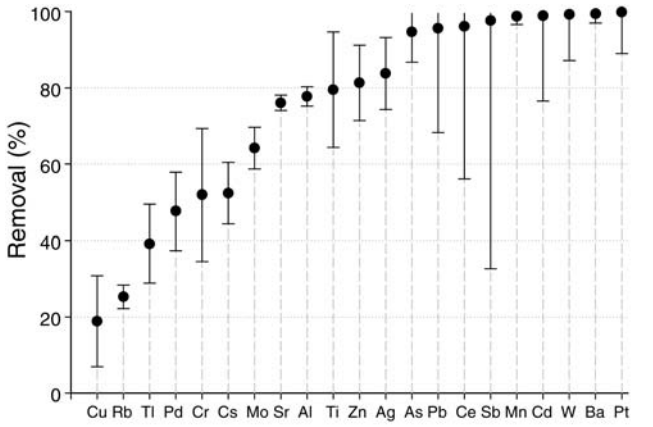

Figure 7. Synthetic lung fluid cleanup: efficiency of trace element removal on Chelex resin. Error bars indicate the standard error of the average.

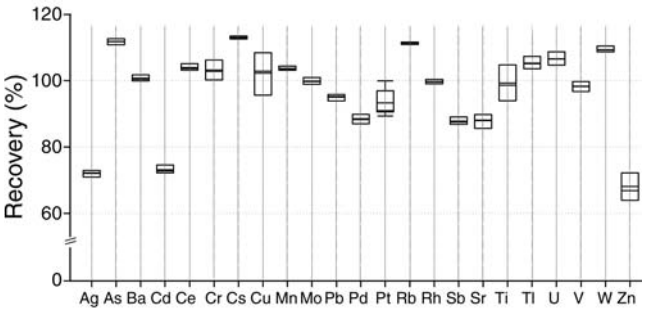

Figure 8. Recovery of 1 µg/L spikes of trace elements from synthetic lung fluid. The boxes span the 75% confidence interval. The two lines inside each box represent the mean and the median.

Clean, Teflon-coated impactor inlets (URG Corp) and filter holders were used to collect samples in the two roadway tunnels and at the three urban sampling sites. Duplicate, collocated samples were collected for analyses of total and leachable metals. Particulate matter samples used for leaching studies were collected inside a roadway tunnel, and mass loadings were 110 to 260 µg per filter. These samples reflected all particulate matter present in the tunnel, including background urban ambient particulate matter, not solely emissions from motor vehicles. Ambient particulate matter was collected at the Milwaukee, Waukesha, and Denver sites. Samples were composited in pairs of filters collected in the same month; total composite masses were 280 to 1150 µg. Eight pairs were composited at each of the three sites; of these, seven were samples obtained on identical dates at identical times at all three sites.

To leach the samples in the synthetic lung fluid, polypentene support rings were removed from the membrane filters. The filters were placed in clean polypropylene centrifuge tubes (Nalgene, Oak Ridge screw cap; Nalge Nunc International, Rochester NY) with 20 mL of synthetic lung fluid that had been passed through Chelex resin twice, and the tubes were capped. They were triple bagged before being taken from the clean laboratory. They were shaken in a water bath at 37°C for 8 hours at 80 rpm. The clean inner bags holding sample tubes were returned to the clean laboratory for sample filtration.

Sample extracts were transferred to precleaned syringe barrels (Norm-Ject, Henke Sass Wolf GMBH, Tuttlingen, Germany) with acid-cleaned Leur-lock syringe filters (Puradisc PP, 25 mm in diameter, 0.2 µm thick, polypropylene membrane; Whatman Inc, Clifton NJ). Approximately 1 mL of the sample extract was discarded to rinse and equilibrate each filter, and the remainder was portioned into two polypropylene graduated tubes (Falcon Blue Max, 15 mL; Becton Dickinson, Franklin Lakes NJ) for storage and analysis. Each portion of final extract filtrate was acidified with 0.2 mL of 8 N high-purity nitric acid.

To provide a metric of external method precision as well as a gauge of overall method performance, NIST SRMs were incorporated into the synthetic lung fluid protocol. Though no SRM can exactly duplicate complex environmental samples, the two we chose (Urban Dust, NIST 1649a; and Used Auto Catalyst, NIST 2556) most likely captured some of the environmental phases of our samples. Figure 9 shows the results of two separate trials on each SRM in synthetic lung fluid subjected to the leaching protocol. The leachable fraction of a trace metal was computed as the ratio of the leachable component to the total metal present in the identical sample.

As demonstrated by the repeatability of measurements for each SRM, overall method precision was good for the elements being investigated (Figure 9). Major solubility differences among elements are apparent. Differences can also be seen in the solubility of a given element between the two SRMs, reflecting the unique phase associations present in each SRM. The most notable differences in leachability between the two SRMs were for Ba, which was present in more soluble phases in the Auto Catalyst, and Zn, Pb, Mn, and Cu, all of which were more leachable in the Urban Dust.

Classes of elements also exhibited trends. Crustal elements (Al, Ti, and Fe) and highly polarizable oxide-forming elements (Ba and Ce) exhibited very low solubility (< 10%). In Urban Dust, alkali metals (Rb and Cs) and mobile divalent transition metals (Mn, Cu, Cd, and Ag), particularly those with filled d-shells, showed high solubility (30%–50%). Oxyanions (Sb) and metals that form strong solution complexes (W) also exhibited high solubility. Leachability of Pb and Zn fell in between, at approximately 10%.

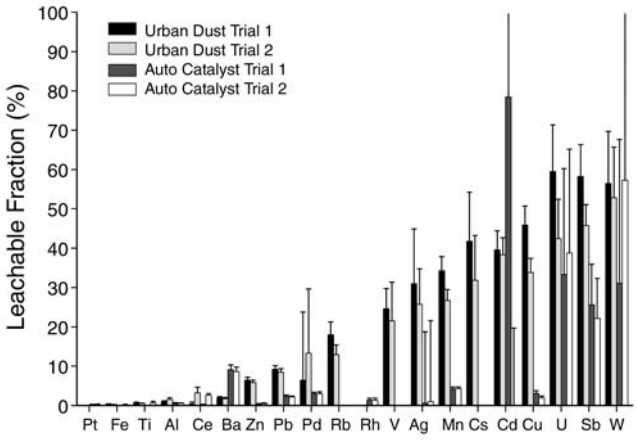

Figure 9. Solubility of trace metals associated with two SRMs in synthetic lung fluid. Urban Dust is NIST SRM 1649a; Used Auto Catalyst is NIST SRM 2556. Error bars indicate the standard error of the average.

STATISTICAL ANALYSIS

CMB Model

Sample collection and analysis methods were parallel for the tunnel tests of total roadway emissions and for the tests of different sources, to ensure direct comparability of the data. Emission rates of species measured in the 16 tunnel tests were categorized by test type and averaged within each type to create five roadway profiles for source apportionment, which were used as the receptors in the source–receptor model. Table 4 briefly summarizes the test types: summer, Kilborn Tunnel, weekdays; summer, Howell Tunnel, weekdays; summer, Howell Tunnel, weekends; winter, Howell Tunnel, weekdays; and winter, Howell Tunnel, salt affected.

Development of emission profiles for brake wear, tire wear, and resuspended road dust are described earlier (Source Sampling/Brake and Tire Wear Tests, and Resuspension Tests). Although we found tire dust to contribute negligible amounts of any element, it is likely to be an important source of OC and particulate matter mass emissions. Thus, we included it in the CMB model for completeness.

Only $PM_{2.5}$ (not PM_{10}) tailpipe emissions were measured, because combustion emissions are primarily in the fine fraction. Because metal emissions from all vehicles, even during different driving cycles, were remarkably similar on a mass-normalized basis, the measured emissions were averaged to create single profiles for tailpipe emissions of gasoline- and diesel-powered motor vehicles.

A source profile for the effect of winter salt application to roadways (to melt ice) was constructed from one of the winter Howell Tunnel tests (test P). This test had mass emission

Table 4. Tunnel Test Types Used as PM_{10} Receptor Profiles and CMB Model Results

Test Type	Number of Tests in Average	Total Number of Vehicles	r^2	χ^2	% Mass Apportioned	Measured Mass (mg/km ± 1 SD)	Calculated Mass (mg/km ± 1 SD)
Summer							
Kilborn, weekdays	5	13,534	0.90	2.52	63	117 ± 14.0	73.8 ± 7.31
Howell, weekdays	3	12,420	0.90	2.68	160	124 ± 17.6	198 ± 39.4
Howell, weekends	2	4957	0.90	2.71	589	24.9 ± 35.6	146 ± 29.9
Winter							
Howell, weekdays	5	37,185	0.89	2.24	94	56.3 ± 3.4	52.7 ± 12.5
Howell, salt affected	1	7977	1.00	0.12	106	375 ± 19.1	396 ± 25.0

rates several times higher than any other test, with much of the increase comprising Cl^-, Na, and other crustal elements. These results and the weather conditions during that test indicated that resuspended road salt was the source of the large mass. The profile for this source was defined by the differences in species emission rates between the salt-affected test and the average of the other winter tests. The road salt profile was used in the CMB model only to apportion emissions from the salt-affected tunnel test.

Emission measurements from the tunnel tests, in milligrams per kilometer, were combined in a CMB model (EPA software CMB 8.2) with the profiles for the different specific emission sources developed in this work (resuspended road dust, brake wear, tire wear, gasoline tailpipe, and diesel tailpipe). Because the goal of the study was to understand the sources of metals, not total mass, metals were emphasized as tracer species. The fit of the total mass by the model was used as one way to judge the accuracy of the results.

The species used to fit the model were chosen for their abundance in the PM_{10} emitted in tunnel tests and their even distribution over the periodic table. The tracer species were OC and EC, Al, Fe, Ti, Cr, Mn, Cu, Zn, Sr, Sb, Ba, and Pb. Cl^- was added as a fit species for the salt-affected tunnel profile only. Seven crustal elements (Na, Mg, Al, K, Ca, Fe, and Ti) were present in considerable amounts in all tunnel tests; however, only three (Al, Fe, and Ti) were used to fit the model. The other four (Na, Mg, K, and Ca) were not included as fit species in order to avoid overestimating the effect of resuspended road dust, their expected primary source. The inclusion of OC and EC with the elements used as fit species was necessary to separate the contributions of gasoline and diesel tailpipe emissions.

ICFA

Several approaches to pollution source apportionment are based on the simple model

$$\mathbf{x}_t = \Lambda \mathbf{f}_t + \mathbf{e}_t, \quad (1)$$

where $\mathbf{x}_t$ is the vector of p chemical species observed at time t, $\mathbf{f}_t$ is the vector of k pollution source contributions at time t, $\mathbf{e}_t$ is the vector of measurement errors associated with the p species observed at time t, and Λ is a $p \times k$ matrix with the k pollution source profiles as its columns. The simplest approach for identifying the pollution source contributions $\mathbf{f}_t$ involves standard regression methods (eg, Gatz 1975; Mayrsohn and Crabtree, 1976; Kowalczyk et al 1978), but it requires that the pollution source profiles Λ are known. When little or nothing is known about the nature of the pollution sources, exploratory factor analysis models have been employed (eg, Thurston and Spengler 1985; Koutrakis and Spengler 1987; Henry et al 1994).

Figure 10 illustrates the variety of approaches to estimating the nature of pollution sources along the continuum of a priori knowledge about them. Techniques other than exploratory factor analysis include confirmatory factor analysis models (eg, Yang 1994; Gleser 1997; Christensen and Sain 2002), Bayesian analysis (eg, Park et al 2001, 2002), and measurement error modeling (Watson et al 1984; Christensen and Gunst 2004).

In recent years, interest has increased in more flexible approaches that assume little knowledge about the nature of pollution source profiles. Both the UNMIX approach (outlined in Henry 1997) and the positive matrix factorization (PMF) approach (Paatero and Tapper 1994) are examples of this type of analysis. UNMIX and PMF attempt to extract nonnegative estimates of source profiles and source contributions from measured chemical species using a factor analysis model. Although each approach attempts to reduce factor indeterminacy through the use of nonnegativity constraints and other computational tools, neither these nor any other purely exploratory approaches can guarantee a uniquely identified solution without additional constraints on the source profiles (which act like factor loadings when the receptor model is viewed as a factor analysis model). Confirmatory factor analysis can guarantee a uniquely estimable solution, but it requires that at least k rows of the source pollution matrix Λ be fixed to equal a full-rank matrix of constants.

Notable among the factor analysis approaches used in source apportionment studies is target transformation factor analysis (TTFA), developed by Malinowski and colleagues (1970) and implemented in receptor modeling by Hopke and coworkers (1980) and others. TTFA uses exploratory factor analysis to extract factors from the data and then rotates the factors to align as closely as possible with the hypothesized factors. This approach is similar to the ICFA approach used in this study, in that each approach utilizes both the factor analysis structure and a priori profile information when estimating source profiles. However, the ICFA approach is advantageous because it is more robust in the presence of poorly specified a priori source profiles.

The ICFA approach can take on aspects of both confirmatory factor analysis and exploratory factor analysis by assigning varying degrees of constraint to each element of the source pollution matrix Λ during the estimation process. Before describing the factor analysis solutions obtained, we first recall that when a k-factor model holds, the factor loadings for the k factors are uniquely estimable when a $k \times k$ submatrix of the $p \times k$ factor loading matrix is fixed to equal a $k \times k$ full-rank matrix of constants. An implication of this property is that if a $k \times k$ submatrix of Λ is fixed when

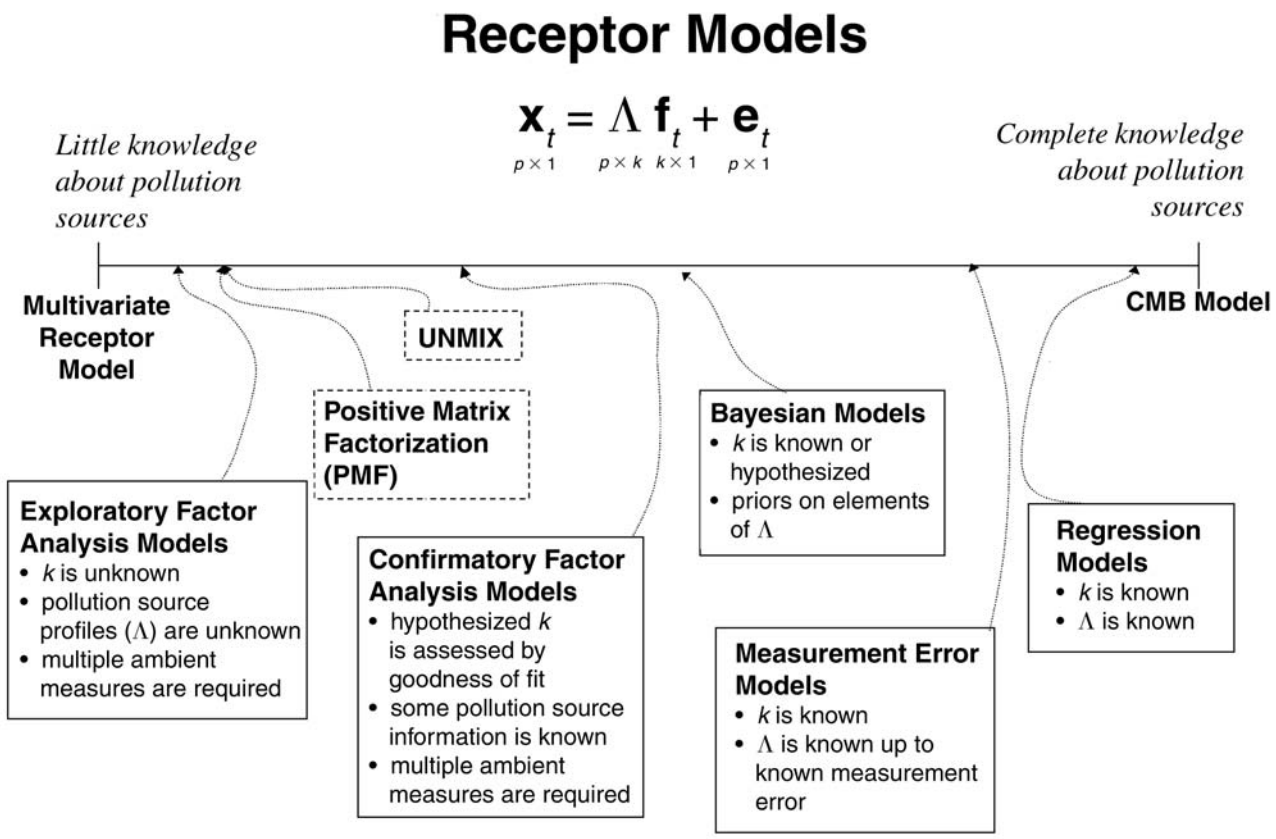

Figure 10. Approaches for estimating pollution source contributions using receptor models. Approaches depend on the a priori knowledge about the number and nature of pollution sources. The term $\mathbf{x}_t$ is the vector of p chemical species observed at time t; Λ is a $p \times k$ matrix with the k pollution source profiles as its columns; $\mathbf{f}_t$ is the vector of k pollution source contributions at time t; and $\mathbf{e}_t$ is the vector of measurement errors associated with the p species observed at time t.

obtaining a factor analysis solution to the multivariate receptor model, then the factors represented by the estimated factor loadings will retain the physical interpretation implied by the choice of the constraint matrix.

We consider here the case in which some or all of the elements in a hypothesized source profile (factor loading) matrix are estimated, but with error. We allow for some other elements to be unknown. When the k-factor model holds, but errors are present in the estimated profiles, we can use the factor analysis model to update $p - q$ rows of the factor loading matrix based on a full-rank constraint matrix consisting of q rows of the source profile matrix, where q is equal to or greater than k.

Beginning with all elements of the profile matrix for which data are available, we can use a factor analysis solution to obtain estimates for the unknown elements. We employed a maximum likelihood estimate of the factor model parameters and constrained factor loading estimates to the interval [0, 1]. Such constraints, along with restrictions to ensure nonnegativity of error variances and factor variances, are easily implemented in standard software (such as the CALIS procedure in SAS software [SAS Institute, Cary NC]). As is common in factor analysis approaches, we constrained estimated parameters to take on physically meaningful values to reduce the probability of selecting a nonoptimal solution. After obtaining a complete $p \times k$ factor loading matrix in the first iteration, we allowed the factor analysis model to update the factor loading estimates to be consistent with the observed ambient data by successively reestimating $p - q$ randomly chosen rows of the factor loading matrix by using the data and the $q \times k$ constraint matrix, consisting of a full-column-rank subset of $q > k$ rows of the factor loading matrix estimate from the previous iteration.

If the k-factor model holds and the sources have been properly identified, then each iteration will yield source profile matrix estimates that improve upon the starting values. If one or more of the actual source profiles are erroneously omitted, or if an incorrect profile is used, the source profile matrix estimates will diverge from the starting values toward a more plausible solution. After

repeated iterations of the algorithm, during which each element of the factor loading matrix has been reestimated many times, the source profile matrix will converge toward an estimate that is associated with a smaller χ^2 goodness-of-fit statistic.

In each iteration of our implementation, we randomly selected a row of the source profile matrix to be reestimated with probability in the interval [0.1, 0.5], so each iteration would estimate a random number of rows; we could also have randomly selected a fixed number of rows to be reestimated in each iteration. However one chooses the rows to be reestimated in each iteration, in order for the model in each update step to be conditionally identified (that is, identified given the $q \times k$ constraint matrix obtained from the previous update), the constraint matrix must not only have at least k rows but also be of rank k. If the model in each update is not conditionally identified, then the algorithm can yield final profile estimates that have rotated away from a starting value matrix that was correct and completely specified. In practice, conditional identification prevents the profile matrix estimates from vacillating among equally well-fitting but dramatically different solutions, many of which will be uninterpretable.

In some situations, we may be reasonably certain about the nature of one or more source profiles but have only an approximate estimate for other source profiles. For example, we may have an accurate estimate of a gasoline-vehicle exhaust profile but have only a suspicion that either an incinerator or a smelter is the source of a Cl-rich profile. In such cases, we can constrain the profile elements associated with the well-understood source λ_{i1} (where i is 1,..., p) to remain in the interval $[4/5 \times \lambda_{i1}, 5/4 \times \lambda_{i1}]$ while allowing the profile elements associated with the poorly understood source λ_{i2} to take on updated values in the interval $[1/5 \times \lambda_{i1}, 5 \times \lambda_{i1}]$. In other situations, we may want to leave some source profiles completely unrestricted in order to account for possibly unknown sources. In these cases, we would like to have a model-fitting procedure that gives uniqueness (or near uniqueness) for the source profile estimates associated with the well-understood profiles and that still maintains the flexibility to estimate unknown source profiles.

The ICFA approach differs from the TTFA approach in that each update of the ICFA algorithm moves the estimated profiles away from the erroneous values (those not substantiated by the data structure) toward more plausible profiles. In contrast, TTFA first finds an exploratory factor analysis solution, then rotates the profiles until they are in line with the target (or hypothesized) profiles. In fact, if the correct source profile is excluded from the columns of the target profile matrix and an incorrect profile is included in its place, TTFA will rotate the solution in order to find transformed factor loadings that resemble the incorrect profiles. Consequently, all other profiles will be inaccurately represented by the rotated solution. In this sense, TTFA squeezes the data into the hypothesized profiles, whereas ICFA adapts the hypothesized profiles to conform to the data.

Once the ICFA approach has converged to reasonably stable updated estimates of the source profiles, source contribution estimates can be calculated for each ambient observation. In order to constrain the contribution estimates to be nonnegative, we defined the contribution from the jth source as $f_j = h_j^2$ and we employed a nonlinear model of the form

$$x_i = \lambda_{i1}h_1^2 + \ldots + \lambda_{ik}h_k^2,\ i = 1, \ldots, p, \quad (2)$$

where x_i is the ith species and λ_{ij} is the proportional representation of the ith species from the jth source. Estimating h_j in the nonlinear model instead of estimating f_1 in a linear model guarantees that the source contributions will be positive. We used a Gauss-Newton algorithm to fit the model to the data. In order to ensure an estimate that was not merely a local minimum, the model was fit 30 times using 30 different randomly chosen starting values. Among the 30 candidate solutions, we chose the one with the smallest sum of squares error as the final, set source contribution estimate.

RESULTS AND DISCUSSION

Except when otherwise defined, statistical significance refers to the 95% confidence test (the Student t test).

APPORTIONMENT OF ROADWAY EMISSIONS

Tunnel Emissions

Tunnel emission tests were divided into types by season and tunnel: summer, Kilborn Tunnel, weekdays (tests A, B, C, D, and E); summer, Howell Tunnel, weekends (tests G and H); summer, Howell Tunnel, weekdays (tests F, I, and J); and winter, Howell Tunnel, weekdays (tests K, L, M, N, O, and P). Samples from winter test P were greatly affected by road salt application; results of this test had a unique distribution. Therefore, test P was treated as a separate type, and its results are not included in the discussion of averages and statistical summaries for all tests.

Tables 5 and 6 present averages (± SEs) of emission rates of trace elements and other chemical species in PM_{10} and $PM_{2.5}$, respectively, from the different types of tunnel tests. Data for all tests, not averaged, are presented in Appendix B (available on request from HEI). When differences

Table 5. Emission Rates of PM_{10} Mass and Species in Tunnels, by Test Type[a]

	Summer Tests			Winter Tests	
PM_{10} Species	Kilborn Weekdays 1.6%–3.0% Trucks (A,B,C,D,E)	Howell Weekdays 6.1%–9.4% Trucks (F,I,J)	Howell Weekends 1.5%–2.4% Trucks (G,H)	Howell Weekdays 7.0%–7.7% Trucks (K,L,M,N,O)	Howell Weekdays 6.6% Trucks (P)
Mass	120 ± 28	140 ± 33	54.0 ± 8.3	50.0 ± 3.57	446 ± 14.8
OC	34.1 ± 5.4	44.4 ± 11.0	21.5 ± 1.7	10.1 ± 2.35	36.6 ± 3.02
EC	11.4 ± 1.8	14.7 ± 5.2	4.29 ± 1.51	3.16 ± 1.51	2.42 ± 0.52
Inorganic ions[b]	9.7 ± 3.3	15.9 ± 3.6	6.35 ± 6.35	21.8 ± 4.70	135 ± 1.78
Sum of all metals measured	33.1 ± 13.0	28.9 ± 5.8	8.76 ± 0.96	7.21 ± 2.47	192 ± 10.2
Na	0.57 ± 0.33	0.56 ± 0.34	0.20 ± 0.06	2.8 ± 1.0	51 ± 6.0
Mg	0.84 ± 0.22	1.9 ± 0.5	0.55 ± 0.10	0.42 ± 0.20	14 ± 1.6
Al[c]	0.97 ± 0.50	2.6 ± 0.8	0.00 ± 0.00	0.25 ± 0.25	4.9 ± 0.9
Si[c]	8.7 ± 1.4	9.1 ± 2.7	2.1 ± 0.2	0.73 ± 0.73	16 ± 3.5
P[c]	0.15 ± 0.09	0.11 ± 0.07	0.04 ± 0.04	0.00 ± 0.22	0 ± 0.27
S[c]	1.9 ± 0.6	1.2 ± 0.6	1.2 ± 0.6	0.09 ± 0.09	1.8 ± 0.7
Cl[c]	0.45 ± 0.17	0.21 ± 0.07	0.05 ± 0.05	0.33 ± 0.29	74 ± 7.0
K[c]	0.83 ± 0.15	1.1 ± 0.4	0.19 ± 0.18	0.064 ± 0.064	1.9 ± 0.18
Ca[c]	10.2 ± 2.3	8.5 ± 2.5	2.4 ± 0.8	0.70 ± 0.63	16.7 ± 1.6
Sc[c]	0.051 ± 0.033	0.00 ± 0.00	0.00 ± 0.00	0.00 ± 0.00	0.00 ± 0.034
Ti	0.044 ± 0.022	0.10 ± 0.04	0.032 ± 0.032	0.0077 ± 0.0054	0.86 ± 0.10
V	0.0016 ± 0.0006	0.0017 ± 0.00088	0.0023 ± 0.0000	0.0002 ± 0.0002	0.018 ± 0.002
Cr	0.011 ± 0.005	0.017 ± 0.009	0.052 ± 0.030	0.0079 ± 0.0050	0.12 ± 0.02
Mn	0.022 ± 0.007	0.033 ± 0.010	0.031 ± 0.014	0.010 ± 0.004	0.19 ± 0.03
Fe	13 ± 11	2.9 ± 0.9	1.6 ± 0.2	1.6 ± 0.5	9.2 ± 1.3
Co	0.002 ± 0.010	0.0030 ± 0.0091	0.002 ± 0.017	0.000 ± 0.011	0.017 ± 0.003
Ni	0.031 ± 0.074	0.032 ± 0.062	0.17 ± 0.12	0.008 ± 0.027	0.064 ± 0.006
Cu	0.083 ± 0.017	0.10 ± 0.04	0.061 ± 0.029	0.038 ± 0.013	0.15 ± 0.02
Zn	0.11 ± 0.03	0.19 ± 0.04	0.070 ± 0.070	0.028 ± 0.010	0.51 ± 0.09
Ge[c]	0.027 ± 0.020	0.00 ± 0.00	0.00 ± 0.00	0.00 ± 0.00	0.000 ± 0.023
As	0.0002 ± 0.0001	0.0006 ± 0.0003	0.0039 ± 0.00387	0.00010 ± 0.00008	0.0019 ± 0.0005
Se[c]	0.002 ± 0.002	0.004 ± 0.004	0.0036 ± 0.00359	0.00 ± 0.00	0.000 ± 0.018
Br[c]	0.054 ± 0.033	0.005 ± 0.002	0.020 ± 0.020	0.00 ± 0.00	0.000 ± 0.019
Rb	0.00025 ± 0.00015	0.0004 ± 0.00038	0.0014 ± 0.0014	0.0002 ± 0.0001	0.023 ± 0.003
Sr	0.0075 ± 0.0025	0.0070 ± 0.00267	0.0050 ± 0.00409	0.0040 ± 0.0021	0.14 ± 0.01
Mo	0.0035 ± 0.0011	0.0054 ± 0.0010	0.0021 ± 0.00213	0.030 ± 0.030	0.0000 ± 0.0088
Rh	0.00003 ± 0.00003	0.00003 ± 0.00003	0.00023 ± 0.00013	0.00000 ± 0.00000	0.00000 ± 0.00003
Pd	0.00037 ± 0.00036	0.00003 ± 0.00001	0.0022 ± 0.00219	0.00000 ± 0.00000	0.00010 ± 0.00010
Ag	0.00004 ± 0.00003	0.00003 ± 0.00001	0.00001 ± 0.00001	0.0092 ± 0.0074	0.0079 ± 0.0015
Cd	0.00010 ± 0.00005	0.00020 ± 0.00013	0.00014 ± 0.00014	0.00006 ± 0.00006	0.0027 ± 0.0005
Sn	0.008 ± 0.011	0.008 ± 0.010	0.016 ± 0.021	0.000 ± 0.089	0.000 ± 0.032
Sb	0.016 ± 0.003	0.016 ± 0.003	0.012 ± 0.004	0.0067 ± 0.0029	0.017 ± 0.002
I[c]	0.010 ± 0.009	0.014 ± 0.014	0.00 ± 0.00	0.00 ± 0.00	0.000 ± 0.082
Cs	0.0007 ± 0.00065	0.000 ± 0.000	0.0007 ± 0.0007	0.00008 ± 0.00003	0.0013 ± 0.0006
Ba	0.14 ± 0.04	0.33 ± 0.10	0.18 ± 0.05	0.13 ± 0.03	0.31 ± 0.05
La	0.00042 ± 0.00042	0.00086 ± 0.00052	0.013 ± 0.018	0.0002 ± 0.0070	0.0066 ± 0.0012
Ce[c]	0.027 ± 0.024	0.045 ± 0.013	0.00 ± 0.00	0.00 ± 0.00	0.000 ± 0.038
W	0.00053 ± 0.00028	0.00059 ± 0.00035	0.00039 ± 0.00039	0.0003 ± 0.0002	0.0072 ± 0.0014
Pt	0.00015 ± 0.00009	0.00020 ± 0.00017	0.0051 ± 0.00511	0.00001 ± 0.00001	0.00008 ± 0.00004
Tl	0.00001 ± 0.00001	0.00009 ± 0.00006	0.00001 ± 0.00001	0.00000 ± 0.00000	0.00012 ± 0.00004
Pb	0.020 ± 0.007	0.0074 ± 0.0052	0.045 ± 0.006	0.0035 ± 0.0019	0.16 ± 0.03
U	0.00002 ± 0.00001	0.00006 ± 0.00001	0.00009 ± 0.00004	0.00001 ± 0.00001	0.00071 ± 0.00009

[a] Averages for tests (in parentheses) ± SE, in mg/km. When differences between entrance and exit concentrations were slightly negative but not statistically different from 0 (95% confidence interval), values of 0 were entered.

[b] SO_4^{2-}, NO_3^-, NH_4^+, Cl^-.

[c] Analyzed by XRF. All other elements were analyzed by ICP-MS.

Table 6. Emission Rates of $PM_{2.5}$ Mass and Species in Tunnels, by Test Type[a]

	Summer Tests			Winter Tests	
$PM_{2.5}$ Species	Kilborn Weekdays 1.6%–3.0% Trucks (A,B,C,D,E)	Howell Weekdays 6.1%–9.4% Trucks (F,I,J)	Howell Weekends 1.5%–2.4% Trucks (G,H)	Howell Weekdays 7.0%–7.7% Trucks (K,L,M,N,O)	Howell Weekdays 6.6% Trucks (P)
Mass	24.1 ± 6.4	39.3 ± 15.3	67.4 ± 14.8	25.4 ± 3.0	46.3 ± 3.16
OC	6.41 ± 3.29	12.9 ± 6.91	12.9 ± 3.5	8.14 ± 1.47	8.67 ± 1.85
EC	6.87 ± 1.58	10.8 ± 3.88	2.31 ± 0.53	3.69 ± 0.77	2.99 ± 0.40
Inorganic ions[c]	3.65 ± 0.81	6.75 ± 1.85	45.3 ± 21.1	4.96 ± 0.91	13.3 ± 1.27
Sum of all metals measured	3.40 ± 1.11	2.45 ± 0.72	1.25 ± 0.50	3.84 ± 1.68	11.8 ± 0.87
Na	0.98 ± 0.98	0.038 ± 0.038	0.0054 ± 0.0054	0.81 ± 0.30	4.2 ± 0.6
Mg	0.077 ± 0.034	0.044 ± 0.022	0.0046 ± 0.0046	0.10 ± 0.05	2.3 ± 0.3
Al[c]	0.12 ± 0.09	0.00 ± 0.00	0.00 ± 0.00	0.00 ± 0.00	0.46 ± 0.16
Si[c]	0.45 ± 0.16	0.64 ± 0.16	0.00 ± 0.00	0.20 ± 0.12	0.93 ± 0.20
P[c]	0.15 ± 0.06	0.037 ± 0.037	0.070 ± 0.070	0.00 ± 0.00	0.00 ± 0.10
S[c]	1.1 ± 0.4	0.090 ± 0.090	0.15 ± 0.08	0.54 ± 0.04	0.44 ± 0.45
Cl[c]	0.46 ± 0.08	0.19 ± 0.14	0.052 ± 0.052	0.073 ± 0.051	0.23 ± 0.05
K[c]	0.13 ± 0.04	0.065 ± 0.041	0.14 ± 0.13	0.0061 ± 0.0054	0.17 ± 0.03
Ca[c]	0.31 ± 0.07	0.43 ± 0.12	0.013 ± 0.013	0.21 ± 0.08	1.1 ± 0.1
Sc[c]	0.00 ± 0.00	0.0018 ± 0.0018	0.00 ± 0.00	0.00 ± 0.00	0.00 ± 0.012
Ti	0.010 ± 0.007	0.19 ± 0.18	0.47 ± 0.45	0.0063 ± 0.0045	0.18 ± 0.02
V	0.00068 ± 0.00017	0.00040 ± 0.00034	0.00 ± 0.00	0.00010 ± 0.00006	0.0018 ± 0.0004
Cr	0.012 ± 0.007	0.0018 ± 0.0018	0.014 ± 0.014	0.0028 ± 0.0021	0.014 ± 0.006
Mn	0.0058 ± 0.0018	0.0060 ± 0.0038	0.0027 ± 0.0019	0.0071 ± 0.0046	0.026 ± 0.005
Fe	0.51 ± 0.16	0.55 ± 0.12	0.13 ± 0.05	1.8 ± 1.3	1.4 ± 0.2
Co	0.000 ± 0.015	0.0004 ± 0.0060	0.008 ± 0.026	0.00 ± 0.00	0.0013 ± 0.0005
Ni	0.00 ± 0.12	0.009 ± 0.044	0.39 ± 0.17	0.000 ± 0.022	0.0080 ± 0.0025
Cu	0.041 ± 0.007	0.012 ± 0.010	0.016 ± 0.000	0.014 ± 0.008	0.032 ± 0.005
Zn	0.023 ± 0.010	0.028 ± 0.017	0.0085 ± 0.0085	0.024 ± 0.017	0.10 ± 0.02
Ge[c]	0.00 ± 0.00	0.00 ± 0.00	0.013 ± 0.013	0.00 ± 0.00	0.00 ± 0.015
As	0.0021 ± 0.0011	0.00045 ± 0.00014	0.0029 ± 0.0029	0.00023 ± 0.00016	0.00044 ± 0.00036
Se[c]	0.0018 ± 0.0014	0.0055 ± 0.0028	0.00 ± 0.00	0.00 ± 0.00	0.041 ± 0.014
Br[c]	0.0016 ± 0.0009	0.012 ± 0.010	0.00 ± 0.00	0.011 ± 0.011	0.00 ± 0.012
Rb	0.0011 ± 0.0006	0.00046 ± 0.00046	0.00 ± 0.00	0.0001 ± 0.0001	0.0028 ± 0.0009
Sr	0.0016 ± 0.0005	0.0014 ± 0.0010	0.00001 ± 0.00001	0.0014 ± 0.0010	0.024 ± 0.003
Mo	0.0020 ± 0.0008	0.0013 ± 0.0008	0.0011 ± 0.0011	0.017 ± 0.016	0.00 ± 0.0042
Rh	0.00001 ± 0.00000	0.00001 ± 0.00001	0.00 ± 0.00	0.00 ± 0.00	0.00001 ± 0.00002
Pd	0.00012 ± 0.00010	0.00004 ± 0.00003	0.00 ± 0.00	0.00 ± 0.00	0.00 ± 0.00006
Ag	0.00004 ± 0.00002	0.00003 ± 0.00003	0.00 ± 0.00	0.00010 ± 0.00007	0.00052 ± 0.00013
Cd	0.00004 ± 0.00003	0.00005 ± 0.00003	0.00 ± 0.00	0.00012 ± 0.00008	0.00028 ± 0.00012
Sn	0.0016 ± 0.0075	0.016 ± 0.014	0.004 ± 0.032	0.00 ± 0.00	0.14 ± 0.04
Sb	0.0081 ± 0.0022	0.0047 ± 0.0020	0.0011 ± 0.0003	0.0027 ± 0.0016	0.0055 ± 0.0007
I[c]	0.0071 ± 0.0055	0.00 ± 0.00	0.069 ± 0.009	0 ± 0.00	0.00 ± 0.034
Cs	0.00062 ± 0.00053	0.0013 ± 0.0013	0.00 ± 0.00	0.00 ± 0.00	0.00044 ± 0.00041
Ba	0.065 ± 0.013	0.082 ± 0.038	0.031 ± 0.011	0.044 ± 0.020	0.064 ± 0.011
La	0.00008 ± 0.00011	0.00017 ± 0.00033	0.00002 ± 0.00043	0.0000 ± 0.0055	0.00067 ± 0.00023
Ce[c]	0.00 ± 0.00	0.021 ± 0.021	0.056 ± 0.056	0.00 ± 0.00	0.00 ± 0.021
W	0.00020 ± 0.00011	0.00010 ± 0.00005	0.00 ± 0.00	0.00001 ± 0.00001	0.00084 ± 0.00025
Pt	0.00002 ± 0.00001	0.00001 ± 0.00001	0.00 ± 0.00	0.00000 ± 0.00000	0.00002 ± 0.00003
Tl	0.00002 ± 0.00002	0.00001 ± 0.00001	0.00 ± 0.00	0.00000 ± 0.00000	0.00001 ± 0.00003
Pb	0.0031 ± 0.0005	0.0010 ± 0.0010	0.0044 ± 0.0044	0.0053 ± 0.0036	0.024 ± 0.005
U	0.00001 ± 0.00000	0.00 ± 0.00	0.00008 ± 0.00008	0.00001 ± 0.00000	0.00005 ± 0.00003

[a] Averages for tests (in parentheses) ± SE, in mg/km. When differences between entrance and exit concentrations were slightly negative but not statistically different from 0 (95% confidence interval), values of 0 were entered.

[b] SO_4^{2-}, NO_3^-, NH_4^+, Cl^-.

[c] Analyzed by XRF. All other elements were analyzed by ICP-MS.

between entrance and exit concentrations were slightly negative but not statistically different from 0 (95% confidence interval), values of 0 were entered in the tables.

Tunnel tests were 4 or 8 hours long to obtain sample filter loadings in the optimal range for ICP-MS analysis, but for gravimetric mass measurements, the low loadings resulted in relatively high measurement uncertainties. Masses of $PM_{2.5}$ and PM_{10} were therefore also reconstructed by summing measurements of chemicals that had less uncertainty for low filter loadings, including OC, EC, the inorganic ions SO_4^{2-}, NO_3^-, NH_4^+, and Cl^-, and elemental oxides. Individual species concentrations were obtained from collocated filters in each sampler. OC mass was multiplied by 1.4 to estimate the mass of organic compounds, and element masses were added as the mass of the most common oxide (Kleeman et al 2000; Allen et al 2001), which is more relevant for mass comparisons than individual element masses are. The gravimetric measurements showed excellent agreement with the reconstructed mass values, but we used the reconstructed masses as the best estimates of the mass emission rates because they had much lower total uncertainties. The average $PM_{2.5}$ reconstructed mass was 102% ± 24% of the average gravimetric value; PM_{10}, 106% ± 12%.

Emission rates of PM_{10} in the tunnel tests were 38.7 to 201 mg/km, with an average rate of 91.9 ± 14.7 mg/km. $PM_{2.5}$ emission rates were 9.1 to 82.2 mg/km, averaging 33.4 ± 5.3 mg/km. The PM_{10} emissions fall between the emission rates reported previously for light-duty vehicles (9 mg/km) and heavy-duty vehicles (420 mg/km) in the Fort McHenry Tunnel (Pierson et al 1996). Comparable emission rates of 69 ± 30 mg/km for PM_{10} and 52 ± 27 mg/km for $PM_{2.5}$ were reported for tests in the Sepulveda Tunnel, which had traffic volumes and fleet composition similar to those in the present study (Gillies et al 2001).

Average emission rates of OC and EC in PM_{10} were 26.5 ± 4.4 and 8.4 ± 1.7 mg/km, respectively, accounting for 29% ± 3% and 9.3% ± 1.5% of PM_{10} roadway mass emissions. PM_{10} emissions in summer tunnel tests are shown in Figure 11. Emission rates of OC in $PM_{2.5}$ were 1.5 to 23.6 mg/km, average 9.2 ± 1.8 mg/km; of EC, 1.6 to 17.2 mg/km, average 6.0 ± 1.2 mg/km.

The OC measurements in both PM_{10} and $PM_{2.5}$ size fractions are similar in magnitude and mass fraction to measurements in the Sepulveda Tunnel (Gillies et al 2001), Caldecott Tunnel (Allen et al 2001), and Van Nuys Tunnel (Fraser et al 1998). In this study, we found more OC than

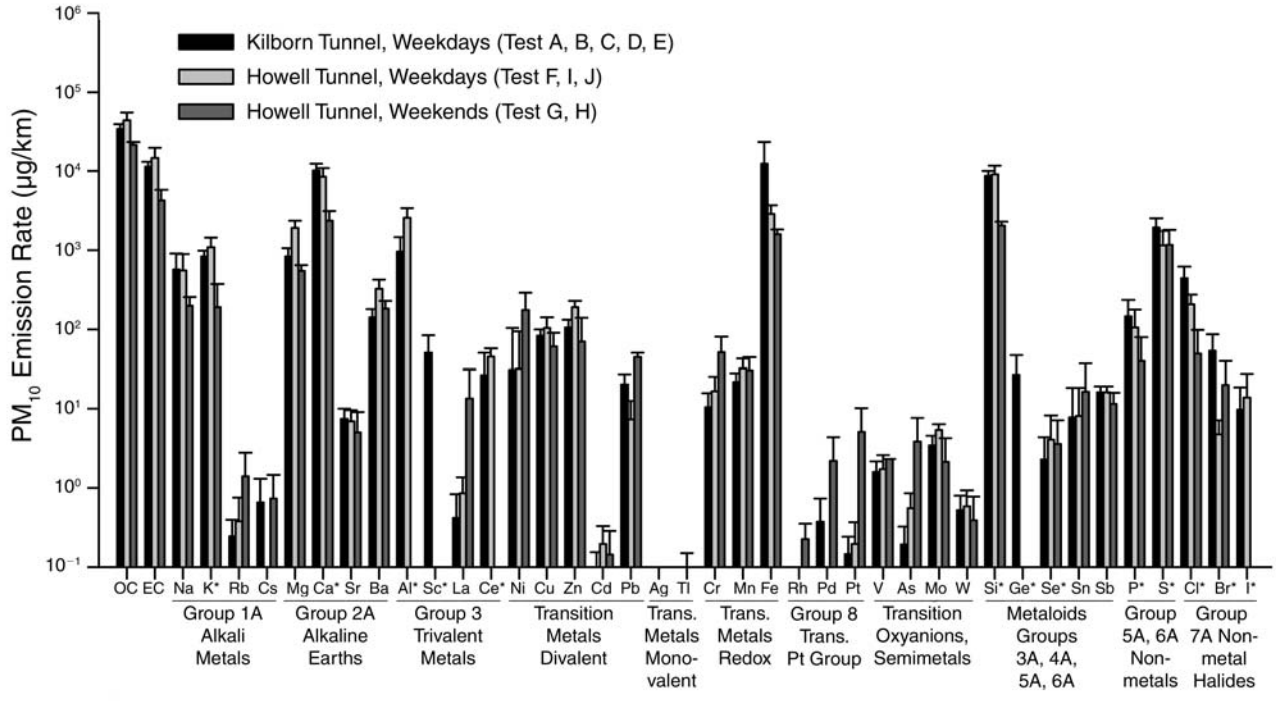

Figure 11. Emission rates of chemical species (by periodic table groups) in PM_{10} from vehicle fleets measured in two Milwaukee tunnels in summer. Error bars indicate the standard error of the average for tests of each type; * indicates analyzed by XRF. All others were analyzed by ICP-MS.

EC in both size fractions, opposite of the findings in the Sepulveda Tunnel and Caldecott Tunnel studies. This discrepancy may be due to differences between the methods used for analyzing EC and OC (Chow et al 2001; Schauer et al 2003). The Van Nuys Tunnel study, which applied the US National Institute for Occupational Safety and Health 5040 method also used in the present study, had very similar ratios of carbon species in the $PM_{2.5}$ fraction to those reported here.

Ratios of EC to OC averaged 0.31 ± 0.04 in PM_{10} emissions for the mixed fleet in this study, but the average ratio in $PM_{2.5}$ was somewhat higher, 0.44 ± 0.06. These results reflect enrichment of PM_{10} with OC from sources such as road dust and wear of organometallic brake pads (Rogge et al 1993). Also, under the low-speed, low-engine-load operating conditions in these tunnels, emissions of EC from heavy trucks are expected to be relatively low (Foster et al 2002; Okada et al 2003; Shah et al 2004); such low values are consistent with the measured $PM_{2.5}$ EC/OC ratio. However, small increases in numbers of heavy-duty trucks affected EC emissions in the Howell Tunnel. Summer weekday and weekend EC/OC ratios in PM_{10} in that tunnel were similar (weekday, 0.31 ± 0.04; weekend, 0.21 ± 0.09) but EC/OC ratios in $PM_{2.5}$ differed: the contribution of EC was more distinct. Weekend tests, with approximately 2% heavy-duty truck traffic, had a $PM_{2.5}$ EC/OC ratio of 0.18 ± 0.01; in weekday tests, with approximately 7% heavy-duty vehicles, the ratio was 0.74 ± 0.01.

The sum of the inorganic ions SO_4^{2-}, NO_3^-, NH_4^+, and Cl^- composed, on average, 20% ± 4.8% of PM_{10} emissions and 20% ± 3.4% of $PM_{2.5}$ emissions. Of these, SO_4^{2-}, NO_3^-, and NH_4^+ emissions were similar across all test types. Cl^- emissions, however, varied distinctly with season, averaging 2.5% ± 0.9% of PM_{10} mass in summer tests and 34% ± 7.9% in winter tests (excluding test P; Figure 12), as a result of salt application on roadways in winter. In contrast, average winter Cl^- emissions for $PM_{2.5}$ were similar to average summer emissions, averaging overall 1.0 ± 0.2 mg/km and 4.1% ± 1.5% of $PM_{2.5}$ mass. Test P had a much higher PM_{10} Cl^- emission rate than any other test, 125 ± 1.1 mg/km, but it contributed 28% ± 1.0% of PM_{10} mass, similar to the other winter tests. Also, distinct weather conditions during test P resulted in much higher emissions of Cl^- in $PM_{2.5}$, 10 ± 0.8 mg/km, 23% ± 2.3% of mass (Figure 12).

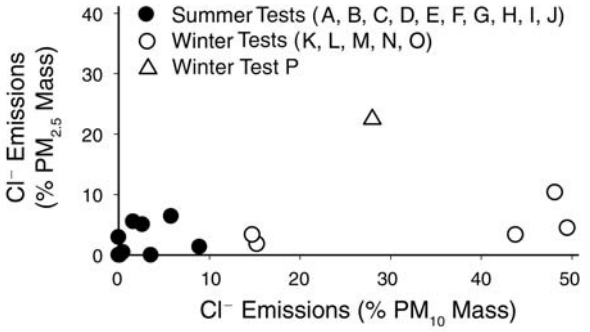

Figure 12. Cl^- emissions as percentage of $PM_{2.5}$ and PM_{10} mass in tests in two Milwaukee tunnels. Data are the average of each test.

Although the weather within the tunnels during all tests was dry, a considerable amount of snow present outside the Howell Tunnel during the winter tests caused the roadway within the tunnel to be wetted by snow and slush carried in with the vehicles. Because the wet roadway attenuated resuspension of road dust, average winter PM_{10} mass emission rates were less than half those in similar summer weekday tests, whereas $PM_{2.5}$ mass emissions were similar in summer and winter (Figure 13).

According to the local climatologic record, average daily temperatures during winter tests K, L, M, N, and O were fairly constant at 0°C to 2°C (32°F to 35°F), warm enough to melt snow and keep the roadway wet. However, the day before test P was slightly warmer, melting even more snow and thoroughly wetting the roadway. The nighttime low before test P was −5°C (23°F), which may have prompted road crews to apply extra salt to prevent freezing. After a warm day and a cold night, the daytime temperature during test P did not exceed 0°C (32°F), promoting drying of the wet, salted roadway. Therefore, the road became relatively drier throughout test P, and resuspension of dried salts and the drying of salty spray were great sources of emissions in both PM_{10} and $PM_{2.5}$. The effect of the drier conditions on emissions of elements from resuspended soil and salts was also apparent in test P, as discussed later in this section.

Emission rates of total elements in PM_{10} measured by XRF and ICP-MS were 1.8 ± 1.6 to 78.5 ± 56.6 mg/km, and the average emission rate accounted for 18.9% ± 2.4% of

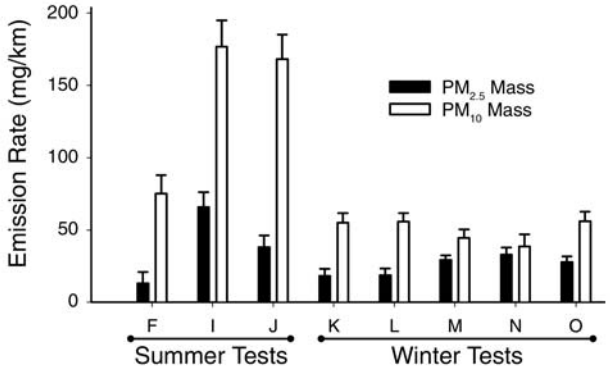

Figure 13. $PM_{2.5}$ and PM_{10} mass emission rates in comparable summer and winter weekday tests in Howell Tunnel. Error bars indicate the standard error of the average for each test.

PM_{10} mass. The most abundant elements emitted in PM_{10} in the tunnel were Fe (average, 4.5% ± 1.7% of PM_{10} mass), Ca (4.2% ± 0.9%), Si (3.9% ± 0.8%), Na (2.2% ± 0.8%), Mg (1.1% ± 0.2%), S (0.84% ± 0.26%), Al (0.69% ± 0.24%), and K (0.41% ± 0.10%). The sum of these eight elements accounted for an average 94% ± 1% of the total PM_{10} emission of 42 measured elements. They were present in $PM_{2.5}$ in much lower amounts, significantly different from 0 in only a few tests.

These eight elements, major components of crustal materials and soil, are predominantly attributed to resuspended road dust because of the large amounts present in PM_{10}. However, a variety of other emission sources may also contribute to their levels, such as combustion of motor-oil additives for Ca, Mg, and S, and wearing of engines, tires, and brakes for Fe, Si, and Al (Cadle et al 1997; Garg et al 2000). S is emitted primarily from emissions of fuel, motor oil, and additives such as zinc dithiophosphate (Cadle et al 1997). For measurements in the Sepulveda Tunnel, Gillies and colleagues (2001) reported S emission rates of 1.05 ± 11.94 mg/km in PM_{10} and 0.32 ± 0.56 mg/km in $PM_{2.5}$, similar to average measurements in our Milwaukee tunnel tests (1.0 ± 0.27 mg/km in PM_{10}; 0.51 ± 0.14 mg/km in $PM_{2.5}$). S was somewhat correlated with crustal elements in PM_{10} (r^2 with Si = 0.49; Ca = 0.42, K = 0.35, and Fe = 0.22) but not in $PM_{2.5}$ ($r^2 < 0.02$) or with other elements in either size fraction.

Significant emissions of Ba, Zn, Cu, Sb, and Pb were also detected in PM_{10} in all tunnel tests (Figure 11; Table 5), which is consistent with the results of other tunnel studies (Gillies et al 2001; Sternbeck et al 2002). Although the sum of these five elements did not exceed 1% of PM_{10} mass, they may be important for health effects, and they can indicate sources of particulate matter emissions, such as brake wear. Brake wear emissions contain significant amounts of Ba, Zn, Cu, and Sb, as well as Fe and other crustal elements (Garg et al 2000).

Sb, which has been suggested as a tracer for brake wear (Dietl et al 1997), was correlated in PM_{10} with Cu ($r^2 = 0.72$) and Ba ($r^2 = 0.52$) and to a lesser extent with Zn, Ca, and Si ($r^2 = 0.30$, 0.28, 0.26, respectively), suggesting that other sources (such as road dust) exist for these elements. Because resuspended road dust is generally too large to dominate the fine particle fraction, correlation between these elements in the $PM_{2.5}$ fraction indicates that brake wear may be an important source. In $PM_{2.5}$, Sb had higher correlations with Cu, Ba, Si, and Ca ($r^2 = 0.77$, 0.64, 0.58, and 0.45, respectively). Correlation between Sb and Zn was not greater in $PM_{2.5}$ than in PM_{10}, indicating that other sources in the $PM_{2.5}$ size range are also important for Zn, including tailpipe emissions of motor oil (Huang et al 1994; Cadle et al 1997) and tire wear (Harrison et al 1996).

Fe, one of the most abundant measured elements, showed no correlations with other elements associated with brake wear because of its ubiquity in possible sources such as crustal materials and tailpipe emissions. Although vehicles tended to brake in the curved Kilborn Tunnel but not in the straight Howell Tunnel, emissions of brake wear elements were not greater in the Kilborn Tunnel. No appreciable differences were found in PM_{10} emission rates between the two tunnels. In $PM_{2.5}$, Cu and Sb emissions were higher in the Kilborn Tunnel, but not significantly so (Figure 14). Sternbeck and associates (2002) suggested that brake wear particles can accumulate on wheelrims during braking and later be resuspended, which would account for similar per-kilometer emission rates of wear-related elements in both tunnels in this study.

Pb can be emitted from several sources, including fuel and motor oil combustion, brake wear, and resuspension of enriched road dust (Cadle et al 1997; Garg et al 2000; Young et al 2002). In tests with significant Pb emissions, the fraction in $PM_{2.5}$ accounted for only up to 17% of that in PM_{10}, indicating that resuspended road dust was likely the predominant source of Pb. Industrial sources and tailpipe emissions prior to the phaseout of leaded gasoline have been proposed as the causes of Pb enrichment in roadway dirt; a more likely source of this persistent Pb enrichment is Pb wheel weights, which are dropped from vehicle wheels and pulverized by traffic (Root 2000). A number of cars manufactured before 1980, which used leaded fuel before it was phased out, were noted and videotaped on the weekend in the Howell Tunnel. But Pb levels were an order of magnitude lower in $PM_{2.5}$ than in PM_{10}, and not significantly so, indicating that tailpipe emissions from older cars were not an important source of emissions in this study.

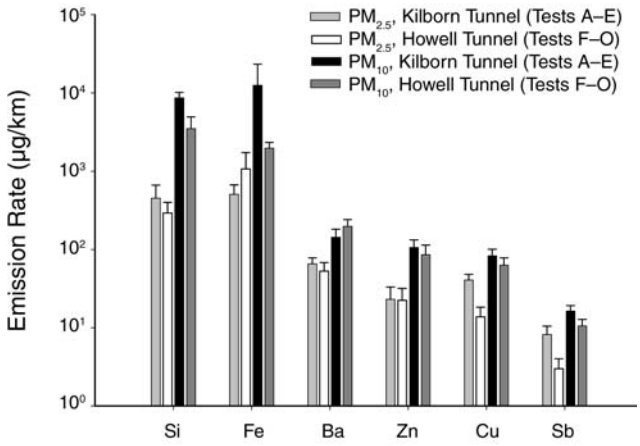

Figure 14. Emissions of elements in PM_{10} and $PM_{2.5}$ associated with brake wear. Error bars indicate the standard error of the average for tests of each type.

Although older vehicles did not appear to affect Pb emissions, they did appear to affect emissions of the Pt group metals (Pt, Rh, and Pd). These elements, components of catalytic converters, have been detected in automobile emissions and road dust in many studies. In a study in Germany (cited by Zereini et al 2001), estimated roadway emissions of Pt from catalytic converters, from measurements in soil and traffic volume, averaged 270 ng/km; in a second bench experiment, average Pt emission rates were 9 to 124 ng/km. Zereini and colleagues (2001) also noted that noble-metal emissions vary with the age of the catalytic converter. Quantities of Pt detected in tunnel tests of this study (Figure 11; Tables 5 and 6) are similar to the quantities found in those studies.

In all weekday tests (except test P), average PM_{10} emission rates of Pt were 100 ± 49 ng/km; Rh, 17 ± 11 ng/km; and Pd, 150 ± 130 ng/km. In summer weekend test H conducted in the Howell Tunnel, however, emission rates were at least an order of magnitude higher than those in any other test: Pt, 10,200 ± 2500 ng/km; Rh, 350 ± 85 ng/km; and Pd, 4400 ± 2800 ng/km. This test was conducted on Sunday afternoon, when several older, classic vehicles passed through the tunnel. Significant emissions of these elements were probably from these older cars, suggesting differences in emissions related to early catalytic converter technologies.

To investigate the contribution of heavy-duty vehicles in the fleet to overall roadway metal emissions, we compared weekday tests (F, I, J) and weekend tests (G, H) in the Howell Tunnel during summer. These tests were conducted under similar temperature and road surface conditions but much different traffic compositions. The weekday tests had higher traffic volume and a higher proportion of trucks (~7%) than the weekend tests (~2%) (Table 1). Although light-duty vehicles constituted the vast majority of the vehicle fleets, a small fraction of heavy-duty trucks can considerably affect particulate matter emissions, through tailpipe emissions as well as increased resuspension of soil. Corresponding with increased traffic and fraction of heavy-duty trucks, weekday PM_{10} emissions (140 ± 33 mg/km) were much greater than weekend emissions (54 ± 8 mg/km). Weekday PM_{10} emissions of EC and total metals were greater than weekend emissions by a factor of approximately 3, whereas OC emissions were doubled.

These large differences in emission rates of PM_{10} elements between weekday and weekend tests were generally attributable to the contribution of crustal elements (Na, Mg, Al, Si, Ca, and Fe) from resuspended road dust (Figure 15; Table 5). The greater number of large trucks on weekdays resulted in increased resuspension of road dust, which has also been observed in other studies (Moosmuller et al 1998). The greater weekday traffic volume, with a more constant flow of traffic and fewer gaps between groups of vehicles, may also have contributed to the difference. Higher weekday PM_{10} emissions of some wear elements (Cu, Zn, Sb, and Ba) were also observed (Figure 15), reflecting increased resuspension of enriched road dust and possibly also greater tire and brake wear from heavy-duty trucks.

The effect of heavy-duty trucks in the Howell Tunnel in summer was apparent in the higher weekday than weekend EC/OC ratio in $PM_{2.5}$, but the low levels of metals in $PM_{2.5}$ were not statistically differentiable between tests. S, which is expected to be emitted in much higher amounts from heavy-duty vehicles because S levels are higher in diesel fuel (Lowenthal et al 1994), was not present in significant amounts in either size fraction. The average ratio of $PM_{2.5}$ emissions to PM_{10} emissions for weekday tests was 0.26 ± 0.06, much smaller than the 0.84 ± 0.39 ratio for the weekend tests, showing greater weekday contribution of coarse particles from resuspension.

Figure 16 presents emission rates of mass and Si in $PM_{2.5}$ and PM_{10} with the percentage of heavy-duty trucks

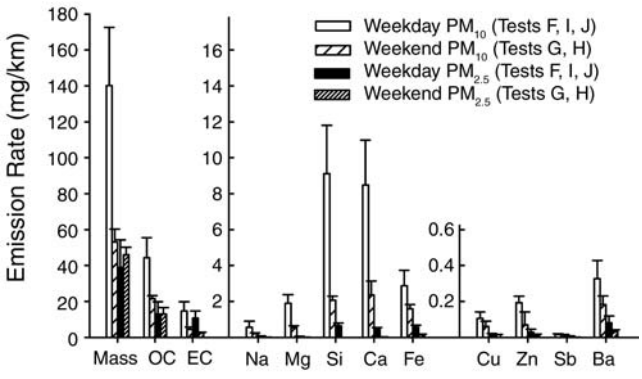

Figure 15. Howell Tunnel weekday and weekend emissions of selected elements in PM_{10} and $PM_{2.5}$, summer tests. Error bars indicate the standard error of the average for tests of each type.

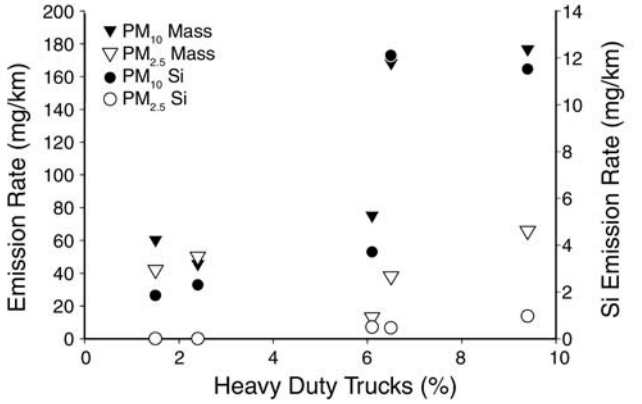

Figure 16. Mass and Si emissions in PM_{10} and $PM_{2.5}$ versus percentage of heavy-duty trucks in the Howell Tunnel summer tests. Data are the averages for each test (F, G, H, I, J).

in the vehicle fleet during summer tests in the Howell Tunnel. Increased percentages of heavy-duty trucks were associated with relatively low increases in $PM_{2.5}$ emission rates and much larger increases in PM_{10} emissions.

Winter tests (K, L, M, N, O, and P) conducted in the Howell Tunnel during weekdays were similar in traffic volume and composition to the summer weekday tests (F, I, and J). Again, test P was treated separately from the five other winter tests because of its unique profile. Emission rates were lower in winter tests than in summer tests by a factor of approximately 2, largely because wetting of the road surface by melting snow limited road dust resuspension in winter.

Elemental emission rates from summer and winter Howell Tunnel tests were also compared (PM_{10} data shown in Figure 17). Few elements were present at significant levels in PM_{10} in winter tests. However, test P showed a unique distribution of elements and had the highest PM_{10} mass emission rate (446 ± 14 mg/km) of any summer or winter tunnel test. The measured mass and chemically reconstructed mass values for test P agreed well. The contribution of elements measured by ICP-MS and XRF in test P was 192 ± 10 mg/km, or 43% ± 2.7% of the PM_{10} mass. Metal emissions in test P were predominantly (57% ± 5%) composed of elements that are components of road salts and crustal materials (Si, Na, Mg, Fe, K, and Ca). Increased emissions of enriched road dust also affected emissions of less abundant elements (including Cu, Zn, Sb, Ba, and Pb). Size distributions of Na and Mg were similar to that of Cl^-, with both elements contributing a much larger fraction of $PM_{2.5}$ mass in test P than in other tests.

In summer weekday tests in the Howell Tunnel, Na and Mg each accounted for significantly less than 1% of $PM_{2.5}$ mass; however, in winter test P, Na contributed 9.2% ± 1.4% and Mg contributed 4.9% ± 0.68%. For the other elements, percentages in $PM_{2.5}$ and PM_{10} were very similar between test P and other tests, indicating that their high emissions in test P were primarily due to weather conditions that promoted resuspension of enriched road dust. The high levels of emissions in test P could also have resulted from brake and tire wear particles being more freely emitted under dry roadway and wheel conditions than in the wetter conditions of the other winter tests, although ratios of brake wear elements did not differ significantly between test P and the other winter tests.

These results show that the resuspension of road dust, which plays an important role in emissions of metals from roadways, depends on weather and road surface conditions, including wetness and presence of excess dirt. Thus simply averaging the contribution of road dust under different roadway conditions could easily overestimate or underestimate direct vehicle emission rates.

To investigate size distributions of particulate matter emissions in the Howell Tunnel, MOUDIs were collocated and operated in winter tests O and P in parallel with the other aerosol samplers. To obtain enough mass for analysis, the impactors were operated with one set of substrates on the two consecutive days, for 16 hours total. Figure 18 shows size distributions of roadway emissions for eight elements (Mg, Fe, Ca, Cu, Sr, Sb, Ba, and Pb) collected by MOUDIs in significant amounts. These samples include emissions in test P, the winter test that involved a road-dust resuspension event.

Elemental size distributions showed primary modes in the coarser range of particles (1.0–18 µm), consistent with resuspension of road dust and particles from tire and brake wear. Emissions of wear elements (Sb and Ba) showed size

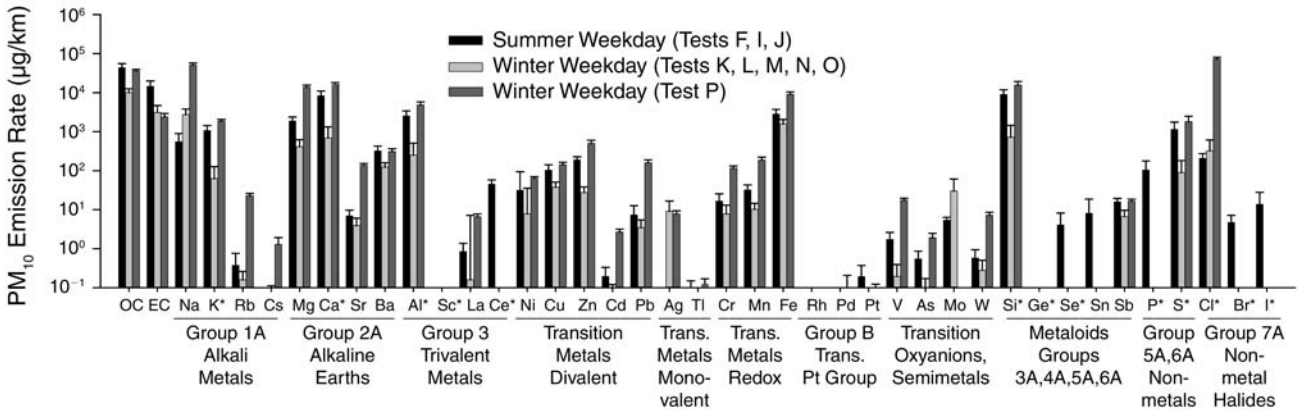

Figure 17. Weekday Howell Tunnel emissions of chemical species (by periodic table groups) in PM_{10}: summer tests, winter test P, and the other winter tests. Error bars indicate the standard error of the average for tests of each type. *, analyzed by XRF. All others were analyzed by ICP-MS.

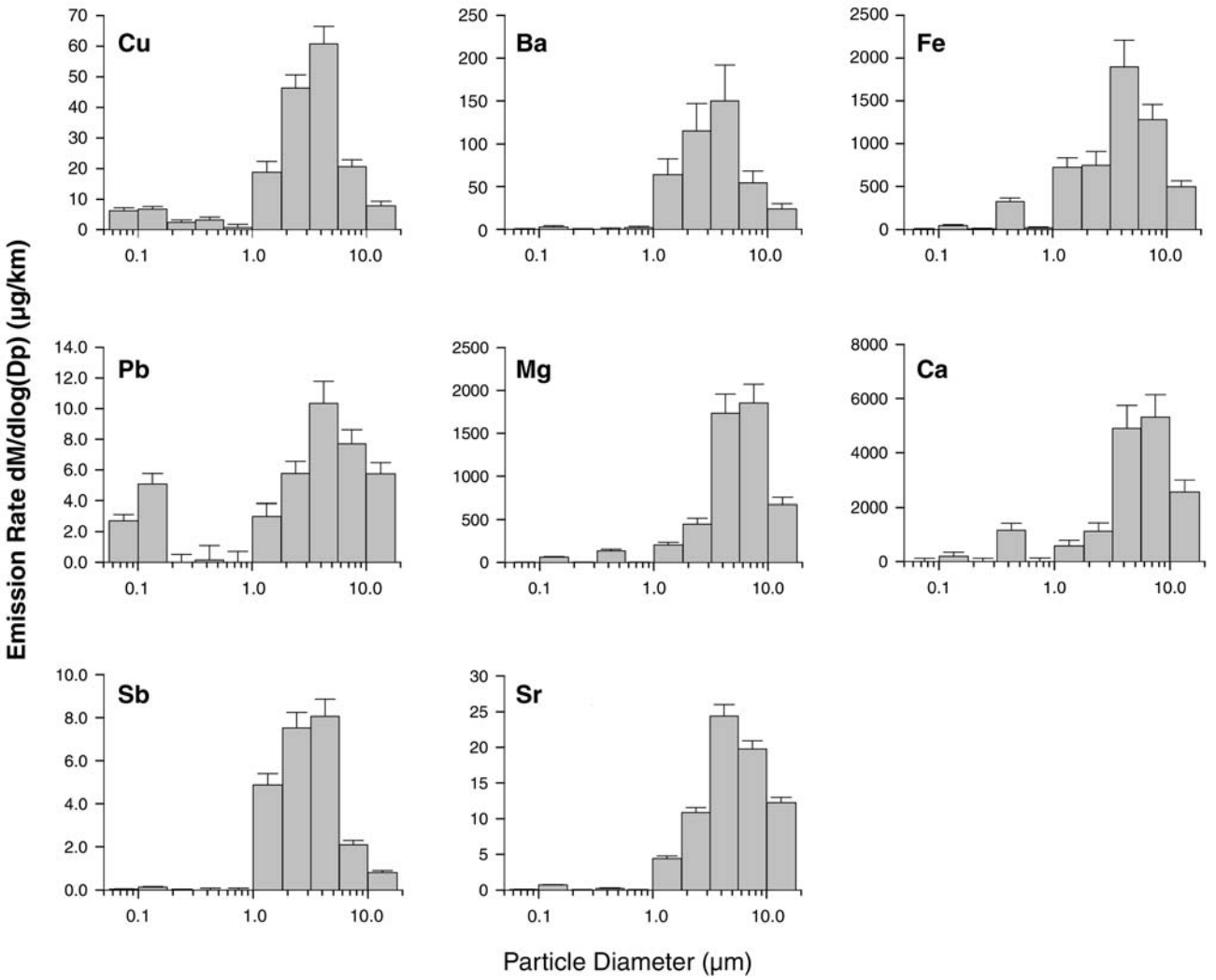

Figure 18. Size-resolved metal emissions from Howell Tunnel winter tests O and P. Samples were collected with 11-stage MOUDIs and analyzed by ICP-MS. Error bars indicate the standard error of the average over the 16 hours of sampling on two consecutive days. Note different y-axis scales among the panels.

distributions similar to those of the crustal elements, consistent with their emission from enriched road dust. Submicron modes, indicative of nonmechanical processes such as combustion of fuel and lubricating oil or vaporization from hot brake surfaces, were also seen for some elements (Pb, Ca, Fe, and Cu). Pb and Cu had bimodal distributions. Submicron emissions of Ca and Fe were less, which can be attributed to tailpipe emissions of lubricating oil as their source and is consistent with previous studies (Gertler et al 2002).

Brake and Tire Wear Profiles

The particulate matter emissions in the RL-SHED tests came from both brake wear and tire wear. Wearing of external engine parts, such as fan belts, could also have contributed to these emissions, but such contributions are probably negligible, particularly because the vehicles tested were late models in good working order.

To investigate the contributions of tire wear to particulate matter levels in the chamber, we measured the chemical compositions of tires from vehicles used in the dynamometer tests. The chemical analysis of resuspended tire samples, which showed that emissions from tire wear were predominantly OC and EC with very low metal levels, indicated that tires were an insignificant contributor to metal emissions in the RL-SHED. In these tire samples, OC accounted for 69% ± 2% (average ± SE) of PM_{10} mass and 64% ± 1% of $PM_{2.5}$ mass. If this fraction of OC were converted to mass of organic compounds, it would account for nominally 100% of the measured mass if an empirical factor of 1.5 were applied to compare OC and compound mass.

Zn was the only element measured in the three tested tires that was present in significant amounts, indicating that metal emissions from tire wear in the RL-SHED were negligible. Zn levels in resuspended PM_{10} samples of tires were 0.054% ± 0.018% (average ± SE) of the OC mass. If the maximum PM_{10} mass fraction of total OC in the RL-SHED tests, 0.36 ± 0.06, were entirely due to tire wear, and if the tires had the maximum Zn/OC ratio, Zn emissions in PM_{10} would still be much greater than would be possible from tire wear. No metals other than Zn were significantly affected by tire wear in the dynamometer tests.

Emission rates of bulk species in PM_{10} and $PM_{2.5}$ from the RL-SHED are shown, by driving cycle test, in Figure 19. The measured concentrations in the chamber in all tests are presented in Appendix C (available on request from HEI). Because of analytic problems, PM_{10} samples were available for only four of the eight tests. To represent organic compound mass, OC was multiplied by 1.4. Metals are shown as metal mass, rather than oxides, because many are present as metallic species (Blau 2001) and because the dominant oxide, sulfide, and other metal species present are not known.

For both vehicles in the driving cycle tests, OC and Fe dominated the emission composition. Differences occurred between test types and between the two vehicles. For both vehicles, emission rates were highest in the UC tests, which had the most extreme vehicle accelerations and decelerations. $PM_{2.5}$ emissions in the two FTP tests for each vehicle were similar in magnitude and composition; PM_{10} data were available for only one FTP test of each vehicle and cannot be compared. Although SS tests included no braking, the results showed low but measurable $PM_{2.5}$ emissions, greater than levels in blank tests. This result indicates that dust from brake wear built up in the vehicle's brake housing during the hard decelerations of the UC tests and was emitted in subsequent tests.

Emissions for individual species in $PM_{2.5}$ and PM_{10} for the UC test and one of the two FTP tests of each vehicle are shown in Figure 20. Among the measured elements, Fe and Ba were the most abundant, with levels an order of magnitude higher than those of most other elements. The next most abundant were light crustal elements (Mg, Al, Ca, Na, K, and Ti); in roadway emissions these likely to have resulted from resuspended road dust. They are not presented in Figure 20, therefore, in order to show comparisons between trace elements that are more likely to reflect brake wear. After crustal elements, the most abundant measured metals were Zn, Mn, Cu, Cr, V, Sr, Mo, and Sb.

MOUDI samples differed in chemical composition among the size-resolved particles emitted in different types of driving cycle tests. Figure 21 shows emission rates for total measured mass, overlaid with organic compound mass (1.4 × OC) and EC, for four sets of samples. The bottom panels present MOUDI samples that were collected on one set of substrates used over two test periods for each of the two vehicles, whereas the top panels give results of

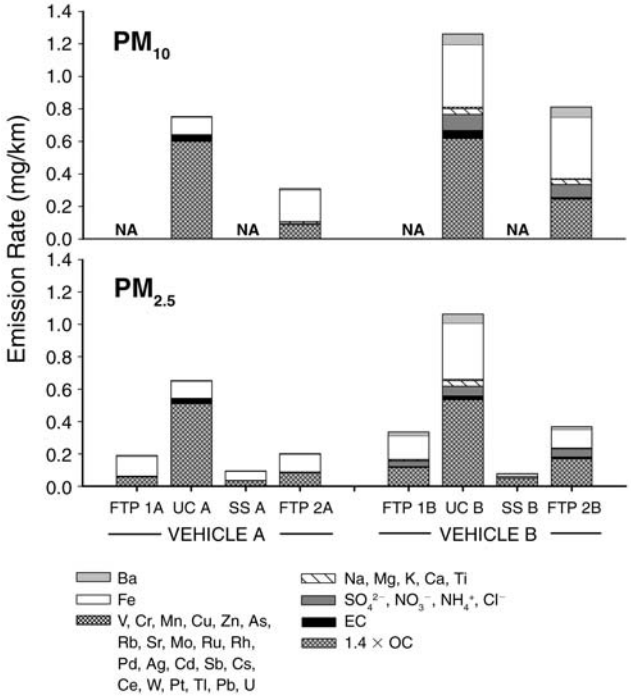

Figure 19. Emission rates in RL-SHED for eight driving cycle tests. Rates are corrected for the results of blank tests (not shown). NA indicates that PM_{10} samples were not available.

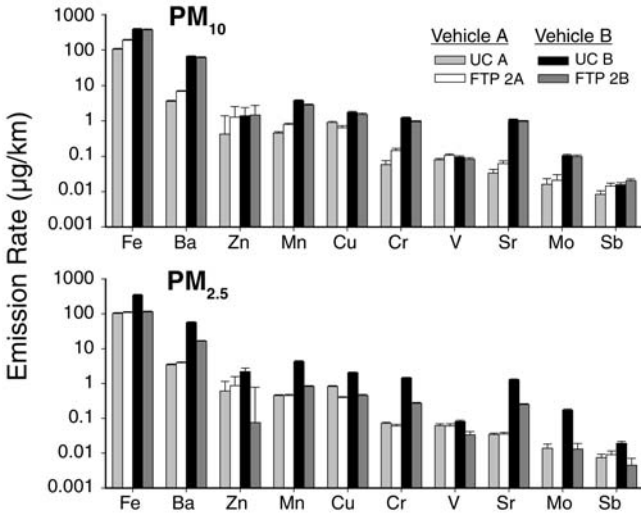

Figure 20. Emission rates of abundant noncrustal species in RL-SHED for four driving cycle tests. Rates are corrected for the results of blank tests (not shown). Error bars indicate the standard error of the average.

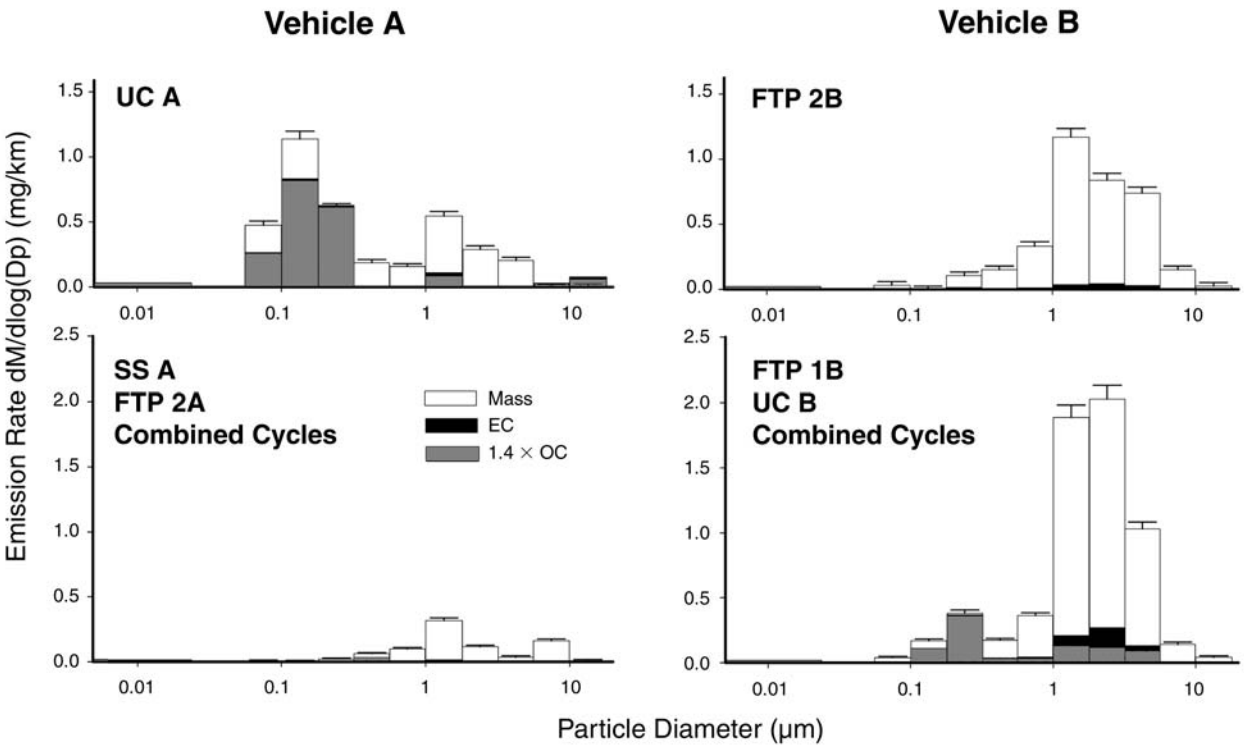

Figure 21. Size-resolved emission rates for driving cycle tests. Error bars indicate the standard error of the average. *Combined cycles* refer to samples collected on one set of substrates used over two test periods.

single tests. Although results from the two vehicles are not directly comparable, similar tendencies can be seen in the results. SS and FTP cycles had low mass emissions, high measurements in the size range 1.0 to 3.2 μm, and no significant OC content. In contrast, UC test emissions show bimodal size distributions, with some in the submicron size range, composed predominantly of organic compounds.

The single UC test of vehicle A and the combined sample of FTP and UC cycles of vehicle B are the only MOUDI tests that showed significant mass in the 0.1 μm size range, the majority of which was organic (Figure 21). The presence of submicron-size organic mass only in UC tests demonstrates that hard acceleration and deceleration created small particles, probably through volatilization and condensation of species from the hot surfaces of brakes and tires. This conclusion is supported by observations of the aluminum MOUDI substrates from both UC tests (not shown). Substrates in the smallest cutpoint stages of the MOUDI (0.056, 0.10, 0.18, and 0.32 μm) had distinct deposition patterns that appeared to be due to liquid droplets impacting the surface. These patterns were not at all similar to patterns of particle bounce. Rather, the substrate surface appeared to be coated by a thin film, as liquid droplets impacted at the nozzles and were spread toward the edges of the substrate by air flowing through the sampler.

In contrast to organic compounds, metals are more likely to be emitted in size fractions larger than 1 μm. Figure 22 presents elemental distributions for MOUDI samples that were collected on one set of substrates over two test periods for vehicle B. The highest mass of Fe was in the 3.2 μm size range; for all other measured elements, the highest mass was in the 1.0 or 1.8 μm size cuts. Levels of all measured elements decreased sharply below 1 μm, and none were present in significant amounts in the size range of 0.1-μm or smaller (the range for which organic compound content was significant). Because mechanically generated particles are expected to be primarily in the coarse fraction of aerosol, the peak emissions of metals within the $PM_{2.5}$ fraction indicates that normal grinding was not the sole mechanism of these brake wear emissions. Chemical processes on the friction-heated surfaces of brake pads and rotors also contribute, most likely through volatilization and condensation (Garg et al 2000; Sanders et al 2002).

Figure 23a shows the compositions of PM_{10} in the RLSHED test emissions, resuspended brake housing dust, and crushed brake pads from each vehicle. (Resuspension and sampling of brake housing dust and crushed brake pads are discussed fully in the next section.) Fe was the predominant contributor to every profile. Only elements that were present in large enough amounts appear in the

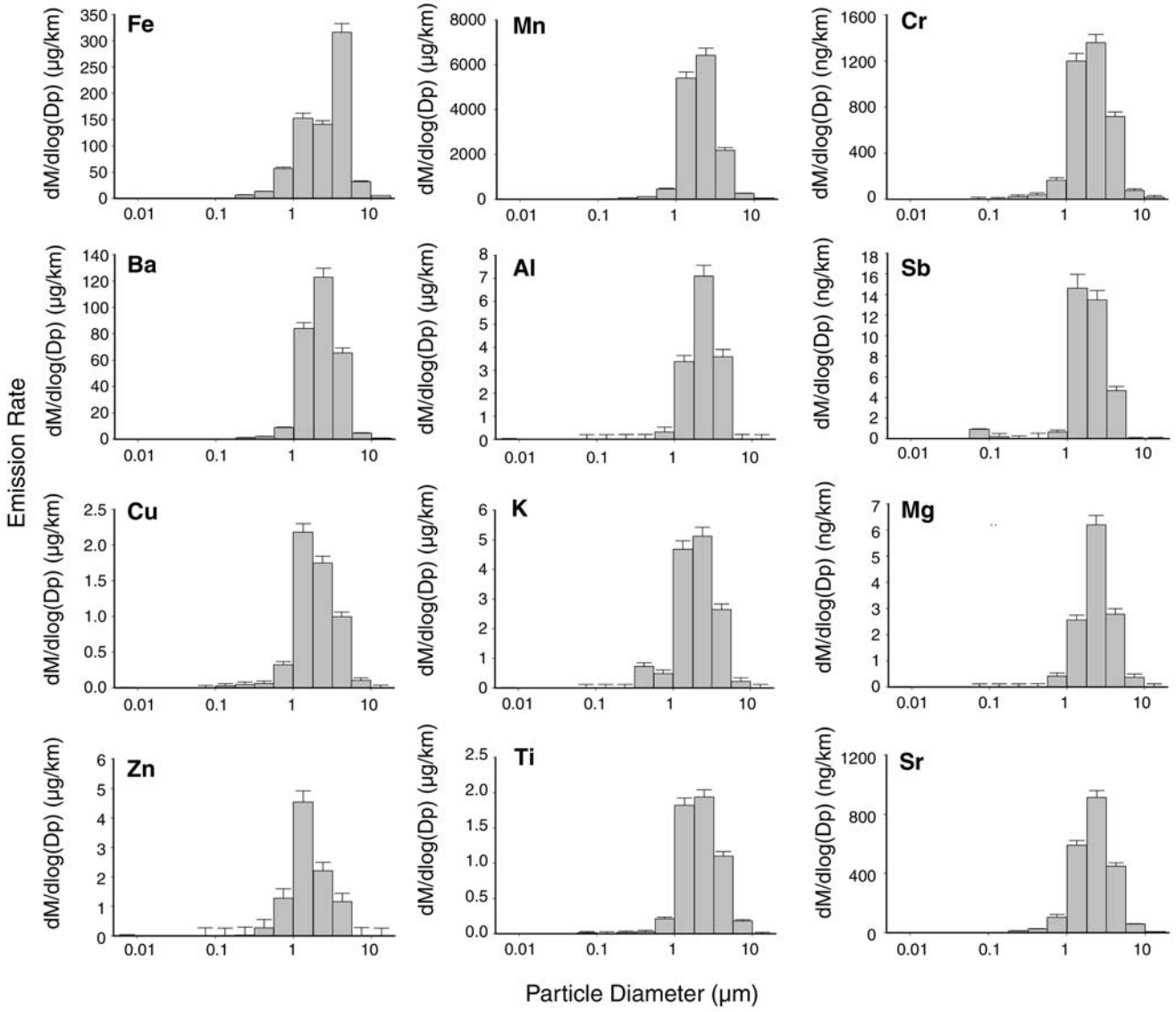

Figure 22. Size-resolved vehicle B metal emission rates, FTP 1B and UC B tests combined. Error bars indicate the standard error of the average. Note different y-axis scales and units among the panels. The mass distribution for these combined tests is in the bottom right panel of Figure 21.

bar graph; those present in smaller amounts are represented by gray shading in the legend. Figure 23b shows the same data but with Fe omitted in order to magnify the relative contributions of the other trace elements.

The measured PM_{10} RL-SHED emissions of each vehicle were more similar in metals composition to brake housing dust than to the crushed brake pad. The contribution of Fe was greater, and the contributions of Ba and light elements (Na, Mg, K, and Ca) were lesser, in the brake housing dust and emissions samples than in the crushed brake pad samples. Other trace elements, notably Cu, were present in significant amounts in brake housing dust and emissions samples but were not present or were present in very small amounts in crushed brake pad samples.

These results could be due to several factors, two in particular. First, the rotor or drum that the brake pad presses against is worn simultaneously with the pad. Rotors on automobiles and trucks are almost always cast iron (Blau 2001), so rotor wear could cause the increased contribution of Fe to the brake housing dust. This increase would be especially likely for vehicle A in our tests, a minivan model that requires new rotors when the brake pads are replaced because of rotor wear (personal correspondence, 9/01, University of Wisconsin Vehicle Fleet staff). Rotor wear also best explains the appearance in brake housing dust and emissions samples of elements that are not present in significant amounts in the brake pads themselves, such as Cu. Wearing of the rotor or other components of the brake

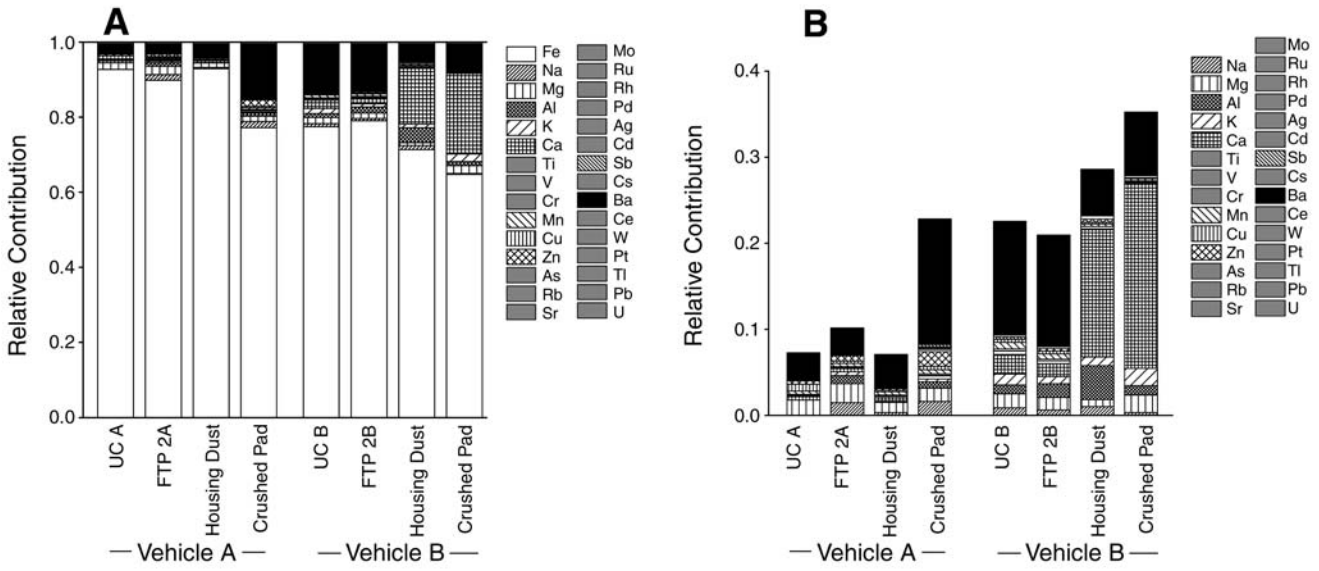

Figure 23. Relative metal contributions to total PM_{10} mass. ***A*****:** RL-SHED test emission rates, brake housing dust, and crushed brake pads from test vehicles. ***B*****:** Excluding iron. Data are the average of the two tests of each type for each vehicle. Note different y-axis scales between the panels. Elements indicated with gray shading do not appear because their relative contributions were too small to show.

system, such as rivets in the pads, could cause increased Cu in the brake housing dust.

A second possible explanation for the differences in relative composition between crushed brake pads and brake housing dust is that some components wear or aggregate into different size fractions. For example, barium sulfate, a major component of many brake pads, is used as a stable filler that accounts for up to 40% of brake pad weight (Blau 2001). The contribution of Ba to brake housing dust mass was much less than its contribution to brake pad mass, however. The increased fraction of Fe from rotor wear may have decreased the relative fraction of Ba in the housing dust, or a portion of the Ba may have been present in particles larger than 10 µm, which were not sampled.

The average size of particulate matter emissions from brake wear has been reported as 1 to 3 µm (Cha et al 1983; Garg et al 2000; Sanders et al 2002), consistent with size-resolved measurements made in the current tests (Figure 21). Because wear processes are likely to emit particles larger than 2.5 µm, however, wear of some components of the brake pad could result in emission of particles larger than 10 µm. Such wear could affect Ba and other components that were less present in the brake housing dust, such as Ti. Wearing into larger particles may also explain why a large fraction of Ca was present in the brake pad and brake housing dust samples of vehicle B but not in emission samples.

These observations indicate that brake wear emissions have a metal composition that is more similar to brake housing dust than to bulk brake pad emissions. Wear of components other than brake pads, and other processes such as oxidation of the brake pad (Blau 2001), alter the composition of brake housing dust relative to that of bulk brake pad material. Dynamometer driving cycle tests with no braking showed significant metal emissions, which also indicates that brake housing dust constitutes much of brake wear emissions. These results suggest that the chemical composition of brake wear emissions for a fleet of vehicles can be best estimated by resuspension and sampling of a range of appropriate brake housing dusts.

Resuspension Profiles

Road Dust Profiles of the relative composition of road dust were similar for PM_{10} and $PM_{2.5}$. Because of analytic problems, reports of trace metals analyzed by ICP-MS do not include Si, which we expected to be a large fraction of the total mass of crustal material samples. Figure 24 presents the relative compositions of the road dust samples for PM_{10} and $PM_{2.5}$ (compositions of all samples are presented in Appendix D, available on request from HEI). PM_{10} accounted for a much larger fraction of total resuspended road dust, but the relative compositions were similar in both PM_{10} and $PM_{2.5}$. In both, OC composed the largest measured fraction, followed by the inorganic ions SO_4^{2-} and Cl^-.

OC is a large component of most soil samples and paved road dusts (Hildemann et al 1991; Ashbaugh et al 2003; Chow et al 2003), including the roadway dust sampled in this study. Water-soluble SO_4^{2-} is also present in soil; here, it constituted 2% to 6% of PM_{10} and $PM_{2.5}$ measured mass, similar to levels found in other soil samples (Chow

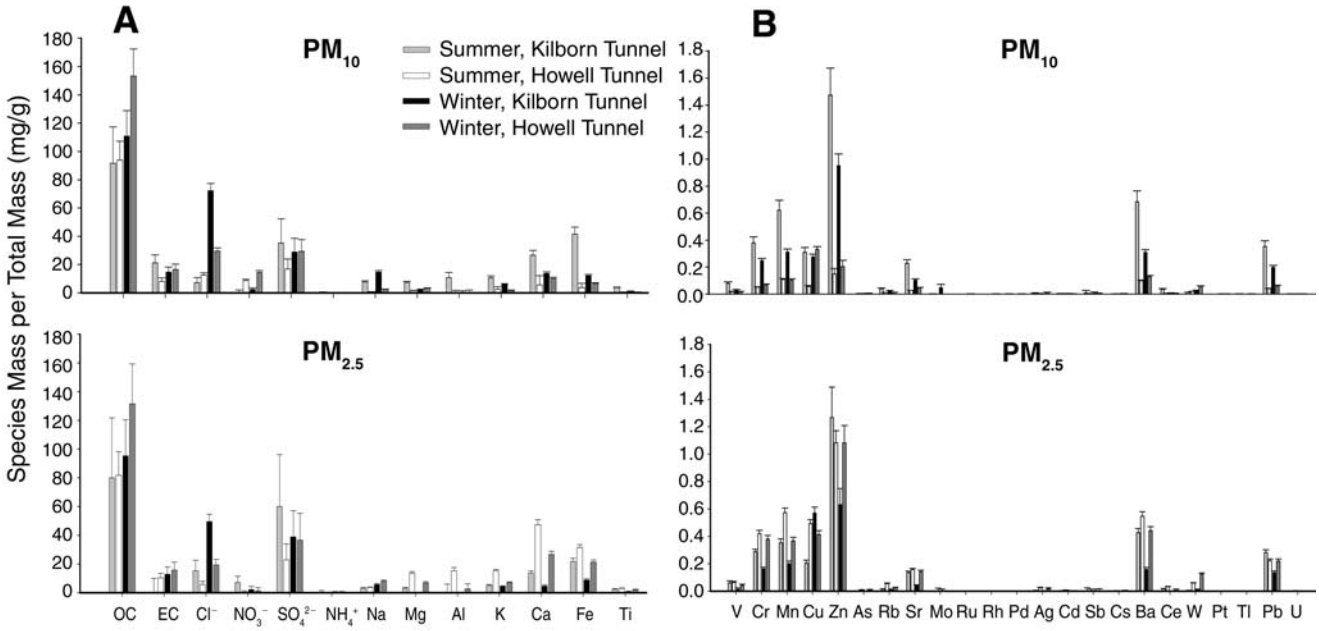

Figure 24. Relative contributions of (*A*) bulk species and crustal elements and (*B*) trace metals to total mass of resuspended road dust. Dust was collected from roadway in two Milwaukee tunnels in summer and winter. Error bars indicate the standard error of the average. Si is not shown because it was not measured.

et al 2003). The large amounts of Cl^- in these road dust samples were predominantly due to the winter application of salt to deice the roads; the percentage of the mass due to Cl^- was at least twice as high in the winter samples for each tunnel and size fraction.

Other major components of these road dust samples included EC, Ca, and Fe, all of which can constitute up to several percent of the mass of nonroad soil (Chow et al 2003). Although all three are emitted from motor vehicles (Cadle et al 1999; Schauer et al 2002), enrichment of road dust by vehicle emissions is probably negligible compared with the amounts of EC, Fe, and Ca also present in nonroad soils. Other components present in these samples (in order of decreasing magnitude) are the crustal elements Na, Mg, Al, and K. Na, like Cl^-, is increased in winter samples by road salt application.

The profiles of measured trace elements in these road dust samples were dominated by Zn, Ba, Mn, Cr, Cu, and Pb, the high concentrations of which reflect enrichment from traffic emissions. Ba, a major component of many brake pad formulations (Blau 2001), is found in relatively large amounts in brake wear emissions (Garg et al 2000). Zn, Mn, and Cu are also found in brake wear emissions and in some tailpipe emissions (Cadle et al 1999; Garg et al 2000; Schauer et al 2002). Cr has not been reported in vehicle tailpipe or brake wear emissions, but it is found in higher concentrations in urban soil and paved road dust than in nonurban soil (Ho et al 2003). Pb is present in crustal materials, but its high levels found in urban soils and road dust are due to previous deposition of Pb from industries or to tailpipe emissions from combustion of leaded gasoline before its phaseout.

Brake Dust Compositions of corresponding crushed brake pads and brake housing dust are shown as relative contribution of metals to total PM_{10} mass in Figure 25 (all data are available in Appendix D). Si was not measured by ICP-MS but was expected to constitute a large fraction of the total mass (Blau 2001). Brake housing dust contained a larger fraction of Fe and a smaller fraction of Ba than did crushed brake pads. Cu constituted a large fraction of several brake housing dust samples but a very small fraction of the corresponding crushed brake pads. Two factors could explain these differences in relative composition between bulk brake pads and brake housing dust (discussed in more detail in the section before last).

First, the rotor (often cast iron) or drum against which the brake pad presses can wear simultaneously with the pad, which would validate the increased contribution of Fe to the dust in our samples. Wearing of components other than the brake pad may also increase the level of Cu. In fact, the two samples that showed a large increase in Cu in the brake housing dust (samples 2 and 3 in Figure 25) were the front and back brakes of the same vehicle, the only two samples from a single vehicle. This unique result indicates that some other component of the brake system on that vehicle wore and contributed Cu to the housing dust.

Second, some components may wear or aggregate into different size fractions, leading to differences between bulk pads and housing dust. The primary example of this factor is barium sulfate. The contribution of Ba to housing dust mass in these tests was much less than the contribution to brake pad mass. In brake pads, Ba content may have been diluted by additional wear from other sources, or a portion may have been present in particles larger than 10 µm, which were not sampled. These resuspension tests do not measure the actual bulk composition of brake pad materials (Blau [2001] and others), rather, the composition of crushed and sieved brake materials.

Overall, wear and other processes such as oxidation alter the composition of brake housing dust relative to bulk brake pad material (Blau 2001), so the housing dust is more relevant to actual brake wear emissions. Therefore, sampled brake housing dust was used to create source profiles for apportioning the total roadway emissions measured in tunnel tests. To construct average source profiles, the brake housing dust samples were divided into semimetallic and low-metallic categories, which relate to different compositions of brake pads. Here, semimetallic refers to dusts with more than 0.1% Cu, 0.2% Zn, 1.0% Ba, and 0.1% Sb by weight. Average compositions for PM_{10} and $PM_{2.5}$ are listed in Table 7.

The semimetallic and low-metallic designations are types of brake pads discussed in the literature, but the range of actual brake pad formulations on the market is vast. The pads randomly collected in this study were classified on the basis of elemental composition only, with five samples in each. Dusts with a markedly higher relative abundance of any trace element tended to also have higher fractions of several other trace elements.

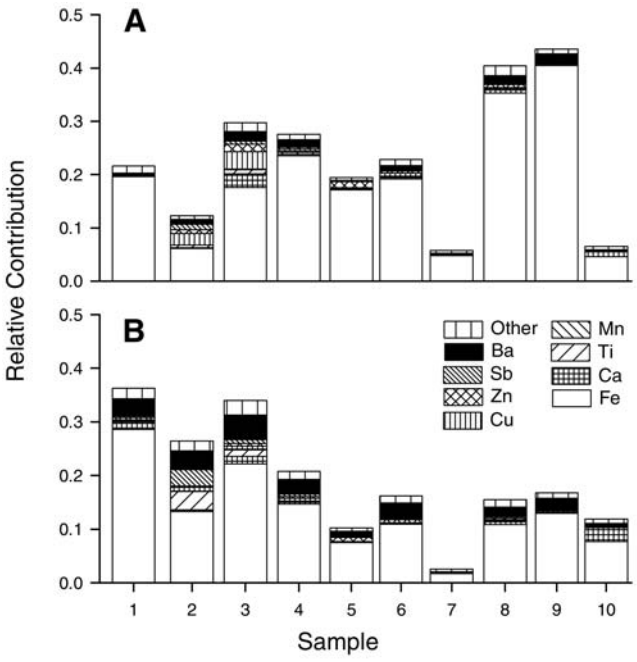

Figure 25. Relative contributions of abundant metals to total PM_{10} mass. (*A*) Resuspended brake housing dust and **(*B*)** corresponding crushed brake pads from sampled vehicles. Si is not shown because it was not measured.

Table 7. Average PM_{10} and $PM_{2.5}$ Resuspended Brake Housing Dust Composition[a]

	Semimetallic Brake Pads[c]		Low-Metallic Brake Pads[c]	
Species[b]	PM_{10}	$PM_{2.5}$	PM_{10}	$PM_{2.5}$
OC	**81.2 ± 11.2**	**67.6 ± 18.9**	**65.6 ± 10.6**	**49.5 ± 24.3**
EC	**44.0 ± 7.9**	26.4 ± 14.9	**34.0 ± 9.1**	16.8 ± 11.2
Na	**5.1 ± 1.1**	**3.5 ± 1.3**	**1.9 ± 0.5**	**2.4 ± 0.8**
Mg	**2.7 ± 0.7**	**2.8 ± 0.8**	**1.7 ± 0.7**	**2.9 ± 0.7**
Al	**1.4 ± 0.3**	**1.4 ± 0.5**	**1.9 ± 0.8**	1.4 ± 1.1
K	**1.6 ± 0.5**	**1.0 ± 0.4**	**0.5 ± 0.1**	0.6 ± 0.3
Ca	7.7 ± 4.6	4.4 ± 2.7	6.2 ± 3.6	10.1 ± 9.3
Fe	**203 ± 47**	**217 ± 89**	**154 ± 57**	**223 ± 38**
Ti	**3.7 ± 1.2**	**3.2 ± 1.0**	0.4 ± 0.3	**0.5 ± 0.1**
V	0.04 ± 0.02	0.05 ± 0.02	**0.07 ± 0.03**	**0.05 ± 0.03**
Cr	**0.3 ± 0.1**	**0.3 ± 0.1**	**0.2 ± 0.0**	**0.2 ± 0.0**
Mn	**1.7 ± 0.5**	**1.6 ± 0.7**	**1.0 ± 0.3**	**1.2 ± 0.2**
Cu	**12.8 ± 6.0**	**7.3 ± 2.5**	**0.3 ± 0.1**	**2.6 ± 0.9**
Zn	**6.9 ± 2.0**	**4.7 ± 1.4**	2.7 ± 1.8	**3.8 ± 1.8**
As	0.05 ± 0.04	**0.09 ± 0.04**	**0.11 ± 0.04**	0.01 ± 0.01
Rb	0.01 ± 0.01	**0.01 ± 0.00**	0.01 ± 0.01	0.00 ± 0.00
Sr	**0.23 ± 0.04**	**0.20 ± 0.04**	**0.06 ± 0.02**	**0.16 ± 0.04**
Mo	**0.02 ± 0.01**	**0.02 ± 0.01**	**0.04 ± 0.01**	**0.09 ± 0.04**
Ru	0.00 ± 0.00	0.00 ± 0.00	0.00 ± 0.00	**0.01 ± 0.00**
Rh	0.00 ± 0.00	0.00 ± 0.00	0.00 ± 0.00	0.00 ± 0.00
Pd	0.00 ± 0.00	0.00 ± 0.00	0.00 ± 0.00	0.00 ± 0.00
Ag	0.00 ± 0.00	0.00 ± 0.00	0.00 ± 0.00	**0.01 ± 0.00**
Cd	0.00 ± 0.00	0.00 ± 0.00	0.00 ± 0.00	0.00 ± 0.00
Sb	**3.8 ± 1.85**	**2.7 ± 0.65**	0.04 ± 0.04	**0.28 ± 0.09**
Cs	0.01 ± 0.01	0.00 ± 0.00	0.01 ± 0.00	0.00 ± 0.00
Ba	**14.2 ± 1.9**	**13.4 ± 3.2**	**5.8 ± 2.2**	**13.2 ± 3.1**
Ce	0.00 ± 0.00	0.00 ± 0.00	0.00 ± 0.00	0.00 ± 0.00
W	0.00 ± 0.00	0.00 ± 0.00	0.01 ± 0.01	**0.01 ± 0.00**
Pt	0.00 ± 0.00	0.00 ± 0.00	0.00 ± 0.00	0.00 ± 0.00
Tl	0.00 ± 0.00	0.00 ± 0.00	0.00 ± 0.00	0.00 ± 0.00
Pb	**0.02 ± 0.01**	**0.01 ± 0.00**	**0.01 ± 0.00**	0.00 ± 0.00
U	0.00 ± 0.00	0.00 ± 0.00	0.00 ± 0.00	0.00 ± 0.00

[a] Values are mg/g of particulate matter ± SD, averaged among five or six samples for each pad type. Bold values are greater than twice the level of uncertainty.

[b] Does not include silicon, which was not measured.

[c] Semimetallic and low-metallic are experimentally defined categories, not definite brake pad types. Semimetallic refers to dusts with more than 0.1% Cu, 0.2% Zn, 1.0% Ba, and 0.1% Sb by weight.

Tire Dust Figure 26 shows the average relative chemical compositions of sampled tires for PM_{10} and $PM_{2.5}$ size fractions, as species mass per total mass. Mass of tire samples was 65% to 75% OC in both size fractions. This fraction of OC would account for the vast majority of the measured mass if an empirical factor of 1.3 to 1.5 were used to compare OC and OC mass. EC was 0.4% to 0.9% of the mass for the three tires sampled. The only element that was present in significant amounts in all three tires was Zn, accounting for 0.02% to 0.06% of the PM_{10} mass. Therefore, the contribution of tire wear to trace metal emissions from motor vehicles is negligible compared with contributions of other specific sources.

Actual brake wear emissions were similar in relative metal composition to vehicle brake housing dust; therefore, size-resolved brake housing dust composition is a good estimate for real-world brake wear emissions of metals from a fleet of vehicles. Source profiles for brake wear were constructed for experimentally defined semimetallic and low-metallic brake pads from on-road vehicles. These profiles showed that concentrations of certain elements present at trace levels in the environment may be affected by brake wear emissions (ie, Cr, Mn, Cu, Zn, Sr, Mo, Sb, and Ba). Analysis of size-resolved samples of pulverized tires indicated that tire wear may be an important contributor to on-road motor vehicle emissions of OC, but its contribution to metals emissions is negligible.

Tailpipe Emission Profiles

Individual emission rates of particulate matter mass and metals showed great variation within classes of vehicle and driving cycle. When metals were normalized to mass emitted, however, variation among emission profiles for individual vehicles was greatly reduced. This reduction was due to the parallel effects of lubricating oil combustion on mass emission and metals emission rates.

Many metals in tailpipe emissions are expected to be from lubricating oil additives and engine wear debris accumulated in the oil. The emission of unburned or partially combusted lubricating oil greatly increases the mass emission of particulate matter, which is likely accompanied by an increase in metal emissions. In previous laboratory studies of diesel particulate matter emissions, lubricating oil dominated the emission rates of many metals (Okada et al 2003). Because these effects were not related to the type of fuel used, large differences were not expected between the mass-normalized metal emission profiles for gasoline and diesel vehicles.

Vehicles were divided into several classes for construction of average emission profiles. All gasoline vehicles were averaged together, weighted by the total mass emitted in each test, to obtain an overall emissions profile. Two more gasoline profiles were created by separating results by newer gasoline vehicles (model years 1986 and later)

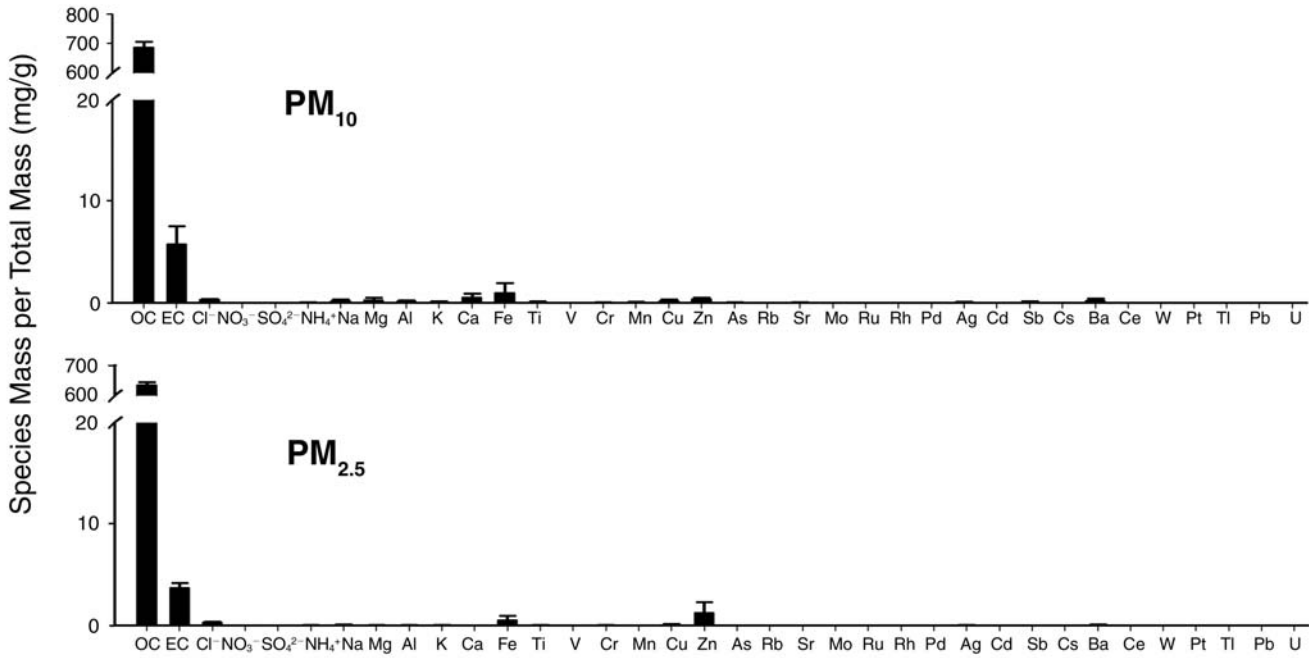

Figure 26. Relative compositions of sampled tire dust PM_{10} and $PM_{2.5}$. Error bars indicate the standard error of the average.

and older gasoline vehicles (model years 1985 and earlier). Gasoline vehicles that visibly emitted smoke were classified as old vehicles, regardless of model year.

Diesel vehicles were averaged according to driving cycle, weighted by the total mass emitted in each test, for another three profiles: average cold-start city–suburban heavy vehicle route, average warm-start city–suburban heavy vehicle route, and average highway. The emission composition profiles for the three gasoline vehicle classes and the three diesel vehicle driving cycle classes are shown in Figure 27, as milligrams of species per gram of total $PM_{2.5}$ mass. Despite the variety of vehicles and driving cycles, the mass-normalized emission profiles were remarkably similar.

Gasoline vehicle emissions were predominantly OC, 65% to 83% of total $PM_{2.5}$ mass; EC was between 17% and 28% of total $PM_{2.5}$ mass. The percentage of Ca was significant and similar for all three gasoline vehicle averages, 0.37% to 0.40%. The percentage of Zn was also notable but more variable in gasoline vehicle emissions, 0.24% to 0.65%. Other elements present in significant amounts in gasoline vehicle emissions included Cu, Fe, Mo, and Pb.

Diesel vehicle profiles by driving cycle were also relatively similar. OC comprised 17% to 35% of the $PM_{2.5}$ mass; EC, 70% to 84%. In all diesel averages, between 1.0% and 2.1% of the $PM_{2.5}$ mass was SO_4^{2-}. These low levels are consistent with the use of California low-S diesel fuel (maximum 0.05% S) in the tailpipe emission tests but not with diesel emissions in regions that do not require low-S fuel. Therefore, SO_4^{2-} in these tailpipe emissions cannot be compared directly with the tunnel SO_4^{2-} measurements or used for source apportionment. Gasoline vehicles varied greatly in SO_4^{2-} emissions. S emissions from catalyst-equipped gasoline vehicles are predominately in the form of gaseous sulfur dioxide, but small amounts of sulfur dioxide can oxidize to SO_4^{2-} in the catalytic converter. Therefore, variation in gasoline SO_4^{2-} emissions is probably due to differences in catalyst performance. Ca was present in diesel vehicle emissions at levels similar to those in gasoline vehicle emissions, 0.27% to 0.6% of total $PM_{2.5}$ mass. Fe constituted a larger but more variable percentage in diesel, 0.03% and 0.58%, as did Zn, 0.03% to 0.77%.

Because the several mass-weighted, mass-normalized profiles constructed for gasoline and for diesel vehicles were so similar, they were easily combined to create composite relative emission profiles for each fuel type. Uncertainties in the profiles were estimated from the standard deviation of the emissions averaged in the profile and from the analytic uncertainty. The final profiles chosen to apportion the emissions in roadway tunnel tests to gasoline and diesel vehicles are listed in Table 8.

Mass-normalized emissions of gasoline and diesel vehicles operated through cold-start tests, hot-start tests, and a variety of driving cycles showed similar patterns. One reason for this similarity is the influence of lubricating oil combustion on the ratios of individual metals to total mass. All gasoline vehicle results were averaged, weighted by total $PM_{2.5}$ mass emitted by each vehicle and vehicle age and performance classification, to create a single gasoline profile. All diesel vehicle results were averaged according to driving cycle, weighted by total $PM_{2.5}$ mass emission, and then averaged to create a single diesel profile. The metals contributing the largest mass fractions to the final profiles were Ca, Fe, Cu, Zn, and Mg.

Source Attribution

Figures 28–31 present tunnel emission test profiles, as well as profiles of specific particulate matter sources, for PM_{10} and $PM_{2.5}$. The figures allow a simple visual comparison of the different components that contributed to the total roadway emissions profiles. Tunnel emissions (ie, receptor samples) are presented in milligrams per kilometer driven; source profiles, as milligrams of species mass per gram of total measured PM_{10} or $PM_{2.5}$ mass. The profiles are shown on a scale that reflects the largest component contribution; Figures 29 and 31 show trace metals on a scale one-tenth of that in Figures 28 and 30. Resuspended road dust is shown from the two sampled tunnels in both summer and winter. Brake dust profiles shown are from resuspended brake housing dust, for experimentally defined semimetallic and low-metallic brake pads. The tire dust profile is an average of sampled resuspended tires. $PM_{2.5}$ emissions from gasoline- and diesel-powered vehicles are weighted averages of results from many vehicles tested on dynamometers. Tailpipe emissions are predominantly due to combustion and are below the $PM_{2.5}$ size range (Kleeman et al 2000). Therefore, emissions from tailpipes do not substantially affect total roadway emissions in the coarse size range (PM_{10}–$PM_{2.5}$), which will be dominated by other sources. In the tunnel tests apportioned here, $PM_{2.5}$ accounted for 20% to 50% of PM_{10} mass, a considerable fraction in which the effect and composition of tailpipe emissions is important.

The road dust profile contains not only crustal elements but also metals, reflecting enrichment from other sources and urban pollutants. However, this is the only source profile with significant amounts of Cl^-, which was detected in the tunnels and is probably from road salt application. Brake dust appears to be the only source that explains the relatively large amounts of Ba and small but significant

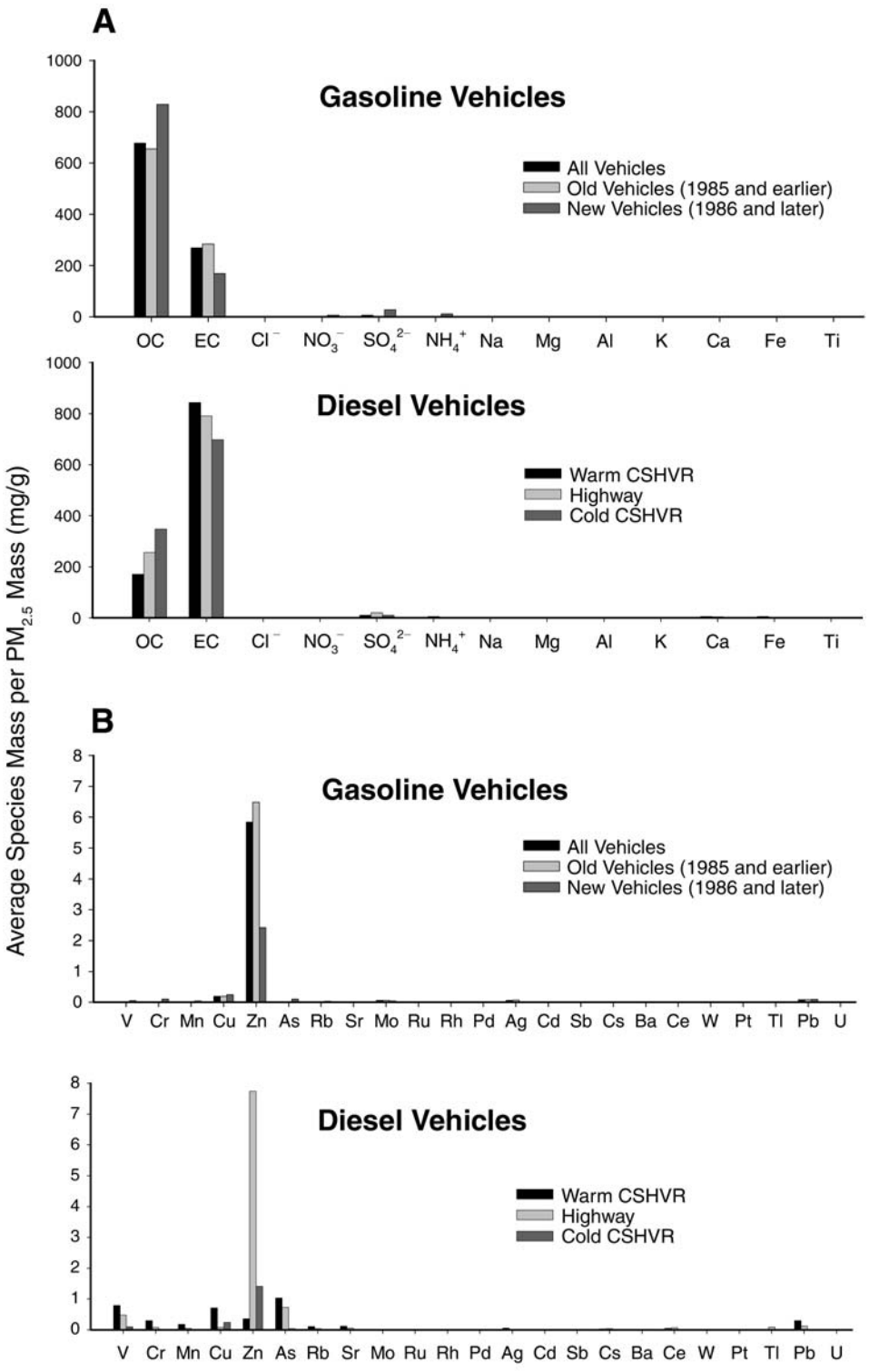

Figure 27. Emissions of (*A*) bulk species and crustal elements and (*B*) trace metals in $PM_{2.5}$ emitted from tailpipes. CSHVR indicates city–suburban heavy vehicle route. Note different y-axis scales between A and B.

Table 8. Average $PM_{2.5}$ Tailpipe Emission Composition Profiles[a]

$PM_{2.5}$ Species	Profile	
	Gasoline Vehicles	Diesel Vehicles
OC	**724,800 ± 126,000**	**241,400 ± 87,000**
EC	**241,600 ± 68,400**	**726,900 ± 104,000**
Cl^-	1792 ± 1520	0.0 ± 2517
NO_3^-	2788 ± 3330	1086 ± 1880
SO_4^{2-}	12,281 ± 14,100	**12,911 ± 5810**
NH_4^+	4852 ± 6070	**3106 ± 1390**
Na	327 ± 329	662 ± 1150
Mg	**1208 ± 297**	945 ± 1080
Al	38.0 ± 35.2	417 ± 724
K	99.0 ± 83.4	808 ± 1060
Ca	**3856 ± 461**	**4004 ± 1610**
Fe	**796 ± 303**	2797 ± 2590
Ti	16.2 ± 9.9	114 ± 95
V	18.8 ± 23.6	428 ± 325
Cr	51.4 ± 46.7	123 ± 144
Mn	22.5 ± 19.4	74.3 ± 88.9
Cu	**215 ± 39**	321 ± 310
Zn	**4953 ± 2270**	2966 ± 3750
As	41.3 ± 50.6	565 ± 480
Rb	13.7 ± 16.8	47.4 ± 50.4
Sr	12.5 ± 10.2	57.6 ± 49.5
Mo	**56.4 ± 13.1**	0.00 ± 30.4
Ru	0.00 ± 5.03	0.00 ± 17.3
Rh	0.01 ± 0.01	0.00 ± 46.9
Pd	6.79 ± 6.99	0.00 ± 47.9
Ag	47.1 ± 36.1	20.4 ± 32.8
Cd	0.07 ± 0.11	15.4 ± 13.7
Sb	0.43 ± 0.75	0.19 ± 0.32
Cs	0.00 ± 2.01	24.9 ± 18.6
Ba	7.50 ± 6.04	6.58 ± 6.86
Ce	**3.71 ± 1.66**	40.1 ± 33.4
W	5.44 ± 6.40	0.00 ± 89.4
Pt	2.59 ± 2.56	0.00 ± 36.3
Tl	0.00 ± 36.2	27.8 ± 48.2
Pb	**83.5 ± 12.80**	137 ± 133
U	5.15 ± 6.00	0.00 ± 39.7

[a] Values are average species mass per total $PM_{2.5}$ mass (μg/g) ± SD. Bold values are statistically different from zero (95% confidence interval).

amounts of Sb emitted in the tunnels. Fe and other metals (such as Cr, Mn, Cu, and Zn) are present in both brake dust and road dust. Zn was also present in significant amounts in gasoline and diesel tailpipe emissions; it was the only element found at significant levels in tire wear emissions.

Results of the CMB model are summarized in Table 4. Although the purpose of using the CMB model was to apportion to sources the metals emitted in the tunnels, good apportionment of the total particulate matter mass indicated that the model results are reasonable. All five tunnel emission averages were fit well by the model, with r^2 of 0.89 to 1.00, and χ^2 of 0.12 to 2.71. The percentage of mass apportioned for four of the five test types was 63% ± 9.8% to 160% ± 39%. The fifth test type, weekend traffic in the summer (Howell Tunnel), had very low measured mass emission rates (24.9 ± 35.6 mg/km), and the model fit 589% of the mass (146 ± 29.9 mg/km); the measured and calculated mass values did not differ significantly, however.

In the CMB model, profiles for gasoline tailpipe emissions and tire wear emissions were collinear and could not be separated. For both profiles, OC constituted approximately 70% of the total mass, with small but significant amounts of Zn. When tire wear was included in the model, the model reported a collinearity cluster and could not separately apportion these two sources. The effective variance solution sought to maximize the CMB fit by weighing OC importance over Zn because the relative uncertainty in the OC contribution to the source profiles was lower. Therefore, the profile for tire wear emissions was omitted from the model and the profile for gasoline vehicle tailpipe emissions was used to represent the sum of gasoline vehicle tailpipe emissions and tire wear. Hence, in the metal apportionment results, contributions of tire wear and gasoline tailpipe emissions are combined as one source.

Although necessary, this combination affects interpretation of the results, because tire wear may contribute much more than gasoline tailpipe emissions to total particulate matter mass. Because the primary constituent of tire wear emissions is OC, the mass of tire wear emissions was apportioned, correctly, to the combined profile, resulting in apportionment of much more mass to the combined profile than would be from tailpipe emissions alone.

Both semimetallic and low-metallic brake wear profiles were used in the CMB model for all test types. Because these brake types are experimentally defined, the contributions attributed by the model to semimetallic and low-metallic brakes were combined into a single value for total brake wear contributions. Road dust profiles were individually applied to corresponding tunnel profiles in appropriate seasons; however, the results of apportionment of each separate road dust profile are discussed as one.

The CMB model apportioned the mass balance species effectively, as demonstrated by the agreement between calculated and measured emission rates from summer Howell Tunnel tests (Figure 32). Table 9 gives a summary of the range of each species' relative contribution that was apportioned to each source profile in any of the tests. Brake wear emissions and resuspended road dust were the primary contributors to metal mass. Few metals were apportioned to the diesel tailpipe emissions profile or the combined

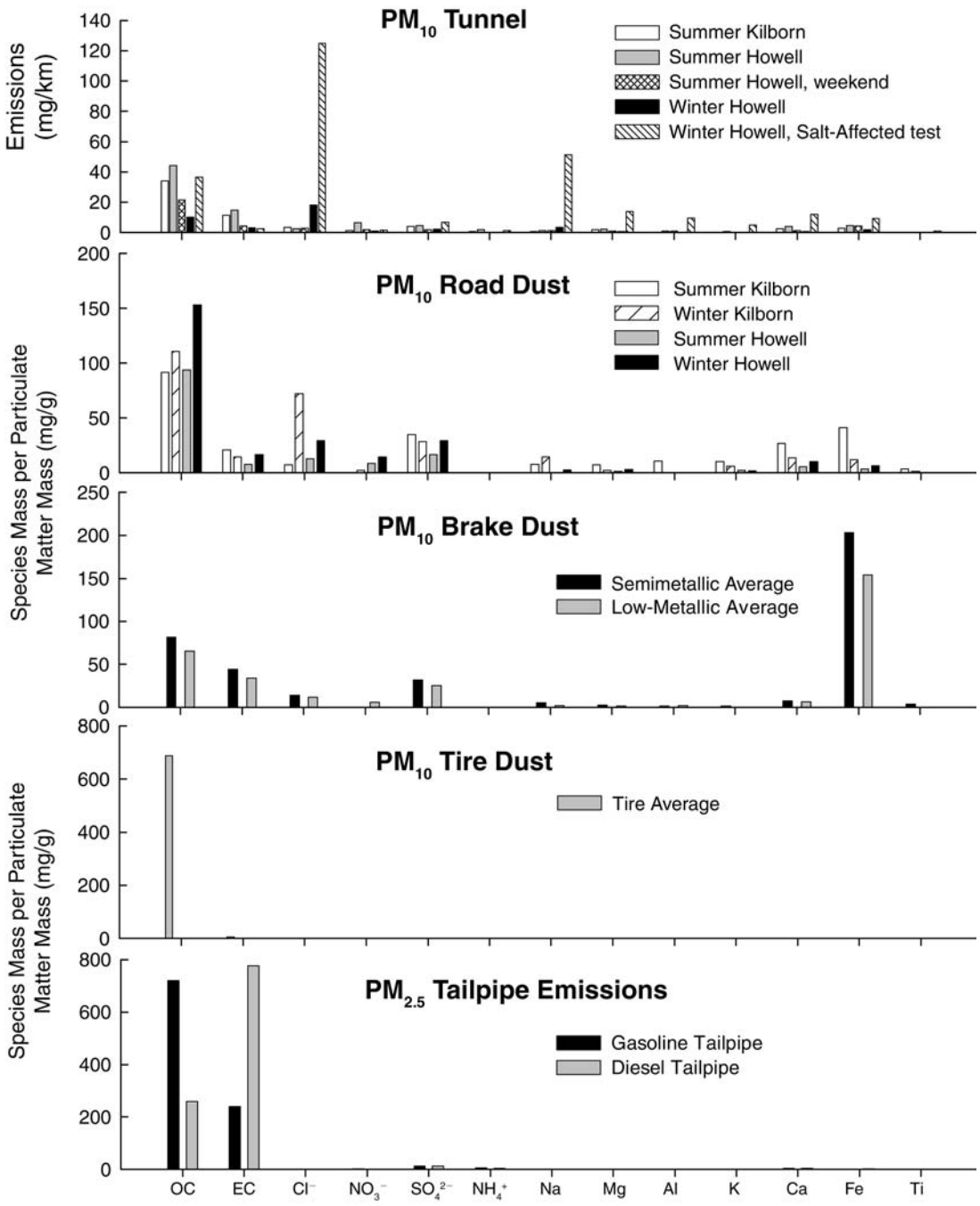

Figure 28. Emission rates in tunnels of bulk species and crustal elements in particulate matter and measured source profiles. Tunnel, brake and tire dust, and emissions data are averages; road dust data are from single resuspended samples. Note different y-axis scales among the panels.

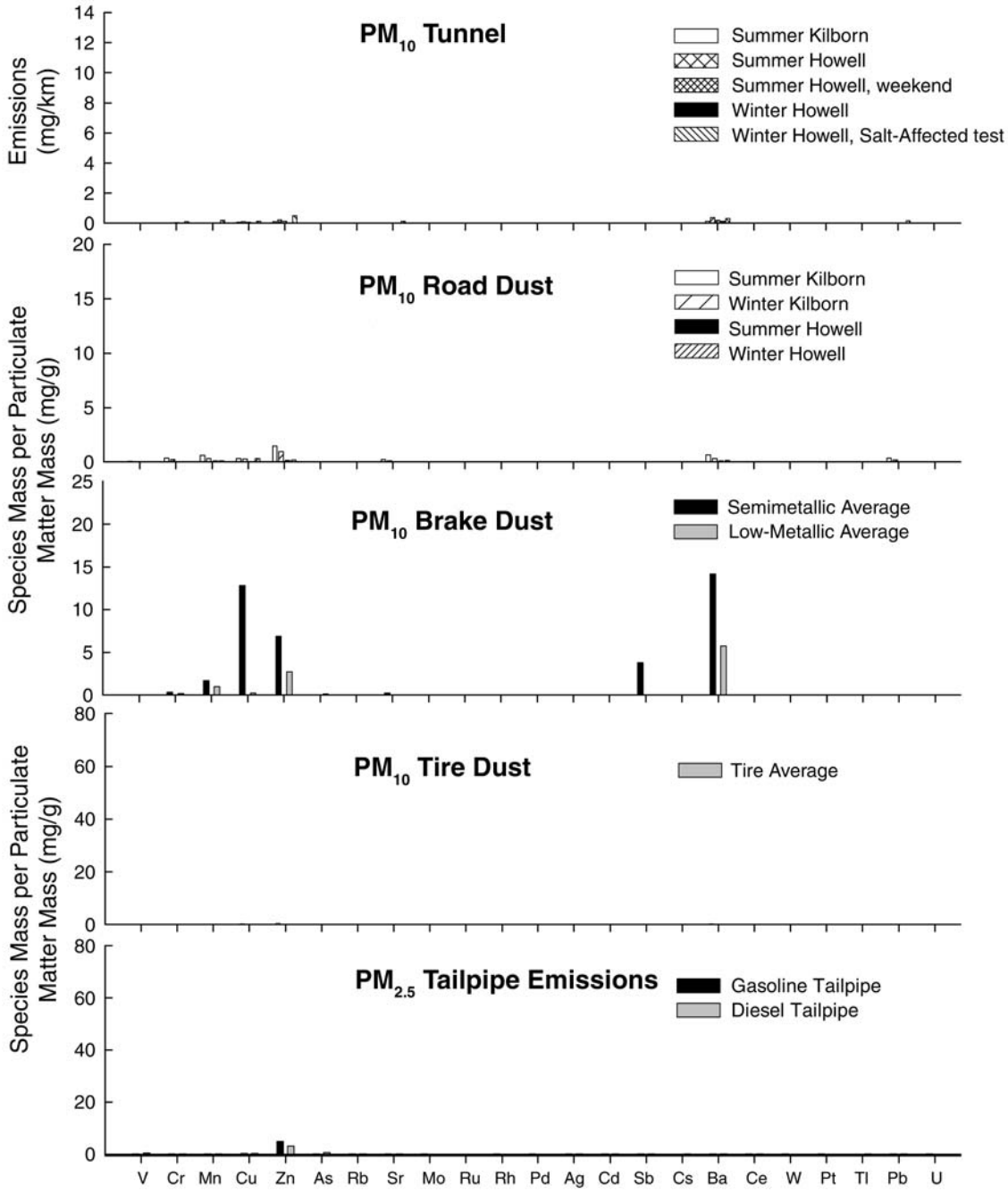

Figure 29. Emission rates in tunnels of trace metals in particulate matter and measured source profiles. Tunnel, brake and tire dust, and emissions data are averages; road dust data are from single resuspended samples. Note different y-axis scales among the panels.

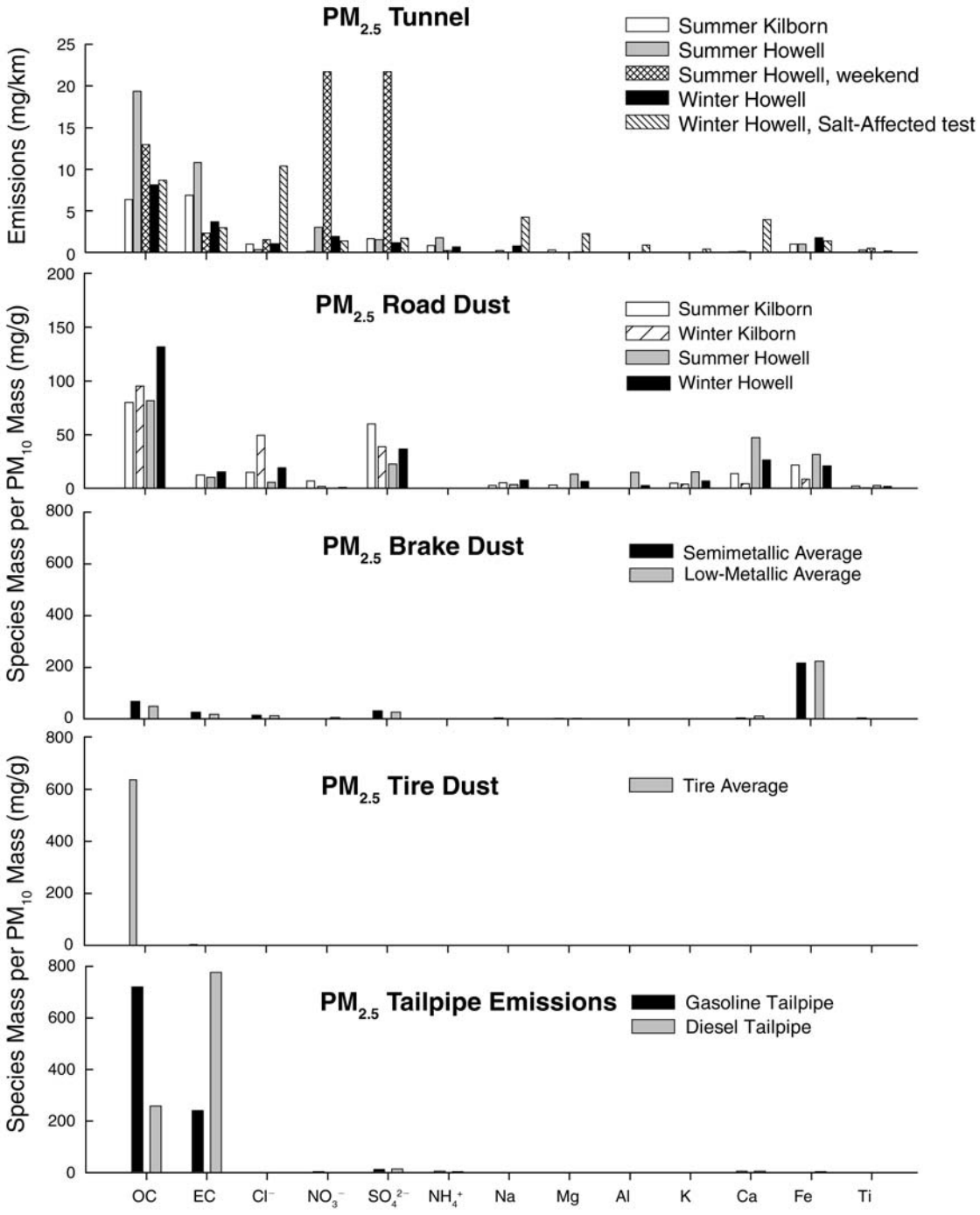

Figure 30. Emission rates in tunnels of bulk species and crustal elements in $PM_{2.5}$ and measured source profiles. Tunnel, brake and tire dust, and emissions data are averages; road dust data are from single resuspended samples. Note different y-axis scales among the panels.

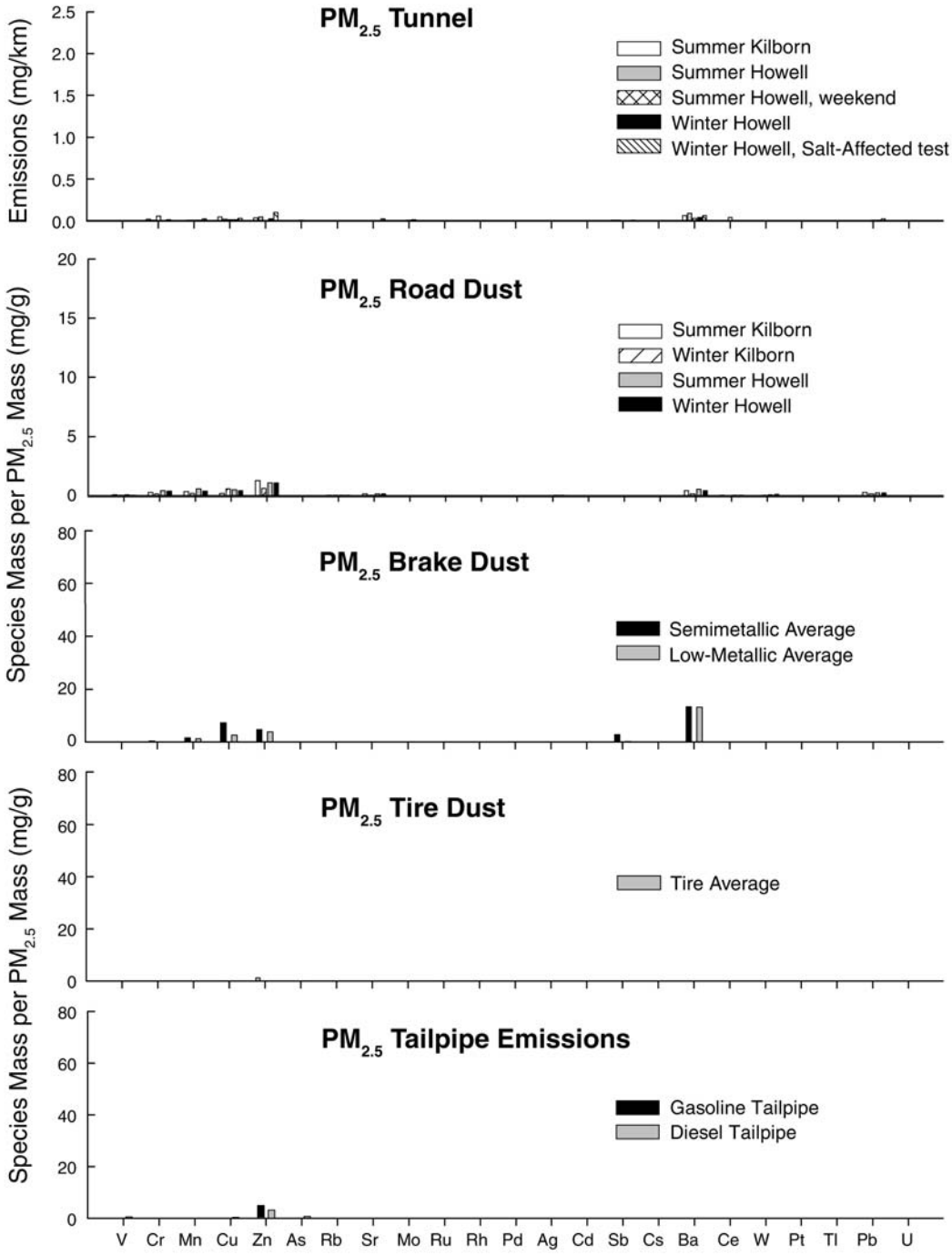

Figure 31. Emission rates in tunnels of trace metals in $PM_{2.5}$ and measured source profiles. Tunnel, brake and tire dust, and emissions data are averages; road dust data are from single resuspended samples. Note different y-axis scales among the panels.

gasoline tailpipe and tire wear emissions profile. This result was expected, because tailpipe emissions and tires contained relatively low concentrations of metals compared with other sources. Apportionment to gasoline and diesel tailpipe emissions must be interpreted carefully, however; more EC and more metals may have been apportioned to the combined gasoline tailpipe and tire wear emissions profile than to the diesel tailpipe emissions profile.

Table 9 shows that more EC was apportioned to gasoline vehicles (18%–77% of EC) than to diesel vehicles (0%–50%). Diesel vehicles constituted a relatively small fraction of the vehicle fleet (up to 7%); however, operating conditions in the tunnel also affected the results for diesel tailpipe emissions. The driving cycle strongly affects the amount of EC that diesel vehicles emit; large emissions of EC would not be expected at the low engine loads and low speeds consistent with cruising conditions in the tunnel tests (Foster et al 2002; Shah et al 2004). The effects of engine load and operation on diesel emissions of EC are often erroneously neglected in analyses, leading to overemphasis of the importance of diesel vehicles to ambient EC concentrations.

Table 9 also shows that somewhat higher fractions of metals were attributed to the combined gasoline tailpipe and tire wear emissions profile than to the diesel tailpipe emissions profile. This result is likely due to the fact that tire wear and gasoline tailpipe emissions could not be separated in the CMB model. Tire wear may contribute a large fraction of the OC in PM_{10}, increasing the mass apportioned to this profile. However, Zn was the only element found in resuspended tire dust samples at significant levels, with levels much higher in tire dust samples (0.03% ± 0.07%) than in gasoline tailpipe emission samples (0.5% ± 0.2% of total mass). Therefore, metals apportioned to this combined profile could be assumed to be due to gasoline tailpipe emissions.

One consequence of using a combined gasoline tailpipe and tire wear profile is that the large PM_{10} and OC masses apportioned to the combined profile as a result of tire wear will increase the fractions of metals attributed to gasoline tailpipe emissions at the expense of the metals from the diesel profile. This result must be interpreted cautiously. The individual elements apportioned to gasoline tailpipe and diesel tailpipe emissions were those expected, but the fractions apportioned to each may be skewed by the mass of tire wear OC that was collinear with the gasoline tailpipe profile. Although the gasoline tailpipe and diesel tailpipe emission profiles were analyzed separately, the true fractions of metals due to gasoline and diesel emissions are likely some combination of the fractions apportioned by the CMB model. Nonetheless, the total emissions of metals from gasoline and diesel tailpipes are a small fraction of the total metal emissions. Split between these two tailpipe sources, they will not greatly affect the total metal apportionment.

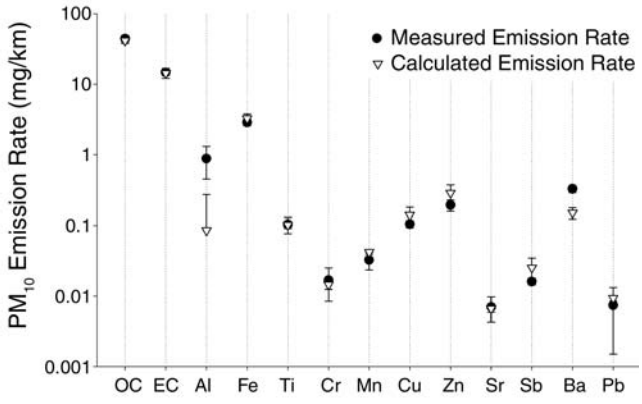

Figure 32. Emission rates of species in PM_{10} measured in summer weekday Howell Tunnel tests and emission rates calculated by CMB model for the same tests. Only mass balance species are shown. Error bars indicate the standard error of the average.

For each of the five tunnel test types, Figures 33–37 present the relative contributions to 23 individual elements in PM_{10} of each of the four model sources: combined gasoline tailpipe and tire wear emissions; diesel tailpipe emissions; brake wear emissions; and resuspended road dust. These 23 elements were present in significant amounts in at least one of the tunnel test type averages. The large contribution of resuspended road dust to concentrations of many elements is visible in every plot. In addition to the lighter crustal elements (Na, Mg, Al, K, Ca, Fe, and Ti), relatively large portions of trace elements such as Sr (53%–70%), Cd (54%–65%), and Pb (58%–91%) were attributed to road dust. These elements are likely present in road dust as part of the crustal matrix or from previous deposition of pollutants.

For the winter salt-affected test P (Figure 37), the road dust profile was replaced with the assigned salt effect profile, and the majority of almost every element was attributed to salt. This finding is a result of defining the salt profile as having the composition of the difference in mass between the heavily salt-affected test P and the other winter tests. Hence, the salt effect profile is equivalent to a large portion of the test P mass, and consequently most of the mass was apportioned to that profile. Although this experimentally defined profile interferes with more specific apportionment of the metals, it is useful to note the enormous effect of resuspended road salt under certain conditions. Drying of salted roadways and evaporation of wet, salty spray from the roadway can contribute great levels of many elements to PM_{10} emissions.

Table 9. Ranges of Relative Source Contributions to Total PM_{10} Mass and Species Emission Rates, from CMB Model, for Tunnel Tests[a]

PM_{10} Species	Source Profile			
	Combined Gasoline Tailpipe and Tire Wear[b]	Diesel Tailpipe[b]	Brake Wear	Resuspended Road Dust
Mass	0.05–**0.51**	0.00–0.04	0.11–0.20	0.29–**0.72**
OC	0.20–**0.89**	0.00–0.06	0.03–0.08	0.06–**0.73**
EC	0.18–**0.77**	0.00–**0.50**	0.04–0.19	0.04–0.38
Cl^-	0.00–0.18	0.00–0.00	0.09–0.42	0.41–**0.90**
NO_3^-	0.01–**0.68**	0.00–0.02	0.06–0.30	0.00–**0.90**
SO_4^{2-}	0.02–0.29	0.00–0.02	0.17–0.22	0.47–**0.77**
NH_4^+	0.48–**0.94**	0.00–0.27	0.02–0.15	0.00–0.10
Na	0.00–0.07	0.00–0.02	0.18–0.38	**0.52–0.77**
Mg	0.02–0.20	0.00–0.02	0.11–0.15	**0.68–0.85**
Al	0.00–0.00	0.00–0.03	0.36–**0.52**	0.46–**0.64**
K	0.00–0.02	0.00–0.01	0.04–0.05	**0.92–0.96**
Ca	0.02–0.18	0.00–0.02	0.09–0.13	**0.71–0.88**
Fe	0.00–0.01	0.00–0.00	**0.64–0.84**	0.15–0.35
Ti	0.01–0.01	0.00–0.01	0.20–0.29	**0.69–0.79**
V	0.03–0.17	0.00–0.34	0.17–0.25	0.37–**0.72**
Cr	0.02–0.14	0.00–0.05	0.23–**0.43**	0.49–**0.66**
Mn	0.00–0.03	0.00–0.01	**0.53–0.75**	0.24–0.45
Cu	0.01–0.08	0.00–0.01	**0.72–0.91**	0.06–0.25
Zn	0.20–**0.69**	0.00–0.11	0.17–**0.56**	0.07–0.21
Sr	0.01–0.07	0.00–0.05	0.22–0.36	**0.53**–0.70
Mo	0.25–**0.84**	0.00–0.00	0.16–**0.75**	0.00–0.00
Rh	0.00–0.00	0.00–0.00	0.58–**0.58**	0.42–0.42
Pd	0.33–0.33	0.00–0.00	0.67–**0.67**	0.00–0.00
Ag	0.20–**0.95**	0.00–0.08	0.00–0.02	0.02–**0.69**
Cd	0.00–0.00	0.00–0.41	0.04–0.05	**0.54–0.65**
Sb	0.00–0.00	0.00–0.00	**0.99–1.00**	0.00–0.01
Ba	0.00–0.00	0.00–0.00	**0.85–0.92**	0.08–0.14
W	0.01–0.37	0.00–0.00	0.04–0.17	0.46–**0.95**
Pt	1.00–**1.00**	0.00–0.00	0.00–0.00	0.00–0.00
Pb	0.07–0.32	0.00–0.10	0.01–0.03	**0.58–0.91**

[a] Values reflect only apportioned mass from tests with significant emission rates for the species, omitting salt-affected test *P.* Values reflecting > 0.5 contribution are in bold type; those reflecting > 0.25 contribution are underlined.

[b] See text for discussion of contributions of gasoline and diesel tailpipe emissions.

In every calculation, brake wear contributed significantly to metal emissions, notably for Fe (64%–84%), Cr (23%–43%), Mn (53%–75%), Cu (72%–91%), Zn (17%–56%), Sr (22%–36%), Sb (99%–100%), and Ba (85%–92%). The vast majorities of Sb, Cu, and Ba were attributed to brake wear in every test, except salt-affected test P. Cu has other possible emission sources in the urban atmosphere, such as metal fabricators, but Sb and Ba may be useful tracers for brake wear emissions.

In this study, diesel tailpipe emissions were applied as a source in all models except the summer Howell Tunnel weekend tests (Figure 35). In that test type, collinearity problems and model instability were observed when the diesel tailpipe profile was included, consistent with the fact that the weekend tests had minimal heavy-duty truck traffic. In the other tunnel tests, diesel was generally calculated to be a large contributor to PM_{10} emissions of V (0%–34%) and Cd (0%–41%) and a smaller but significant

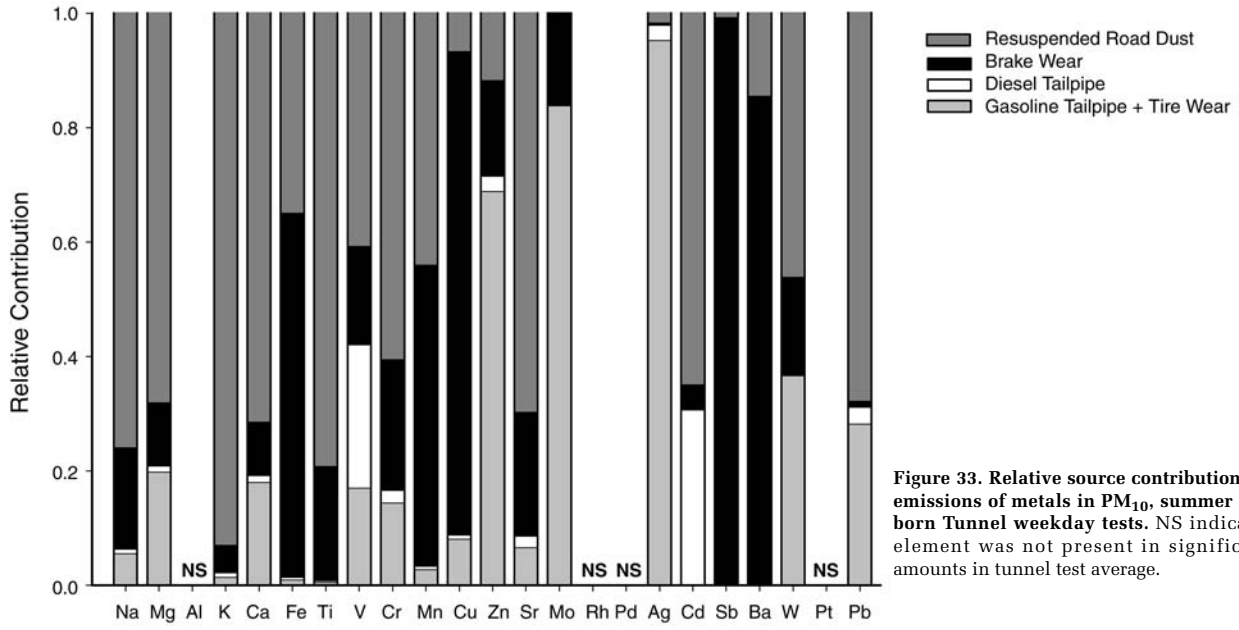

Figure 33. Relative source contributions to emissions of metals in PM_{10}, summer Kilborn Tunnel weekday tests. NS indicates element was not present in significant amounts in tunnel test average.

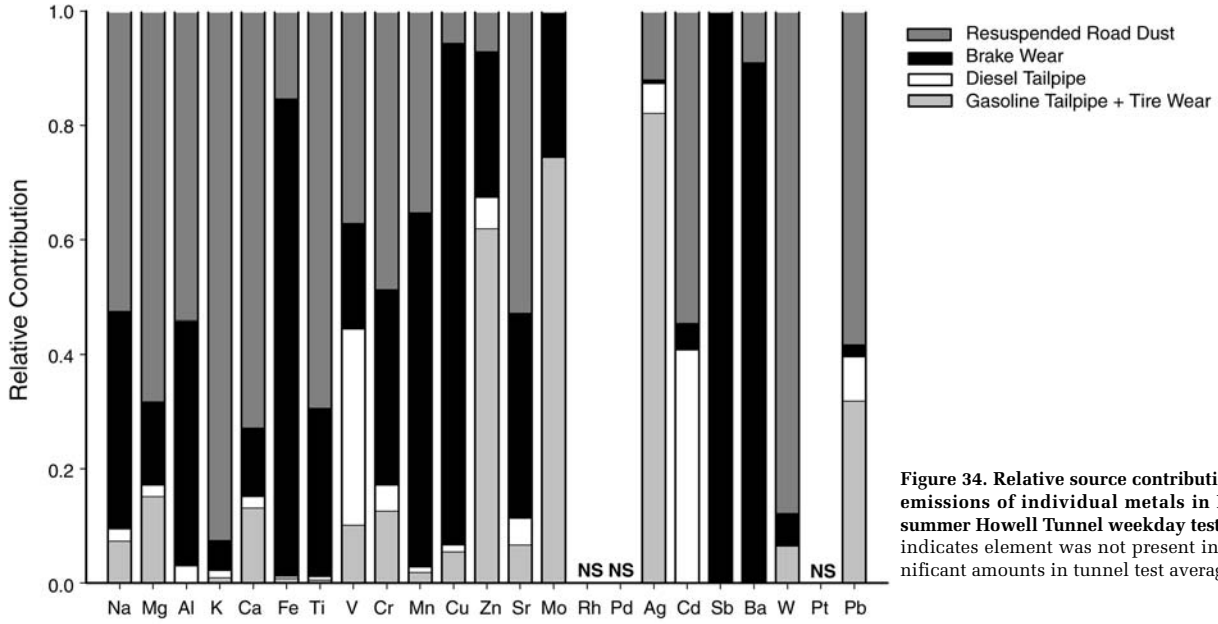

Figure 34. Relative source contributions to emissions of individual metals in PM_{10}, summer Howell Tunnel weekday tests. NS indicates element was not present in a significant amounts in tunnel test average.

contributor to Ca, Cr, Zn, Sr, and Pb. Diesel tailpipe emissions have relatively low metal content compared with other vehicle sources; they are not the dominant source of most metals. Although heavy-duty trucks constituted less than 7% of the vehicle fleets in these tests, amounts of metals apportioned to diesel tailpipe emissions would still be proportionally very small in fleets with larger fractions of heavy trucks, owing to the simultaneous increases in emissions from other sources with increased truck traffic.

The combined gasoline tailpipe and tire wear emissions profile was calculated to contribute significant amounts of many metals. Although the elements apportioned to this profile are representative of the composition of gasoline tailpipe emissions, the fractions attributed to the profile may be somewhat high. The true fractions are expected to be some combination of the fractions apportioned to this profile and those apportioned to the diesel tailpipe emissions profile. For instance, Ca and Mg, components of engine lubricating oil additives, are expected in tailpipe emissions. These elements are also major components of road dust and crustal material, however, and the attribution of up to 20% of their mass to gasoline tailpipe emissions is high.

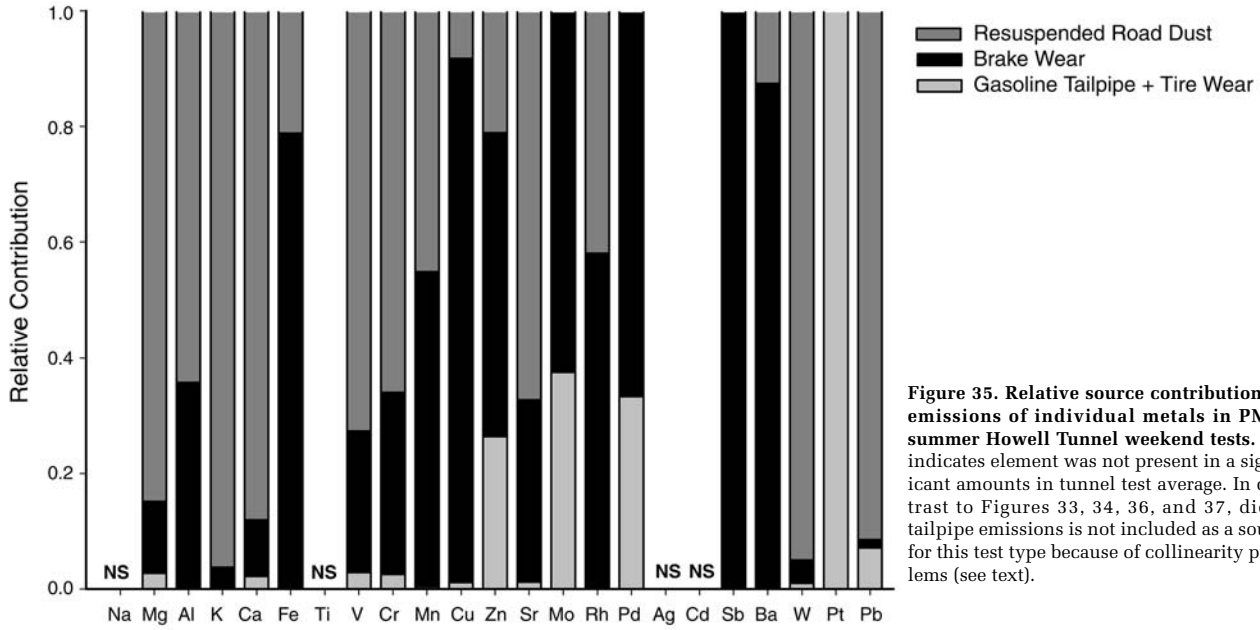

Figure 35. Relative source contributions to emissions of individual metals in PM_{10}, summer Howell Tunnel weekend tests. NS indicates element was not present in a significant amounts in tunnel test average. In contrast to Figures 33, 34, 36, and 37, diesel tailpipe emissions is not included as a source for this test type because of collinearity problems (see text).

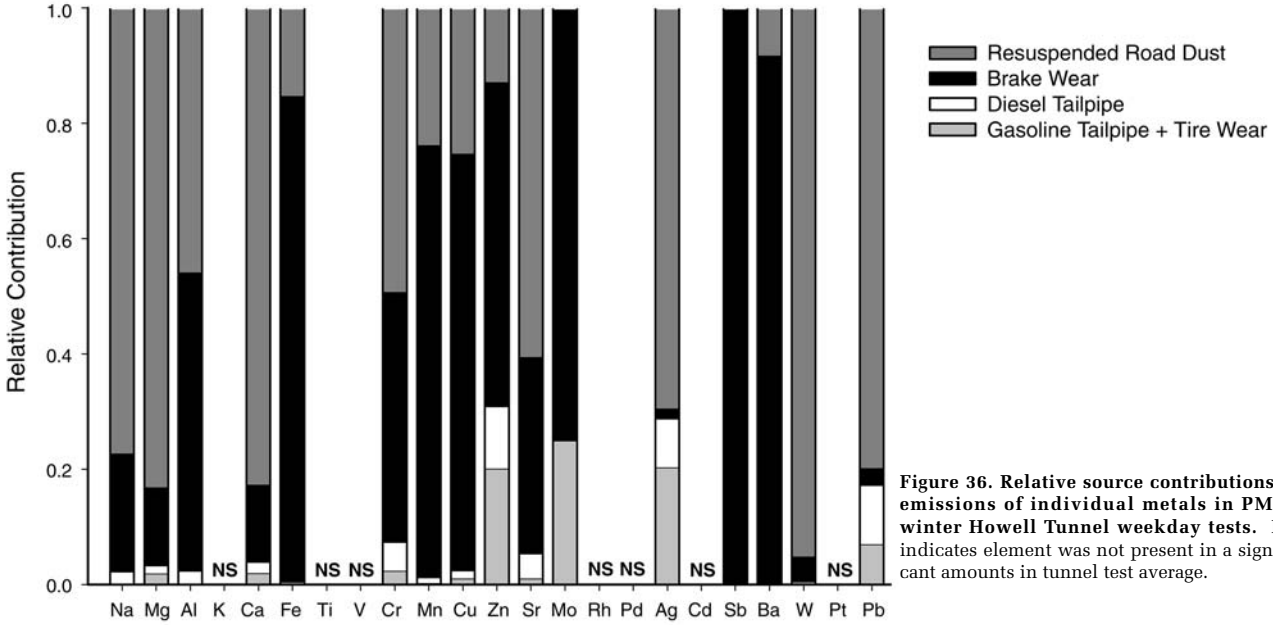

Figure 36. Relative source contributions to emissions of individual metals in PM_{10}, winter Howell Tunnel weekday tests. NS indicates element was not present in a significant amounts in tunnel test average.

Like the diesel tailpipe emissions profile, the combined gasoline tailpipe and tire wear emissions profile contributed to V, Cr, Zn, Sr, and Pb in varying amounts. No Cd was attributed to the combined gasoline tailpipe and tire wear emissions profile, although up to 41% was apportioned to the diesel tailpipe emissions profile. Gasoline vehicles contributed up to 32% of the Pb, which was greater than the diesel vehicle contribution. Mo and Ag were measured in significant amounts in most tunnel tests, attributed predominantly to the combined gasoline tailpipe and tire wear emissions profile (Mo, 25%–84%; Ag, 20%–95%). Again, the true fractions of these metal emissions that were due to gasoline tailpipe and diesel tailpipe emissions are expected to be some combination of those apportioned to each profile.

Pt, Rh, and Pd were found in significant amounts only in the summer weekend tests at the Howell Tunnel. Levels of these noble metals were thought to be due to the catalytic converters of the older, classic automobiles present during those tests. However, the gasoline tailpipe profiles used in the model did not contain enough Pt, Pd, or Rh to account for the emissions in those tests.

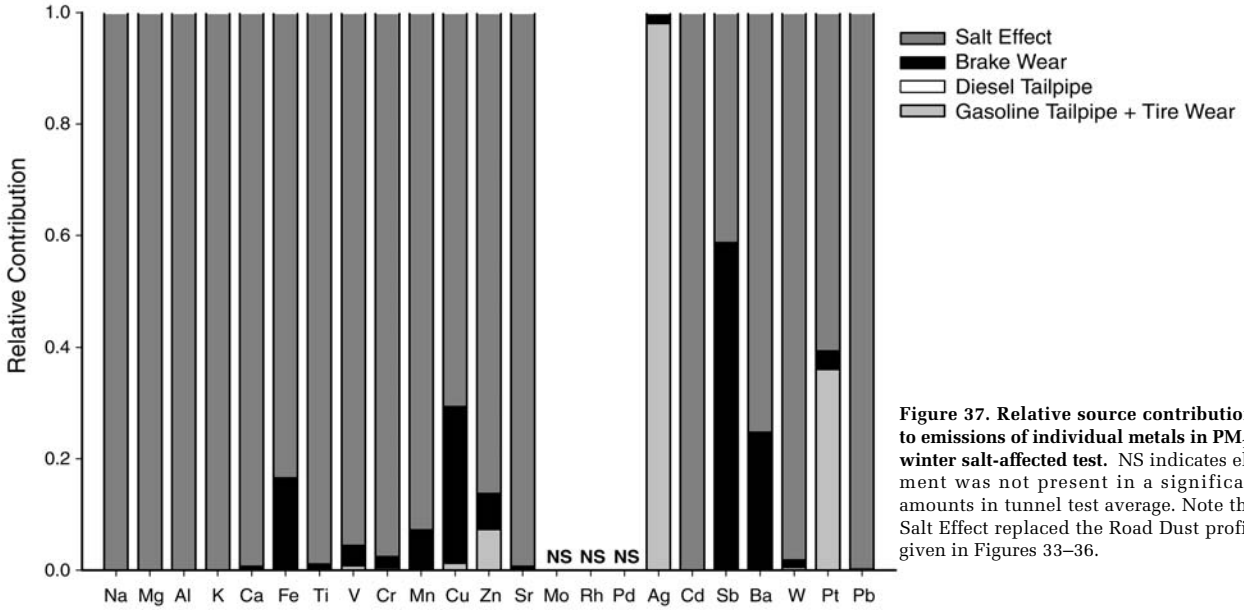

Figure 37. Relative source contributions to emissions of individual metals in PM_{10}, winter salt-affected test. NS indicates element was not present in a significant amounts in tunnel test average. Note that Salt Effect replaced the Road Dust profile given in Figures 33–36.

Despite the variety in the tunnel emissions measured, source attribution of the total roadway emissions by the CMB model was considerably consistent. Road dust, enriched by previous deposition of emissions from other sources, was calculated to contribute to the levels of most elements measured in the tunnel tests. Brake wear was the source of most Cu and Ba and nearly all Sb measured in the tunnels. Apportionments to the diesel tailpipe emissions profile and the combined gasoline tailpipe and tire wear emissions profile were fairly similar; combustion of lubricating oil and engine wear were likely the dominant sources of metal emissions from both gasoline and diesel vehicles. Because of the effect of tire wear mass on the gasoline tailpipe profile, the true fractions of metals that are due to gasoline and to diesel tailpipe emissions are probably a combination of the fractions apportioned to each profile.

SOURCES OF AMBIENT METALS

Descriptive Analysis

Concentrations of all measured species from the Milwaukee, Waukesha, and Denver sites were compared (data are presented in Appendix E, available on request from HEI). Mass and bulk composition of particulate matter samples collected at Milwaukee and Waukesha were very similar, as expected for sites close to one another. (Hereafter, these two sites are referred to as *the Wisconsin sites*.) One aspect of quality control for the field samples was comparison of mass data to measurements made by the Wisconsin Department of Natural Resources (WDNR) at the same sites and times. The WDNR uses the EPA federal reference method for $PM_{2.5}$ and PM_{10} mass measurements. Mass data were available from the WDNR for $PM_{2.5}$ at both the Milwaukee and Waukesha sites and for PM_{10} at the Waukesha site only. The entire WDNR data set and our University of Wisconsin data set for PM_{10} and $PM_{2.5}$ mass were regressed; r^2 was 0.91, slope was 1.00 ± 0.03, and y-intercept was 0.32 ± 0.60 μg/m^3.

Seasonal average compositions of bulk chemical species in PM_{10} and $PM_{2.5}$ at all three sites are shown in Figure 38. We classified February and March 2001 as winter, April through June as spring, July through September as summer, and October through December as fall; January 2002 was included separately as a second winter average.

Mass measurements in Denver were, on average throughout the year, 53% higher for PM_{10} mass and 8% higher for $PM_{2.5}$ mass than those in the Wisconsin sites. High PM_{10} measurements are normal for the Denver site, which is near a quarry. Different seasonal trends in bulk chemistry were apparent at the Denver and Wisconsin sites for PM_{10} and $PM_{2.5}$. Whereas the OC concentration was highest in the warmer months at the Wisconsin sites, OC levels in Denver appeared to be lowest in summer and highest in fall and winter. These slight seasonal differences in OC concentrations may have been due to weather and formation of secondary organic aerosol.

EC levels were fairly constant among seasons at all three sites, but in Denver they were slightly higher in both PM_{10} and $PM_{2.5}$ size fractions during fall and winter. Although in Denver the average concentrations of OC and EC in

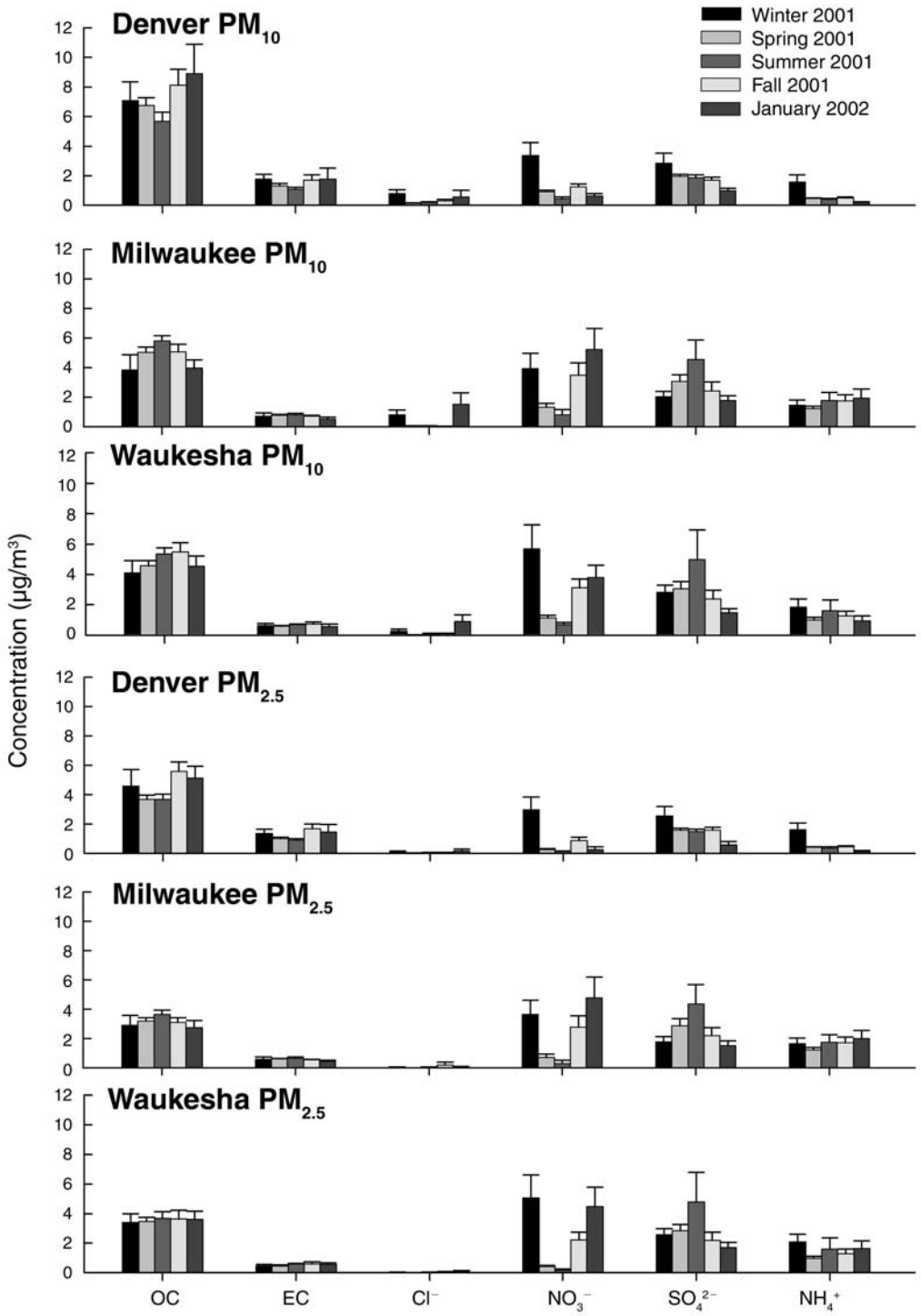

Figure 38. Seasonal average ambient species concentrations in PM_{10} and $PM_{2.5}$ measured at three sites. Error bars indicate the standard error of the average.

winter did not differ significantly from those in other seasons, these trends could be interpreted to corroborate the conclusion of the Northern Front Range Air Quality Study that motor vehicle cold-engine starts in very cold temperatures are a major contributor to fine particle mass (Watson et al 1998). However, EC data from the Wisconsin sites do not show a similar trend, even though temperatures in Wisconsin were lower than those in Denver during winter; January, February, and March monthly averages of daily low temperature were 5°F (2.8°C) lower in Milwaukee than in Denver. Thus, small changes in the EC/OC ratio observed in Denver as a function of season do not support the Northern Front Range Air Quality Study conclusion.

The average Cl^- concentration at all three sites was largest in PM_{10} and highest in winter, most likely because of the application of salt on icy roads. This seasonal difference was especially great at the Wisconsin sites. NO_3^- concentrations were also highest at the Wisconsin sites in winter and fall, more than twice as high as in summer. Semivolatile NO_3^- levels increase during cooler seasons in part because of changes in phase distribution and artifacts (Hering et al 1988; Hering and Cass 1999), which were not accounted for in this study. NH_4^+ is also a semivolatile species, but its seasonal differences were not as distinct. SO_4^{2-} data showed a seasonal trend: maximum concentrations at the Wisconsin sites in the summer, possibly from increased photochemical formation.

In Denver, NO_3^-, SO_4^{2-}, and NH_4^+ were all highest from February through March. Although most Denver measurements from individual dates in that period were low, three dates had very high mass and ion concentrations in both PM_{10} and $PM_{2.5}$. The SO_4^{2-}, NO_3^-, and NH_4^+ concentrations were 2 to 4 times larger than other, typical concentrations measured in that season and over the rest of the year, and measured mass and mass reconstructed from chemical measurements agreed well. On those three dates, EC and OC concentrations were also high but were within the typical range. This result probably reflects the effect of meteorologic conditions that allowed pollutants to accumulate in the airshed.

Figure 39 presents seasonal average PM_{10} profiles for the most abundant measured elements at the three ambient sampling sites; Figure 40 shows the less abundant measured elements. The most abundant elements included light, crustal elements that accounted for most of the measured metal mass, as well as heavier elements.

Measurements of Al, K, Ca, Fe, and Ti were much higher in Denver than at the Wisconsin sites, consistent with the Denver site being near a quarry. Because these elements are major components of soil, their ambient concentrations are expected to be predominantly from resuspended soil. Therefore, the observed differences between the measurements at Denver and the Wisconsin sites measurements reflect differences in geology, soil composition, and ground cover. These elements are also emitted from sources other than soil, however. K is emitted from wood and biomass burning; Ca, a component of some detergents used in engine lubricating oils, is emitted from motor vehicles. Though the higher levels of these elements in Denver were likely due in large part to crustal contributions, vehicle emissions and biomass burning may have contributed to a lesser extent.

At all three sites, the amount of Na was higher in the winter than in other seasons; at the Wisconsin sites, it was higher by an order of magnitude. This was an expected result of road salt application.

Trace elements of interest for source apportionment of metals associated with motor vehicle operation in atmospheric particulate matter were detected routinely at all three sites (Figures 39 and 40). Ba, expected from brake wear (Garg et al 2000), was more than twice as high in Denver than at the Wisconsin sites. The seasonal average concentrations were relatively constant. In Denver, Ba was 17.1 ± 5.1 to 21.8 ± 4.5 ng/m^3; Milwaukee and Waukesha had less Ba on average, 3.5 ± 0.8 to 7.4 ± 1.7 ng/m^3. The greater Ba levels in Denver could be related to driving patterns, as is suggested by the significantly higher levels of Ba as well as other brake wear elements (Fe, Zn, Sb, and Sr) in Denver than in Wisconsin. Variations in composition of resuspended crustal material in these areas could affect ambient concentrations of elements present in soil, even at trace levels.

Other elements of interest are Cu and Zn, which have been associated with motor vehicle tailpipe emissions and with metal foundries. Zn measurements were higher in Denver than in Wisconsin, which could be related to these sources or to soil resuspension. Cu concentrations were highest in Waukesha, where the highest seasonal average was 29.3 ng/m^3 and individual measurements were as high as 75 ± 4.4 ng/m^3. WDNR permit records show that a metal casting company registered as an emitter of Cu is located approximately 1 km due west of the Waukesha sampling site, which is a reasonable explanation for the high levels of Cu found in these samples.

Several other trace metals quantified at the three sites could be important as source tracers. High levels of Pb are expected from industry (particularly metal processing [Ramadan et al 2000]) and from contamination of soils by industrial emissions or by emissions from motor vehicles before the phaseout of leaded gasoline; seasonal average Pb concentrations at the three sites were 1.1 to 9.0 ng/m^3. Roadway soil is also enriched in Pb through the pulverization of wheel weights dropped from vehicles (Root 2000).

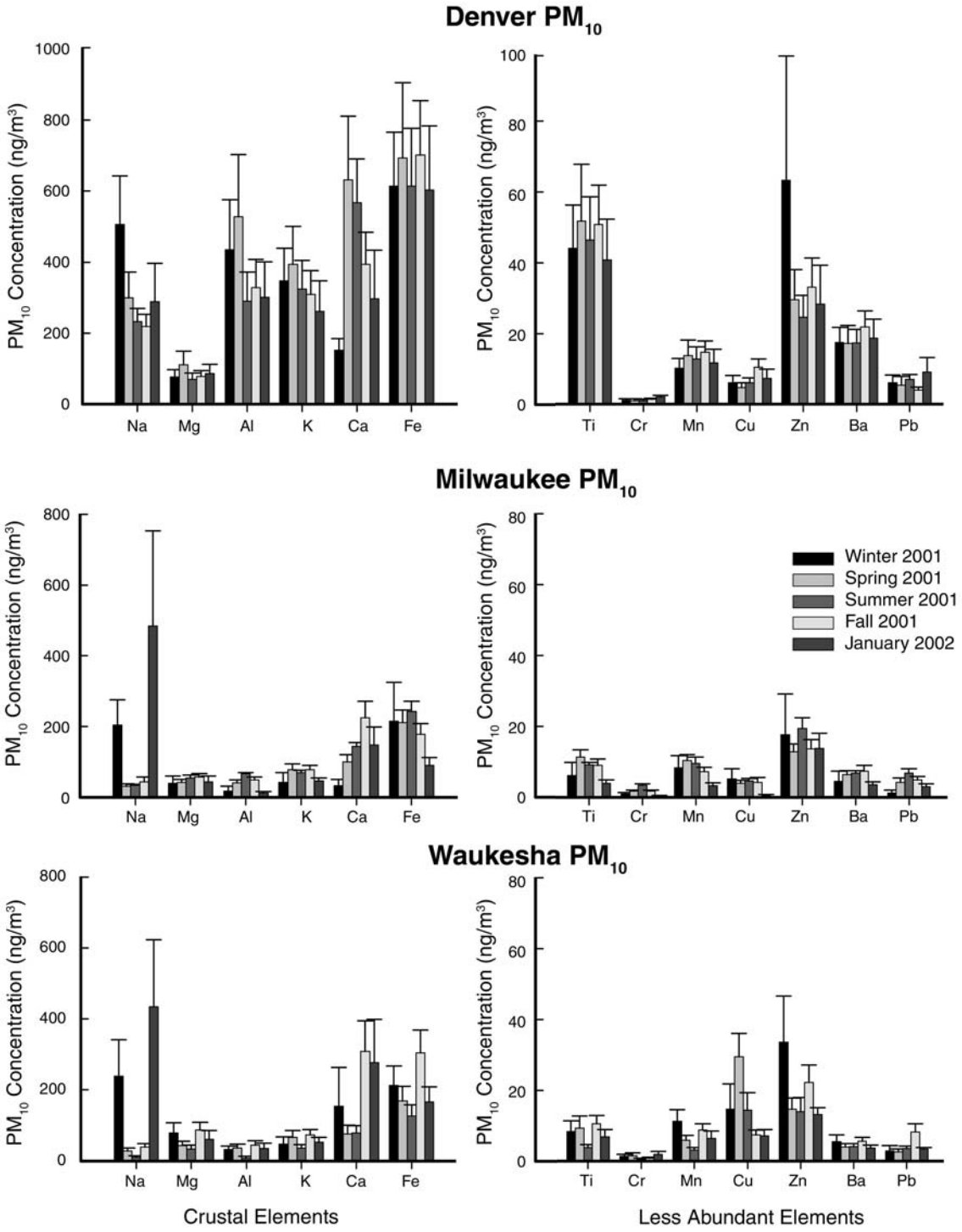

Figure 39. Seasonal average ambient concentrations of measured elements in PM_{10} at three sites. Error bars indicate the standard error of the average. Note different y-axis scales among the panels.

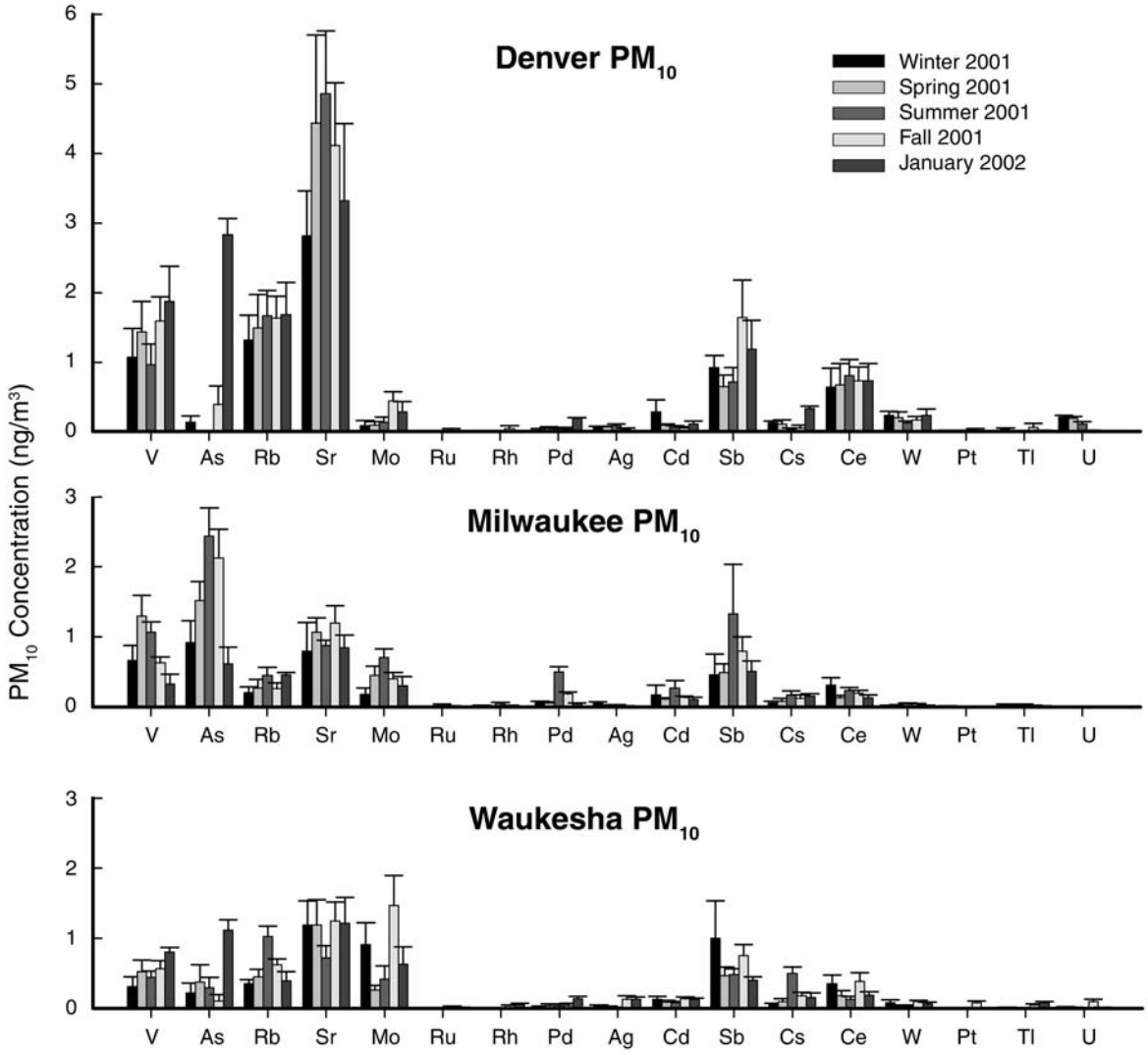

Figure 40. Seasonal average ambient concentrations of less-abundant measured elements in PM_{10} at three sites. Error bars indicate the standard error of the average.

V, which has been suggested as a tracer for combustion of fuel oil and heavy petroleum products, was present in seasonal averages at all three sites in concentrations of 0.31 to 1.9 ng/m^3. Elements such as As and Cd (up to 2.4 ng/m^3 and 0.3 ng/m^3, respectively, in seasonal site averages) may be markers for metal smelting (Ramadan et al 2000) or incineration. Although one local source in Denver is an incinerator, elevated concentrations of As and Cd were not observed there.

The very low levels of the noble metals Rh, Pd, and Pt detected were expected to be from catalytic converters (Figure 40). Though these elements are easily measured with ICP-MS at levels less than 0.01 ng/m^3, few measurements of these metals in the entire year of the study were significantly different from 0. The low concentrations we observed are consistent with work in Vienna by Kanitsar and colleagues (2003), who reported PM_{10} concentrations of Rh, Pd, and Pt of less than 5 pg/m^3.

Significant measurements of any of these three elements were obtained on a total of 14 days in Milwaukee and Waukesha and on 10 days in Denver. Of these, Pd concentrations were highest and were often accompanied by higher than usual Rh and Pt measurements. Excluding values that were not statistically different from 0, the average of the few detectable measurements (in ng/m^3) were as follows: in Milwaukee, Rh, 0.047 ± 0.006; Pd, 0.36 ± 0.048; and Pt, 0.010 ± 0.001; in Waukesha, Rh, 0.077 ± 0.013; Pd, 0.23 ± 0.03; and Pt, 0.10 ± 0.03. Milwaukee and

Waukesha measurements tended to be higher in colder winter months, but significant measurements in Denver were scattered throughout the year, with averages of 0.21 ± 0.20 ng/m^3 for Rh, 0.23 ± 0.037 ng/m^3 for Pd, and 0.079 ± 0.042 ng/m^3 for Pt. These averages reflect only the samples of highest concentration, which were outnumbered by samples below the detection limit.

The variations in concentrations of bulk chemical species and elements at the three ambient sampling sites (Figures 38–40) show that different sources influenced the particulate matter composition at these sites. To investigate these variations further, we compared particulate matter and species concentrations measured at the two Wisconsin sites, which are located only 20 km apart, in more detail. Figure 41 shows daily measurements of mass, SO_4^{2-}, OC, and EC in PM_{10} and $PM_{2.5}$ from the Waukesha site against those from the Milwaukee site. Table 10 gives values of correlation coefficient (r^2), slope, and intercept for these species and trace metals in PM_{10}. Samples from the two sites were very similar in composition for measurements that are regionally influenced, such as mass and SO_4^{2-}. Mass was highly correlated in PM_{10} (r^2 = 0.85, slope = 1.04 ± 0.07, intercept = −1.00 ± 1.74 µg/m^3). $PM_{2.5}$ mass at both sites was strongly correlated (r^2 = 0.88) and accounted for 32% to 83% (average, 56%) of PM_{10} mass at both sites.

The observed correlations between mass measurements at the two Wisconsin sites reflect the species of which the mass is composed. In this study, SO_4^{2-} contributed an average of 12% of PM_{10} mass and 20% of $PM_{2.5}$ mass at both sites. Because SO_4^{2-} is formed through atmospheric reactions and predominantly associates with fine particles, the SO_4^{2-} in $PM_{2.5}$ at each site constituted an average of 90% of the PM_{10} SO_4^{2-}. Also, because of the uniformity of atmospheric photochemistry in an urban region, correlations between SO_4^{2-} values were strong and nearly identical for both size fractions (PM_{10} r^2 = 0.93, $PM_{2.5}$ r^2 = 0.94; both, slope = 1.1 ± 0.04 and intercept = −0.2 ± 0.17 µg/m^3).

At both Wisconsin sites OC was a major contributor to mass, constituting on average 22% of PM_{10} mass and 29% of $PM_{2.5}$ mass. OC is strongly affected by local emissions but reflects a wide array of sources that are dispersed throughout an airshed. One major component of OC is secondary organic aerosol. Because, like SO_4^{2-}, secondary organic aerosol is formed by chemical processes in the atmosphere rather than being emitted from a point source, its concentration is fairly constant over a region. The mass of secondary organic aerosol therefore insulates the total OC measurement from variation with local sources, and OC levels were reasonably well correlated between PM_{10} and $PM_{2.5}$ measurements at the two sites (PM_{10} r^2 = 0.72, slope = 0.9 ± 0.1, intercept = 0.5 ± 0.4 µg/m^3; $PM_{2.5}$ r^2 = 0.68, slope = 1.1 ± 0.1, intercept = −0.2 ± 0.4 µg/m^3). Overall, OC concentrations are affected by regional concentrations of secondary organic aerosol and by local sources that are

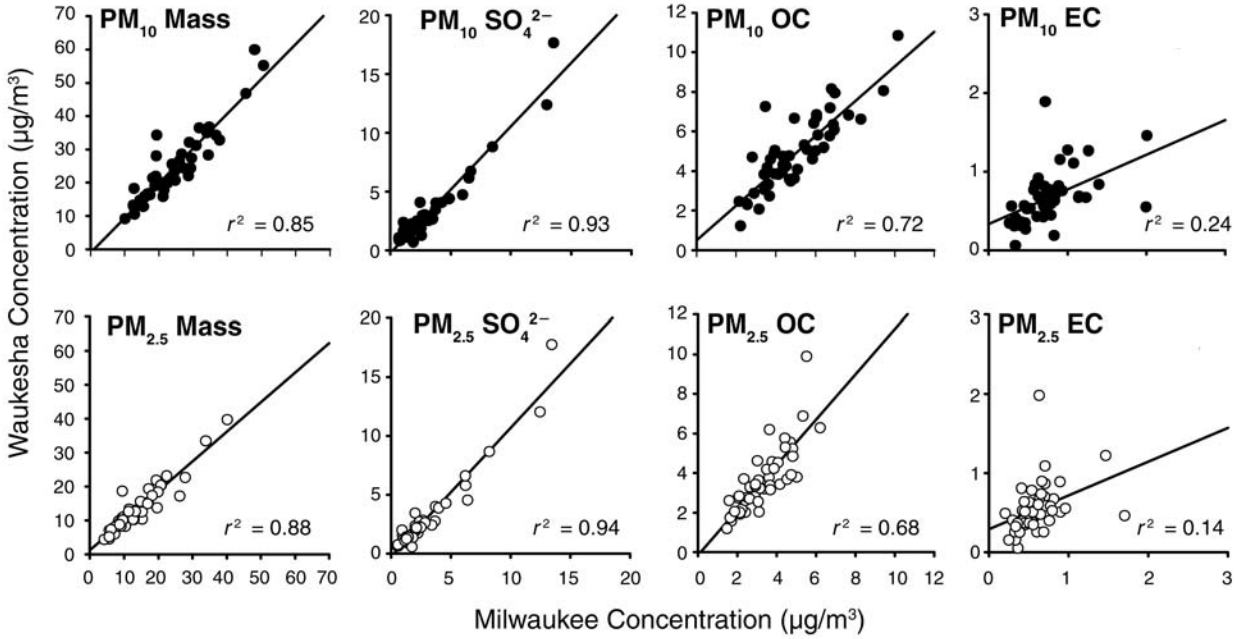

Figure 41. Ambient daily measurements of mass, SO_4^{2-}, OC, and EC in PM_{10} and $PM_{2.5}$ at the two Wisconsin sites. For regression equation values, see Table 10. Note different y-axis scales among the panels.

dispersed throughout urban areas and therefore have similar effects at different sites.

Local sources had a greater effect on EC concentrations, which differed between the two Wisconsin sites. Linear regression of the Wisconsin EC data produced a poor correlation, with an r^2 of only 0.24 for PM_{10} and 0.14 for $PM_{2.5}$. These values can be attributed to the fact that EC is emitted from combustion of organic matter, which is not spatially uniform across the urban region. Variations in local diesel traffic or combustion sources could affect EC at one site but not at the other. Like EC concentrations, ambient concentrations of metals were dominated by local sources.

Table 10. Statistics for Species Measured in PM_{10} at Waukesha vs Milwaukee for 1 Year of Ambient Samples

PM_{10} Species	r^2	Slope ± 1 SD	Intercept ± 1 SD
Mass	0.85	1.0 ± 0.07	−1.0 ± 1.7
OC	0.72	0.9 ± 0.08	0.5 ± 0.4
EC	0.24	0.4 ± 0.12	0.3 ± 0.1
Cl^-	0.85	0.5 ± 0.03	0.0 ± 0.0
NO_3^-	0.80	0.7 ± 0.05	0.4 ± 0.2
SO_4^{2-}	0.93	1.1 ± 0.04	−0.2 ± 0.2
NH_4^+	0.82	0.8 ± 0.05	−0.1 ± 0.1
Na	0.87	0.7 ± 0.04	3.9 ± 11.3
Mg	0.30	0.9 ± 0.20	10.7 ± 12.3
Al	0.03	0.2 ± 0.18	22.9 ± 9.9
K	0.48	0.8 ± 0.12	4.3 ± 10.6
Ca	0.50	1.3 ± 0.22	−39.0 ± 43.5
Fe	0.00	0.1 ± 0.19	189.5 ± 47.3
Ti	0.40	0.8 ± 0.16	0.5 ± 1.8
V	0.01	0.1 ± 0.08	0.5 ± 0.1
Cr	0.01	0.2 ± 0.23	0.9 ± 0.5
Mn	0.04	0.2 ± 0.15	5.2 ± 1.6
Cu	0.08	1.2 ± 0.67	11.7 ± 4.0
Zn	0.11	0.4 ± 0.18	12.0 ± 3.5
As	0.00	0.0 ± 0.07	0.3 ± 0.2
Rb	0.32	0.6 ± 0.13	0.4 ± 0.1
Sr	0.41	0.8 ± 0.17	0.1 ± 0.2
Mo	0.01	−0.3 ± 0.43	0.9 ± 0.3
Ru	0.01	−0.1 ± 0.24	0.0 ± 0.0
Rh	0.06	−0.3 ± 0.18	0.0 ± 0.0
Pd	0.04	0.1 ± 0.05	0.0 ± 0.0
Ag	0.03	−1.0 ± 0.82	0.1 ± 0.0
Cd	0.08	0.1 ± 0.05	0.1 ± 0.0
Sb	0.05	0.1 ± 0.07	0.5 ± 0.1
Cs	0.33	0.7 ± 0.16	0.1 ± 0.0
Ba	0.28	0.4 ± 0.09	2.1 ± 0.7
Ce	0.01	0.3 ± 0.34	0.2 ± 0.1
W	0.01	0.2 ± 0.31	0.1 ± 0.0
Pt	0.02	1.3 ± 1.45	0.0 ± 0.0
Tl	0.01	−0.2 ± 0.27	0.0 ± 0.0
Pb	0.03	0.2 ± 0.15	3.4 ± 0.9
U	0.02	1.8 ± 1.96	0.0 ± 0.0

Figure 42 shows plots of Wisconsin data for Cl^- and 11 elements measured in PM_{10}. Data points represent individual measurements grouped by season. Linear regression statistics for all measured species are listed in Table 10; however, 20 of 30 species have an r^2 of less than 0.1, suggesting no correlation between sites.

As seen in Figure 38, Cl^- concentrations were higher in winter than in other seasons at both sites, owing to the use of salt to melt ice on roadways in winter. Cl^- levels in PM_{10} were also similar at the two sites ($r^2 = 0.85$, slope = 0.49 ± 0.03, intercept = 0.02 ± 0.03 μg/m^3). More Cl^- was present at the Milwaukee site than at the Waukesha site because of greater salt application or greater resuspension of road dust and salt by downtown traffic. Every individual Milwaukee Cl^- measurement greater than 0.3 μg/m^3 occurred in the winter (January, February, or March).

The same pattern occurred for Na, also a major component of road salt. Na concentrations in PM_{10} were markedly higher in winter, and the linear regression was similar to that of Cl^- ($r^2 = 0.87$, slope = 0.7 ± 0.04, intercept = 3.9 ± 11.3 ng/m^3). As both Wisconsin sites were affected by the same source, road salt, Na at those sites had the highest correlation coefficient of any measured element.

Several other elements had reasonable correlations between the two sites, including Ca ($r^2 = 0.50$), K ($r^2 = 0.48$), and Ti ($r^2 = 0.40$). These elements are largely emitted from resuspended soil but can also be emitted from other sources, including motor vehicle exhaust (Ca) and wood smoke (K). That correlations for these three elements are only moderate suggests that their atmospheric concentrations were influenced by similar sources and activity patterns that occurred at similar times in the airshed, such as meteorologic factors.

Contributions of local sources to ambient concentrations of metals can also be seen in Figure 42. Ba measurements at the two Wisconsin sites were moderately correlated ($r^2 = 0.28$), which suggests the effects of similar sources and area dispersions at the two sites. Ba is a major component of motor vehicle brake pads and is usually associated with motor vehicle emissions (Gillies et al 2001; Sternbeck et al 2002; Pakkanen et al 2003). The moderate correlation may indicate that although the patterns and volumes of motor vehicle traffic at the two sites are not highly correlated, they are related. Sr ($r^2 = 0.41$) is a significant component of motor vehicle brake wear emissions; therefore, Sr concentrations, like Ba concentrations, will be influenced by traffic patterns.

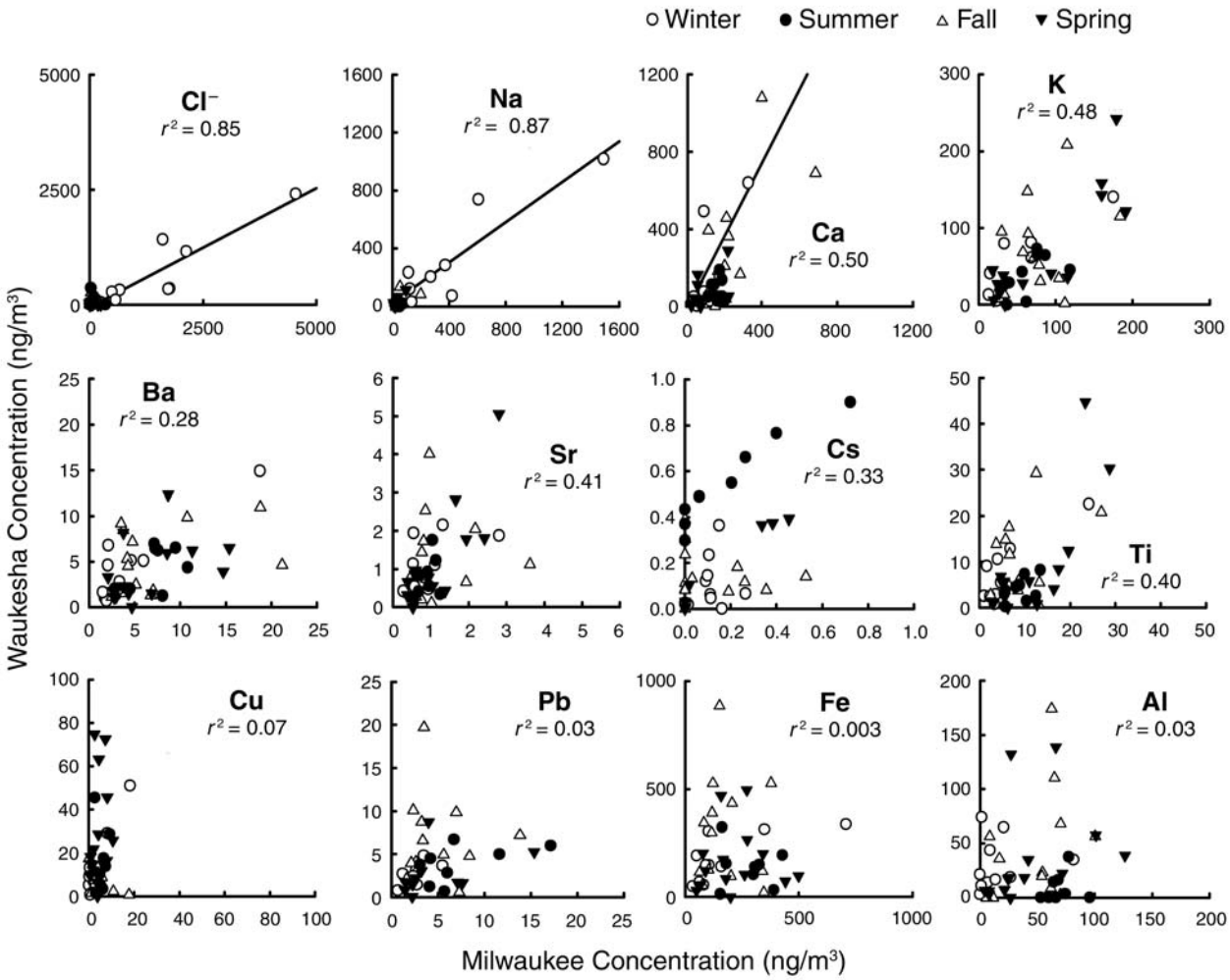

Figure 42. Ambient daily measurements of 12 elements in PM_{10} at the two Wisconsin sites. Note different scales among the panels.

Cs had an interesting seasonal pattern that resulted in a moderate correlation between sites ($r^2 = 0.33$). Three high Cs measurements were obtained in late June (spring, Figure 42), just before the high measurements of summer. An additional source influenced concentrations at both sites during this time; however, Cs is rare in the environment, so the source is unknown. Although Cs is present in soil, levels of other trace elements related to soil did not increase during the same period. Rb showed a similar seasonal pattern, and Cs was highly correlated with Rb at both the Milwaukee site ($r^2 = 0.87$) and the Waukesha site ($r^2 = 0.81$), but not at the Denver site ($r^2 = 0.04$).

The bottom row of Figure 42 illustrates an extreme: elements for which there was no correlation between concentrations at the two sites. Cu measurements were unique, being much larger in Waukesha than in Milwaukee. Variability in measurements in the low range resulted in a minimal correlation ($r^2 = 0.07$). Cu levels in Waukesha were up to 75 ng/m^3, nearly 4 times higher than the maximum of 20 ng/m^3 in Milwaukee. Cu is emitted from motor vehicles and other sources, but the relative effects of those sources in Waukesha were overshadowed by the local metal casting company registered as an emitter of Cu.

Pb, Fe, and Al also had very low correlation coefficients but, unlike Cu, showed no apparent trends in concentrations. Although the dominating sources of Pb, Fe, and Al at the two sites are unknown, the data suggest that local point sources had a great affect. All three metals are present at significant levels in crustal material and soils, but the correlations of their concentrations between the two sites were much lower than those of the other crustal elements (such as Na, Ca, K, and Ti); therefore, concentrations of Pb, Fe, and Al must be affected by local sources other than soil. Cd also showed the effect of local sources. Often associated with

incineration, a localized point source of emissions that are not spatially uniform across an urban area, Cd had an r^2 of only 0.08 between the two sites (Table 10).

For elements measured in PM_{10} at the Wisconsin sites, correlations indicated contributions of similar sources or activity patterns; large variations between the sites reflected effects of local sources. To identify sources of metals, however, consistent relations among different elements measured at the same site are more useful. Some components of crustal material, including Ti, were reasonably correlated between the two sites (Figure 42, Table 10). Fe and Al are also present in soil (Ramadan et al 2000; Chow et al 2003), but their low correlations between the Wisconsin sites indicate that local sources heavily influenced their ambient concentrations.

Concentrations of Ti, Al, and Fe in PM_{10} at all three ambient sampling sites are shown in Figure 43. In Denver, Ti was highly correlated with Fe ($r^2 = 0.97$), as was Al ($r^2 = 0.86$). Correlations between these elements in Wisconsin were much lower: Ti and Fe had r^2 of 0.68 in Waukesha and 0.40 in Milwaukee, and Al and Fe had r^2 of 0.70 in Waukesha and 0.27 in Milwaukee. Linear regressions of Ti and Al against Fe were not significantly different at the Milwaukee and Waukesha sites but both were much different from Denver regressions. Additionally, levels of all three elements were lower at the Wisconsin sites. These data suggest that concentrations of Ti, Al, and Fe in Denver samples were from resuspended soil and that crustal materials were a larger component of the PM_{10} in Denver. Low correlations between the Wisconsin sites for Al and Fe (Figure 42), however, indicate that other sources dominated the concentrations of those elements.

Large contributions of crustal materials to ambient metal concentrations also suggest that other elements, present in trace amounts in soil, are dominated by large emissions of resuspended soil. To investigate that possibility, we compared concentrations of Ba and Sr to concentrations of Cu at each ambient sampling sites. These three elements are known to be emitted by motor vehicle brake wear, but they are also present in low levels in crustal materials.

As suggested in Figure 44, different sources influenced the concentrations of Cu, Sr, and Ba at the three sites. Levels of Cu were much higher in Waukesha than in Milwaukee or Denver, owing to a local Cu emitter. Levels of Ba and Sr were higher in Denver than in the Wisconsin sites. This result may have been associated with the large concentrations of crustal elements, which in turn could have contributed to the higher correlations between Ba and Cu ($r^2 = 0.77$) and between Sr and Cu ($r^2 = 0.60$) at that site. Although all three elements are associated with motor vehicle brake wear, these contributing sources caused the linear regressions for Ba and Sr versus Cu at the three sites to diverge markedly.

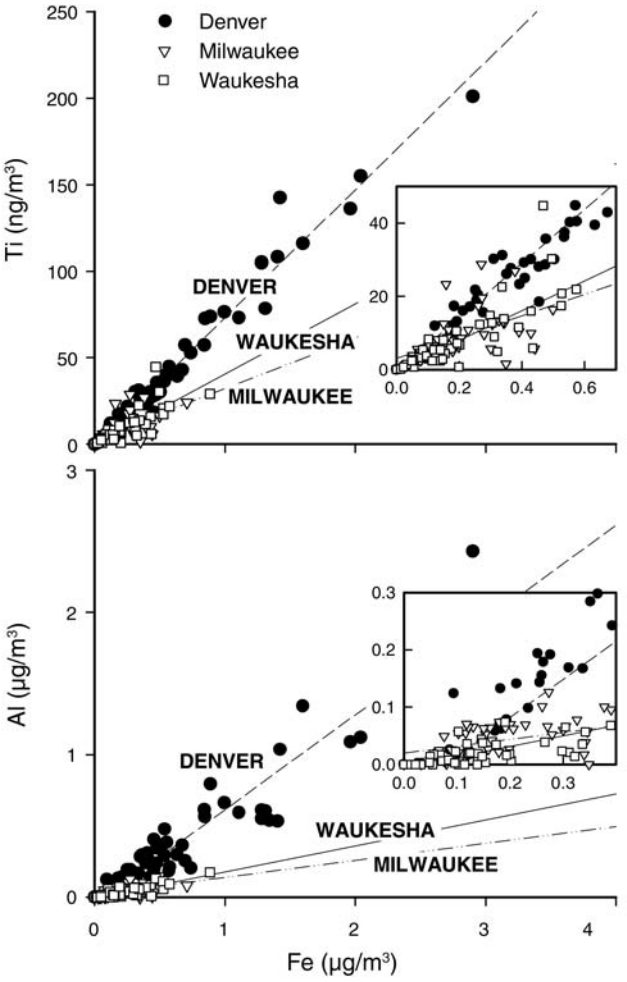

Figure 43. Ambient daily concentrations of Ti, Al, and Fe in PM_{10} at three sites. Note different y-axis scales between the panels.

To eliminate the influence of the local Cu emitter in Waukesha, we compared Sr and Ba concentrations directly (Figure 45). The two elements were relatively well correlated in Denver ($r^2 = 0.85$), but somewhat less so in Milwaukee ($r^2 = 0.58$) and Waukesha ($r^2 = 0.52$). The linear regressions have similar slopes for all three sites (0.21 ± 0.01 for Denver, 0.20 ± 0.03 for Waukesha, and 0.12 ± 0.01 for Milwaukee), however. This similarity indicates that Ba and Sr were present in consistent ratios in the emissions from a source that affected all three sites. The concentrations of Ti, Al, and Fe we compared suggested a different composition of crustal material in Denver than in Milwaukee and Waukesha. Therefore, the consistent relation of Ba and Sr indicates that motor vehicle brake wear affected the ambient concentrations of these elements at all three sites.

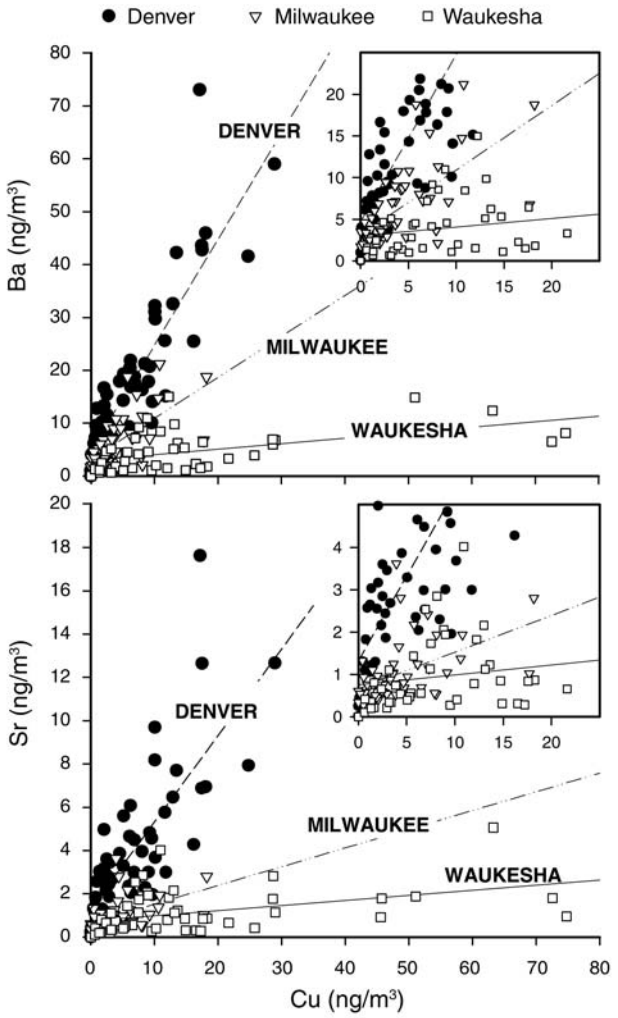

Figure 44. Ambient daily concentrations of Ba, Sr, and Cu in PM_{10} at three sites. Note different y-axis scales between the panels.

In addition to helping to elucidate the sources of metals, these results are important for understanding the distribution of exposures to different categories of air pollutants in the Milwaukee area in particular, and in Wisconsin in general. Conclusions about the spatial distribution of particulate matter derived from particle mass and SO_4^{2-} measurements do not accurately represent other species in particulate matter that may be important to human health. As more evidence emerges of the role of trace metals in health effects, new approaches are needed to assess the public's exposure to trace metals and other potentially harmful components of atmospheric particulate matter.

ICFA

Analysis of 22 Species Including OC and EC We also considered source apportionment of the combined Waukesha and Milwaukee data using ICFA. The primary focus of our study was the effect of metals, but we also studied OC and EC because their presence greatly facilitates identification of several sources. Although we conducted much exploratory analysis in order to select species for inclusion in the study and to determine the model structure, we present here only some final analyses for interpretation.

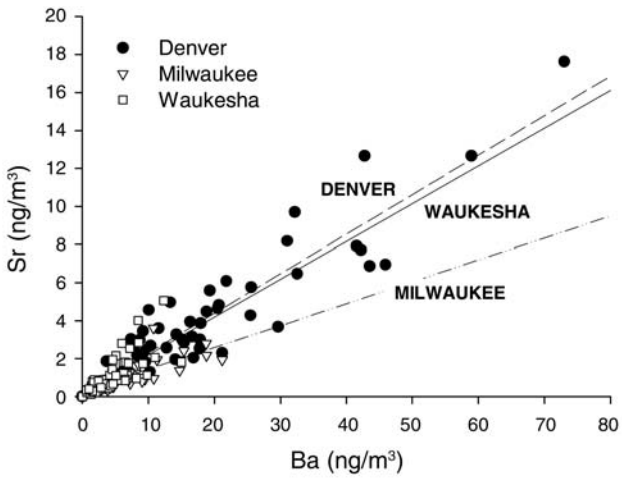

Figure 45. Ambient daily concentrations of Ba and Sr in PM_{10} at three sites.

We began by hypothesizing a model with six a priori source profiles that varied in believability. The profiles for roadway emissions and road salt were based on tunnel measurements and were thus highly credible. The profiles for wood burning and for a municipal incinerator were obtained from the EPA SPECIATE database (*www.epa.gov/ttn/chief/software/speciate*) and hence were created from measurements taken at a different time and location from those in this study; therefore, these profiles had only limited credibility. The final two profiles were virtually unspecified in order to identify unknown sources: one is referred to as *Unknown*; the other, *Copper*, because of relatively large amounts of Cu in some samples.

Although methods for measuring OC, EC, and other constituents varied among the profiles, the ICFA algorithm allows profiles to adapt to the correlation structure in the observed data during the iterative process. Only the profiles created for this study were constrained to remain relatively unchanged by the algorithm. Profiles borrowed from other studies were only loosely constrained. Table 11 shows the hypothesized source profiles used for the starting values in the ICFA algorithm. The 19 species included in the model were selected by using prescreening tools that eliminated elements that were largely below

detection and emphasized elements with high specificity for sources and relevance to human health.

In the first update step, the known elements of the profile matrix (or factor loading matrix) were fixed to their hypothesized values and the elements in the Unknown profile were estimated along with all other unspecified parameters in the model. In this and every step of the algorithm, elements of the profile matrix were constrained to be nonnegative.

We then began a series of updates, each involving the reestimation of randomly selected rows of the profile matrix. Each row of Λ was selected for reestimation with the same fixed probability. Thus the number of reestimated rows changed from iteration to iteration, with the constraint that never more than $p - k$ rows were estimated (to retain the conditional identifiability property). Once the rows for reestimation were chosen, a confirmatory factor analysis model was fitted with factor loadings in the $p - q$ estimated rows, and q rows were fixed to equal the factor loading estimates obtained from the previous iteration.

Each reestimation is an improvement in the sense that the χ^2 goodness-of-fit statistic measuring lack of fit is reduced at each iteration. (The statistic can be calculated using -2 times the log likelihood evaluated at the estimated parameter vector.) The amount of improvement generally decreases for successive iterations as the procedure is successively iterated. A decrease (or rather, nonincrease) of the χ^2 goodness-of-fit statistic is in fact guaranteed at each iteration.

Because of the varying degrees of credibility associated with the profiles in the initial source profile matrix, we assigned different degrees of constraint to the acceptable values for reestimated profile elements. For the Roadway and Road Salt profiles, all reestimated elements were required to fall in the interval $[3/4 \times \lambda_{ij}, 4/3 \times \lambda_{ij}]$, where λ_{ij} is the proportional representation of the ith species from the jth source. For the Wood Burning and Incinerator profiles, reestimated elements were constrained to fall in the interval $[1/10 \times \lambda_{ij}, 10 \times \lambda_{ij}]$. All reestimated elements of the Copper

Table 11. Starting Source Profile Matrix for ICFA of 22 Chemical Species in PM_{10}

PM_{10} Species	Profile[a]					
	Roadway	Unknown[b]	Road Salt	Wood Burning[b]	Copper	Incinerator
OC	0.285805	—	0.075576	0.450000	0.000000001	0.00570
EC	0.077378	—	0.000000	0.100000	0.000000001	0.03500
Cl^-	0.163631	—	0.304239	0.010000	0.000000001	0.27000
Na	0.050220	—	0.135893	0.001000	0.000000001	0.06200
Mg	0.021079	—	0.037860	0.000730	0.000000001	0.01420
Al	0.011669	—	0.026836	0.001000	0.000000001	0.00230
K	0.005302	—	0.013830	0.030000	0.000000001	0.07600
Ca	0.025878	—	0.031830	0.001000	0.000000001	0.00230
Fe	0.044138	—	0.020640	0.000000	0.000000001	0.00220
V	0.000031	—	0.000049	0.000000	0.000000001	0.00001
Mn	0.000447	—	0.000473	0.000000	0.000000001	0.00016
Cu	0.000905	—	0.000285	0.000000	0.01	0.00120
Zn	0.001670	—	0.001314	0.000370	0.000000001	0.09800
As	0.000037	—	0.000004	—	0.000000001	0.00007
Sr	0.000152	—	0.000379	0.000000	0.000000001	0.00009
Ag	0.000044	—	0.000000	0.000000	0.000000001	0.00007
Cd	0.000004	—	0.000007	0.000000	0.000000001	0.00110
Sb	0.000167	—	0.000017	0.000000	0.000000001	0.00140
Ba	0.002420	—	0.000506	0.000000	0.000000001	0.00083
Ce	0.000072	—	0.000042	0.000000	0.000000001	0.00000
W	0.000008	—	0.000020	0.000000	0.000000001	0.00000
Pb	0.000377	—	0.000443	0.000000	0.000000001	0.05800

[a] Values are relative contributions.

[b] A dash (—) indicates that the value was unknown and therefore unspecified.

and Unknown profiles, except for the Cu element of the Copper profile, were allowed to take any value in [0, 1].

These general rules for profile constraints had some exceptions. For example, one element in each source profile except Unknown was fixed to remain at the starting value in order to fix the scale for the profile. Thus the values for the OC element of Roadway and of Wood Burning, the Cl^- element of Road Salt, the EC element of Incinerator, and the Cu element of the Copper profile never changed during the updates. Also, any element with a value in Table 11 that was undefined or defined to be 0.000000001 was always allowed to take any value in [0, 1], regardless of the profile. Because the Roadway profile is affected by Road Salt, and because Road Salt was an added source in the model, we allowed the Cl^- and Na values in the Roadway profile to be as low as 0 to allow the mass associated with these elements to be included in the updated Road Salt profile. (Note that we chose asymmetric intervals to allow for the right-skewness typically associated with air quality data. One could also specify a separate interval for each element in the source profile matrix on the basis of source profile uncertainty estimates.)

After 50 updates of the source profile matrix, we rescaled the Roadway and Road Salt profiles to ensure that the individual values in each profile summed to no more than 1, and we rescaled the remaining (loosely constrained) profiles to also sum to 1. Examination of the estimated source profile matrix led us to relabel some of the sources. We changed Unknown and Wood Burning to Organic 1 and Organic 2, respectively, because of the dominant role of OC in these profiles. After revising the Incinerator profile, we renamed it Roadway 2 because of its EC/OC ratio. The final estimates and their final labels are given in Table 12.

After using the nonlinear model in equation (2), we estimated the source contribution at each date of measurement and plotted the estimates (Figure 46). Using the total mass measured at each time, a range of possible contribution values for each source was specified. Starting values were chosen at random from a uniform distribution with range from 0 to a constant proportional to the measured

Table 12. Final Source Profile Matrix Estimated by Using ICFA of 22 Chemical Species in PM_{10}

	Profile[a]					
PM_{10} Species	Roadway 1	Organic 1	Road Salt	Organic 2	Copper	Roadway 2
OC	0.2858	0.7455	0.1629	0.8239	0.0175	0.4497
EC	0.0904	0.0800	0.0000	0.1348	0.0000	0.2761
Cl^-	0.0000	0.0044	0.4930	0.0018	0.0000	0.0000
Na	0.0000	0.0099	0.1652	0.0002	0.0000	0.0000
Mg	0.0158	0.0158	0.0460	0.0061	0.0000	0.0112
Al	0.0088	0.0104	0.0326	0.0044	0.0000	0.0078
K	0.0055	0.0153	0.0168	0.0081	0.0000	0.0600
Ca	0.0220	0.0584	0.0521	0.0183	0.0000	0.0179
Fe	0.0331	0.0518	0.0251	0.0000	0.0000	0.0479
V	0.0000	0.0001	0.0001	0.0000	0.0000	0.0002
Mn	0.0006	0.0016	0.0010	0.0000	0.0000	0.0014
Cu	0.0007	0.0005	0.0003	0.0000	0.9825	0.0009
Zn	0.0021	0.0034	0.0028	0.0024	0.0000	0.0773
As	0.0000	0.0001	0.0000	0.0002	0.0000	0.0001
Sr	0.0001	0.0002	0.0005	0.0000	0.0000	0.0006
Ag	0.0000	0.0000	0.0000	0.0000	0.0000	0.0001
Cd	0.0000	0.0000	0.0000	0.0000	0.0000	0.0009
Sb	0.0002	0.0001	0.0000	0.0000	0.0000	0.0011
Ba	0.0018	0.0011	0.0006	0.0000	0.0000	0.0011
Ce	0.0001	0.0001	0.0001	0.0000	0.0000	0.0000
W	0.0000	0.0000	0.0000	0.0000	0.0000	0.0000
Pb	0.0005	0.0014	0.0009	0.0000	0.0000	0.0458

[a] Values are relative contributions.

mass. Thus no effort was made to obtain starting values near the true or estimated source contribution.

Among the 30 estimators obtained from the nonlinear least squares fit, the majority were near the value that minimized the sum of squares error, but several always converged to local minimums in the function being minimized. The source contributions estimated for Milwaukee and Waukesha tended to be reasonably well correlated. As expected, the contribution of the Road Salt profile was relatively low for most of the year but spiked in winter (February 2001 and January 2002), when road salt was being used. Because the contribution of the Organic 2 profile was slightly higher during summer than during winter, we suspect that this source profile may be associated with secondary organic formations.

Figure 47 shows box plots of the calculated mass versus measured mass for each of the 22 species. Figure 48 shows the contribution of pollution sources to total PM_{10} mass for each of the 22 species. The relative dominance of OC and EC seems to drive the formation of the pollution source profiles. The Organic 1 and Organic 2 sources contributed much larger amounts to total PM_{10} mass than the other sources. Figure 49 gives noncarbon pollution source contributions for each of the 20 noncarbon species. In the noncarbon analysis, the difference between the Organic 1

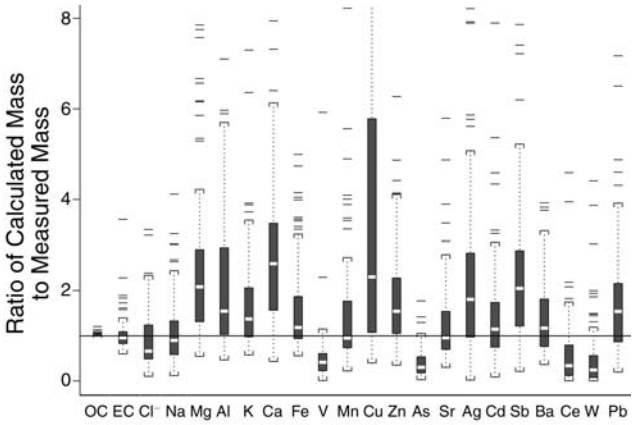

Figure 47. Box plots for ratios of calculated mass to measured mass of PM_{10} at the two Wisconsin sites for 22 species in the analysis. The contributions of each species to each source profile were averaged over all measurement times and both locations. For each species, the central white bar represents the average; and the shaded bars and the dotted lines represent 1 SD and 2 SD, respectively.

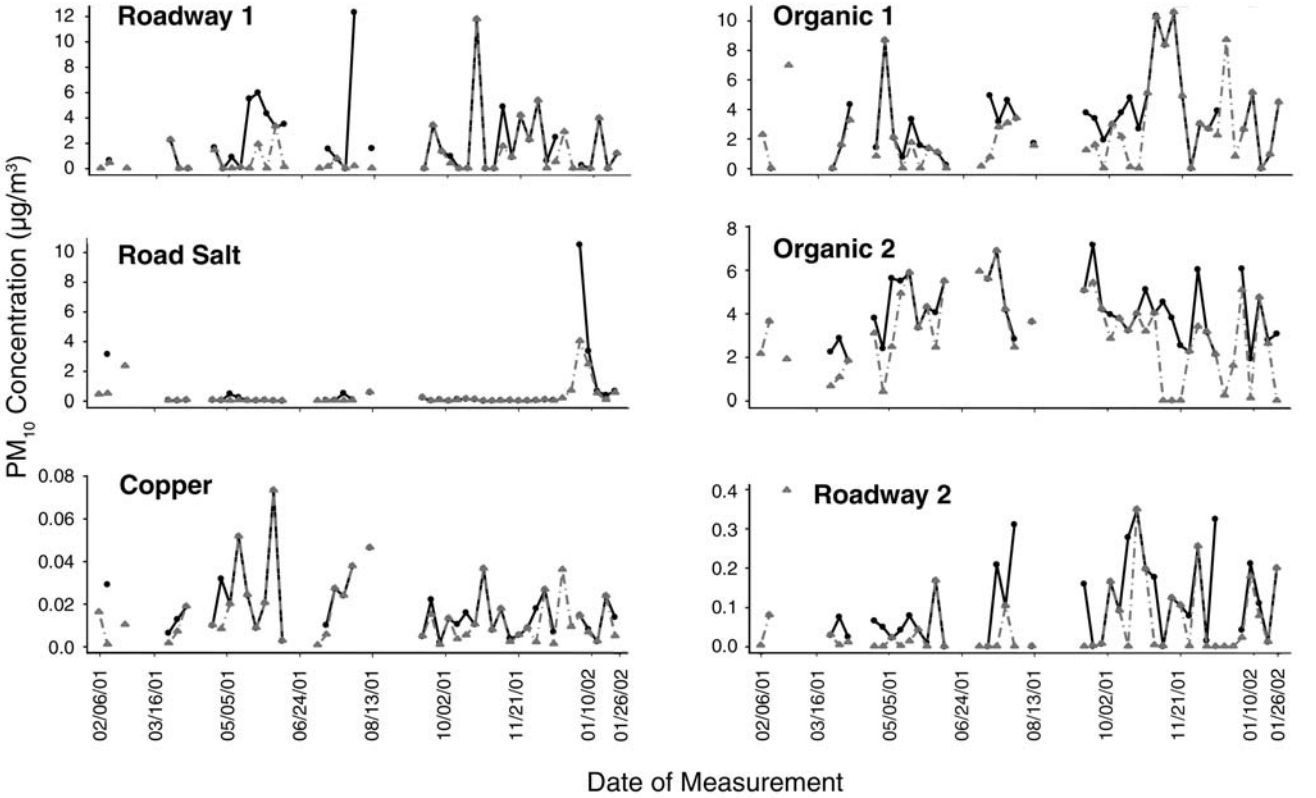

Figure 46. Source contribution estimates to PM_{10} mass based on analysis of 22 chemical species in particulate matter samples, by date of measurement, in Milwaukee (black lines) and Waukesha (gray dashed lines). Note different y-axis scales among the panels.

and Organic 2 source contributions and those of the Roadway 1, Roadway 2, and Road Salt sources were not as dramatic as those in the total PM_{10} analysis. Finally, Figure 50 shows the complete source contributions for each species. For example, most of the ambient Cl^- mass originated from the Road Salt source, and most of the Cu originated from the Copper source. This apportionment indicated that the Organic 1 source was the leading contributor to most of the heavier metals.

Analysis Based on Metal-Heavy Sources Because one of the primary goals of the study was to assess the effects of metals and metal-heavy sources on air quality, we decided to conduct analyses without OC and EC in an effort to identify metal sources that might be overshadowed by their presence. First the values for all species other than OC and EC in the final source profile matrix estimated by ICFA were used as starting values (Table 12), with one exception: elements estimated to be 0 in Table 12 were

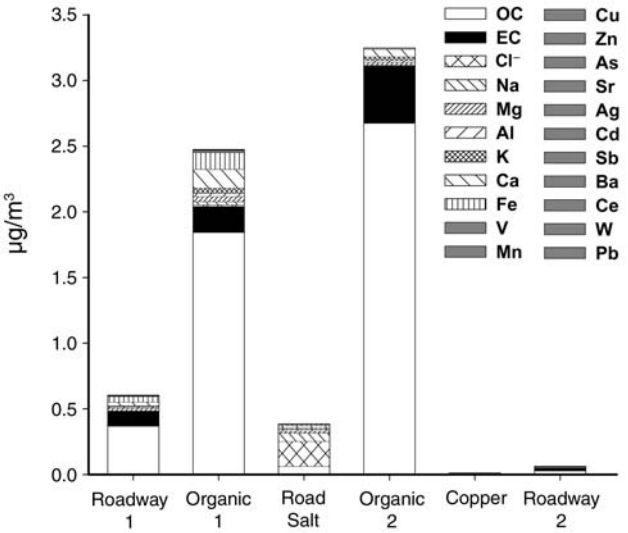

Figure 48. Source contributions to PM_{10} mass at the two Wisconsin sites for 22 species in the analysis. The contributions of each species to each source profile were averaged over all measurement times and both locations. Elements indicated with gray shading do not appear because their relative contributions were too small to show.

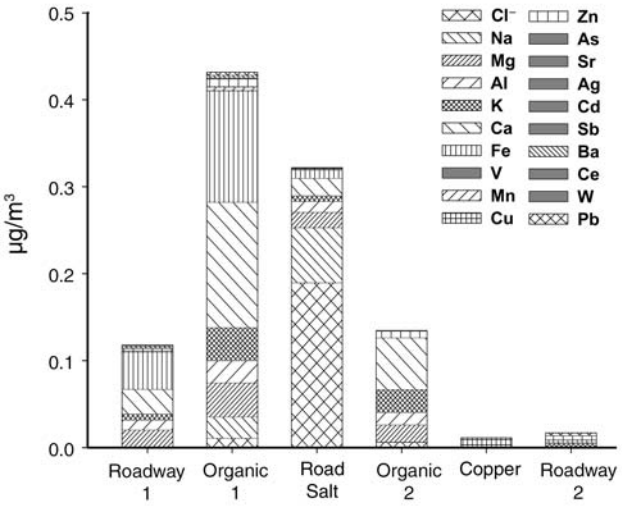

Figure 49. Source contributions to PM_{10} mass at the two Wisconsin sites for 20 noncarbon species in the analysis. The contributions of each species to each source profile were averaged over all measurement times and both locations. Elements indicated with gray shading do not appear because their relative contributions were too small to show.

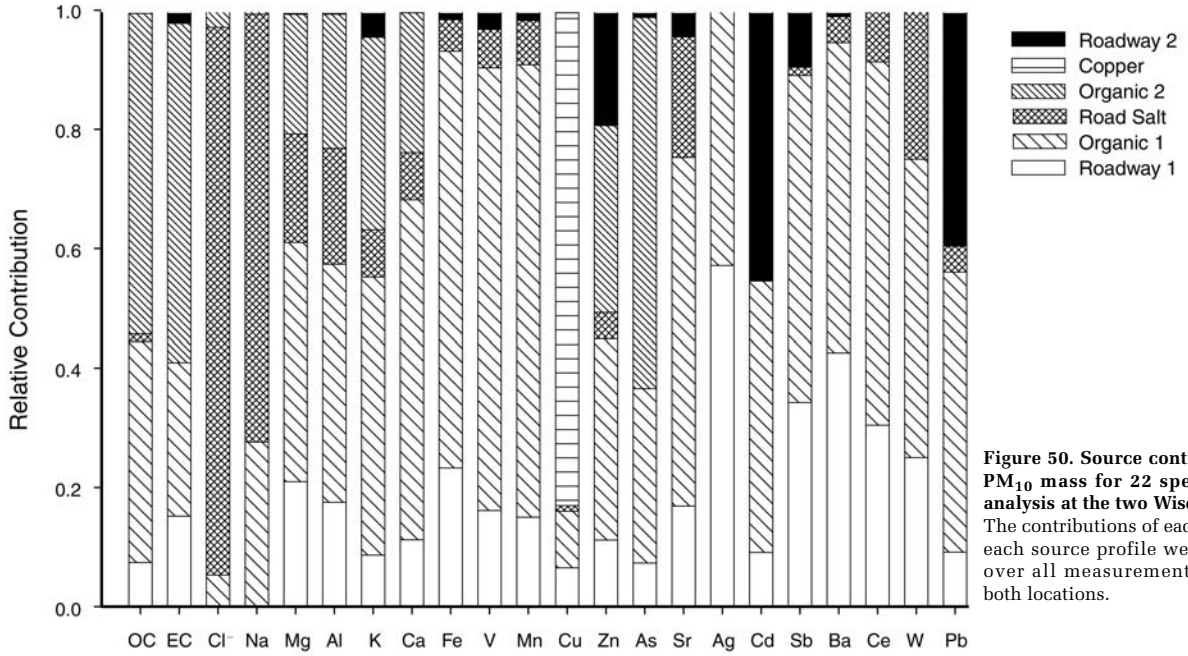

Figure 50. Source contributions to PM_{10} mass for 22 species in the analysis at the two Wisconsin sites. The contributions of each species to each source profile were averaged over all measurement times and both locations.

changed to 0.000000001, which allowed each element to be updated. The Cl^- element in the Road Salt profile was fixed at the starting value, but all other elements in the Roadway 1 and Road Salt profiles were constrained to the interval $[4/5 \times \lambda_{ij}, 5/4 \times \lambda_{ij}]$, where λ_{ij} is the proportional representation of the ith species from the jth source. The elements in the other four source profiles were constrained only to be nonnegative, but the factor variance was constrained to equal a constant. The size of this constant was irrelevant because the four profiles originally labeled Organic 1, Organic 2, Copper, and Roadway 2 would be rescaled to sum to 1 after the final update. Because the most prominent chemical constituents (OC and EC) were excluded, scaling the 20 noncarbon profile elements to sum to 1 would overestimate these elements, making the scale of the resulting source contribution estimates incorrect. The estimated profiles based on the noncarbon species were expected to be more sensitive to the metal-heavy sources than the profiles based on all 22 species (Table 12), but the scale of the source profile elements needed to be adjusted. Thus the following approach was developed for assessing the metal-heavy source contributions:

1. Estimate the source profiles using the 20 noncarbon species.
2. Estimate the two rows of profile elements associated with OC and EC using estimates of the noncarbon species in a confirmatory factor analysis model.
3. Rescale all previously unspecified source profiles to sum to 1.

This approach yields source profiles and associated source contributions that are of the appropriate scale but are not overly influenced by the dominance of the carbon species.

In step 2, the estimates of the OC and EC elements of the source profile matrix were constrained by using not only the source profile estimates from step 1, but also the OC and EC starting values in the Roadway and Road Salt profiles in Table 11. The resulting complete source profile matrix, after estimating the profile matrix rows for OC and EC and rescaling, is given in Table 13. In addition to the Roadway and Road Salt sources, we identified the other updated source profiles as EC with Light Metals, Organic (which is dominated by OC), Metals (which consists of OC, EC, Cl^-, and metals), and OC with Heavy Metals.

Figure 51 plots the source contributions to total PM_{10} mass that are based on our approach for assessing metal-heavy sources. The Road Salt source profile shows roughly the same structure as in the first analysis (Figure 46). Similar to the Organic 2 source profile estimated for all 22 species (Figure 46), the Organic source concentrations estimated for noncarbon PM_{10} species tend to be greater during summer, which is typical of secondary organics formation.

Figure 52 shows box plots of the calculated mass versus measured mass for each of the 22 PM_{10} species when we used the approach for assessing metal-heavy source contributions. Figure 53 gives total pollution source contributions for PM_{10} mass for each of the 22 species using this approach. Figure 54 gives noncarbon pollution source contributions for each of the 20 noncarbon species using this approach. Because the Organic source accounts for much of the OC, it contributed vastly more to the total PM_{10} mass than the other sources did. This contribution is illustrated by comparing Figure 53, which includes OC and EC, and Figure 54, which gives only the noncarbon contributions to PM_{10} mass (note the different scale in each).

Figure 55 shows the complete contributions to each of the 22 PM_{10} species in the analysis by the six pollution sources. The Organic source was the leading contributor to the mass of 14 species (OC, EC, Mg, Al, K, Ca, Fe, V, Mn, As, Sr, Cd, Ba, and Ce). Although the contributions of the Road Salt and OC with Heavy Metals sources to the total mass were an order of magnitude smaller than the Organic source contribution, they were the largest contributors to the mass of some species. Road Salt was the leading contributor to the mass of Cl^- and Na, and OC with Heavy Metals was the leading contributor to the mass of Cu, Zn, Ag, Sb, W, and Pb.

The ICFA method allowed us to define some sources with high specificity (as in confirmatory factor analysis), while using the structure of the data to identify sources that were unknown, misspecified, or poorly defined a priori. In further developing ICFA, we propose an approach that maximally utilizes source profile information to reduce indeterminacy and increase interpretability when multivariate receptor models are employed. Though the ICFA approach is not flawless, we believe that it provides unique insights and that its development as a new source apportionment approach has potential value.

In this study, PM_{10} data from Milwaukee and Waukesha were apportioned to sources using ICFA. The ICFA method is used to specify metal-heavy sources, although such sources are often not the major contributors to total PM_{10} mass. In this analysis, we identified organic sources as the leading contributors to the PM_{10} mass. Our approach for assessing metal-heavy sources then allowed identification of other sources that made important contributions to the mass of individual species of interest.

Table 13. Final Source Profile Matrix Estimated by Using Approach for Assessing Metal-Heavy Source Contributions to PM_{10}

	Profile[a]					
PM_{10} Species	Roadway	EC with Light Metals	Road Salt	Organic	Metals	OC with Heavy Metals
OC	0.2858	0.1611	0.0756	0.8219	0.3275	0.5535
EC	0.0774	0.6442	0.0000	0.0697	0.1635	0.0236
Cl^-	0.0000	0.0577	0.3042	0.0000	0.1875	0.0500
Na	0.0628	0.0150	0.1087	0.0000	0.0000	0.0018
Mg	0.0214	0.0083	0.0473	0.0154	0.1736	0.0011
Al	0.0093	0.0080	0.0215	0.0060	0.0000	0.0490
K	0.0066	0.0097	0.0161	0.0160	0.0375	0.0689
Ca	0.0258	0.0530	0.0398	0.0238	0.0000	0.0622
Fe	0.0552	0.0361	0.0165	0.0430	0.0515	0.1042
V	0.0000	0.0001	0.0001	0.0001	0.0011	0.0003
Mn	0.0004	0.0012	0.0006	0.0016	0.0085	0.0155
Cu	0.0007	0.0008	0.0002	0.0000	0.0283	0.0097
Zn	0.0021	0.0026	0.0011	0.0009	0.0094	0.0352
As	0.0000	0.0001	0.0000	0.0002	0.0000	0.0000
Sr	0.0002	0.0002	0.0005	0.0001	0.0024	0.0016
Ag	0.0001	0.0000	0.0000	0.0000	0.0000	0.0002
Cd	0.0000	0.0001	0.0000	0.0000	0.0022	0.0000
Sb	0.0001	0.0000	0.0000	0.0000	0.0000	0.0067
Ba	0.0019	0.0008	0.0006	0.0006	0.0000	0.0003
Ce	0.0001	0.0001	0.0001	0.0000	0.0013	0.0002
W	0.0000	0.0000	0.0000	0.0000	0.0004	0.0001
Pb	0.0003	0.0010	0.0004	0.0006	0.0055	0.0160

[a] Values are relative contributions.

SYNTHETIC LUNG FLUID EXTRACTIONS

Figure 56 presents results of tests to determine the solubility of trace metals in roadway tunnel emissions of PM_{10}, in synthetic lung fluid. Data from samples collected inside a roadway tunnel in four separate tests are shown for elements measured in considerable amounts in samples and with low background in lung fluid. The leachable fraction was generally higher than that observed with the SRMs (Figure 9), but interelement patterns were quite similar. A high degree of reproducibility was observed among tests, attesting to the robustness of the leaching protocol and uniformity of chemical phases among these tunnel aerosols.

Crustal elements exhibited relatively low solubility (Ti, 5%–10%; Al, 10%–15%; Ce, 5%–20%; and Fe, 10%–25%), whereas the two very mobile transition metals Mn and Cd approached 90% solubility. The leachable fractions of Cu, Zn, and Sb were also high, approximately 50% to 60%, consistent with known solution chemistry. Ba and Pb solubility fractions were similar, averaging 25%. The relatively low leachable fraction of Ba was not unexpected given the low solubility of most common anions and likely source compounds, including barium sulfate from brake wear (Blau 2001). Many Pb species, except the NO_3^-, are only slightly soluble in saline, with pH nearly neutral; the Pb cation is extracted into most environmental phases. These facts likely explain the low fraction of Pb that was leachable.

These experiments measured the fraction of metals leachable by a fixed volume of synthetic lung fluid in 8 hours, not the total soluble fraction. Therefore, mass loadings may have had a distinct effect on the fraction of a species that was leachable, similar to that expected from short-term dissolution of particle masses in lung fluid.

In all ambient composites from the same dates, masses of particulate matter collected at the Milwaukee and Waukesha sites were very similar, but masses of samples at the Denver site were nearly twice as high. Figure 57 shows

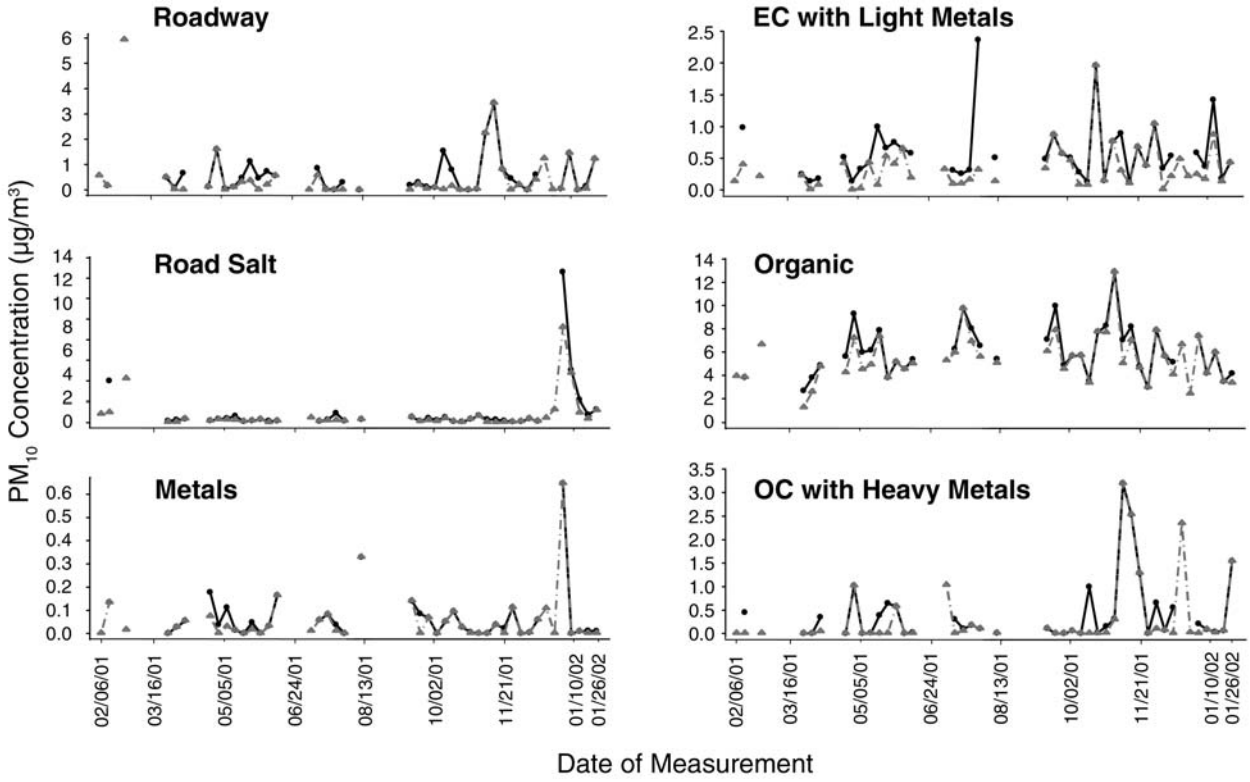

Figure 51. Source contribution to total PM_{10} mass based on assessment of metal-heavy source contributions, by date of measurement, in Milwaukee (black solid line) and Waukesha (gray dashed line). Note different y-axis scales among the panels. The contributions of each species to each source profile were averaged over all measurement times and both locations.

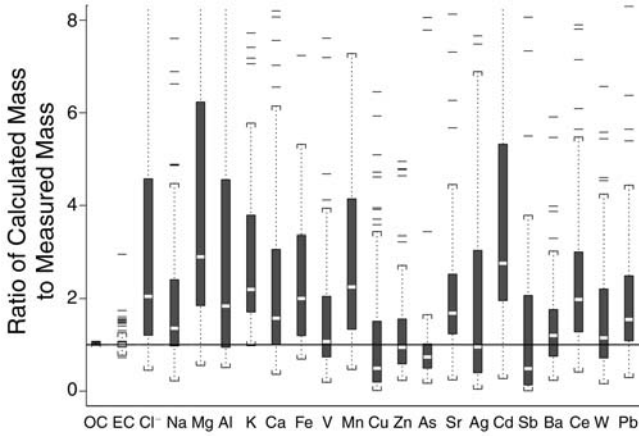

Figure 52. Box plots for ratios of calculated mass to measured mass of PM_{10} at the two Wisconsin sites obtained by using the approach for assessing metal-heavy source contributions. The contributions of each species to each source profile were averaged over all measurement times and both locations. For each species, the central white bar represents the average, and the shaded bars and dotted lines represent 1 SD and 2 SD, respectively.

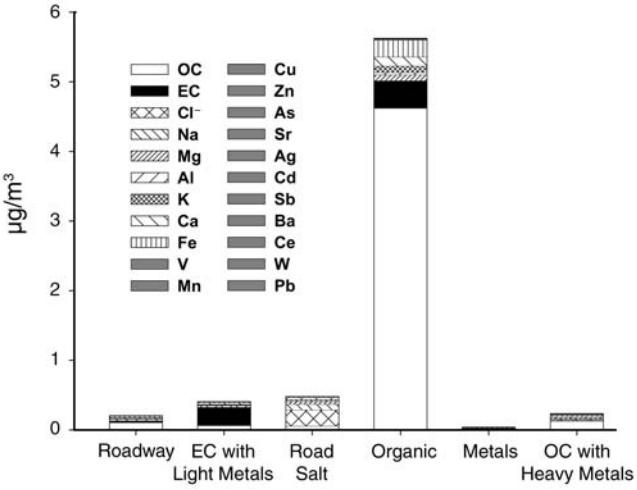

Figure 53. Source contributions to PM_{10} mass at the two Wisconsin sites for each of the 22 species obtained by using the approach for assessing metal-heavy source contributions. The contributions of each species to each source profile were averaged over all measurement times and both locations. Elements indicated with gray shading do not appear because their relative contributions were too small to show.

leachable fractions of metals at the three ambient sampling sites for samples collected at the same dates and times in November 2001. The elements shown are those measured in considerable amounts in samples and with low background in lung fluid. For nearly all of the metals measured in November samples, the leachable fraction was lowest in the Denver sample. This consistent result may reflect that the Denver metals were associated with less soluble phases or may be due in part to the high mass loading of the Denver composite (1150 µg), which was nearly twice the mass of the Wisconsin samples.

Also, results of our exploration of a set of detailed ambient data (see Descriptive Analysis) suggests that measured Denver PM_{10} was affected much more by crustal elements than Wisconsin PM_{10} was; many of these elements are expected to be associated with stable, less soluble crustal materials. For the November 2001 composites, the leachable fractions of Ce, Pb, Sb, Ba, and W were highest in the Milwaukee samples; the leachable fractions of Cu, Mn, and Mo were highest in the Waukesha samples.

Concentrations of metals vary with point sources over relatively small geographic areas. Hence, although the Milwaukee and Waukesha sites were only 20 km apart and had similar particulate matter mass and regionally influenced species, total concentrations of individual metals were influenced by a variety of local sources. The differences in sources and chemical compositions of metals at the two sites are consistent with the differences between leachable fractions of individual metals.

Leachabilities of individual metals in the ambient aerosol composites are compared in Figure 58. The composites represent 2 individual sampling days in a month and are not meant to represent seasonal or monthly averages. February samples were available only in Denver; April samples, only in Wisconsin. Two composites were available in May, labeled May A and May B.

The fraction of Ba soluble in the synthetic lung fluid (Figure 58A) ranged from 10% to 65% for all three sites, with no distinct trends among sites. Pb, however, did show differences by site (Figure 58B): on average, the leachable

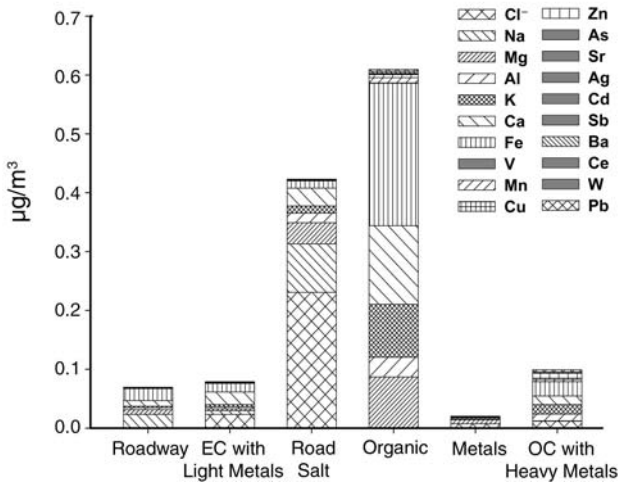

Figure 54. Source contributions to PM_{10} mass for each of the 20 non-carbon species at the two Wisconsin sites obtained by using the approach for assessing metal-heavy source contributions. The contributions of each species to each source profile were averaged over all measurement times and both locations. Elements indicated with gray shading do not appear because their relative contributions were too small to show.

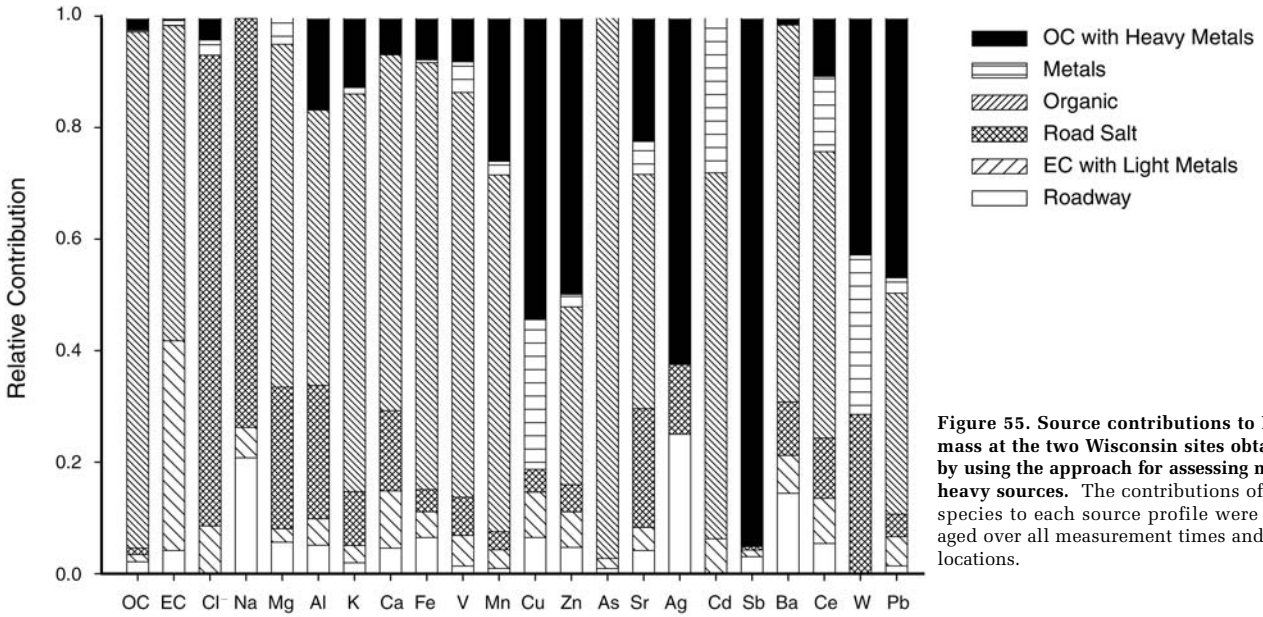

Figure 55. Source contributions to PM_{10} mass at the two Wisconsin sites obtained by using the approach for assessing metal-heavy sources. The contributions of each species to each source profile were averaged over all measurement times and both locations.

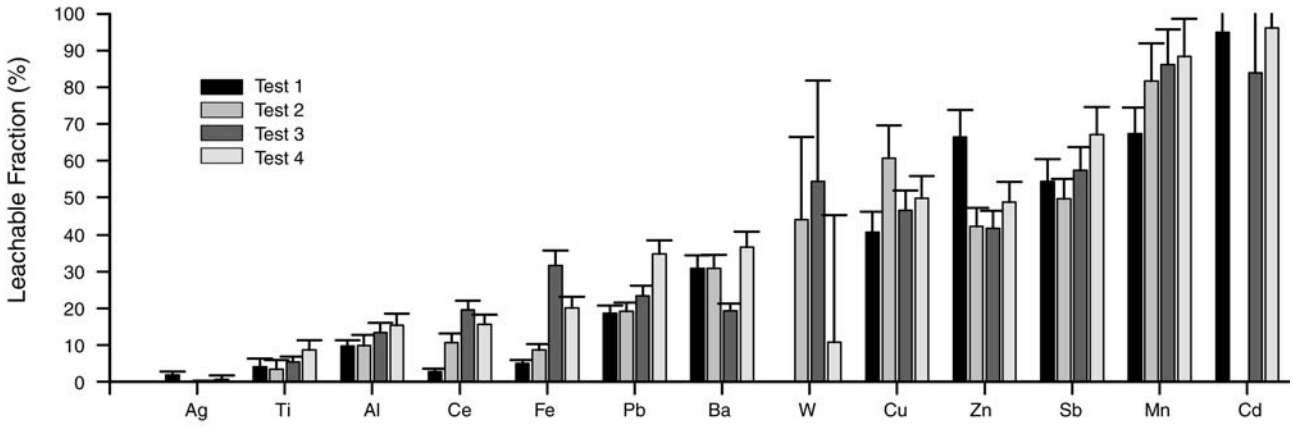

Figure 56. Solubility of PM_{10} trace metals in synthetic lung fluid after 8 hours. Data are from samples of motor vehicle emissions from a roadway tunnel. Error bars indicate the standard error of the average. The absence of bars for some metals in some tests indicates that the metal was not present in the sample, the leachate, or both.

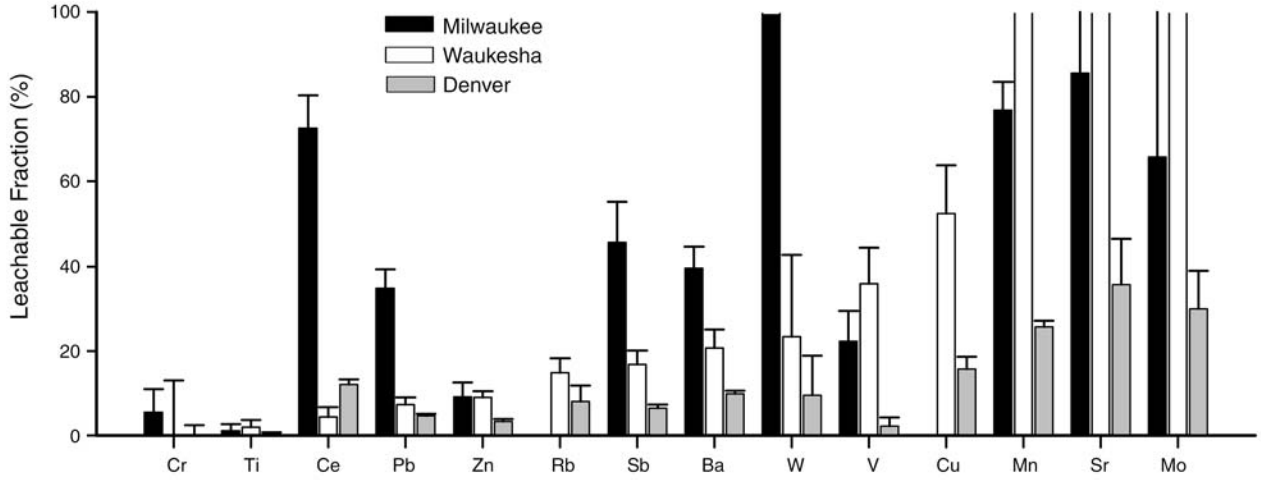

Figure 57. Solubility of PM_{10} trace metals in synthetic lung fluid. Ambient aerosol samples obtained for samples collected at the same dates and times from three sites in November 2001. Error bars indicate the standard error of the average. The absence of bars for some metals at some sites indicates that the metal was not present.

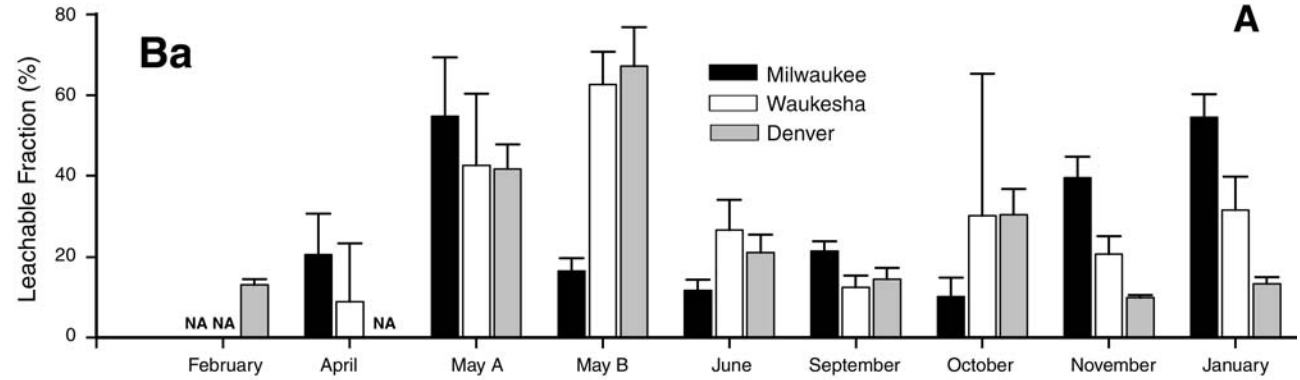

Figure 58. Solubility of PM_{10} trace metals in synthetic lung fluid. Two-day composites of ambient aerosol samples obtained at three sites, February 2001 through January 2002. Two composites were available in May (labeled A and B). NA indicates samples were not available. The absence of bars for some sites in some months indicates that none of the metal was leachable. Error bars indicate the standard error of the average. (*Panel A only; figure continues on next page.*)

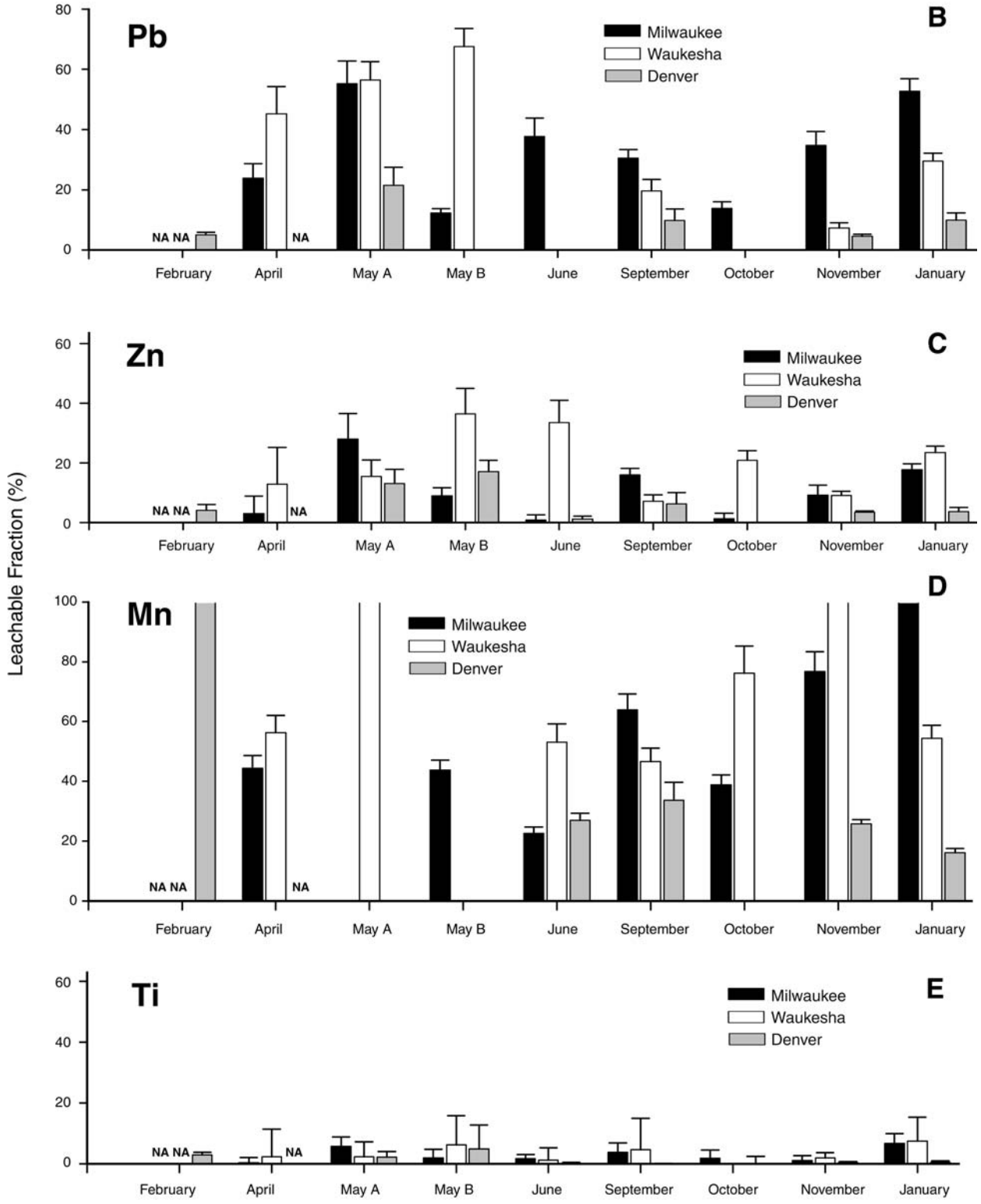

Figure 58 (*continued: Panels B, C, D, and E*).

fraction of Pb (15% to 55%) was much higher in Milwaukee samples, and a noticeable fraction of Pb in Milwaukee samples was leached in every composite. Several Waukesha samples had soluble fractions of Pb, but several did not. The leachable fraction of Pb in Denver samples was never greater than 22%, probably owing to the effect of additional Pb in stable crustal material at that site.

For Zn (Figure 58C), the greatest leachable fractions were in the Waukesha samples in five of the nine composites—possibly because a nearby industry emitted Zn in a different chemical form than was present at the other sites. The largest soluble fraction of Zn was 36%, in Waukesha. The leachable fraction of Mn varied greatly, from 15% to 100% (Figure 58D). The wide range of mass fractions leached by the synthetic lung fluid suggests that a variety of sources contributed different forms of Mn to the total. Very little Ti was leachable from any composite at any site (Figure 58E); the maximum soluble fraction was 7%, indicating that Ti was present in very stable phases in crustal materials.

The fraction of metals in atmospheric particulate matter that is likely to be dissolved in the fluid lining the lungs is strongly affected by particle size, oxidation state, complexation, and chemical associations of the metals. Because we expected metal concentrations at urban locations to be greatly affected by local sources, rather than constant across a region, the potential toxicity of metals in particulate matter deposited in the lungs should also vary with local sources. We confirmed this hypothesis with a series of experiments with synthetic lung fluid and PM_{10}.

For a set of samples of similar chemical composition, collected in motor vehicle tunnel tests, the leachable fractions of metals were constant and reproducible among samples. A set of ambient samples from urban sites did, however, show wide variation for individual metals. This result indicates that metals in ambient particulate matter are present in different forms that are influenced by local sources over space and time. Contributions of local sources to concentrations and compositions of trace metals in atmospheric particulate matter can increase or attenuate the dissolution and biological availability of those metals.

This exploratory work indicates that the behavior of metals in the lungs can vary widely with source and chemical and physical composition. To further understand these relations and their health effects, future work must more closely inspect chemical and physical speciation of metals and particulate matter, effects of organic compounds and surfactants, and pathways other than dissolution through which metals can exert toxicity.

SUMMARY AND CONCLUSIONS

In recent years the scientific understanding of the sources, chemical and physical properties, and effects of ambient particulate matter has increased greatly. However, many aspects of chemical speciation, source apportionment, actual human exposures, and health implications of atmospheric particulate matter remain unclear. The relations among measured atmospheric concentrations, chemical composition, human exposure, and adverse health effects are extremely complex. Studies investigating the effects of inhaled particulate matter have widely determined that although health effects are associated with total mass concentrations, they may be greatly affected by key chemical components such as metals. Metal concentrations have been less studied than other components of particulate matter because of the inability to routinely quantify the low levels of metals in most ambient samples. Therefore, the present study was motivated by the need to better understand the concentrations of metals in ambient particulate matter, the sources of metals in ambient air, and the associated implications for human health.

Motor vehicle emissions are a principal source of particulate matter in the urban atmosphere. Roadway emissions from motor vehicles have been investigated as contributors to organic compounds in particulate matter and have also been seen to contribute to emissions of some metals. Although many metals are present at only trace levels in roadway emissions, these contributions may constitute an important fraction of their total atmospheric concentrations. Therefore, roadway emissions may dominate human exposures to many elements, particularly in urban environments.

Human exposure to particulate matter emitted from on-road motor vehicles includes simultaneous exposure to PM_{10} and $PM_{2.5}$ emissions from vehicle tailpipes, brake wear, tire wear, and resuspended road dust. Each of these specific roadway sources contributes to emissions of a characteristic suite of metals. To appropriately describe the associations of roadway metal emissions with ambient concentrations and health effects, the relative contributions of these individual sources to total emissions must be clarified. To that end, we applied a systematic approach to integrate measurements of roadway emissions of particulate matter, emissions from specific roadway sources, and ambient concentrations of metals.

The variety of analytic methods used in different studies of motor vehicle emissions and ambient particulate matter has complicated interpretation of the results. Therefore, an important factor in the design of our study was the use of consistent methods for collection and analysis of samples in all facets of the study, allowing direct comparison of all

results. Particulate matter samples were collected that were representative of total roadway emissions from an on-road fleet of motor vehicles, tailpipe emissions from gasoline and diesel vehicles, motor vehicle brake wear and tire wear, and resuspended road dust. Apportionment of total roadway emissions of metals focused on PM_{10}, which has a larger fraction of metals than $PM_{2.5}$. Although smaller particles are suspected to be more closely linked to health effects, neglecting the relatively larger metals content of the inhalable PM_{10} fraction would be misguided. Also important is that investigation of the chemical composition of both size fractions for resuspended road dust, brake dust, and tire dust indicated that PM_{10} and $PM_{2.5}$ were similar in relative metal composition.

Resuspended road dust was a significant contributor to PM_{10} metal emissions in all roadway emissions tests conducted in this study. Because it is enriched from previous deposition of roadway sources and urban pollutants, the proportion of trace metals in road dust was significantly larger than that in natural geologic crustal material. The resuspension of road dust was influenced by changing roadway conditions, including weather and the fraction of heavy trucks present.

Brake wear contributed significantly to emissions of many elements. The majority of Fe, Cu, Ba, and Sb emissions were attributed to brake wear. Emissions of these elements were correlated in the PM_{10} fraction with elements that dominate crustal material. In the $PM_{2.5}$ fraction, however, Cu, Ba, and Sb were more strongly correlated with one another than with crustal elements, indicating the importance of direct emissions from brake wear. Tire wear had minimal effect on metal emissions, but it contributed to OC concentrations.

Gasoline tailpipe emissions contributed up to 20% of roadway emissions of Mg and Ca, up to 32% of Pb, and more than 20% of Zn and Mo. These emissions were also the sole source of Pt in some tests. Metals were also attributed to diesel tailpipe emissions, including Zn (up to 11%), Pb (up to 32%), Cd (up to 41%), and V (up to 34%). A submicron particle mode observed in the roadway emissions of Pb, Ca, Fe, and Cu was also indicative of tailpipe emissions.

Overall, this study contributes greatly to understanding of the sources and patterns of metal emissions from motor vehicle roadways, particularly the Midwestern fleet. Clearly, the composition of vehicle fleets, weather patterns, and other factors vary widely from one geographic area to another. Therefore, conducting similar studies in other regions of the United States and the world would be beneficial to elucidating the constancy or variability of roadway emissions. Understanding these variables is important to understanding the contributions of roadway emissions to total ambient metal concentrations.

This work demonstrated that the distributions of individual metals in ambient PM were not spatially uniform in the urban airshed comprising Milwaukee and Waukesha. Such spatial variability indicates that contributions of local sources affect metal concentrations on a small scale. Some elements were, however, reasonably well correlated at the two nearby sites because they were emitted from many sources dispersed throughout the area (such as traffic emissions) or because their source activities were correlated (such as Na from the use of road salt in winter).

Also, correlations between metals at a given site can be used to understand sources and the variation or homogeneity of those sources in different areas. One example was the consistent relation between Ba and Sr concentrations, which indicated that brake wear was an important source at all three ambient sampling sites. Statistical analysis of the data with ICFA allowed further investigation of motor vehicle roadway contributions to ambient metal concentrations. The model enabled the profiles for roadway emissions measured in Milwaukee to be highly defined, whereas the compositions of other sources not specific to this study were more flexible. In agreement with the basic review of the ambient data, statistical results indicated that roadway emissions were important to total metal concentrations but that different sources dominated at different times and specific locations.

To further understand the concentrations of metals in the atmosphere, better descriptions of the composition and contributions of different sources are needed. This study improved understanding of metal emissions from roadways, but the concentrations of metals from many other major sources have not been accurately measured in a manner that can be readily integrated into air quality studies. In attempting to understand human exposure to metals and their effects on human health, accurate characterization of the source contributions to ambient metal concentrations is vital.

The results of this study demonstrate the need to better characterize the spatial variability of ambient metals in the urban atmosphere to appropriately represent actual human exposure. The effects of local sources on metal concentrations lead to large variations in human exposures. Furthermore, the speciation of metals from different sources strongly influences whether those metals contribute to health effects. Clearly, then, the potential toxicity of metals in particulate matter will also vary widely among different sources.

For ambient particulate matter samples examined in this study, which had diverse compositions affected by an

array of sources, the fractions of metals leachable in a synthetic lung fluid varied markedly between sites. For a set of samples of similar chemical composition collected in motor vehicle tunnel tests, however, the leachable fractions of metals were constant and reproducible between samples. These results support our expectation that the chemical and physical forms of metal species strongly influence their fate after deposition in the lungs. To further understand potential health effects of ambient metals, future work must more closely inspect chemical and physical speciation of metals and particulate matter, effects of organic compounds and surfactants, and pathways other than dissolution through which metals can exert toxicity.

Through a systematic design, this study integrated measurements of metal emissions from roadways, metal composition of specific roadway sources, and ambient concentrations of metals with more detail than has previously been available. Although this study holistically described interactions of these factors, it is only one step toward increased understanding of human exposure to metals and associated health effects. In general, much uncertainty remains concerning the sources, concentrations, and speciation of metals in ambient particulate matter. Future studies must address variation in roadway emissions in other geographic areas, metal emissions from a range of other sources, and spatial variation in concentrations and speciation of ambient metals.

ACKNOWLEDGMENTS

The EPA funded the XRF analysis of tunnel samples, and Jason Weinstein at the EPA performed that analysis. Joan Bursey of Eastern Research Group helped in many ways. Tailpipe emissions were measured as part of the Gasoline/Diesel Split Study funded by the DOE. The trace metal analyses were funded as part of the HEI study; all other measurements were funded by DOE. Mike O'Connor, Tom Valencia, Wilson Chao, and staff of the California Air Resources Board Haagen-Smit Laboratory coordinated and helped with the RL-SHED dynamometer tests at their facility. John Strauss, Al Spallato, and Dustan Helmer at the Wisconsin State Laboratory of Hygiene analyzed many samples and assisted with sample preparation. Rei Rasmussen performed carbon monoxide, carbon dioxide, and methane analyses. Sample collection would not have been possible without the help of Min-Suk Bae. Dr Robert Smith and students at the University of Wisconsin–Madison videotaped and characterized tunnel vehicle fleets. Sara Bruening, Clifton Hackbarth, Dr Michael Hannigan, and Art Pinkert assisted with collection of ambient samples. The City of Milwaukee Police and Public Works Departments assisted with tunnel testing.

REFERENCES

Adgate JL, Ramachandran G, Pratt GC, Waller LA, Sexton K. 2003. Longitudinal variability in outdoor, indoor, and personal $PM_{2.5}$ exposure in healthy non-smoking adults. Atmos Environ 37:993–1002.

Allen JO, Mayo PR, Hughes LS, Salmon LG, Cass GR. 2001. Emissions of size-segregated aerosols from on-road vehicles in the Caldecott Tunnel. Environ Sci Technol 35:4189–4197.

Ashbaugh LL, Carvacho OF, Brown MS, Chow JC, Watson JG, Magliano KC. 2003. Soil sample collection and analysis for the fugitive dust characterization study. Atmos Environ 37:1163–1173.

Aust AE, Ball JC, Hu AA, Lighty JS, Smith KR, Straccia AM, Veranth JM, Young WC. 2002. Particle Characteristics Responsible for Effects on Human Lung Epithelial Cells. Research Report 110. Health Effects Institute, Boston MA.

Blau PJ. 2001. Compositions, Functions, and Testing of Friction Brake Materials and Their Additives. ORNL/TM-2001/64. Oak Ridge National Laboratory, Oak Ridge TN.

Cadle SH, Mulawa PA, Ball J, Donase C, Weibel A, Sagebiel JC, Knapp KT, Snow R. 1997. Particulate emission rates from in-use high-emitting vehicles recruited in Orange County, California. Environ Sci Technol 31:3405–3412.

Cadle SH, Mulawa PA, Hunsanger EC, Nelson K, Ragazzi RA, Barrett R, Gallagher GL, Lawson DR, Knapp KT, Snow R. 1999. Composition of light-duty motor vehicle exhaust particulate matter in the Denver, Colorado area. Environ Sci Technol 33:2328–2339.

Cha S, Carter P, Bradow RL. 1983. Simulation of Automobile Brake Wear Dynamics and Estimation of Emissions. SAE Technical Paper 831036. Society of Automotive Engineers International, Warrendale PA.

Chow JC, Watson JG, Ashbaugh LL, Magliano KL. 2003. Similarities and differences in PM_{10} chemical source profiles for geological dust from the San Joaquin Valley, California. Atmos Environ 37:1317–1340.

Chow JC, Watson JG, Crow D, Lowenthal DH, Merrifield T. 2001. Comparison of IMPROVE and NIOSH carbon measurements. Aerosol Sci Technol 34:23–34.

Christensen WF, Gunst RF. 2004. Measurement error models in chemical mass balance analysis of air quality data. Atmos Environ 38:733–744.

Christensen WF, Sain SR. 2002. Accounting for dependence in a flexible multivariate receptor model. Technometrics 44:328–337.

Claiborn CS, Larson T, Sheppard L. 2002. Testing the metals hypothesis in Spokane, Washington. Environ Health Perspect 110(Suppl 4):547–552.

Davis AP, Shokouhian M, Ni SB. 2001. Loading estimates of lead, copper, cadmium, and zinc in urban runoff from specific sources. Chemosphere 44:997–1009.

Dietl C, Reifenhauser W, Peichl L. 1997. Association of antimony with traffic: Occurrence in airborne dust, deposition and accumulation in standardized grass cultures. Sci Total Environ 205:235–244.

El-Fadel M, Hashisho Z. 2001. Vehicular Emissions in Roadway Tunnels: A Critical Review. Crit Rev Environ Sci Technol 31:125–174.

Environmental Protection Agency (US). 2002. Third External Review Draft of Air Quality Criteria for Particulate Matter (April, 2002): Volume I. EPA/600/P-99/002aC. Office of Research and Development, Research Triangle Park NC.

Evans GF, Highsmith RV, Sheldon LS, Suggs JC, Williams RW, Zweidinger RB, Creason JP, Walsh D, Rodes CE, Lawless PA. 2000. The 1999 Fresno particulate matter exposure studies: Comparison of community, outdoor, and residential PM mass measurements. J Air Waste Manage Assoc 50:1887–1896.

Foster DE, Kweon C-B, Schauer J, Okada S. 2002. Detailed Chemical Composition and Particle Size Assessment of Diesel Engine Exhaust. SAE Technical Paper 2002-01-2670. Society of Automotive Engineers International, Warrendale PA.

Fraser MP, Cass GR, Simoneit BRT. 1998. Gas-phase and particle-phase organic compounds emitted from motor vehicle traffic in a Los Angeles roadway tunnel. Environ Sci Technol 32:2051–2060.

Fraser MP, Cass GR, Simoneit BRT. 1999. Particulate organic compounds emitted from motor vehicle exhaust and in the urban atmosphere. Atmos Environ 33(17):2715–2724.

Gabele P. 2003. Final Report: Support of the Gasoline/Diesel Particulate Matter Split Study. DE-AI04-2001AL67138. US Department of Energy and US Environmental Protection Agency, Research Triangle Park NC.

Garg BD, Cadle SH, Mulawa PA, Groblicki PJ, Laroo C, Parr GA. 2000. Brake wear particulate matter emissions. Environ Sci Technol 34:4463–4469.

Gatz DF. 1975. Relative contributions of different sources of urban aerosols: Application of a new estimation method to multiple sites in Chicago. Atmos Environ 9:1–18.

Gauvin S, Reungoat P, Cassadou S, Déchenaux J, Momas I, Just J, Zmirou D. 2002. Contribution of indoor and outdoor environments to $PM_{2.5}$ personal exposure of children: VESTA study. Sci Total Environ 297:175–181.

Gavett SH, Koren HS. 2001. The role of particulate matter in exacerbation of atopic asthma. Int Arch Allergy Immunol 124:109–112.

Gertler AW, Gillies JA, Pierson WR, Rogers CF, Sagebiel JC, Abu-Allaban M, Coulombe W, Tarnay L, Cahill TA. 2002. Real-world particulate matter and gaseous emissions from motor vehicles in a highway tunnel. In: Emissions from Diesel and Gasoline Engines Measured in Highway Tunnels. Research Report 107. Health Effects Institute, Boston MA.

Gillies JA, Gertler AW, Sagebiel JC, Dippel WA. 2001. On-road particulate matter ($PM_{2.5}$ and PM_{10}) emissions in the Sepulveda Tunnel, Los Angeles, California. Environ Sci Technol 35:1054–1063.

Gleser LJ. 1997. Some thoughts on chemical mass balance models. Chemometrics and Intelligent Laboratory Systems 37:15–22.

Goswami E, Larson T, Lumley T, Liu LJS. 2002. Spatial characteristics of fine particulate matter: Identifying representative monitoring locations in Seattle, Washington. J Air Waste Manage Assoc 52:324–333.

Harrison RM, Smith DJT, Luhana L. 1996. Source apportionment of atmospheric polycyclic aromatic hydrocarbons collected from an urban location in Birmingham, UK. Environ Sci Technol 30:825–832.

Henry RC. 1997. History and fundamentals of multivariate air quality receptor models. Chemometrics and Intelligent Laboratory Systems 37:37–42.

Henry RC, Lewis CW, Collins JF. 1994. Vehicle-related hydrocarbon source compositions from ambient data: The GRACE/SAFER method. Environ Sci Technol 28:823–832.

Hering S, Cass G. 1999. The magnitude of bias in the measurement of $PM_{2.5}$ arising from volatilization of particulate

nitrate from teflon filters. J Air Waste Manage Assoc 49:725–733.

Hering SV, Lawson DR, Allegrini I, Febo A, Perrino C, Possanzini M, Sickles JE, Anlauf KG, Wiebe A, Appel BR, John W, Ondo J, Wall S, Braman RS, Sutton R, Cass GR, Solomon PA, Eatough DJ, Eatough NL, Ellis EC, Grosjean D, Hicks BB, Womack JD, Horrocks J, Knapp KT, Ellestad TG, Paur RJ, Mitchell WJ, Pleasant M, Peake E, Maclean A, Pierson WR, Brachaczek W, Schiff HI, Mackay GI, Spicer CW, Stedman DH, Winer AM, Biermann HW, Tuazon EC. 1988. The nitric-acid shootout: Field comparison of measurement methods. Atmos Environ 22:1519–1539.

Hildemann LM, Cass GR, Markowski GR. 1989. A dilution stack sampler for collection of organic aerosol emissions: Design, characterization and field-tests. Aerosol Sci Technol 10:193–204.

Hildemann LM, Markowski GR, Cass GR. 1991. Chemical-composition of emissions from urban sources of fine organic aerosol. Environ Sci Technol 25:744–759.

Ho KF, Lee SC, Chow JC, Watson JG. 2003. Characterization of PM_{10} and $PM_{2.5}$ source profiles for fugitive dust in Hong Kong. Atmos Environ 37:1023–1032.

Hopke PK, Lamb RF, Natusch DFS. 1980. Multielemental characterization of urban roadway dust. Environ Sci Technol 14:164–172.

Huang X, Olmez I, Aras NK, Gordon GE. 1994. Emissions of trace elements from motor vehicles: Potential marker elements and source composition profile. Atmos Environ 28:1385–1391.

Jaecker-Voirol A, Pelt P. 2000. PM_{10} emission inventory in Ile de France for transport and industrial sources: PM_{10} resuspension, a key factor for air quality. Environ Modelling Software 15:575–581.

Kanitsar K, Koellensperger G, Hann S, Limbeck A, Puxbaum H, Stingeder G. 2003. Determination of Pt, Pd and Rh by inductively coupled plasma sector field mass spectrometry (ICP-SFMS) in size-classified urban aerosol samples. J Anal Atom Spectrometry 18:239–246.

Kellog R, Winberry W Jr. 1999. EPA Compendium Method 10-3.3: Determination of Metals in Ambient Particulate Matter Using X-Ray Fluorescence (XRF) Spectroscopy. EPA/625/R-96/010a. US Environmental Protection Agency, Washington DC.

Kleeman MJ, Schauer JJ, Cass GR. 2000. Size and composition distribution of fine particulate matter emitted from motor vehicles. Environ Sci Technol 34:1132–1142.

Knaapen AM, Shi TM, Borm PJA, Schins RPF. 2002. Soluble metals as well as the insoluble particle fraction are involved in cellular DNA damage induced by particulate matter. Mol Cell Biochem 234-235:317–326.

Kodavanti UP, Schladweiler MCJ, Ledbetter AD, Hauser R, Christiani DC, Samet JM, McGee J, Richards JH, Costa DL. 2002. Pulmonary and systemic effects of zinc-containing emission particles in three rat strains: Multiple exposure scenarios. Toxicol Sci 70:73–85.

Koutrakis P, Spengler JD. 1987. Source apportionment of ambient particles in Steubenville, OH using specific rotation factor analysis. Atmos Environ 21:1511–1519.

Kowalczyk GS, Choquette CE, Gordon GE. 1978. Chemical element balances and identification of air pollution sources in Washington, DC. Atmos Environ 12:1143–1153.

Kumata H, Yamada J, Masuda K, Takada H, Sato Y, Sakurai T, Fujiwara K. 2002. Benzothiazolamines as tire-derived molecular markers: Sorptive behavior in street runoff and application to source apportioning. Environ Sci Technol 36:702–708.

Laden F, Neas LM, Dockery DW, Schwartz J. 2000. Association of fine particulate matter from different sources with daily mortality in six US cities. Environ Health Perspect 108:941–947.

Lin S, Munsie JP, Hwang SA, Fitzgerald E, Cayo MR. 2002. Childhood asthma hospitalization and residential exposure to state route traffic. Environ Res 88:73–81.

Liu LJS, Box M, Kalman D, Kaufman J, Koenig J, Larson T, Lumley T, Sheppard L, Wallace L. 2003. Exposure assessment of particulate matter for susceptible populations in Seattle. Environ Health Perspect 111:909–918.

Lowenthal DH, Zielinska B, Chow JC, Watson JG, Gautam M, Ferguson DH, Neuroth GR, Stevens KD. 1994. Characterization of heavy-duty diesel vehicle emissions. Atmos Environ 28:731–743.

Malinowski ER, Weiner PH, Levinston AR. 1970. Factor analysis of solvent shifts in proton magnetic resonance. J Phys Chem 74:4537–4542.

Mayrsohn H, Crabtree JH. 1976. Source reconciliation of atmospheric hydrocarbons. Atmos Environ 10:137–143.

Molinelli AR, Madden MC, McGee JK, Stonehuerner JG, Ghio AJ. 2002. Effect of metal removal on the toxicity of airborne particulate matter from the Utah Valley. Inhalation Toxicol 14:1069–1086.

Moosmuller H, Gillies JA, Rogers CF, DuBois DW, Chow JC, Watson JG, Langston R. 1998. Particulate emission rates for unpaved shoulders along a paved road. J Air Waste Manage Assoc 48:398–407.

National Research Council (US). 1998. Research Priorities for Airborne Particulate Matter: I. Immediate Priorities and a Long-Range Research Portfolio. National Academy Press, Washington DC.

Nicholson KW, Branson JR, Giess P, Cannell RJ. 1989. The effects of vehicle activity on particle resuspension. J Aerosol Sci 20:1425–1428.

Okada S, Kweon C-B, Foster DE, Schauer JJ, Shafer MM, Christensen CG, Gross DS. 2003. Measurement of Trace Metal Composition in Diesel Engine Particulate and its Potential for Determining Oil Consumption: ICPMS (Inductively Coupled Plasma Mass Spectrometer) and ATOFMS (Aerosol Time of Flight Mass Spectrometer) Measurements. SAE Technical Paper 2003-01-0076. Society of Automotive Engineers International, Warrendale PA.

Oller AR. 2002. Respiratory carcinogenicity assessment of soluble nickel compounds. Environ Health Perspect 110(Suppl 5):841–844.

Paatero P, Tapper U. 1994. Positive matrix factorization: A non-negative factor model with optimal utilization of error estimate of data values. Environmetrics 5:111–126.

Pakkanen TA, Kerminen V-M, Loukkola K, Hillamo RE, Aarnio P, Koskentalo T, Maenhaut W. 2003. Size distributions of mass and chemical components in street-level and rooftop PM_1 particles in Helsinki. Atmos Environ 37:1673–1690.

Park ES, Guttorp P, Henry RC. 2001. Multivariate receptor modeling for temporally correlated data by using MCMC. J Am Stat Assoc 96:1171–1183.

Park ES, Oh M-S, Guttorp P. 2002. Multivariate receptor models and model uncertainty. Chemometrics and Intelligent Laboratory Systems 60:49–67.

Petrucci F, Bocca B, Alimonti A, Caroli S. 2000. Determination of Pd, Pt and Rh in airborne particulate and road dust by high-resolution ICP-MS: A preliminary investigation of the emission from automotive catalysts in the urban area of Rome. J Anal Atom Spectrometry 15:525–528.

Pierson WR, Brachaczek WW. 1983. Particulate matter associated with vehicles on the road: 2. Aerosol Sci Technol 2(1):1–40.

Pierson WR, Gertler AW, Robinson NF, Sagebiel JC, Zielinska B, Bishop GA, Stedman DH, Zweidinger RB, Ray WD. 1996. Real-world automotive emissions: Summary of studies in the Fort McHenry and Tuscarora mountain tunnels. Atmos Environ 30:2233–2256.

Prieditis H, Adamson IYR. 2002. Comparative pulmonary toxicity of various soluble metals found in urban particulate dusts. Exp Lung Res 28:563–576.

Ramadan Z, Song XH, Hopke PK. 2000. Identification of sources of Phoenix aerosol by positive matrix factorization. J Air Waste Manage Assoc 50:1308–1320.

Rauch S, Morrison GM, Motelica-Heino M, Donard OFX, Muris M. 2000. Elemental association and fingerprinting of traffic-related metals in road sediments. Environ Sci Technol 34:3119–3123.

Reddy CM, Quinn JG. 1997. Environmental chemistry of benzothiazoles derived from rubber. Environ Sci Technol 31:2847–2853.

Rogak SN, Green SI, Pott U. 1998. Use of tracer gas for direct calibration of emission-factor measurements in a traffic tunnel. J Air Waste Manage Assoc 48(6):545–552.

Rogge WF, Hildemann LM, Mazurek MA, Cass GR, Simoneit BRT. 1993. Sources of fine organic aerosol: 3. Road dust, tire debris, and organometallic brake lining dust: Roads as sources and sinks. Environ Sci Technol 27:1892–1904.

Root RA. 2000. Lead loading of urban streets by motor vehicle wheel weights. Environ Health Perspect 108:937–940.

Sagebiel JC, Zielinska B, Walsh PA, Chow JC, Cadle SH, Mulawa PA, Knapp KT, Zweidinger RB, Snow R. 1997. $PM\text{-}_{10}$ exhaust samples collected during IM-240 dynamometer tests of in-service vehicles in Nevada. Environ Sci Technol 31:75–83.

Sanders PG, Dalka TM, Xu N, Maricq MM, Basch RLH. 2002. Brake Dynamometer Measurement of Airborne Brake Wear Debris. SAE Technical Paper 2002-01-1280. Society of Automotive Engineers International, Warrendale PA.

Schauer JJ, Kleeman MJ, Cass GR, Simoneit BRT. 2002. Measurement of emissions from air pollution sources: 5. C1–C32 organic compounds from gasoline-powered motor vehicles. Environ Sci Technol 36:1169–1180.

Schauer JJ, Mader BT, Deminter JT, Heidemann G, Bae MS, Seinfeld JH, Flagan RC, Cary RA, Smith D, Huebert BJ, Bertram T, Howell S, Kline JT, Quinn P, Bates T, Turpin B,

Lim HJ, Yu JZ, Yang H, Keywood MD. 2003. ACE-Asia intercomparison of a thermal-optical method for the determination of particle-phase organic and elemental carbon. Environ Sci Technol 37:993–1001.

Schauer JJ, Rogge WF, Hildemann LM, Mazurek MA, Cass GR, Simoneit BRT. 1996. Source apportionment of airborne particulate matter using organic compounds as tracers. Atmos Environ 30:3837–3855.

Schauer JJ, Kleeman MJ, Cass GR, Simoneit BRT. 1999. Measurement of emissions from air pollution sources: 2. C1 through C30 organic compounds from medium duty diesel trucks. Environ Sci Technol 33(10):1578–1587.

Shafer MM, Hoffmann SR, Overdier JT, Armstrong DE. 2004. Physical and kinetic speciation of copper and zinc in three geochemically contrasting marine estuaries. Environ Sci Technol 38(14):3810–3819.

Shah SD, Cocker DR III, Miller JW, Norbeck JM. 2004. Emission rates of particulate matter and elemental and organic carbon from in-use diesel engines. Environ Sci Technol 38:2544–2550.

Sternbeck J, Sjödin A, Andréasson K. 2002. Metal emissions from road traffic and the influence of resuspension: Results from two tunnel studies. Atmos Environ 36:4735–4744.

Sun GB, Crissman K, Norwood J, Richards J, Slade R, Hatch GE. 2001. Oxidative interactions of synthetic lung epithelial lining fluid with metal-containing particulate matter. Am J Physiol Lung Cell Mol Physiol 281:L807–L815.

Thurston GD, Spengler JD. 1985. A quantitative assessment of source contributions to inhalable particulate matter pollution in metropolitan Boston. Atmos Environ 19:9–25.

Tsai FC, Apte MG, Daisey JM. 2000. An exploratory analysis of the relationship between mortality and the chemical composition of airborne particulate matter. Inhalation Toxicol 12(Suppl 2):121–135.

Watson JG, Chow JC, Lu ZQ, Fujita EM, Lowenthal DH, Lawson DR, Ashbaugh LL. 1994. Chemical mass-balance source apportionment of PM_{10} during the Southern California Air-Quality Study. Aerosol Sci Technol 21:1–36.

Watson JG, Cooper JA, Huntzicker JJ. 1984. The effective variance weighting for least squares calculations applied to the mass balance receptor model. Atmos Environ 18:1347–1355.

Watson JG, Fujita EM, Chow JC, Zielinska B, Richards LF, Neff W, Dietrich D. 1998. Northern Front Range Air Quality Study Final Report. Colorado State University, Fort Collins CO.

Williams R, Suggs J, Zweidinger R, Evans G, Creason J, Kwok R, Rodes C, Lawless P, Sheldon L. 2000. The 1998 Baltimore Particulate Matter Epidemiology-Exposure Study: Part 1. Comparison of ambient, residential outdoor, indoor and apartment particulate matter monitoring. J Expos Anal Environ Epidemiol 10:518–532.

Wise JP Sr, Wise SS, Little JE. 2002. The cytotoxicity and genotoxicity of particulate and soluble hexavalent chromium in human lung cells. Mutat Res 517:221–229.

Wooley J, Nazaroff WW, Hodgson AT. 1990. Release of ethanol to the atmosphere during use of consumer cleaning products. J Air Waste Manage Assoc 40:1114–1120.

Wrobel A, Rokita E, Maenhaut W. 2000. Transport of traffic-related aerosols in urban areas. Sci Total Environ 257(2-3):199–211.

Yang H. 1994. Confirmatory Factor Analysis and Its Application to Receptor Modeling [dissertation]. University of Pittsburgh, Pittsburgh PA.

Young TM, Heeraman DA, Sirin G, Ashbaugh LL. 2002. Resuspension of soil as a source of airborne lead near industrial facilities and highways. Environ Sci Technol 36:2484–2490.

Zelikoff JT, Schermerhorn KR, Fang KJ, Cohen MD, Schlesinger RB. 2002. A role for associated transition metals in the immunotoxicity of inhaled ambient particulate matter. Environ Health Perspect 110(Suppl 5):871–875.

Zereini F, Wiseman C, Alt F, Messerschmidt J, Muller J, Urban H. 2001. Platinum and rhodium concentrations in airborne particulate matter in Germany from 1988 to 1998. Environ Sci Technol 35:1996–2000.

Zielinska B, Sagebiel JC, Harshfield G, Gertler AW, Pierson WR. 1996. Volatile organic compounds up to C-20 emitted from motor vehicles: Measurement methods. Atmos Environ 30(12):2269–2286.

APPENDICES AVAILABLE ON REQUEST

The following materials may be obtained from HEI's website, *www.healtheffects.org*, or requested by contacting the Health Effects Institute at: Charlestown Navy Yard, 120 Second Avenue, Boston MA 02129-4533, +1-617-886-9330, fax +1-617-886-9335, or email (*pubs@healtheffects.org*). Please give (1) the first author, full title, and number of the Research Report and (2) the title of the appendix requested.

Appendix A. Synopsis of UW–Madison Aerosol Trace Element Protocols

Appendix B. Tunnel Roadway Emission Rates

Appendix C. Brake and Tire Wear Emissions

Appendix D. Source Profiles: Tire Wear, Brake Housing Dust, and Resuspended Road Dust

Appendix E. Ambient Data: Denver 2001 PM_{10}, Milwaukee 2001 PM_{10}, and Waukesha 2001 PM_{10}; Denver 2001 $PM_{2.5}$, Milwaukee 2001 $PM_{2.5}$, and Waukesha 2001 $PM_{2.5}$

ABOUT THE AUTHORS

James J Schauer is associate professor of Civil and Environmental Engineering at the University of Wisconsin–Madison and also carries appointments in the Environmental Chemistry and Technology Program and as the director of air chemistry at the Wisconsin State Laboratory of Hygiene. He is well known for his work with source apportionment of atmospheric particulate matter.

Glynis C Lough is a postdoctoral research associate with Dr Schauer.

Martin M Shafer is an associate scientist in the Environmental Chemistry and Technology Program at University of Wisconsin–Madison. He is an expert in trace metal analytic chemistry, speciation, biogeochemistry, and field sampling.

William F Christensen is an assistant professor in the Department of Statistics at Brigham Young University and is an authority concerning multivariate analysis of spatial and environmental data and factor analysis of air quality data.

Michael F Arndt is an assistant scientist in environmental sciences at the Wisconsin State Laboratory of Hygiene and a specialist in ICP-MS analysis.

Jeffrey T DeMinter is a senior chemist in environmental sciences at the Wisconsin State Laboratory of Hygiene specializing in chemical analysis of atmospheric particulate matter.

June-Soo Park assisted in this research as a postdoctoral fellow at University of Wisconsin–Madison. He is now a researcher in the Medical School in Epidemiology and Preventative Medicine at the University of California at Davis.

OTHER PUBLICATIONS RESULTING FROM THIS RESEARCH

Lough GC, Schauer JJ, Park JS, Shafer MM, Deminter JT, Weinstein JP. 2005. Emissions of metals associated with motor vehicle roadways. Environ Sci Technol 39(3):826–836.

Lough GC. 2004. Sources of Metals and NMHCs from Motor Vehicle Roadways [dissertation]. University of Wisconsin–Madison, Madison WI.

ABBREVIATIONS AND OTHER TERMS

Cl^-	chloride ion
CMB	chemical mass balance
DOE	Department of Energy (US)
EC	elemental carbon
EPA	Environmental Protection Agency (US)
FTP	federal test protocol
HCO_3^-	bicarbonate ion
HPO_4^{2-}	phosphate ion
IC	ion chromatography
ICFA	iterated confirmatory factor analysis
ICP-MS	inductively coupled plasma mass spectrometry
MOUDI	micro-orifice uniform deposit impactor
NH_4^+	ammonium ion
NIST	National Institute of Standards and Technology (US)
NO_3^-	nitrate ion
OC	organic carbon
PM_{10}	particulate matter < 10 µm in aerodynamic diameter
$PM_{2.5}$	particulate matter < 2.5 µm in aerodynamic diameter
r^2	coefficient of determination for bivariate analysis
RL-SHED	running-loss sealed housing for evaporative determinations
SF_6	sulfur hexafluoride
SO_4^{2-}	sulfate ion

SRM	standard reference material
SS	steady state
TOA	thermal-optical analyses
TTFA	target transformation factor analysis
UC	unified cycle
XRF	x-ray fluorescence spectrometry
WDNR	Wisconsin Department of Natural Resources

INTRODUCTION

Metals comprise a complex group of elements with a broad range of toxicity, including effects on genes, nervous and immune systems, and the induction of cancer (Goyer 1996). Some metals (eg, lead) are toxic at very low levels; others (eg, manganese) are essential to living systems at low concentrations, but may be toxic at higher concentrations. Metals may exist in several valence states that differ in toxicity and may be associated with organic matter and inorganic materials that can affect their toxicity. The presence of metals in the environment has received a great deal of attention in recent years. Their accumulation in the environment is of concern because of their persistence. Some scientists believe that transition metals (eg, nickel and vanadium) are particularly toxic components of particulate matter (PM)*(Carter et al 1997; Ghio et al 1999).

Metals are used in a variety of ways in motor vehicles. In addition to their structural contribution and their use in batteries and brake pads, metals are used in catalytic converters and as fuel additives to reduce certain emissions (eg, PM) or improve engine performance. Although metals are useful, they can cause deleterious health effects if they are emitted in sufficient amounts. They can also cause changes in the composition of emissions that may increase their toxicity.

In 1998, HEI issued Request for Preliminary Applications 98-4, *Research on Metals Emitted by Motor Vehicles.* The goal of the Request was a broad investigation of metals that may be found in automobile emissions, in particular those found in tailpipe exhaust. Metallic components of fuel additives were a top priority, but metals found in other emissions (such as those derived from fuel lubricant, engine wear, catalytic converter, or brake pads) were also of interest. Several other, more general issues of exposure to and health effects of metals were also considered. These were as follows: characterization of metals in tailpipe and nontailpipe emissions, the particle size distribution of such emissions, and their transformation in ambient air; research leading to the development of scientifically robust models to evaluate the relation between metallic emissions from motor vehicles and human exposure; uptake, distribution, and pharmacokinetics; effects of prolonged exposure to metals at low doses; factors affecting susceptibility; risk-assessment issues; improved assessment of neurotoxicity; and immunologic effects.

On the basis of a preliminary application submitted in January 1999, the HEI Health Research Committee invited Dr Schauer to submit a full application to HEI. The application, "Characterizations of Emissions and Human Exposure to Metals Emitted from Motor Vehicles," was submitted in April 1999. In the application, he proposed to evaluate the use of tunnels for identifying the source contributions of metals from different types of automobile emissions, including tire and brake dust, roadside dust, and tailpipe emissions. The proposal's objectives addressed the use of improved methods for measuring many metals that occur at low levels and application of these methods to tunnels, tire wear, brake wear, tailpipe emissions, and ambient air.

The Research Committee recommended the Schauer study for funding because they believed that it would provide important new information about the levels and types of metals in mobile source emissions and, ultimately, the contribution of these emissions to personal exposure to these metals. The proposed measurements from tunnels were thought to be useful for evaluating exposures to composite emissions from large numbers of in-use vehicles. The Committee believed that supplementing the study with dynamometer tests would lead to better characterization of metals in tailpipe emissions of individual vehicles.†

The Investigators' Report by Schauer and colleagues describes the application of two new methods, inductively coupled plasma mass spectrometry (ICP-MS) and iterated confirmatory factor analysis (ICFA). Together with more traditional analytic techniques, these methods allow the identification of profiles for various components of mobile source emissions and the subsequent use of these profiles to attribute personal exposures to various sources.

SCIENTIFIC BACKGROUND

Air pollution in the form of PM has been associated with adverse health effects. PM is a heterogeneous mix of both inorganic and organic constituents. It can originate from a

* A list of abbreviations and other terms appears at the end of the Investigators' Report.

† Dr Schauer's 3-year study, "Characterization of Emission and Human Exposure to Metals Emitted from Motor Vehicles", began in January 2000. Total expenditures were $233,402. The draft Investigators' Report from Schauer and colleagues was received for review in August 2003. A revised report, received in May 2004, was accepted for publication in June 2004. During the review process, the HEI Health Review Committee and the investigators had the opportunity to exchange comments and to clarify issues in both the Investigators' Report and in the Review Committee's Commentary.

number of sources, including motor vehicle emissions. Identification of PM components that are responsible for inducing pathological outcomes and identification of sources of PM components that are deleterious to health are important steps in assessing human risk associated with exposure to air pollutants. Metals are among the constituents thought to induce the detrimental health effects that result from PM exposure.

SOURCES OF METALS IN AMBIENT AIR

A number of studies have examined the sources of metals in ambient air pollution. One study by Davis and investigators (2001) analyzed sources that contribute to urban runoff, including building siding and roofs; brakes, tires, and oil leaked from automobiles; and atmospheric deposition under wet and dry conditions. Their results showed that atmospheric deposition was a large source of heavy metals, including cadmium, copper, and lead. In a study in Spokane, Washington, ambient PM was analyzed for metals using energy-dispersive x-ray fluorescence spectrometry (XRF) and instrumental neutron activation analysis (Claiborn et al 2002). The investigators determined correlation coefficients between fine particulate metals and particle sources. Iron, manganese, and titanium were all highly correlated with soil ($r > 0.90$). Zinc was correlated with vegetative sources, whereas antimony, selenium, and arsenic were correlated with motor vehicle sources.

CHARACTERIZATION OF METALS FROM MOBILE SOURCES

Chassis Dynamometer Tests

Chassis dynamometer tests are often used to aid source profiling of automobile emissions. These tests allow brake, tire, and tailpipe emissions to be analyzed in a closed environment. A vehicle's rear wheels are clamped to the floor of the dynamometer chamber and the front wheels are placed on a roller. The vehicle is operated under controlled engine conditions, and the emissions are channeled from the tailpipe into a dilution chamber, where they are collected in a constant-volume sampling system and analyzed (El-Fadel and Hashisho 2001). Usually, dynamometer testing is conducted according to the federal test procedure, a set of operating parameters for the driving cycle (Cadle et al 1999). Samplers may also be placed inside the chamber for analysis of brake and tire emissions. In dynamometer testing, emissions are typically expressed as the weight of the emitted pollutant per unit of distance traveled (g/mi or mg/km). Modeling is used to integrate the results of the dynamometer tests with statistical methods in order to extrapolate and interpolate estimated emissions under various conditions.

In a dynamometer study of the composition of PM from light-duty motor vehicles, using XRF analysis of metals, Cadle and colleagues (1999) found more metal emissions from diesel engines than from gasoline engines. The elements measured averaged less than 1 mg/mi for gasoline vehicles, with the exception of elevated iron during a winter measurement period and silicon during a summer measurement. Metals comprised 9.0% of PM mass during summer but only 3.2% during winter (Cadle et al 1999). In another dynamometer study, investigators used XRF analysis to examine metal composition in emissions from high-emitting vehicles or vehicles with visible tailpipe smoke and emissions of approximately 0.395 g/mi of PM less than or equal to 10 μm in aerodynamic diameter (PM_{10}) (Cadle et al 1997). Elements present at significantly elevated levels included magnesium, aluminum, silicon, phosphorus, sulfur, chloride, calcium, iron, copper, bromine, zinc, and lead, with concentrations from 0.22 to 7.76 mg/mi (0.41% to 12.3% of the PM_{10} mass). Metals commonly found in engine oil (such as zinc, phosphorus, calcium, magnesium, and copper) were all well correlated (r^2 0.55–0.95). Garg and colleagues (2000) studied brake-wear-particle emissions by using a brake dynamometer. They found that, among the metals tested, iron, copper, and barium had the highest concentrations in brake dust.

Dynamometer testing is expensive, so it is often conducted on only one or two vehicle types, which introduces bias because the vehicles tested are not representative of all vehicle models, types, and ages. Therefore, combining dynamometer testing with real-world automobile emissions, such as in tunnels, is important for accuracy.

Tunnel Studies

Specific sources of ambient metals (such as automobile emissions, including those from brakes, tires, and tailpipes) have been investigated in tunnel studies. Roadway tunnels offer an excellent opportunity to study automobile emissions in a somewhat contained real-world environment. Additionally, the tunnel study allows collection of emissions that are effectively the average from many vehicle types and, sometimes, analysis of emissions in different seasons or traffic-flow situations (Gertler et al 2002). Typically studies of tunnel emissions involve PM samplers that are placed at both the tunnel entrance and exit. Video recordings are often used to identify the number and types of vehicles entering the tunnel during the study period. Inert gases may be released at the tunnel entrance and monitored over time in order to give a measurement of airflow

through the tunnel, and road dust samples are often gathered for further analysis.

In a study of motor vehicle emissions in the Caldecott Tunnel in San Francisco, investigators used instrumental neutron activation analysis to measure metals present in PM_{10} and $PM_{1.9}$. Using this method, investigators found 12 metals (barium, iron, chromium, mercury, lanthanum, magnesium, manganese, sodium, antimony, scandium, vanadium, and zinc; Allen et al 2001). Sternbeck and colleagues (2002) compared the metal concentrations in PM in emissions from two different tunnels in Gothenburg, Sweden. Total suspended particles were examined at the tunnel inlets and outlets, and metals in the particles were analyzed by using ICP-MS. Similar concentrations of copper, zinc, antimony, barium, and lead were detected in the inlets and outlets of both tunnels, whereas metals such as aluminum, calcium, iron, magnesium, manganese, and titanium were higher in one tunnel, perhaps owing to higher levels of road dust. By applying a chemical mass balance model to tunnel emissions data, the investigators determined that copper, zinc, cadmium, antimony, barium, and lead derived from wear processes rather than from fuel combustion and that copper, barium, and cadmium derived mainly from brake wear (Sternbeck et al 2002).

Gillies and investigators (2001) analyzed PM_{10} and $PM_{2.5}$ emissions in the Sepulveda Tunnel in Los Angeles, California. Crustal elements comprised 7.8% of $PM_{2.5}$ emissions. Of that percentage, 18.5% was due to Fe, the third-most-dominant element and the most dominant metal; other metals (magnesium, aluminum, silicon, potassium, and manganese) made up an additional 12.6%. In another tunnel study, Gertler and colleagues (2002) estimated emissions from heavy-duty and light-duty vehicles. For both vehicle types, emissions of the crustal metals silicon and cadmium were similar, suggesting that these elements have a source other than tailpipe exhaust, perhaps road dust. The metals emitted at the highest levels by both heavy-duty and light-duty vehicles were magnesium, iron, copper, and zinc.

Rauch and colleagues (2000) conducted a study to examine traffic-related metals in road sediment. The investigators used ICP-MS to quantify metals and to determine which are associated with lead or with platinum-group metals, which are autocatalysts that are added to unleaded fuel. Lead was strongly associated with the following groupings of bulk metals: iron–manganese and calcium–magnesium–strontium. Platinum-group metals were not associated with any particular elements. In another study of road dust, elevated levels of lead, chromium, manganese, nickel, and zinc were found (Hopke et al 1980).

HEALTH EFFECTS OF METALS

Epidemiologic Studies

Epidemiologic studies have found associations between metals in PM and adverse health outcomes. For instance, as part of a larger study on the health effects of PM in Spokane, Washington, Claiborn and associates (2002) examined the effects of particulate metals on emergency room admissions for asthma and respiratory problems (Claiborn et al 2002). Daily PM measurements and metal levels from a central monitoring site in Spokane were analyzed by using energy-dispersive XRF. Statistical analysis showed an association between fine particulate zinc and emergency room admissions for asthma, suggesting that metal constituents in PM play a role in adverse respiratory health.

In Vitro and in Vivo Studies

Metals are thought to exert toxic effects by catalyzing oxidation of proteins and lipids. Dye and colleagues (1999) found that metals (such as vanadium and nickel) in the particulate residual oil fly ash were associated with cytotoxic effects in cultured tracheal epithelial cells. These toxic effects were absent, however, when a free radical was added, implicating oxidative stress as the mechanism of toxicity. Results of a number of studies have demonstrated the toxic effects of zinc, a metal commonly found in PM. Kodavanti and investigators (2002) intratracheally instilled into rats zinc-containing PM from oil combustion, as well as the leachable fraction of this PM. They compared the biological effects of these agents to those of instilled zinc sulfate. All three intratracheal exposures induced dose-dependent increases in the permeability of albumin, whereas only zinc sulfate and the PM leachate induced neutrophilic inflammation. The investigators contend that these similar biological responses were probably due to bioavailable zinc. Prieditis and Adamson (2002) performed a similar experiment to determine the effects of zinc instillation on lung tissue. Rats were instilled with either atmospheric dust (containing 4.8 mg of zinc per 1 g of dust) or a solution of zinc, copper, vanadium, nickel, iron, or lead, all at concentrations similar to the zinc concentration in the atmospheric dust. Zinc, copper, and the atmospheric dust induced lung inflammation and injury, whereas the other metals tested had minimal effects.

Knaapen and colleagues (2002) investigated the role of soluble metals, particularly iron, in DNA damage. Hydroxyl radicals that damage DNA were generated in the presence of PM and hydrogen peroxide. The damaging effect was no longer observed when an iron chelator was added, suggesting that iron mediated the generation of the radicals. The researchers also observed the modified DNA

lesion 8-hydroxydeoxyguanosine, which is specific for hydroxyl radicals, in calf thymus DNA, and DNA damage in epithelial cells after incubation with PM. In another study, Molinelli and investigators (2002) analyzed the effect of metal removal on the toxicity of ambient PM. PM extracts were treated with a chelating agent that removes all cations (including transition metals) from the sample. Epithelial cells (BEAS-2B) were incubated with PM extracts that were either treated or not treated with the chelating agent, and the inflammatory mediator interleukin-8 was measured. Higher levels of interleukin-8 were observed in the cell cultures incubated with untreated than with treated PM extract, suggesting that the removal of metal ions attenuated the inflammatory response. Aust and colleagues (2002) examined iron-containing coal fly ash of different sizes for its potential to produce reactive oxygen species and inflammatory mediators in cultured lung epithelial cells. Investigators found that more iron was released from the smaller particles than from larger ones. They confirmed that soluble extracts of coal fly ash generated reactive oxygen species in vitro and that transition metals were likely responsible. Further, the smallest particles, which were rich in iron, were the most active. Further research found that the coal fly ash particles entered the cells and stimulated synthesis of the protein ferritin, suggesting that iron was released intracellularly and was available to provoke an inflammatory response by forming reactive oxygen species. Costa and Dreher (1997) found an association between concentrations of acid-soluble metals in PM and toxicity in an animal model for cardiopulmonary injury. This and other studies suggest that the oxidation potential of water-soluble metals may contribute to PM toxicity. Collectively, these studies provided a plausible connection among the intracellular release of transition metal from particles, formation of reactive oxygen species, and resulting toxicity.

MEASURING METALS

A variety of techniques have been used to analyze the metal composition of PM samples, including ICP-MS and XRF. Prior to ICP-MS analysis, PM emission samples are digested and concentrated in acid (Rauch et al 2000). For most elements, ICP-MS is more sensitive than XRF, but the difference in sensitivity varies considerably across elements.

ICP-MS

In ICP-MS, analytes in solution are nebulized into an argon plasma in which atomization and ionization occur (Sutton and Caruso 1999). The nebulizing gas carries the analyte into the plasma, where atomization and ionization occur. The ions move down a pressure gradient into a series of focusing lenses and subsequently into the mass analyzer, most often a quadrapole. The quadrapole separates the ions according to mass–charge ratio, creating an output profile that is then used to identify the species (Sutton and Caruso 1999). When levels of light elements (eg, aluminum, calcium, iron, potassium, magnesium, manganese, sodium, sulfur, silicon, and zinc) are sufficiently high, optical techniques can be used to quantify the levels with inductively coupled plasma optical emission spectrometry (described in Investigators' Report Appendix A, available on request from HEI).

XRF

In XRF, samples are irradiated with and absorb x-rays and then emit light in a spectrum that is characteristic of the elements present. This technique allows elements in complex samples to be quantified on the basis of the intensity of the emitted spectral lines meeting the detector. Although XRF does not destroy samples, it lacks the sensitivity of ICP-MS for the analysis of many metals.

STATISTICAL TECHNIQUES FOR IDENTIFYING SOURCES OF METALS

Statistical techniques are often used to identify the sources and relative source contributions of air pollutants. Such efforts to attribute human exposure and risks to specific components and sources can ultimately provide a basis for control measures to attenuate that risk.

Chemical Mass Balance Modeling

One statistical approach is to use the chemical mass balance (CMB) model, based on the law of conservation of mass. In CMB modeling, a mass balance is achieved between the concentrations of chemical components in an ambient sample and a linear combination of the chemical compositions of the potential sources of these components. CMB modeling involves identification of all potential sources, along with determination of chemical profiles, or fingerprints, for those sources (Gleser 1997). Source profiles may include the relative contributions of all components emitted by the source or a tracer component unique to that source. Included in the CMB model are fractionation coefficients that describe the selective loss of pollution components as they travel from the source to the site where pollution from a combination of sources is measured, the receptor site. Selective losses of components may occur due to gravitational settling, chemical transformation, or evaporation (Schauer et al 1996). Difficulties arise in CMB modeling when source profiles vary because of inconsistency over time or chemical instability or when multicollinearities among sources render them indistinguishable.

ICFA

Other methods used to attribute ambient levels to sources include various types of factor analysis, among them confirmatory and exploratory factor analysis. Confirmatory factor analysis is guided by a priori assumptions about the relations among and the underlying construct of the variables. In short, it is used to test the validity of a previously defined model (Dempster et al 2004). Exploratory factor analysis is used when little is known about the underlying construct of the variables and a priori assumptions are lacking. It is used to identify the underlying construct. ICFA combines elements of both confirmatory and exploratory factor analysis in a way that makes use of a priori knowledge of some profiles while generating updated profiles for sources that are less well defined.

Studies with Synthetic Lung Fluid

In addition to the use of in vivo animal models and in-vitro cell systems, an alternative way of examining the toxic effects of metals is the use of synthetic lung lining fluid. Epithelial fluid obtained from human lungs is diluted as a result of the saline lavage technique used to extract it. Because methods for concentrating this human fluid back to its original form are not yet available, synthetic lung fluid is often used in studies. Synthetic lung fluid often includes apotransferrin or lactoferrin (for iron binding), phosphatidylcholine (a lipid constituent), albumin, and lysozyme, adjusted to a pH of 7.4 (Sun et al 2001).

STUDY DESIGN AND METHODS

In this study, Schauer and colleagues collected and characterized samples from a variety of sources associated with on-road motor vehicles, including tailpipe emissions (from both gasoline and diesel vehicles), dust from brake wear and tire wear, roadway dust, and roadway dust containing salt applied to roadways in winter (Commentary Figure). In addition, total roadway emissions were measured in two roadway tunnels. Use of sensitive analytic techniques such as ICP-MS allowed measurement of a variety of elements in these emissions (Commentary Table) and subsequent development of profiles for each source. These profiles were compared to the profiles developed for the roadway tunnels by using a CMB model, in order to determine the relative contribution of various sources to

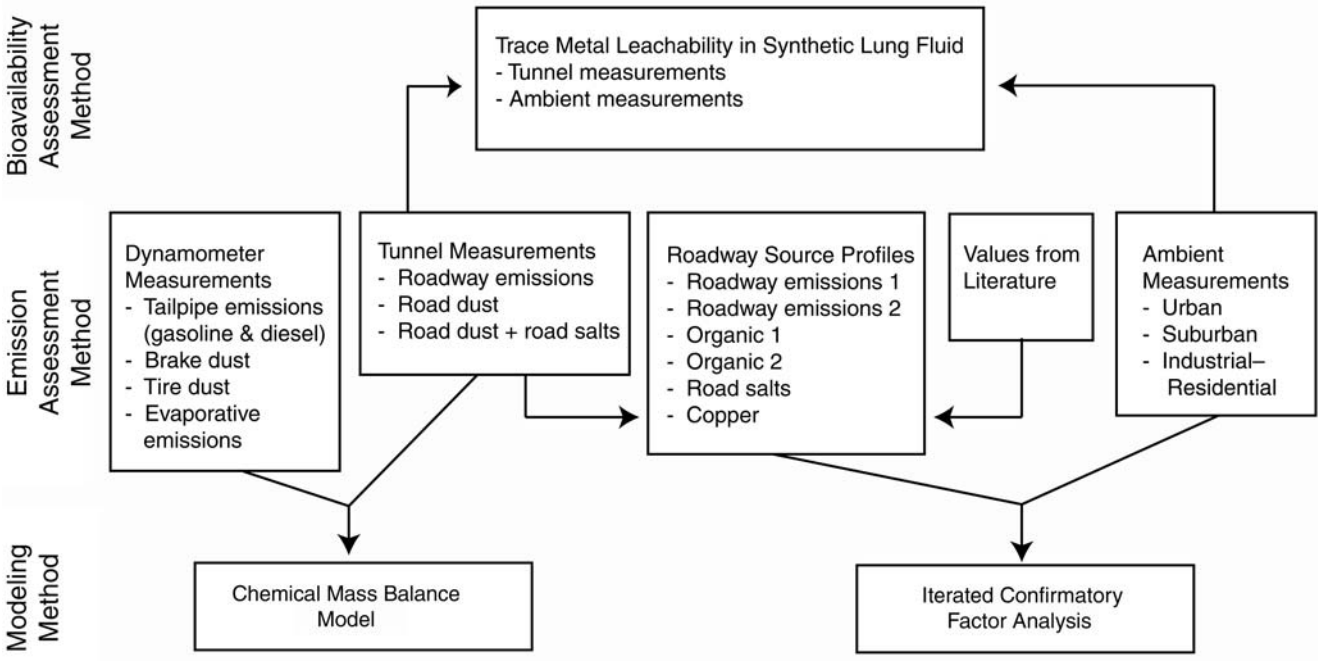

Commentary Figure. Design of the study by Schauer and colleagues. Dynamometer measurements included measurements of specific sources (tailpipe, brakes, tires) and evaporative emissions. Tunnel measurements were taken in the Kilborn Tunnel (summer weekday rush hour) and the Howell Tunnel (summer weekday rush hour, summer weekend, winter weekday rush hour). Both tunnels are in Milwaukee WI. Ambient measurements were taken at monitors at three locations: Milwaukee WI (urban), Waukesha WI (suburban), and Denver CO (industrial–residential). Roadway source profiles developed from dynamometer tests and tunnel sampling were combined in a chemical mass balance model to determine sources of on-road emission measurements. Ambient measurements were combined with estimated roadway source profiles in an iterated confirmatory factor analysis to determine sources of ambient measurements. Samples from tunnel and ambient measurements were incubated in a synthetic lung fluid to establish leachability of the associated metals.

Commentary Table. Elements, Ions, and Carbon Measurements in Schauer Study[a]

Name	Symbol or Abbreviation	Analytic Method Used	Measurement						
			Brake Dust	Tire Dust	Tailpipe Emissions[b]	RL-SHED Emissions[c]	Tunnel	Ambient	Synthetic Lung Fluid[d]
Carbons									
Organic carbon	OC	Thermal optical	+	+	+	+	+	+	−
Elemental carbon	EC	Thermal optical	+	+	+	+	+	+	−
Ions									
Chloride	Cl^-	Ion chromatography, XRF	+	+	+	+	+	+	−
Nitrate	NO_3^-	Ion chromatography	+	+	+	+	+	+	−
(Sulfate	SO_4^{2-}	Ion chromatography	+	+	+	+	+	+	−
Ammonia	NH_4^+	Ion chromatography	+	+	+	+	+	+	−
Elements									
Nonmetals									
Phosphorus	P	XRF	−	−	−	−	+	−	−
Sulfur	S	XRF	−	−	−	−	+	−	−
Selenium	Se	XRF	−	−	−	−	+	−	−
Alkali metals									
Sodium	Na	ICP-MS	+	+	+	+	+	+	−
Potassium	K	XRF	+	+	+	+	+	+	−
Rubidium	Rb	ICP-MS	+	+	+	+	+	+	+
Cesium	Cs	ICP-MS	+	+	+	+	+	+	+
Alkali earth metals									
Magnesium	Mg	ICP-MS	+	+	+	+	+	+	−
Calcium	Ca	XRF	+	+	+	+	+	+	−
Strontium	Sr	ICP-MS	+	+	+	+	+	+	+
Barium	Ba	ICP-MS	+	+	+	+	+	+	+
Transition metals									
Scandium	Sc	XRF	−	−	−	−	+	−	−
Titanium	Ti	ICP-MS	+	+	+	+	+	+	+
Vanadium	V	ICP-MS	+	+	+	+	+	+	+
Chromium	Cr	ICP-MS	+	+	+	+	+	+	+
Manganese	Mn	ICP-MS	+	+	+	+	+	+	+
Iron	Fe	ICP-MS	+	+	+	+	+	+	+
Cobalt	Co	ICP-MS	−	−	−	−	+	−	−
Nickel	Ni	ICP-MS	−	−	−	−	+	−	−
Copper	Cu	ICP-MS	+	+	+	+	+	+	+
Zinc	Zn	ICP-MS	+	+	+	+	+	+	+
Molybdenum	Mo	ICP-MS	+	+	+	+	+	+	+
Ruthenium	Ru	ICP-MS	+	+	+	+	+	+	+
Rhodium	Rh	ICP-MS	+	+	+	+	+	+	+
Palladium	Pd	ICP-MS	+	+	+	+	+	+	+
Silver	Ag	ICP-MS	+	+	+	+	+	+	+
Cadmium	Cd	ICP-MS	+	+	+	+	+	+	+
Tungsten	W	ICP-MS	+	+	+	+	+	+	+
Platinum	Pt	ICP-MS	+	+	+	+	+	+	+

Table continues on next page

[a] Plus sign = analyzed in sample. Minus sign = not analyzed.

[b] From vehicle on dynamometer.

[c] All emissions from vehicle on dynamometer other than tailpipe.

[d] Combined with tunnel or ambient samples to determine leachability.

Commentary Table (*continued*). Elements, Ions, and Carbon Measurements in Schauer Study[a]

Name	Symbol or Abbreviation	Analytic Method Used	Measurement						
			Brake Dust	Tire Dust	Tailpipe Emissions[b]	RL-SHED Emissions[c]	Tunnel	Ambient	Synthetic Lung Fluid[d]
Elements (*continued*)									
Lanthanides									
Lanthanum	La	ICP-MS	−	−	−	−	+	−	−
Cerium	Ce	XRF	+	+	+	+	+	+	+
Actinides									
Uranium	U	ICP-MS	+	+	+	+	+	+	+
Halogens									
Bromine	Br	XRF	−	−	−	−	+	−	−
Iodine	I	XRF	−	−	−	−	+	−	−
Metals									
Aluminum	Al	XRF	+	+	+	+	+	+	+
Tin	Sn	ICP-MS	−	−	−	−	+	−	−
Thallium	Tl	ICP-MS	+	+	+	+	+	+	−
Lead	Pb	ICP-MS	+	+	+	+	+	+	+
Metalloids									
Silicon	Si	XRF	−	−	−	−	+	−	−
Germanium	Ge	XRF	−	−	−	−	+	−	−
Arsenic	As	ICP-MS	+	+	+	+	+	+	−
Antimony	Sb	ICP-MS	+	+	+	+	+	+	+

[a] Plus sign = analyzed in sample. Minus sign = not analyzed.

[b] From vehicle on dynamometer.

[c] All emissions from vehicle on dynamometer other than tailpipe.

[d] Combined with tunnel or ambient samples to determine leachability.

total roadway emissions. ICFA was used to determine the relative contribution of various sources to ambient PM collected at three locations.

The specific aims of the study were to:

- Measure and speciate metals in fine PM ($PM_{2.5}$) and PM_{10} emissions from several large fleets of motor vehicles in two tunnels.
- Measure and speciate metals in fine and coarse PM emitted from winter and summer cold-start engine emissions.
- Measure metals in fine and coarse PM from tire dust, brake dust, and tailpipe emissions.
- Measure and speciate metals in ambient fine and coarse PM at ambient air-monitoring sites in Midwestern cities.
- Measure human exposure to metals from motor vehicles, such as those experienced by people conducting activities near motor vehicle traffic.

METAL AND SOURCE CHARACTERIZATION

To date, most source characterizations of vehicles have been based primarily on measurements from a limited number of vehicles operated on dynamometers. These characterizations have also largely depended on analysis of gas-phase compounds and speciation of organic compounds from PM. Some investigators have measured emissions from vehicles traveling through tunnels, giving a more realistic view of in-use vehicles, but these studies also tend to be focused on volatile organic compounds and their speciation. In the study described in Investigators' Report, Dr Schauer and colleagues used ICP-MS, an approach for analyzing metals in PM from different sources. This technique is important because it is more sensitive than traditional techniques, such as XRF, for analysis of trace metals. Detailed characterization of metals allows identification of source profiles that can be used to investigate the contribution of specific roadway sources to metal emissions associated with mobile sources.

To understand the metal content of different components of mobile sources, the investigators collected tailpipe emissions (from gasoline- and diesel-powered vehicles), brake dust, tire dust, and resuspended road dust. They analyzed them for elemental carbon (EC), organic carbon (OC), nitrate (NO_3^-), sulfate (SO_4^{2-}), ammonia (NH_4^+), and trace elements. Together, these components comprise the majority of chemicals making up the mass of PM. They also collected samples from two tunnels in Wisconsin: the Kilborn Tunnel during summer weekdays, and the Howell Tunnel during summer and winter weekends and weekdays. A CMB model was used to evaluate the relative contribution of each source to the metal emissions measured in the tunnels.

Investigators also collected ambient air samples from Milwaukee, Waukesha, and Denver, analyzed their trace-element contents, and used these data to develop source profiles for urban, suburban, and industrial–residential settings, respectively. These profiles, combined with source profiles from the published literature for tunnels and other sources, profiles for roadway sources, organic sources, and road salt, were used in an ICFA model to determine the origin of pollutants in ambient settings. Six initial source profiles were used in this model (roadway emissions, municipal incinerator, road salt, unspecified source, copper, and wood burning). After allowing the model to update the source profile matrix 50 times, the sources were redesignated on the basis of the profiles (roadway emissions 1, roadway emissions 2, road salt, copper, organic 1, and organic 2).

LEACHABILITY

To preliminarily address bioavailability of metals, ambient and tunnel samples were examined in a study that determined the solubility in a synthetic fluid that was designed to mimic human epithelial lung lining fluid. The synthetic lung fluid was purified of metals with a Chelex resin and then incubated with filter samples from tunnel studies or from ambient air at 37°C for 8 hours with shaking (80 rpm) to allow extraction (leaching) of material from the filters. Synthetic lung fluid was then analyzed for trace metals by using ICP-MS and XRF.

RESULTS

The combined use of ICP-MS and XRF allowed detection of 43 elements (Commentary table). The concentrations of 13 elements (aluminum, silicon, phosphorus, sulfur, potassium, calcium, scandium, germanium, bromine, iodine, chlorine, and cerium) were determined by XRF elemental analysis. The application of ICP-MS allowed measurement of concentrations of 31 additional elements. Use of ICP-MS, with its greater sensitivity for trace metals, allowed the detailed profiling of elements that was necessary for the subsequent identification of profiles that can be used for source apportionment as a way of assessing emissions in the tunnel.

Using a CMB model, the investigators compared source profiles for total roadway emissions, as measured in tunnels, to profiles for resuspended road dust, brake dust, tire dust, and tailpipe emissions from gasoline- and diesel-powered vehicles. Using these source profiles, and excluding results from light, weekend traffic in summer in one tunnel (traffic conditions which were considerably different than traffic in the other tunnel sampling times), CMB modeling predicted 63% to 160% of the total PM mass in the tunnels. Calculated and measured emission rates in the excluded tunnel were in good agreement, adding further support for the modeling results.

The results of the CMB model allowed the investigators to trace back individual elements measured in the tunnels (roadway emissions) to one of four model sources: the combination of gasoline-vehicle tailpipe emissions and tire dust, diesel-vehicle tailpipe emissions, brake dust, and resuspended road dust. They conclude that much of the lighter crustal elements (sulfur, magnesium, aluminum, potassium, calcium, iron, and titanium), as well as the trace elements strontium, cadmium, and lead, were attributable to road dust. They also conclude that brake dust contributed to a large proportion of the roadway emissions of iron, chromium, manganese, copper, zinc, strontium, antimony, and barium. The investigators report that diesel-vehicle tailpipe emissions contributed a large percentage of PM_{10}, vanadium, and cadmium and a small amount of calcium, chromium, zinc, strontium, and lead. The combination of gasoline-vehicle tailpipe emissions and tire dust were shown to account for a large percentage of the roadway emission of vanadium, chromium, zinc, strontium, lead, molybdenum, and silver.

ICFA results indicated that the two organic source profiles were dominant contributors of ambient PM_{10} and that the road salt profile was a dominant contributor to ambient chloride. Not surprisingly, OC and EC dominated the results of the analysis; however, by removing these values from the model, the investigators were able to perform a source attribution for metals. They concluded that the organic sources were major contributors for 14 species in ambient PM_{10}: OC, EC, magnesium, aluminum, potassium, calcium, iron, vanadium, manganese, arsenic, strontium, cadmium, barium, and cerium. Road salt was found to be a major contributor of chloride and sodium.

The solubility tests used samples from ambient air and from tunnels in a synthetic lung fluid. The results indicated that many elements could be leached into the fluid. The investigators found eight transition metals (silver, titanium, iron, tungsten, copper, zinc, manganese, and cadmium) from tunnel samples, and eight (titanium, tungsten, copper, zinc, manganese, chromium, vanadium, and molybdenum) from ambient samples, in the leachate, with a high solubility observed for several elements, including barium (10%–65%), lead (15%–50%), zinc (≤ 36%), manganese (15%–100%), and titanium (≤ 7%).

DISCUSSION

This was a valuable study, performed by an investigator team with expertise in measuring trace levels of metals in environmental samples. The methods they used to approach the study problem were excellent, and the study generated solid information that could be important for a range of activities, including emissions inventories. The team took a multidisciplinary approach to the examination of metals from mobile sources (including vehicle sources besides the tailpipe), weaving together biology, chemistry, and source apportionment techniques. An important aim of this study, to measure exposure in people conducting activities near traffic, was not addressed, however, the results from the other aims are valuable individually, and even more valuable when examined together.

Dr Schauer and colleagues performed source characterization for metals by using ICP-MS and XRF. This combination of analytic techniques is sufficiently sensitive for analysis of trace metals to allow development of source profiles for brake dust, tire dust, resuspended road dust, and tailpipe emissions from diesel and gasoline vehicles. These profiles were analyzed with the use of a CMB model to determine the relative contribution of various sources to on-road emissions from motor vehicles. Using another new technique, ICFA, Dr Schauer and his colleagues compared the CMB results with results from an analysis of metals from ambient PM at three locations. This comparison provides information about the influence of metals from different sources on the concentrations of metals in ambient air. Dr Schauer and colleagues posit that insoluble metals trace back to area sources and soluble metals to local sources. Finally, they examined the solubility of metals in synthetic lung fluid to estimate the bioavailability of these metals.

The solubility tests used samples from ambient air and from tunnels in a synthetic lung fluid. The results indicated that many elements could be leached into the fluid. High solubility was observed for several elements, implying that many elements could become bioavailable if inhaled. This aspect of the study may be an important contribution to understanding the bioavailability of metals from mobile sources. The data identify some soluble species of metals and link them with potential health effects. For example, the soluble forms of transition metals are thought to lead to free-radical production in the lung and cause lung damage. The data from solubility tests in a biologically relevant fluid may also reflect chemical properties of the elements similar to those often measured by ion chromatography.

Although this study provides a large amount of useful information, several limitations should be noted before more general conclusions are drawn. Care should be taken if extending the roadway emissions results from this study more broadly. The Investigators' Report does not outline the sampling strategy, especially with respect to what vehicles were sampled on what days and at what times of day, so it is not clear how representative the data are of the general fleet or how these measurements contribute to the general population's exposure to metals (which can also come from other sources). Such details are necessary in order to be confident in using the results to understand human exposures. More variation in the percentages of diesel vehicles in the tunnels would also have made the study more powerful.

Similar care should be taken in extending the ambient air sampling and subsequent source apportionment results, because the criteria used for selection of the sites (including considerations about weather, proximity to traffic, and season) are insufficiently described. Furthermore, the Waukesha sampling site was influenced by nearby sources (such as a copper-emitting facility) and thus may not represent ambient levels of pollutants.

Owing to the small amount of mass collected in the tunnel tests, which was necessary for optimal loading in the ICP-MS analyses, the gravimetric mass measurements for PM carried high uncertainties. Therefore, the investigators calculated a reconstructed mass for PM by summing the measurements of components that had less uncertainty (EC, OC, SO_4^{2-}, NO_3^- chloride, and elemental oxides). Investigators found that these reconstructed mass values agreed well with the direct, gravimetric analyses (with their uncertainties), giving greater confidence to their use.

Although solubility is not the same as bioavailability, the tests with synthetic lung fluid do give a sense of which metals may present health hazards. However, the synthetic lung fluid used in this study is not the same as true lung fluid, which contains components such as proteins, peptides, nucleotides, and lipids that can react with metals. Therefore, care should be exercised in interpreting these results, because a metal being soluble does not necessarily mean that it will become bioavailable in the lung. The rate at

which metals leach from particles is also important and may influence toxicity. The investigators are appropriately cautious in interpreting their data. Nevertheless, transition metals must be in soluble form to become free radicals in the presence of oxygen, even though the insoluble forms may be made bioavailable through mechanisms of chelators.

The data generated from this study should be considered exploratory in nature, providing new information for and insight into the application of techniques to studies of air pollution related to mobile sources. Although the statistical techniques employed by Schauer and colleagues are not sophisticated (means, standard deviations, regression analyses), they do appear appropriate to the study. They also, however, do not give the conclusions of the study the same sort of confidence that a more rigorous statistical analysis would. If the data set were larger, comprising more cars and trucks under a variety of driving conditions and road surfaces, more sophisticated statistical techniques would be essential for drawing other important conclusions which could also be generalized across a wider set of circumstances.

Finally, as a source apportionment technique, ICFA needs validation. It needs to be replicated in other studies, including studies in different environments and with different compositions of vehicles; it also needs evaluation against other methods. However, the Investigators' Report provides useful information about automotive emissions as one part of attributing personal and health effects to any particular source or component of PM. ICFA analysis of the data represents an important first step in characterizing the contribution of nontailpipe emissions.

CONCLUSIONS

This was a valuable study, performed by an investigator team with expertise in measuring trace levels of metals in environmental samples. The methods they used to approach the study problem were excellent, and the study generated solid information that could be important for a range of activities, including emissions inventories. The team took a multidisciplinary approach to the examination of metals from mobile sources (including vehicle sources besides the tailpipe), weaving together biology, chemistry, and source apportionment techniques. An important aim of this study, to measure exposure in people conducting activities near traffic, was not addressed, however, the results from the other aims are valuable individually, and even more valuable when examined together. Although this study provides a large amount of useful information, several limitations should be noted before more general conclusions are drawn: (1) Care should be taken if extending the roadway emissions results from this study more broadly. (2) Similar care should be taken in extending the ambient air sampling and subsequent source apportionment results. (3) ICFA needs to be validated through replication in other studies, including studies in different environments and with different compositions of vehicles, and evaluated against other methods. (4) The data generated from this study should be considered exploratory in nature, providing new information for and insight into the application of techniques to studies of air pollution related to mobile sources. The study provides useful data, especially with respect to exposure from all types of mobile sources (not just tailpipes). It brings a novel approach, ICP-MS, to the characterization of metals in PM, which has been a problem because measurement of trace elements has heretofore been hindered by limits of detection. This technique lowers the detection limits significantly, making measurement of trace metals possible. The application of another new technique, ICFA, allows these measurements to be used in subsequent source apportionment. This research also involved using synthetic fluid to determine the fraction of metals that is soluble in a biological environment and thus may interact with cellular components. This study, with its multidisciplinary approach, provides important tools and presents a useful approach for gathering information about which metals (and sources of these metals) are linked with pathology of the respiratory systems in asthma and other diseases.

ACKNOWLEDGMENTS

The Health Review Committee thanks the ad hoc reviewers for their help in evaluating the scientific merit of the Investigators' Report. The Committee is also grateful to Martha Richmond and Geoffrey Sunshine for their oversight of the study, to Debra Kaden and Joanne Sordillo for their assistance in preparing its Commentary, to Jenny Lamont and Genevieve MacLellan for science editing this Report and its Commentary, and to Melissa R Harke, Carol Moyer, and Ruth E Shaw for their roles in publishing this Research Report.

REFERENCES

Allen JO, Mayo PR, Huges LS, Salmon LG, Cass GR. 2001. Emissions of size-segregated aerosols from on-road vehicles in the Caldecott Tunnel. Environ Sci Technol 35:4189–4197.

Aust AE, Ball JC, Hu AA, Lighty JS, Smith KR, Straccia AM, Veranth JM, Young WC (2002) Particle Characteristics Responsible for Effects on Human Lung Epithelial Cells.

Research Report 110. Health Effects Institute, Boston MA.
Cadle SH, Mulawa PA, Ball J, Donase C, Weibel A, Sagebiel JC, Knapp KT, Snow R. 1997. Particulate emission rates from in-use high-emitting vehicles recruited in Orange County, California. Environ Sci Technol 31:3405–3412.

Cadle SH, Mulawa PA, Hunsanger EC, Nelson K, Ragazzi RA, Barrett R, Gallagher GL, Lawson DR, Knapp KT, Snow R. 1999. Composition of light-duty motor vehicle exhaust particulate matter in the Denver, Colorado area. Environ Sci Technol 33:2328–2339.

Carter JD, Ghio AJ, Samet JM, Devlin RB. 1997. Cytokine production by human airway epithelial cells after exposure to an air pollution particle is metal-dependent. Toxicol Appl Pharmacol 146(2):180–188.

Claiborn CS, Larson T, Sheppard L. 2002. Testing the metals hypothesis in Spokane, Washington. Environ Health Perspect 110(Suppl 4):547–552.

Costa DL, Dreher KL. 1997. Bioavailable transition metals in particulate matter mediate cardiopulmonary injury in healthy and compromised animal models. Environ Health Perspect 105(Suppl 5):1053–1060.

Davis AP, Shokouhian M, Ni S. 2001. Loading estimates of lead, copper, cadmium, and zinc in urban runoff from specific sources. Chemosphere 44:997–1009.

Dempster M, Donnelly M, O'Loughlin C. 2004. The validity of the MacNew quality of life in heart disease questionnaire. Health Qual Life Outcomes 2:6–12.

Dye JA, Adler KB, Richards JH, Dreher KL. 1999. Role of soluble metals in oil fly ash-induced airway epithelial injury and cytokine gene expression. Am J Physiol Lung Cell Mol Physiol 277(21):L498–L510.

El-Fadel M, Hashisho Z. 2001. Vehicular emission in roadway tunnels: A critical review. Crit Rev Environ Sci Technol 31(2):125–174.

Garg BD, Cadle SH, Mulawa PA, Groblicki PJ, Laroo C, Parr GA. 2000. Brake wear particulate matter emissions. Environ Sci Technol 34(21):4463–4469.

Gertler AW, Gillies JA, Pierson WR, Rogers CF, Sagebiel JC, Abu-Allaban M, Coulombe W, Tarnay L, Cahill TA. 2002. Real-world particulate matter and gaseous emissions from motor vehicles in a highway tunnel. In: Emissions from Diesel and Gasoline Engines Measured in Highway Tunnels. Research Report 107. Health Effects Institute, Boston MA.

Ghio AJ, Stonehuerner J, Dailey LA, Carter JD. 1999. Metals associated with both the water-soluble and insoluble fractions of an ambient air pollution particle catalyze an oxidative stress. Inhalation Toxicol 11(1):37–49.

Gilles JA, Gertler AW, Sagebiel JC, Dippel WA. 2001. On-road particulate matter (PM2.5 and PM10) emissions in the Sepulveda Tunnel, Los Angeles, California. Environ Sci Technol 35:1054–1063.

Gleser LJ. 1997. Some thoughts on chemical mass balance models. Chemometr Intell Lab 37:15–22.

Goyer RA. 1996. Toxic effects of metals. Chapter 23 in: Casarett and Doull's Toxicology: The Basic Science of Poisons (Klaassen CD, Watkins JB III, eds), pp 578–633. 5th edition. McGraw-Hill, New York NY.

Hopke PK, Lamb RE, Natusch DFS. 1980. Multielemental characterization of urban roadway dust. Environ Sci Technol 14(2):164–172.

Knaapen AM, Shi T, Borm PJA, Schins RPF. 2002. Soluble metals as well as the insoluble particle fraction are involved in cellular DNA damage induced by particulate matter. Mol Cell Biochem 234-235:317–326.

Kodavanti UP, Schladweiler MCJ, Ledbetter A, Hauser R, Christiani DC, Samet JM, McGee J, Richards JH, Costa DL. 2002. Pulmonary and systemic effects of zinc-containing emissions particles in three rat strains: Multiple exposure scenarios. Toxicol Sci 70:73–85.

Molinelli AR, Madden MC, McGee JK, Stonehuerner JG, Ghio AJ. 2002. Effect of metal removal on the toxicity of airborne particulate matter from the Utah Valley. Inhalation Toxicol 14:1069–1086.

Prieditis H, Adamson IYR. 2002. Comparative pulmonary toxicity of various soluble metals found in urban particulate dusts. Exp Lung Res 28:563–576.

Rauch S, Morrison GM, Motelica-Heino M, Donard OFX, Muris M. 2000. Elemental association and fingerprinting of traffic-related metals in road sediments. Environ Sci Technol 34:3119–3123.

Schauer JJ, Rogge WF, Hildemann LM, Mazurek MA, Cass GR, Simoneit BRT. 1996. Source apportionment of airborne particulate matter using organic compounds as tracers. Atmos Environ 30(22):3837–3855.

Sternbeck J, Sjödin Å, Andréasson K. 2002. Metal emissions from road traffic and the influence of resuspension: Results from two tunnel studies. Atmos Environ 36:4735–4744.

Sun G, Crissman K, Norwood J, Richards J, Slade R, Hatch GE. 2001. Oxidative interactions of synthetic lung epithelial

lining fluid with metal-containing particulate matter. Am J Physiol Lung Cell Mol Physiol 281:L807–L815.

Sutton KL, Caruso JA. 1999. Liquid chromatography-inductively coupled plasma mass spectrometry. J Chromatogr A 856:243–258.

RELATED HEI PUBLICATIONS: PARTICULATE MATTER AND DIESEL EXHAUST

Number	Title	Principal Investigator	Date*
Research Reports			
131	Characterization of Particulate and Gas Exposures of Sensitive Subpopulations Living in Baltimore and Boston	P Koutrakis	2005
	Mechanisms of Particulate Matter Toxicity in the Respiratory System	KE Pinkerton	In Press
130	Relationships of Indoor, Outdoor, and Personal Air (RIOPA)		
	Part I. Collection Methods and Descriptive Analyses	CP Weisel	2005
	Part II. Analyses of Concentrations of Particulate Matter Species	BJ Turpin	In Press
127	Personal, Indoor, and Outdoor Exposures to $PM_{2.5}$ and Its Components for Groups of Cardiovascular Patients in Amsterdam and Helsinki	B Brunekreef	2005
126	Effects of Exposure to Ultrafine Carbon Particles in Healthy Subjects and Subjects with Asthma	MW Frampton	2004
124	Particulate Air Pollution and Nonfatal Cardiac Events		
	Part I. Air Pollution, Personal Activities, and Onset of Myocardial Infarction in a Case–Crossover Study	A Peters	2005
	Part II. Association of Air Pollution with Confirmed Arrhythmias Recorded by Implanted Defibrillators	DW Dockery	2005
123	Time-Series Analysis of Air Pollution and Mortality: A Statistical Review	F Dominici	2004
122	Evaluation of a Personal and Microenvironmental Aerosol Speciation Sampler (PMASS)	AS Geyh	2004
121	Field Evaluation of Nanofilm Detectors for Measuring Acidic Particles in Indoor and Outdoor Air	BS Cohen	2004
119	Manganese Toxicokinetics at the Blood–Brain Barrier	RA Yokel	2004
118	Controlled Exposures of Healthy and Asthmatic Volunteers to Concentrated Ambient Particles in Metropolitan Los Angeles	H Gong Jr	2003
117	Peroxides and Macrophages in Toxicity of Fine Particulate Matter	DL Laskin	2003
114	A Personal Particle Speciation Sampler	S Hering	2003
112	Health Effects of Acute Exposure to Air Pollution *Part I.* Healthy and Asthmatic Subjects Exposed to Diesel Exhaust *Part II.* Healthy Subjects Exposed to Concentrated Ambient Particles	ST Holgate	2003
110	Particle Characteristics Responsible for Effects on Human Lung Epithelial Cells	AE Aust	2002
107	Emissions from Diesel and Gasoline Engines Measured in Highway Tunnels		
	Part I. Real-World Particulate Matter and Gaseous Emissions from Motor Vehicles in a Highway Tunnel	AW Gertler	2002
	Part II. Airborne Carbonyls from Motor Vehicle Emissions in Two Highway Tunnels	D Grosjean	2002
101	Epithelial Penetration and Clearance of Particle-Borne Benzo[*a*]pyrene	P Gerde	2001
99	A Case-Crossover Analysis of Fine Particulate Matter Air Pollution and Out-of-Hospital Sudden Cardiac Arrest	H Checkoway	2000

Continued

** Reports published since 1990.*
Copies of these reports can be obtained from the Health Effects Institute and many are available at www.healtheffects.org.

RELATED HEI PUBLICATIONS: PARTICULATE MATTER AND DIESEL EXHAUST

Number	Title	Principal Investigator	Date*
98	Daily Mortality and Fine and Ultrafine Particles in Erfurt, Germany *Part I.* Role of Particle Number and Particle Mass	H-E Wichmann	2000
97	Identifying Subgroups of the General Population That May Be Susceptible to Short-Term Increases in Particulate Air Pollution: A Time-Series Study in Montreal, Quebec	MS Goldberg	2000
95	Association of Particulate Matter Components with Daily Mortality and Morbidity in Urban Populations	M Lippmann	2000
94	The National Morbidity, Mortality, and Air Pollution Study		
	Part I. Methods and Methodologic Issues	JM Samet	2000
	Part II. Morbidity and Mortality from Air Pollution in the United States	JM Samet	2000
	Part III. PM_{10} Concentration–Response Curves and Thresholds for the 20 Largest US Cities	JM Samet	2004
91	Mechanisms of Morbidity and Mortality from Exposure to Ambient Air Particles	JJ Godleski	2000
76	Characterization of Fuel and Aftertreatment Device Effects on Diesel Emissions	ST Bagley	1996
Special Reports			
	Health Effects of Outdoor Air Pollution in Developing Countries of Asia: A Literature Review		2004
	Revised Analyses of Time-Series Studies of Air Pollution and Health		2003
	Reanalysis of the Harvard Six Cities Study and the American Cancer Society Study of Particulate Air Pollution and Mortality: A Special Report of the Institute's Particle Epidemiology Reanalysis Project		2000
	Particulate Air Pollution and Daily Mortality: The Phase I Report of the Particle Epidemiology Evaluation Project		
	Phase I.A. Replication and Validation of Selected Studies		1995
	Phase I.B. Analyses of the Effects of Weather and Multiple Air Pollutants		1997
HEI Communications			
10	Improving Estimates of Diesel and Other Emissions for Epidemiologic Studies		2003
9	Evaluation of Human Health Risk from Cerium Added to Diesel Fuel		2001
HEI Research Program Summaries			
	Research on Particulate Matter		1999
	Research on the Effects of Particulate Air Pollution on Mortality and Morbidity		1996
HEI Perspectives			
	Understanding the Health Effects of Components of the Particulate Matter Mix: Progress and Next Steps		2002
	Airborne Particles and Health: HEI Epidemiologic Evidence		2001

** Reports published since 1990.*
Copies of these reports can be obtained from the Health Effects Institute and many are available at www.healtheffects.org.

HEALTH
EFFECTS
INSTITUTE

Charlestown Navy Yard
120 Second Avenue
Boston MA 02129-4533 USA
+1-617-886-9330
www.healtheffects.org

RESEARCH
REPORT

Number 133
March 2006